MDAC-62364

GPO PRICE	$
CSFTI PRICE(S)	$
Hard copy (HC)	3.00
Microfiche (MF)	.65

ff 653 July 65

N68-36566 (ACCESSION NUMBER)	(THRU)
186 (PAGES)	1 (CODE)
CR-92332 (NASA CR OR TMX OR AD NUMBER)	05 (CATEGORY)

FACILITY FORM 602

EVAPORATIVE COOLING GARMENT SYSTEM (ECGS)

PART I

DOUGLAS MISSILE & SPACE SYSTEMS DIVISION

MCDONNELL DOUGLAS CORPORATION

SEPTEMBER 1968

NASA CR 92332

FINAL REPORT

EVAPORATIVE COOLING GARMENT SYSTEM (ECGS)

SEPTEMBER 1968

MDAC-62364

PART I

PREPARED BY
J.G. BITTERLY
PROGRAM MANAGER
EVAPORATIVE COOLING GARMENT SYSTEM
ADVANCE BIOTECHNOLOGY AND POWER DEPARTMENT

APPROVED BY
DR. K. H. HOUGHTON
CHIEF ENGINEER
ADVANCE BIOTECHNOLOGY AND POWER DEPARTMENT

PREPARED UNDER CONTRACT NO. NAS-9-7207
BY McDONNELL DOUGLAS ASTRONAUTICS COMPANY
WESTERN DIVISION
FOR NATIONAL AERONAUTICS AND SPACE ADMINISTRATION

DOUGLAS
MISSILE & SPACE SYSTEMS DIVISION

PRECEDING PAGE BLANK NOT FILMED.

FOREWORD

McDonnell Douglas Astronautics Company-Western Division (MDAC-WD) gratefully acknowledges program support provided by NASA-Manned Spacecraft Center and the Air Force Aerospace Medical Division. In particular considerable technical assistance and advice was provided by Messrs. Larry E. Bell, Elton M. Tucker (Program Manager), and Joseph T. Barker of the NASA-MSC, Crew Systems Division. From this organization, Mr. Fred A. Spross donned and evaluated the garment configuration for cooling effectiveness, comfort, and mobility in physical exercise tests on the MDAC-WD treadmill. Providing contract cognizance for the Air Force were Mr. Don Bowen of AMRL, Lt. Col. Richard Willis and Maj. Eli Beeding of AMD.

Also participating in physical testing of the cooling garment and contributing to its development were Capt. C. B. Harrah of the Air Force Space and Missile Systems Organization and Dr. Allen Chambers of the NASA-Ames Research Center. Further acknowledgment is extended to other members of SAMSO, including Col. A. I. Karstens, Dr. P. Briska, and Dr. E. Thrasher and to Mr. Roy St. John and Mr. James Blackaby of NASA-ARC for their active interest. On the MDAC-WD team, special thanks are due Mrs. Alice Chatham for her work in garment fabrication and to test engineers R. Weivig, E. Hoyer, D. Miller, and R. Scott.

PRECEDING PAGE BLANK NOT FILMED.

CONTENTS

FIGURES

Section 1
INTRODUCTION AND SUMMARY

The latest Gemini flights have shown that astronaut extravehicular activities (EVA) require more physical effort than had been expected, and this effort causes very high peak metabolic rates. The body heat that is generated during these activities must be dissipated so that a complete body thermal balance is maintained with the need to minimize or eliminate sweating, and lastly to provide a cooling system that will allow maximum sustained metabolic rates with optimum comfort. Other criteria for spacesuit body cooling include immediate response to any dynamic heat problem; minimum or no power required; high reliability, preferably with no moving parts; and applicability to EVA, IVA, or lunar exploration.

This report describes the results of an Evaporative Cooling Garment System (ECGS) program that was conducted for the NASA-MSC Crew Systems Division and was jointly founded by the USAF-AMD. The primary objective of the program was to develop and test an engineering model of the ECGS to determine if this new concept would be able to provide full body cooling for an astronaut in a simulated 4-hour EVA mission. The mission profile was designed to tax the limits of human endurance and to produce maximum heat energy outputs; these conditions were imposed to ascertain if the ECGS could provide all of the cooling necessary to maintain thermal equilibrium and working comfort in a highly variable work duty cycle without heat stress. A target maximum cooling performance level of 5,000 Btu/hr was desired. Another requirement of the program was to determine if the ECGS could be integrated into an Apollo A-6L type of full-pressure suit with only minimum changes to the pressure suit. The USAF also desired that the full body, suited ECGS configuration could be converted to a garment front and back torso with upper arm coverage.

The ECGS operates by conducting body heat through a thin membrane that completely encloses a wick water supply, which is adjacent to a flexible three-dimensional material. A vacuum line penetrates the outer membrane layer, thus exposing the water to low-pressure boiloff to space via a control valve. The phase change and cold steam generated by the heat of vaporization carries the body heat to space. This may be likened to an open-loop refrigeration cycle or may be compared to the natural process of skin cooling by sweat evaporation.

The 14-month program included the research tasks of theory and design, basic laboratory tests, engineering model fabrication, design verification tests, and documentation with hardware delivery. The following pages describe the problems and solutions and present the analysis of the test results as they relate to the several tasks.

Every objective and contract requirement was achieved within the specified time and budget. The highest performance target was easily exceeded. The ECGS heat rejection capacity was found to be highly effective; in fact no matter how hard a test subject worked, more than adequate cooling was available. The program also demonstrated that cooling up to thermal equilibrium could eliminate sweating, even at the highest metabolic rates. The cooling rate response time is virtually instantaneous at any level of heat rejection, and the control of heat removal could be held in the laboratory to within $\pm 1\%$ of the desired values. In summary, the ECGS has shown that a man's useful work output can be increased by 250%, on the basis of thermal equilibrium, over that provided by current flight hardware.

Section 2
ECGS SYSTEM DESCRIPTION AND OPERATION

The ECGS consists of several cooling patches covering nonarticulated portions of the body, associated plumbing and controls, and a supporting garment. The entire system is designed to operate independently, without outside power or storage of material, in a vacuum environment. The system will be compatible with an Apollo-type space pressure suit and will use the suit openings presently provided for the LCG system. A drawing showing the complete ECGS cooling suit is shown in Figure 1.

The ECGS is built up of four basic layers in the patch area. Next to the skin is a layer of absorbent mesh which serves two purposes. First, it improves the "feel" of the patch next to the skin and, second, it provides a wick to absorb any moisture from the skin. This moisture is transported by the mesh wick to the areas between patches where it can be evaporated. The next layer of the ECGS system is the cooling patch. It acts as a low-pressure boiler, removing heat from the skin and carrying it away as low pressure (cold) steam. (See Section 3.1 for detailed patch description.) The third layer is a plastic ballonet which is pressurized to approximately 5 in. of water. This ballonet imposes a uniform pressure on the patch, causing it to conform closely to the local body contours. The outer layer is a nonstretchable fabric cover which protects the ballonet and patch from abrasion and holds the assembly in place.

The patches are connected to form a complete garment with stretch type material at the articulated joint areas. Vacuum lines connect the individual patches to the outlet collector manifold. Water supply lines are routed inside the vacuum lines to the outlet collector. A water reservoir in the form of a belt is attached to the main torso patch. This reservoir supplies water to the individual patch boilers through the water supply lines. The controls for

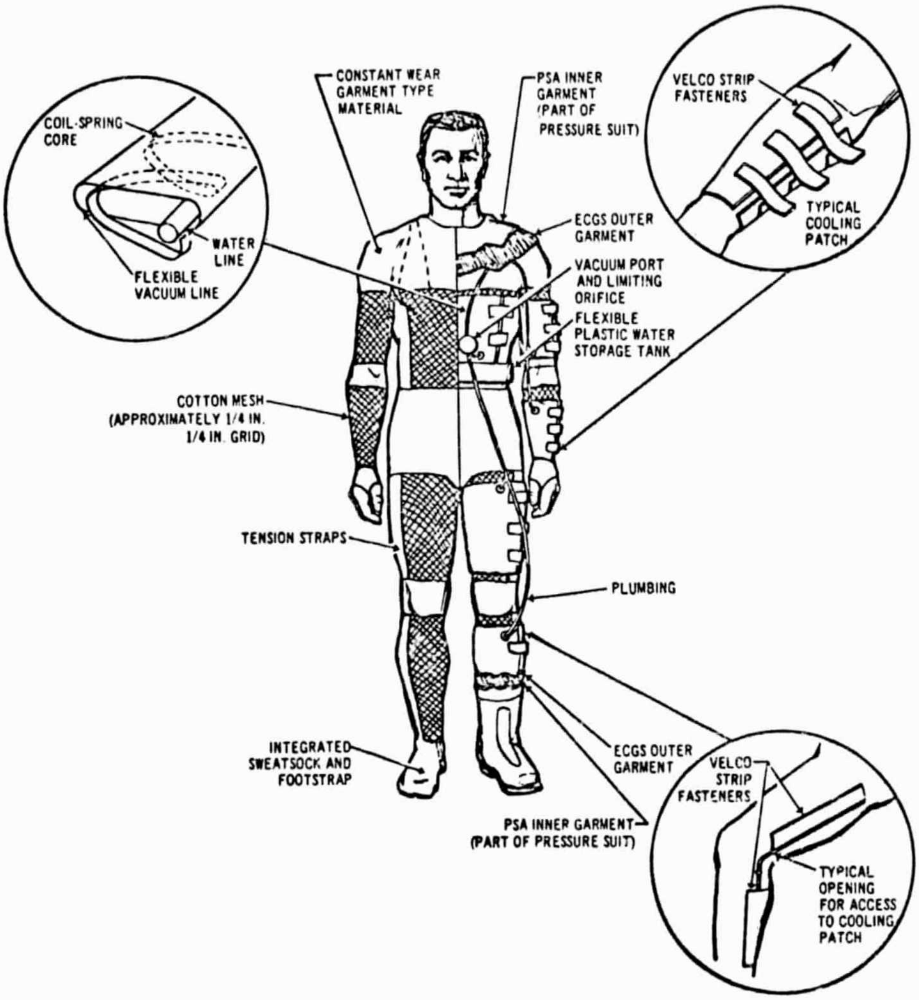

Figure 1. ECGS Suit Cutaway Drawing

regulating water feed rate and steam (heat) removal rate will be located outside the space pressure suit for the first prototype model. Later versions will incorporate all controls on the suit itself.

In operation, the function of the ECGS cooling garment is as follows:

1. Heat is generated in the subject.
2. The water in the cooling patch is heated by conduction from the skin.
3. The pressure in the patch is reduced by exposing the patch vacuum exit to space environment through a throttling valve.
4. The water in the patch boils at a temperature corresponding to the reduced patch internal pressure, carrying off 1,000 Btu of heat for each pound of water vaporized, as "cold" steam.

Patch temperature is controlled by adjusting the vacuum throttling valve which affects patch internal pressure, hence adjusting the boiling temperature of the water. By this means, patch temperature can be adjusted from body temperature down to about the freezing temperature of water. With this wide range of patch temperature adjustment, any conceivable body heat rejection rate can be accomodated at a wide range of skin temperatures. Water which is boiled off from the patch is replenished as required from the water belt reservoir.

PRECEDING PAGE BLANK NOT FILMED.

Section 3
DEVELOPMENT OF ECGS COOLING PATCHES

3.1 ECGS COOLING PATCH AND COMPONENT DESIGN AND FABRICATION

Figure 2 shows a typical ECGS cooling patch. The patch is made up of five basic layers. An inner and outer impermeable membrane, a wicking layer, a boiler void layer, and a reflective foil layer. The inner and outer membranes are sealed together around the edges of the patch to form a vacuum-tight bag. Within this bag are the wicking layer, boiler void, and reflecting foil layers. The wicking layer acts as a small capacity water reservoir and maintains a "wet" contact with the membrane on the skin or cool side of the patch. This wicking layer is attached to a boiler void layer. The boiler void provides a path for the vaporized water to use in leaving the patch. Additional steam collector manifolds are provided between the boiler void and the foil layer to aid in removing steam from the patch and reduce internal flow restrictions. The foil layer acts as a thermal reflector, preventing radiant heat from entering the cooling patch from outside sources thereby preventing unnecessarily high heat loads to the cooling patch.

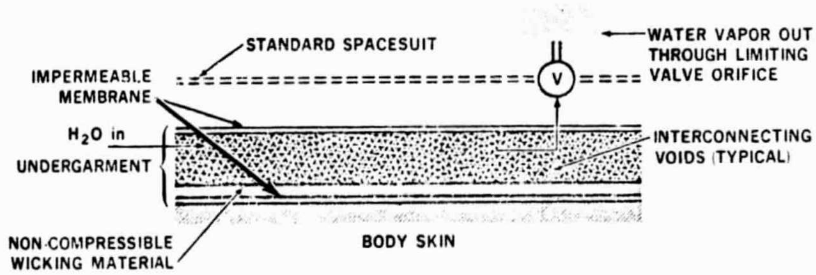

Figure 2. Patch Cross-Section

The cooling patch is fabricated using the Trilock boiler void as a base. The Trilock is cut to the patch shape. The water distribution lines, steam collector manifold lines, and any pressure tap lines are then sewed onto the Trilock. The steam collector manifold lines are made from Spirap, a commercial nylon product used to bundle wire into harnesses. It is a tube made by wrapping nylon strip in a helical pattern onto a rodlike mandrel. For the ECGS application, the Spirap is expanded to leave spaces between the strip of nylon so it resembles a flat wire helical spring. An electrically heated mandrel is used to set the Spirap with the desired "pitch" on the spiral windings. Figure 3 shows a typical piece of Spirap before and after "stretching." This steam collector line is also sewed around the edge of the Trilock to provide a peripheral steam collector and to protect the outer membrane from puncture by the raw Trilock edge. Water distribution lines are 1/16-in. diam PVC tubing. The water distribution lines are all connected to a manifold. The manifold is fed by a single tube which is threaded through the vacuum exhaust fitting. The vacuum exhaust fitting is sewed to the Trilock and all steam collector manifold lines are routed to this central collection point. A cover of 0.020-in.-thick soft PVC sheet is sewed over each steam collector manifold junction and completely around the Spirap on the edge of the patch. This serves two purposes: it protects the outer membrane from abrasion by sharp Spirap ends, and it provides a small pocket to aid steam flow from one steam collector manifold to the other. The next step in patch fabrication is to sew on two layers of wicking material (Dexter Paper No. 195). This is placed on the side opposite the steam collector manifold, vacuum exhaust fitting, and water distribution lines and manifold. The water distribution lines are passed through this wicking layer so they protrude about 1/2 in. The water lines are then sewed down to the wicking to hold them in position. Four layers of wicking paper about 1/2 in. in diameter are then cemented over each water line termination. These provide protection for the remaining wicking, which will cover them, and also a high water storage capacity at each water line termination to aid in water distribution. Two additional layers of wicking are then sewed over the wick side of the patch. A rip-stop-type aluminum foil is then tack stitched to the top (vacuum outlet) side of the patch. The membranes are placed on the top and bottom of the patch; all through connections are made up, and the membranes are heat sealed around the edges of the patch. This completes the fabrication of a typical ECGS cooling patch.

To make a complete patch assembly, a cooling patch, ballonet, and a patch cover are required. The ballonet is simply a plastic bag shaped to match the patch. A small fitting on the top of the ballonet accepts the pressurizing air line. The ballonet is placed between the cooling patch and the outside of the patch cover. The patch cover is made up of two layers of material; an outer fabric, which serves to protect the cooling patch and restrain the ballonet; and an inner layer of nylon mesh, which acts as a perspiration wick and comfort layer. These two layers are sewed together to form a pocket into which the ballonet and cooling patch may be placed. Velcro closing fastenings retain the cooling patch and ballonet once they are in place. Provisions are made for fastening the outer cover fabric to the stretch-type material which joins the patches together. The vacuum outlet and ballonet pressurizing fittings protrude through the outer fabric of the cover where they are accessible for connection to the external plumbing system.

The external plumbing of the ECGS system ducts the steam generated in each patch to a central collecting manifold from which it is ported through a throttling valve to space vacuum. The water supply lines are also routed to each patch through the external vacuum lines. Two types of external vacuum lines were evaluated. One is a built up, flat line made up of 1/4-in. ID Spirap (Figure 4) covered with a plastic membrane. This type of line provides a very low profile while allowing maximum effective flow area. The second type of duct is Penn tube WTF flexible corrugated Teflon tubing. This tubing provides excellent flexibility and is available as off-the-shelf hardware. Preliminary testing of the first type of ducting (plastic covered multiple Spirap) showed that some development work was necessary to obtain good end seals and to provide flexibility at articulated areas. Because of the limited scope of the present program, this development time was not available. The choice, therefore, for the first prototype ECGS system was the Penn tube WTF flexible tubing. Follow-on development of a lower profile ducting will reduce the bulk of the present system and eliminate the necessity of using circular cross-section ducting for the external vacuum lines. The present design, using Penn tube WTF tubing, provides separate 1/2-in. ID ducts from each patch vacuum exit fitting to the collector manifold.

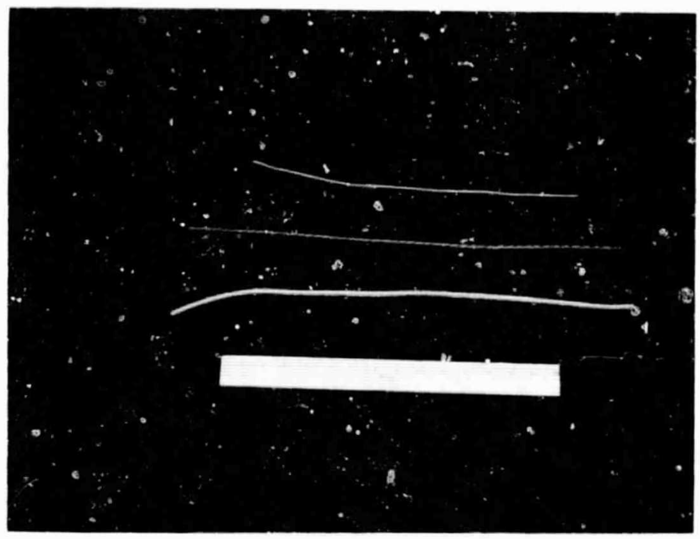

Figure 3. Spirapsteam Line - "Stretched" and As-received Condition

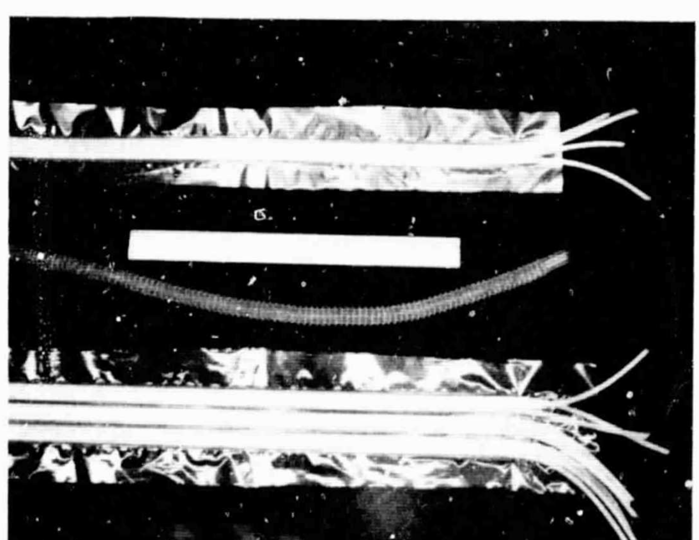

Figure 4. External Plumbing-Line Configurations

The patch vacuum exit fitting is shown in Figure 5. The vacuum exit fitting is designed to seal to the patch membrane with two soft rubber washers which are compressed by the fitting base and a washer with the clamping nut. The external vacuum line is connected to the fitting by slipping the vacuum line over the fitting exit and clamping it in place.

3.2 PREDICTED PATCH PERFORMANCE

An analysis was made to determine the limitations on patch performance inherent in the basic design and to size the external vacuum lines. The results of this analysis showed that heat removal rates would be obtained which far surpass the required 5,000 Btu/hr for a complete suit. External vacuum line plumbing layout was estimated and preliminary line sizes were developed. The complete analysis is included in Appendix A.

The flow characteristics were calculated for two different types of Trilock boiler void materials. Tests were run using air at low pressure, to determine the pressure drop characteristics of each material. The data was reduced to Reynolds' number and friction factor form and is shown in Figure 6. The method of data analysis is shown in Appendix B.

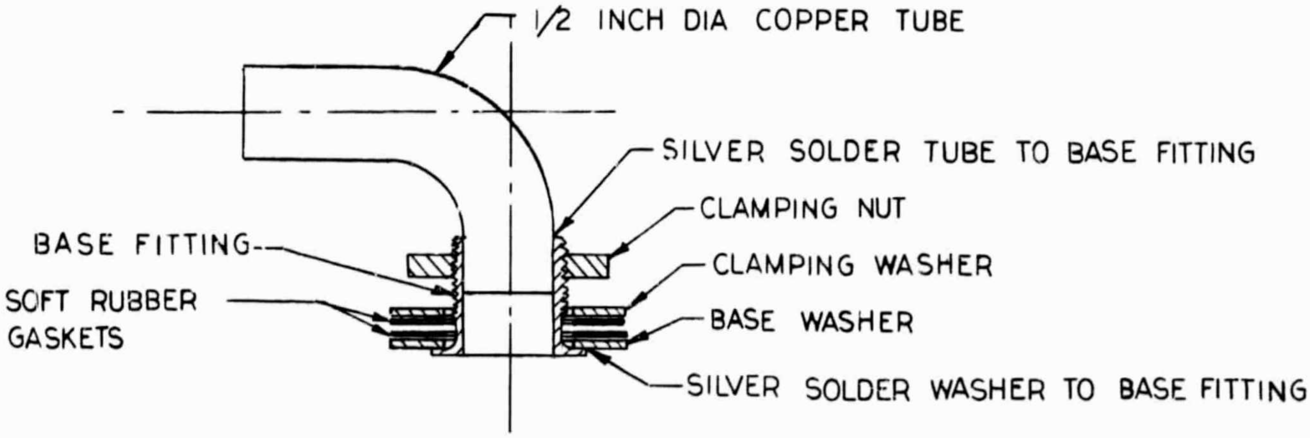

Figure 5. ECGS Patch Exit Vacuum Fitting

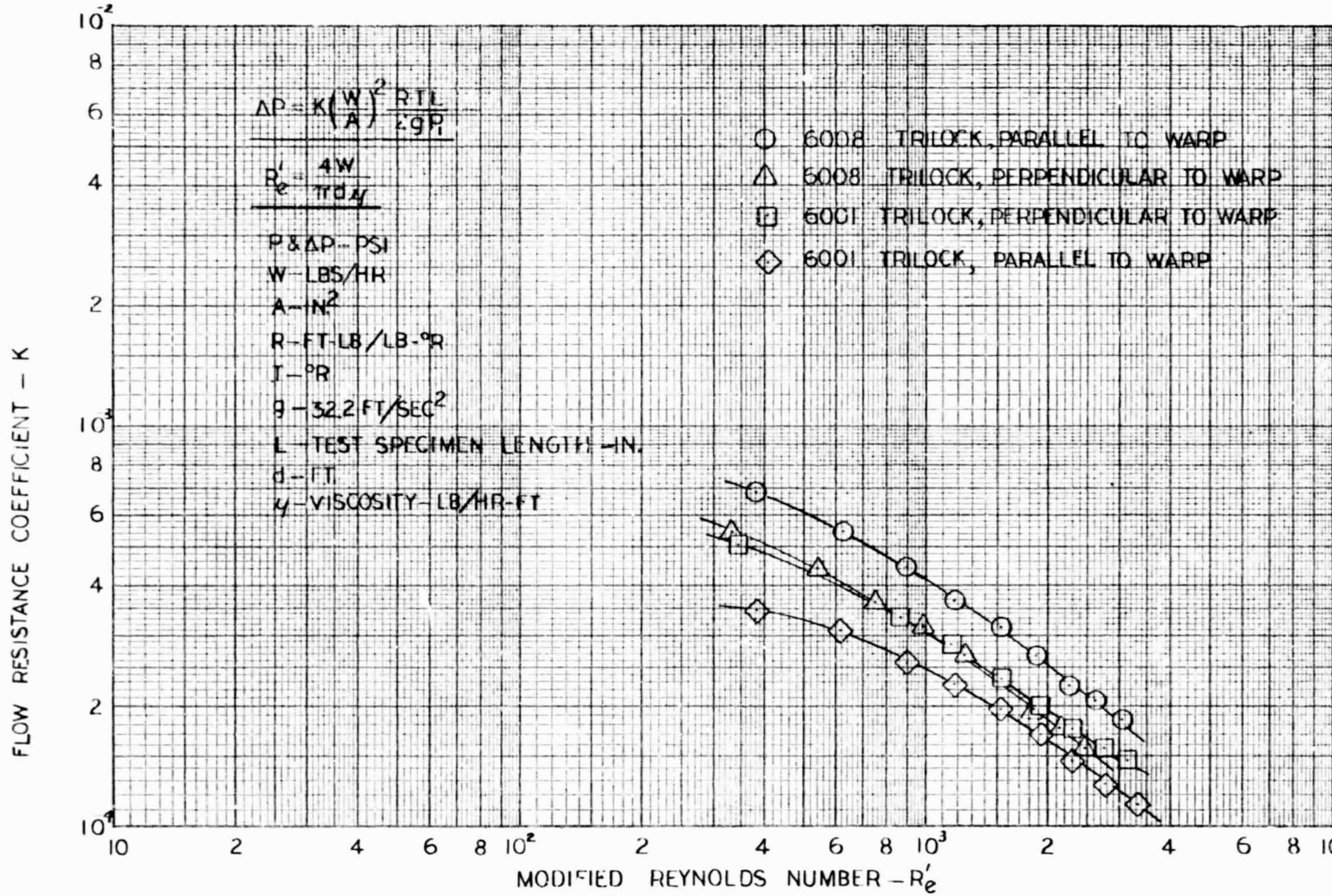

Figure 6. ECGS Boiler Void Pressure Drop Characteristics

3.3 WICKING MATERIAL TESTS

Tests were performed to evaluate several candidate materials for use in the cooling patch wicking layer. The characteristics measured included wicking flow rate and dry wicking rate at a range of simulated external patch pressures and for several layers of material. The results of these tests indicated that Dexter Paper No. 195 was satisfactory for the proposed use.

The tests were run in a setup which closely simulated the conditions to which the wicking material would be exposed in actual patch operation. A typical wicking material test in progress is shown in Figure 7. The test setup consisted of a 1-in.-wide by 15-in.-long test sample supported by a plastic sheet. On top of the sample was a layer of Trilock and on top of the Trilock was a plastic balloon. This whole assembly was retained inside a rigid plastic enclosure. The balloon was inflated through a pressure regulator to simulate the external pressure which an actual patch would encounter in operation. Water was supplied

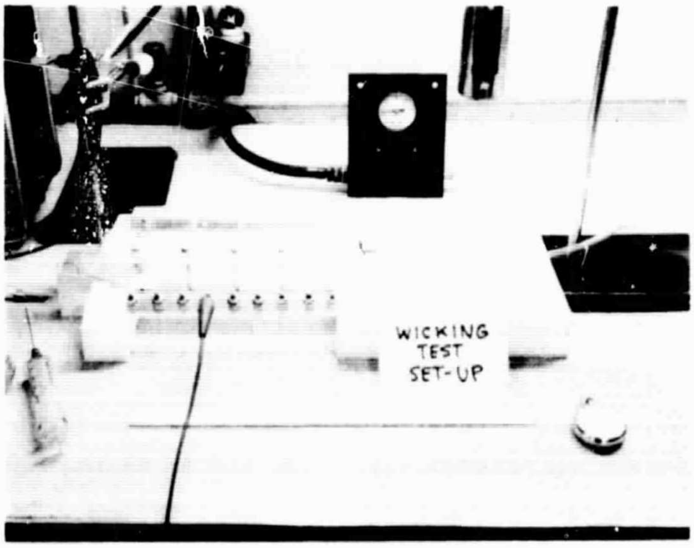

Figure 7. Wicking-Material Test Set-up

to the wick from an open vessel with the water level approximately 1 in. below the level of the wick test sample. The end of the sample was immersed in the water and allowed to soak there. The other end of the sample, where it comes out of the test rig, was held in close contact with a large (12 by 12 in.) piece of wicking material. The large wicking "patch" acts as a water reservoir. To ensure a constant water reservoir in the large patch, a blower is used to accelerate water evaporation from the reservoir patch.

The dry wicking rate tests were conducted by placing a dry test sample into the test rig with one end in the water supply vessel. The position of the wet "front" was noted at several times as it progressed down the test strip. From this data, the wetting rate could be plotted as inches versus time.

The wet wicking flow rate tests were conducted by placing a test sample in the rig, allowing it to saturate throughout its length, and placing the "downstream" end of the sample on a 12-by-12 in. wick reservoir which was force evaporated with a blower. The quantity of water removed from the supply vessel vs. time was recorded to obtain curves of water volume versus time.

The materials which were tested for wicking characteristics are listed in Table I. These materials include both paper and woven fabrics. All materials were tested in the as-received condition with one exception as noted in Table I. Test samples 1 in. wide and 15 in. long were cut from each material. One sample was used for only one test. Subsequent tests on the same material used a new test sample.

The results of the wicking material tests are summarized in Figures 8 through 11. These figures show the average wicking rate per unit flow cross-section of wick sample. Data for material No. 1 is shown at 3.7 and 18.4 psi pressure in Figures 12 through 15. These pressures correspond to actual operating pressures. The data were obtained to provide more complete documentation on the material which appeared most suitable for ECGS patch application. This material was selected for use in the delivery cooling garment because of its excellent wet strength, superior wicking rate, and low linting characteristics.

Table I

MATERIALS TESTED FOR ECGS WICKING APPLICATION

Material Number	Number and/or Description	Thickness (In.)	Manufacturer
1	No. 193	0.0042	C. H. Dexter & Sons, Inc. 1 Elm Street Windsor Locks, Connecticut
2	No. 232	0.0033	C. H. Dexter & Sons, Inc. 1 Elm Street Windsor Locks, Connecticut
3	No. 17V	0.0032	C. H. Dexter & Sons, Inc. 1 Elm Street Windsor Locks, Connecticut
4	No. 10	0.0025	C. H. Dexter & Sons, Inc. 1 Elm Street Windsor Locks, Connecticut
5	Fiberglas Flake Paper (F-5) Specification	0.0045	Owens-Corning
6	Marquisette Non-Textured Beta Fiber	0.0043	NASA Furnished
7	Unbonded AA Beta Fiber	0.025	Owens-Corning
8	Double Knit Orlon	0.043	--
9	Knit Cotton	0.0215	--
10	Hollow Glass Roving 20 End	0.012	Pittsburg Plate Glass Co. Fiberglass Division Shelbyville, Indiana
11	Handi-Wipes-Rayon Fiber Towel	0.013	Colgate-Palmolive Co. New York, New York
12	Electro Phoresis Paper	0.0096	--
13	Filter Paper No. 54	0.0085	W. R. Balston, Ltd.
14	4-Ply Superwipes	0.0130	Borg Products
15	Cotton Fiber Pads	0.037	--

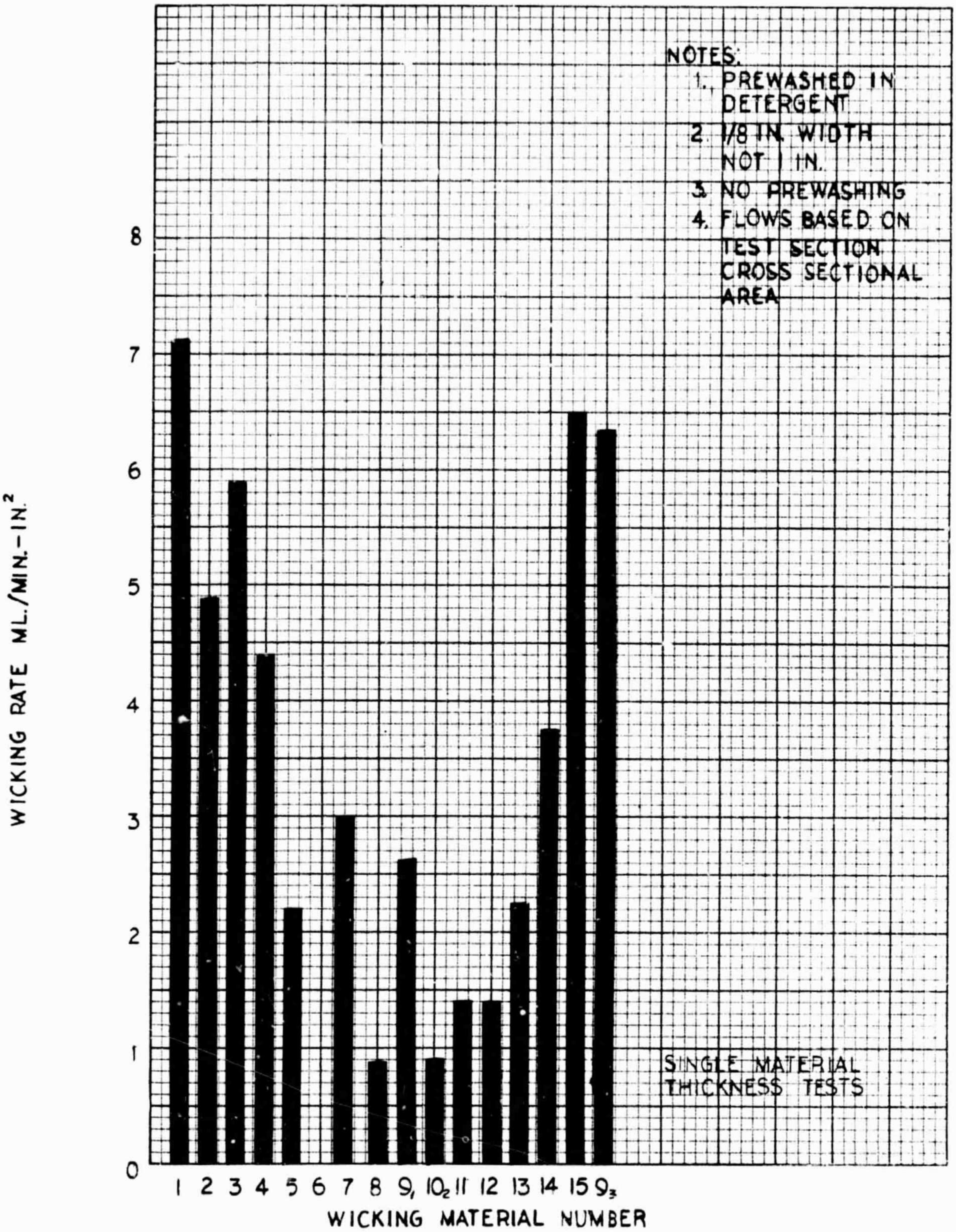

Figure 8. Wet-Wicking Flow Rate at 0 psi

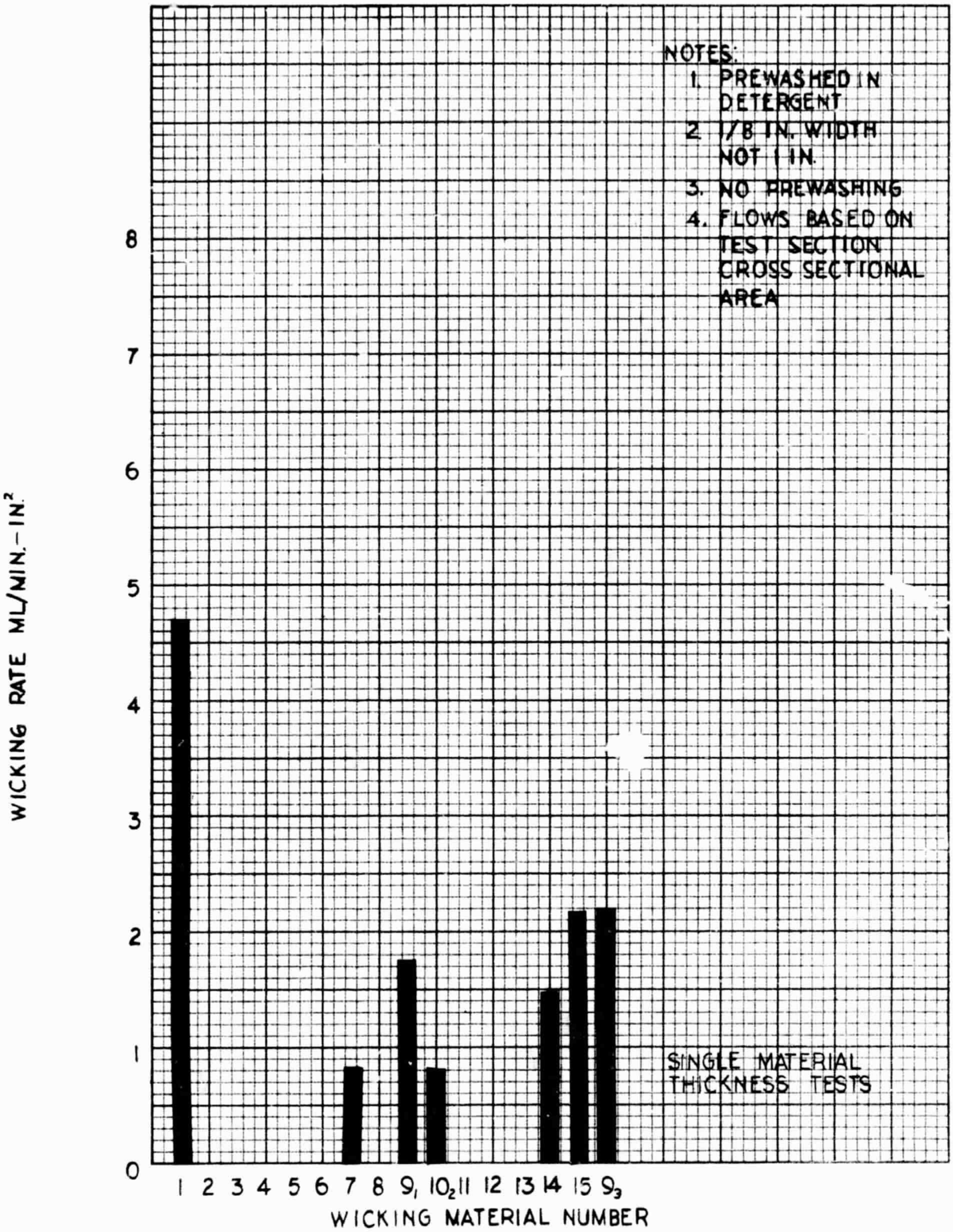

Figure 9. Wet-Wicking Flow Rate at 5 psi

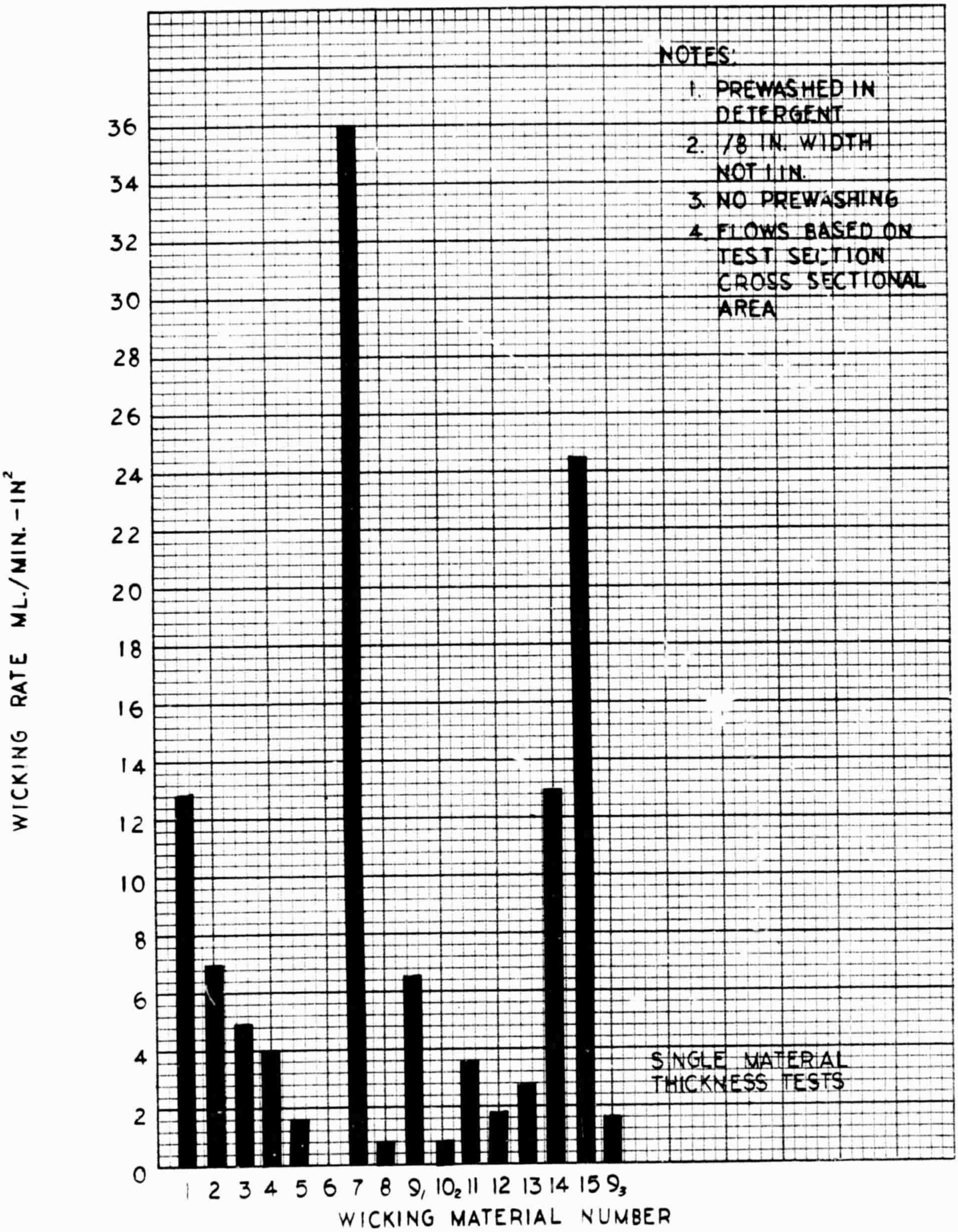

Figure 10. Average Dry-Wicking Rate at 0 psi

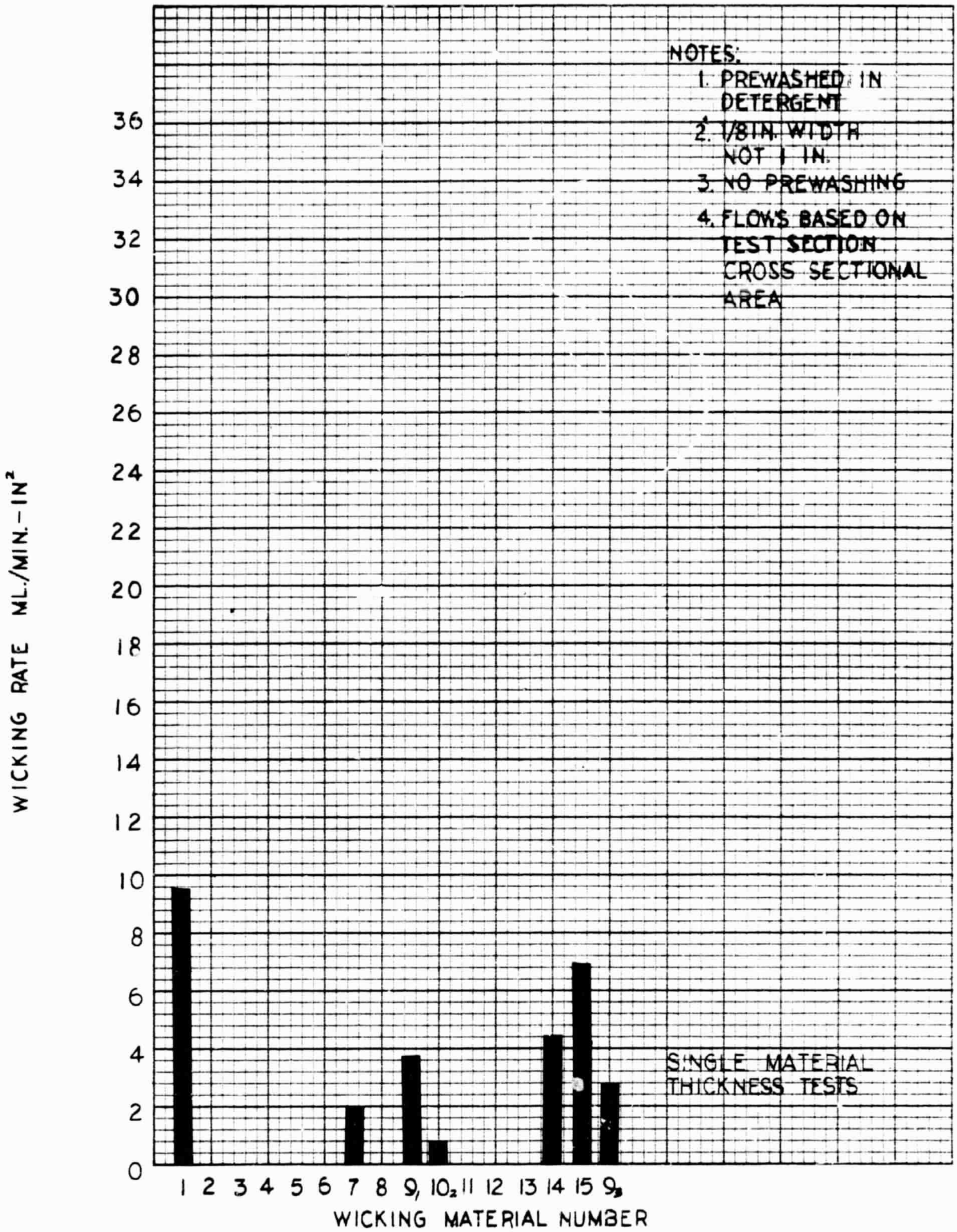

Figure 11. Average Dry-Wicking Rate at 5 psi

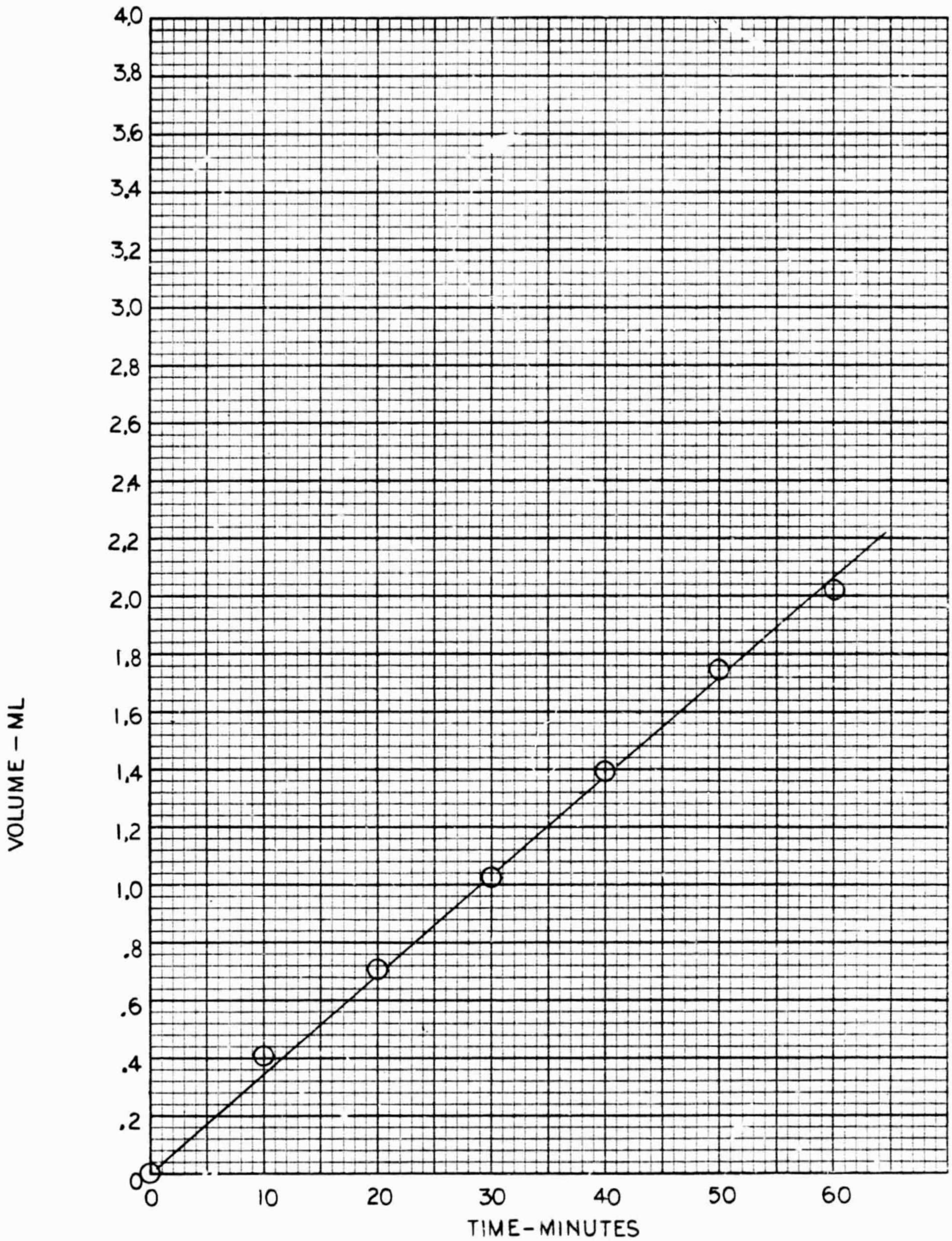

Figure 12. Wet-Wicking Flow Rate - Material No. 1 - 3.7 psi

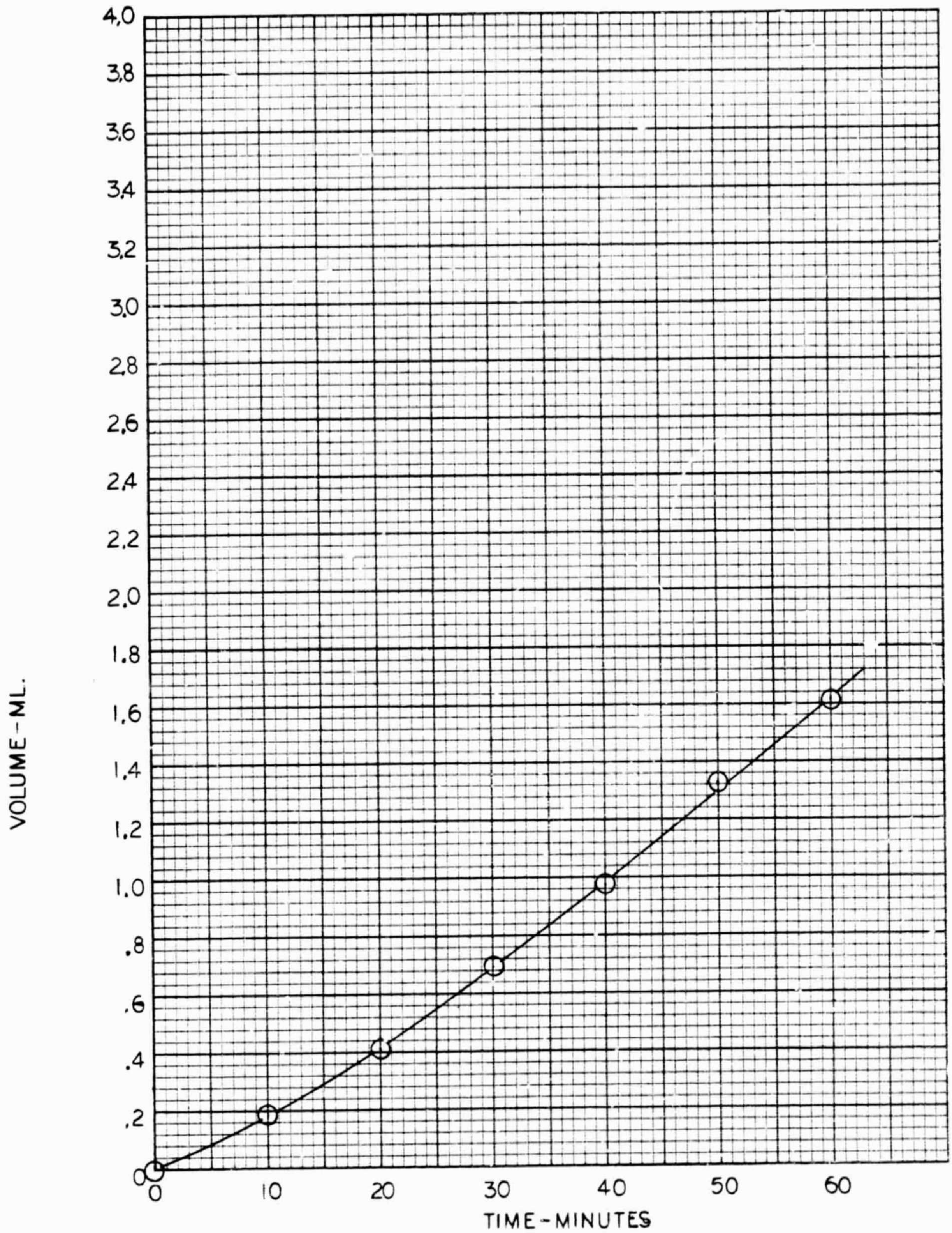

Figure 13. Wet-Wicking Flow Rate - Material No. 1 - 18.4 psi

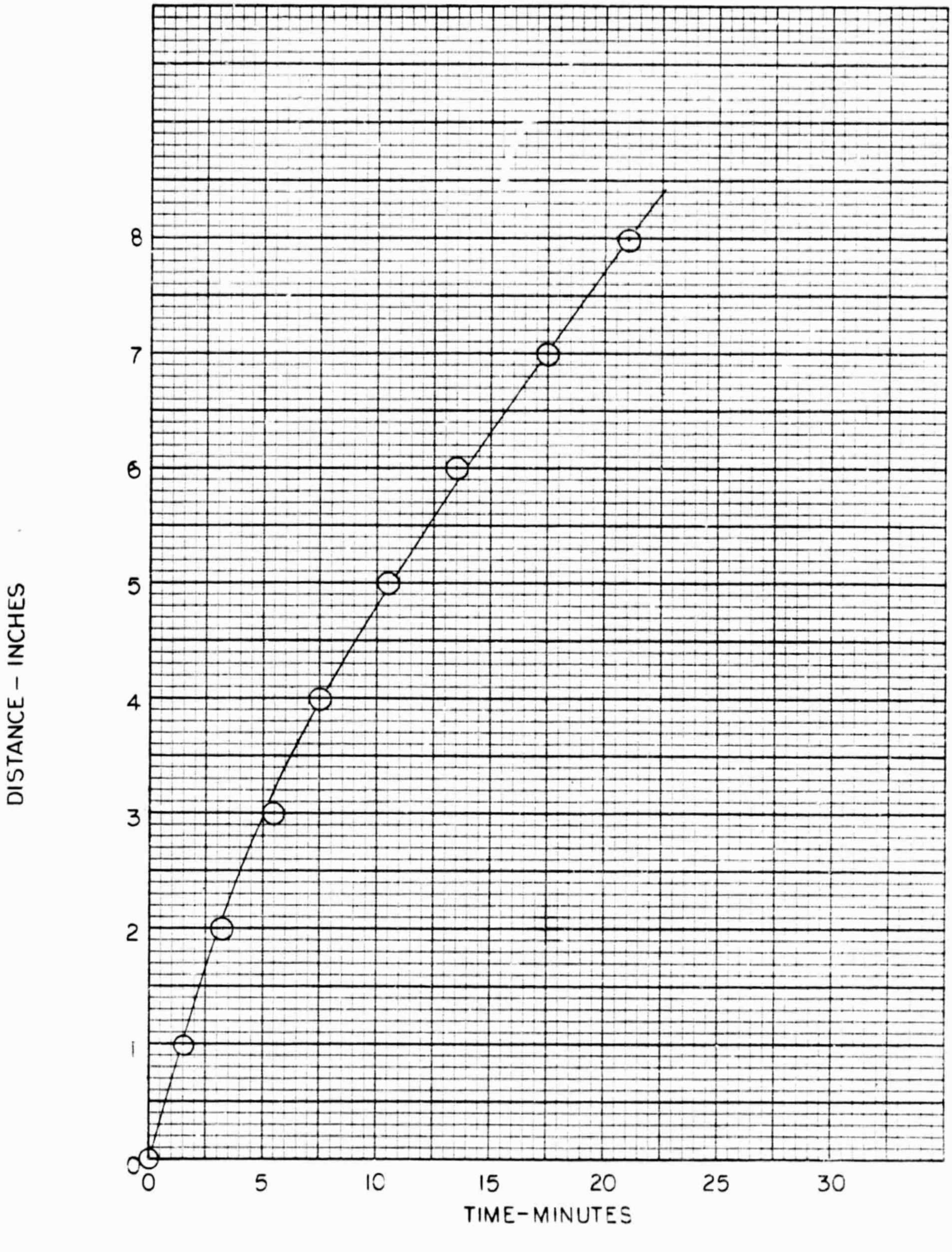

Figure 14. Dry-Wicking Rate - Material No. 1 - 3.7 psi

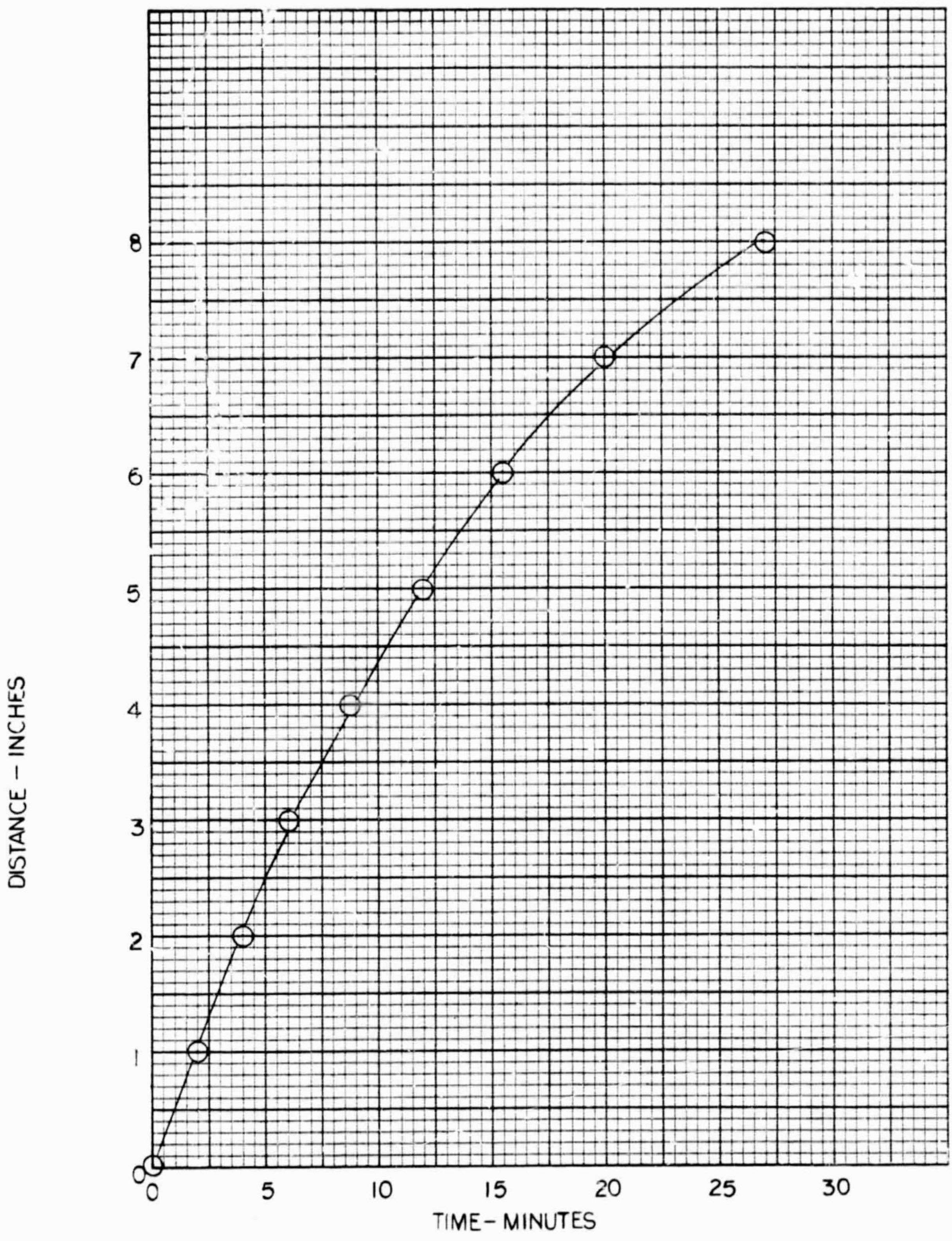

Figure 15. Dry-Wicking Rate - Material No. 1 - 18.4 psi

3.4 BOILER VOID ΔP TESTS

A series of tests was performed to determine the local pressure drop characteristics of two candidate boiler void materials. The tests were conducted using air at ambient temperature as the test fluid. The material to be evaluated was cut to a 6-in.-square shape and enclosed in a plastic envelope. Inlet and outlet manifolds of 1/4-in. Spirap were provided to distribute the flow uniformly across the test section. A photograph of a typical boiler void test section is shown in Figure 16. Instrumentation was provided to measure pressure at the inlet to the test section, differential pressure across the test section, and air flow rate. A throttling valve was included at the inlet and exit of the test section. The exit of the downstream valve was ported to the ECGS laboratory vacuum system. The test setup is shown schematically in Figure 17.

The tests were run by flowing air through the test section at a range of subatmospheric pressures. Pressure differential across the test section and air flow rate were measured. Reynolds number and flow resistance coefficient were calculated from the test data. Tests were run for flow both parallel and perpendicular to the warp of the material. Figure 6 shows the results of these tests. The method of data reduction and analysis is given in Appendix B. The most suitable boiler void material, based on the test data, is Trilock No. 6001-1. This material was used in all subsequent ECGS cooling patches.

3.5 INDIVIDUAL PATCH TESTS

All cooling patch tests were run in the ECGS laboratory. This laboratory is equipped with a large vacuum system, capable of simulating space vacuum pressure at the exit of the ECGS vent system. Ample space is available in the laboratory for full space pressure suit storage, assembly, and testing in conjunction with the ECGS cooling garment. A treadmill and bicycle ergometer are available for generating the required metabolic rates to simulate the anticipated work loads astronauts may encounter during EVA or IVA while wearing a space pressure suit. Two methods of raising metabolic rate were used in the tests which have been performed on ECGS patches to date. These are treadmill walking/running and forearm exercise.

Figure 16. Boiler Void Pressure-Drop Test Specimen

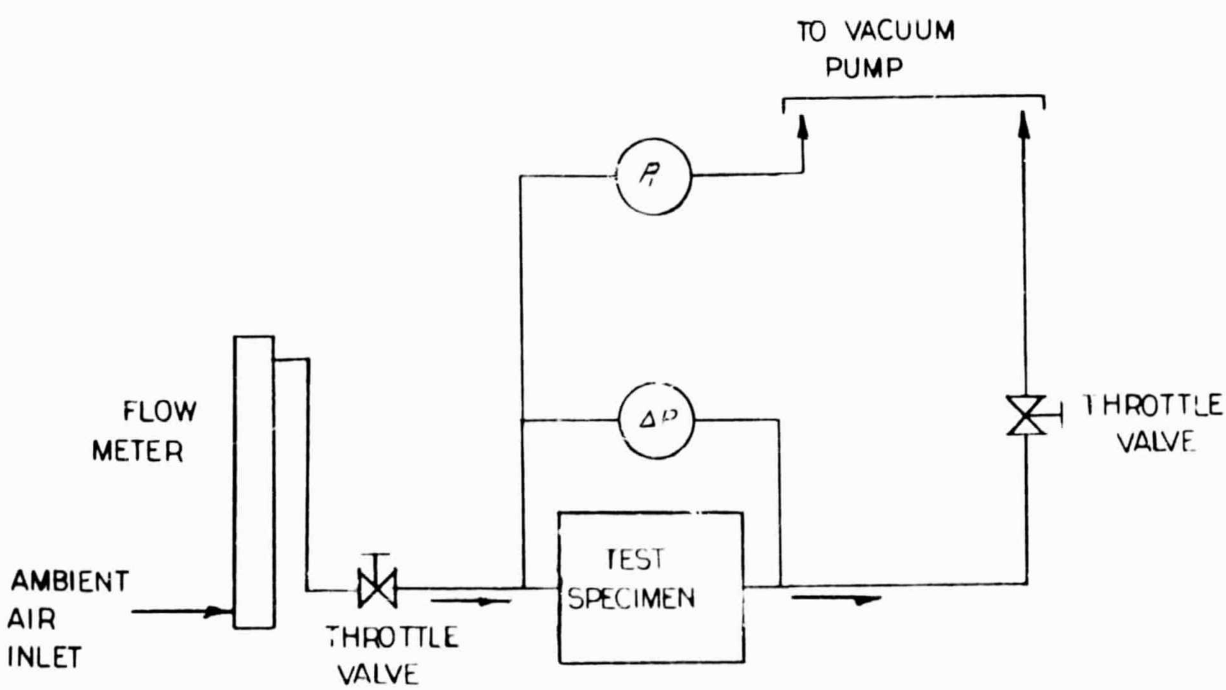

Figure 17. Boiler Void Test Set Up Schematic

Treadmill operation is quite straightforward. A preselected speed and grade are set and the subject walks/runs at these fixed conditions. Available test data from other sources provide a good correlation between treadmill speed and grade and test subject metabolic rate.

The forearm exercise was accomplished using a squeeze bulb similar to that used to inflate a blood pressure cuff. A schematic of this system is shown in Figure 18. In operation, the forearm exercise system requires the subject to squeeze the bulb at such a rate that a constant pressure is maintained in the accumulator. A valve in the accumulator exit line regulates the air flow. The flow is measured by a flowmeter downstream of the flow regulating valve.

The exercise rate can be controlled by changing the pressure or flow rate. When using this form of exercise, the subject is seated upright with the hand and arm which is exercising supported in a specific position. With this restriction of position and the flow and pressure measurements, a very repeatable exercise rate can be accomplished.

Primary test instrumentation measured skin temperature under the test patch, pressure inside the patch, and run time. Secondary data included patch weight before and after a run, and vacuum system manifold pressure. All patch variables were recorded on an analog data system (ADS).

The ADS is shown schematically in Figure 19. This system provides analog recording on an oscillograph of up to 30 thermistor temperature readings and up to 40 pressure readings. In addition, five channels of strain-gage-type instruments can be monitored. The temperature measuring capability is obtained by sequentially scanning up to 30 thermistor inputs. The scanning rate is limited to 30/min in order to get readable oscillograph records. Two channels of thermistor data are continuously monitored and visual readout is provided for these two channels. The pressure measuring capability of this data system is obtained by sequentially scanning up to 48 individual pressure inputs by using a scannivalve. This scannivalve sequentially ports the pressures to a single strain gage transducer.

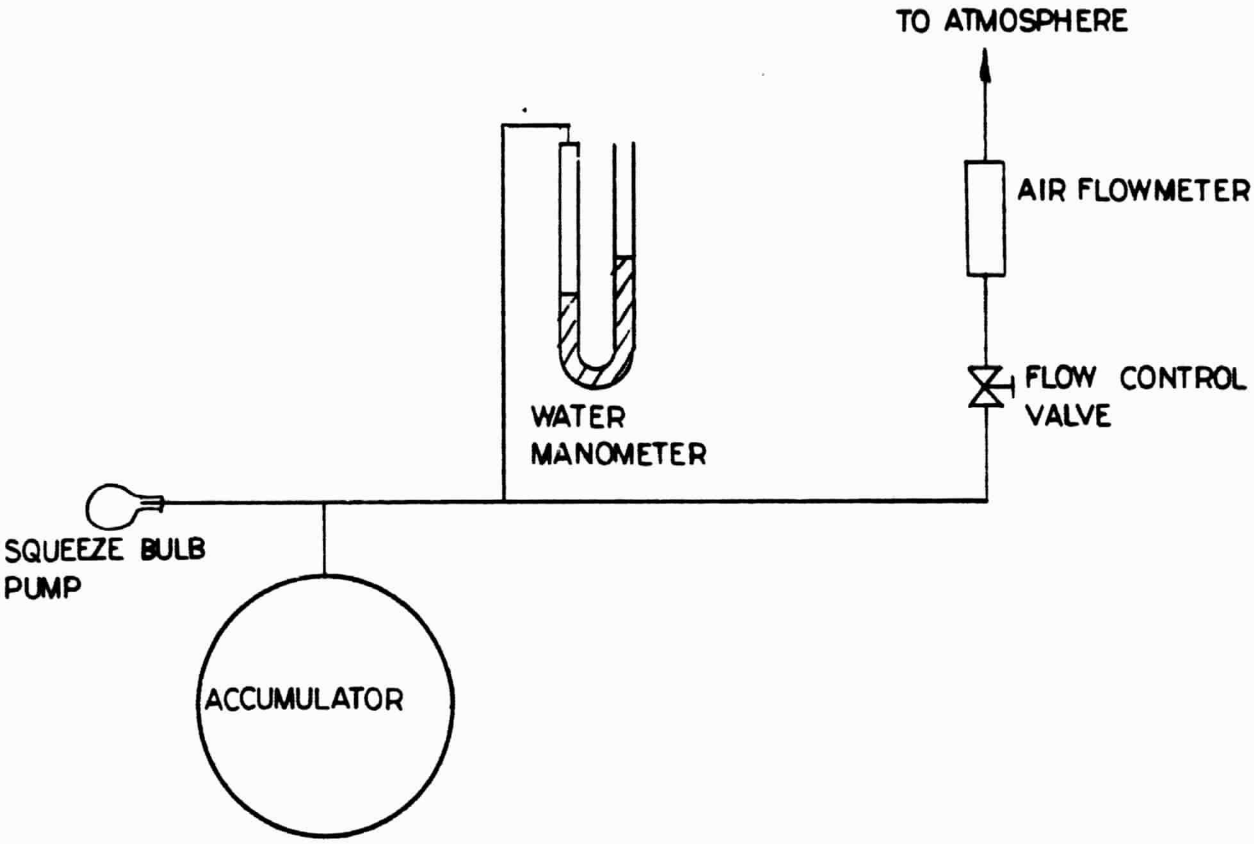

Figure 18. ECGS Forearm Exercise System

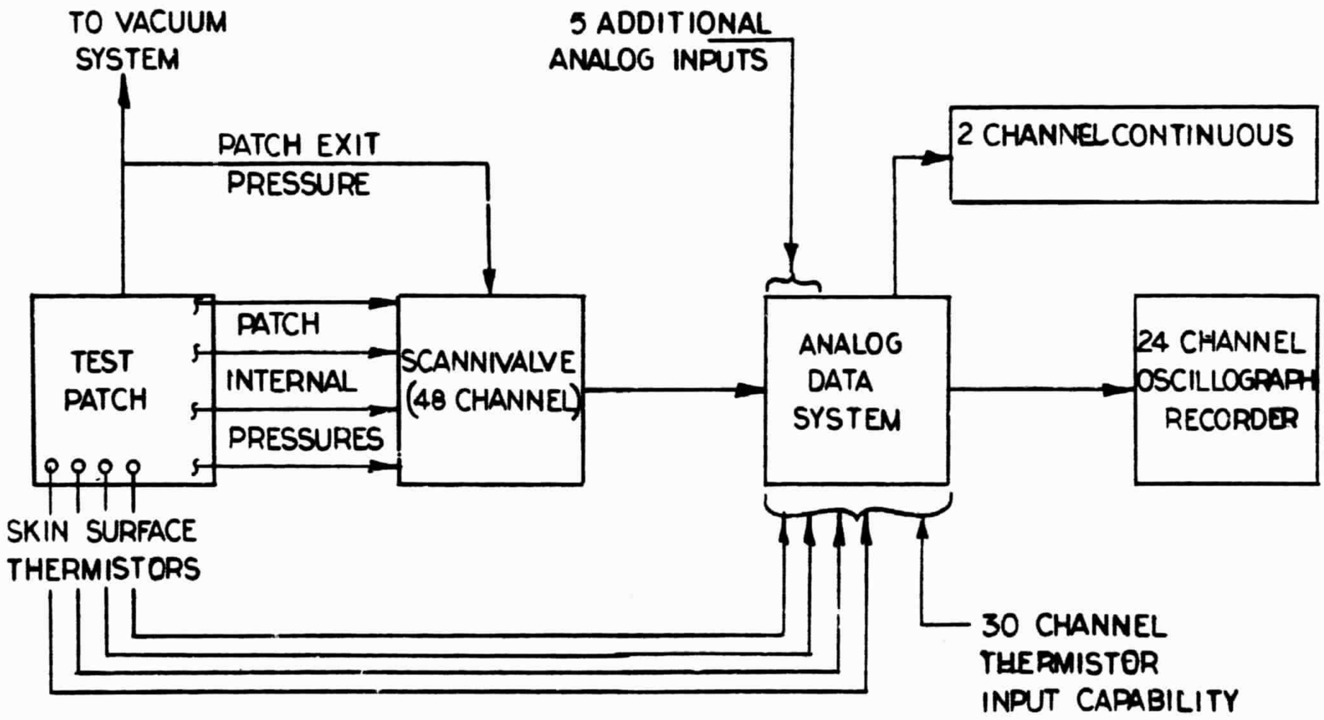

Figure 19. Analog Data System Schematic

The procedure used to test individual patches was as follows, with minor modifications as required for specific tests:

1. Fill patch with water.

2. Weigh patch and record weight.

3. Apply thermistors to test subject.

4. Install patch on test subject and attach patch vacuum and instrumentation line.

5. Operate patch and record data (subject may or may not be exercised depending on run requirements).

Table II lists all individual patch test runs during the Task 2 effort. These tests covered a wide range of variables and as such some served more than one purpose. A brief discussion of the overall test program is presented in the following paragraphs.

The first test series (runs 301 to 304) was run to obtain skin temperature time history data to use as a comparison with future cooling patch data. These runs were made both with and without a lower right arm patch in place to determine the effect of the inactive patch on skin temperature. Data from these tests are shown in Figures 20 through 23. It can be seen that the inactive patch causes the skin temperature to rise higher than when the forearm is exercised without any covering.

A run was made to investigate the effect on blood biochemistry of exercise, fatigue, and local overheating of the forearm. This work was carried out with IRAD funds as a parallel study which might have relevance to the ECGS program. A detailed discussion of this program is included in Appendix C.

Another series of runs (308 to 310) was made to obtain data on forearm temperature while the forearm was being cooled with an ECGS patch. Forearm exercise was included to show what effect it may have on the patch cooling characteristics. Data from these runs (Figures 24, 25, and 26) show that the cooling capability of the patch far exceeds the heat generated locally by the exercise.

Table II

PATCH TEST RUN SUMMARY (page 1 of 6)

Run Number	Date	Maximum Q Patch (Btu/hr)	Run Time (minutes)	Patch Location	Minimum Skin Temperature (°F)	Subject	Remarks
301	9/12/67	0	82.8	Lwr. Rt. Arm	94.5 (max)	E.H.	Temp. profile w/hand exercise
302	9/13/67	0	71.2	No Patch	94.9 (max)	D.C.	Temp. profile w/hand exercise
303	9/13/67	0	145.8	Lwr. Rt. Arm	99.1 (max)	E.H.	Temp. profile w/hand exercise
304	9/18/67	0	188.3	Lwr. Rt. Arm	98.2 (max)	E.H.	Temp. profile w/hand exercise
306	9/21/67	0	176.0	Lwr. Rt. Arm	100.1 (max)	E.H.	Blood Chem./Exercise correlation
308	9/29/67	-	15.0	Lwr. Rt. Arm	72.5	J.B.	Initial cooling w/hand exercise
309	9/29/67	-	45.0	Lwr. Rt. Arm	63.5	G.J.	Cooling w/hand exercise
310	10/2/67	-	71.2	Lwr. Rt. Arm	65.7	J.B.	Cooling w/hand exercise
311	10/11/67	-	15.0	Upper Rt. Arm	--	E.H.	Bad press. data
312	10/13/67	-	--	Upper Rt. Arm	--	D.G.	Bad press. data
313	10/13/67	-	11.0	Upper Lt. Arm	74.0	D.G.	Spiwrap size eval. - no exercise
314	10/13/67	-	12.5	Upper Rt. Arm	70.0	D.G.	Spiwrap size eval. - no exercise
315	10/13/67	-	102.0	Lwr. Rt. Arm	75.5	E.H.	1st attempt to control Q w/exercise
316	10/16/67	-	26.5	Partial Torso	60.7	E.H.	Torso cooling - no exercise
317	10/18/67	189.0	9.0	Upper Rt. Arm	70.5	D.G.	Spiwrap size eval. - no exercise
318	10/18/67	149.0	10.5	Upper Lt. Arm	72.0	D.G.	Spiwrap size eval. - no exercise
319	10/18/67	171.0	9.0	Upper Lt. Arm	83.0	E.H.	Treadmill 7.65 mph
320	10/26/67	67.0	46.0	Upper Rt. Arm	67.5	J.B.	Cooling - no exercise - fixed Q
321	10/27/67	67.6	43.3	Upper Rt. Arm	66.0	J.B.	Cooling - no exercise - fixed Q
322	10/27/67	125.0	21.5	Upper Rt. Arm	57.3	J.B.	Cooling - no exercise - fixed Q
323	10/27/67	174.0	11.2	Upper Rt. Arm	61.5	J.B.	Cooling - no exercise - fixed Q
324	10/30/67	153.0	11.0	Upper Rt. Arm	69.7	J.B.	Cooling - no exercise - fixed Q
325	10/30/67	265.0	3.5	Upper Rt. Arm	74.0	J.B.	Cooling - no exercise - fixed Q
326	10/30/67	302.0	3.0	Upper Rt. Arm	76.6	J.B.	Cooling - no exercise - fixed Q
327	10/30/67	337.0	1.9	Upper Rt. Arm	80.0	J.B.	Cooling - no exercise - fixed Q
328	10/30/67	136.0 avg.	10.0	Upper Rt. Arm	64.6	J.B.	Max. Cooling - no exercise - max. Q

Table II (page 2 of 6)

Run Number	Date	Maximum Q Patch (Btu/hr)	Run Time (minutes)	Patch Location	Minimum Skin Temperature (^oF)	Subject	Remarks
329	11/10/67	--	--	Upper Rt. Arm	--	--	Bad run - patch leaking air
330	11/10/67	73.1	42.0	Upper Lt. Arm	59.7	S.Z.	Cooling - no exercise - fixed Q
331	11/14/67	194.8	9.6	Upper Rt. Arm	56.9	S.Z.	Cooling - no exercise - fixed Q
332	11/15/67	269.0	3.3	Upper Rt. Arm	69.5	S.Z.	Cooling - no exercise - fixed Q
333	11/15/67	423.0	1.2	Upper Rt. Arm	77.0	S.Z.	Cooling - no exercise - fixed Q
334	11/16/67	150.0	19.0	Upper Rt. Arm	53.5	S.Z.	Water added during run Cooling - no exercise - fixed Q
335	11/16/67	66.7	73.0	Upper Rt. Arm	55.7	S.Z.	Water added during run Cooling - no exercise - fixed Q
336	11/22/67	588.0	3.4	Lwr. Lt. Leg	74.7	S.Z.	Cooling - no exercise - fixed Q
337	11/22/67	145.0	9.3	Upper Rt. Arm	71.4	S.Z.	Cooling - no exercise - fixed Q
338	11/22/67	294.0	1.7	Upper Rt. Arm	80.2	S.Z.	Cooling - no exercise - fixed Q
339	11/22/67	129.2 133.0	6.0 6.0	 Upper Rt. Arm	69.5 65.1	S.Z. S.Z.	Cooling - no exercise - fixed Q Cooling w/exercise at 1200 BTU/Hr.
340	11/28/67	162.0	5.6	Upper Rt. Arm	78.1	S.Z.	Cooling w/exercise - 1200 BTU/Hr.
341	11/28/67	173.0	5.9	Upper Rt. Arm	72.6	S.Z.	Cooling following exercise at 1200 BTU/Hr.
342	11/29/67	160.0	8.4	Upper Rt. Arm	70.4	S.Z.	Cooling w/exercise - 1600 BTU/Hr.
343	11/29/67	107.0	27.5	Upper Rt. Arm	62.2	S.Z.	Cooling w/exercise - 1600 BTU/Hr.
344	11/28/67	134.0	16.9	Upper Rt. Arm	56.5	S.Z.	"Zero" ballonet press. Cooling - no exercise - fixed Q
345	11/29/67	--	19.5	Upper Rt. Arm	63.9	J.B.	Cooling w/exercise - 1600 BTU/Hr.
346	11/29/67	175.0	8.7	Upper Rt. Arm	68.5	J.B.	Cooling - no exercise - fixed Q
347	12/1/67	238.0	4.0	Upper Rt. Arm	79.2	S.Z.	"Zero" ballonet press. Cooling - no exercise - fixed Q
348	12/1/67	192.0	6.4	Upper Rt. Arm	71.8	S.Z.	Cooling - no exercise - fixed Q
349	12/1/67	168.0	6.8	Upper Rt. Arm	70.0	S.Z.	Cooling - no exercise - fixed Q

Table II (page 3 of 6)

Run Number	Date	Maximum Q Patch (Btu/hr)	Run Time (minutes)	Patch Location	Minimum Skin Temperature (°F)	Subject	Remarks
350	12/4/67	363.0	2.2	Upper Rt. Arm	79.1	S.Z.	Cooling - no exercise - fixed Q
351	12/4/67	--	2.0	Lwr. Lt. Leg	80.8	S.Z.	*Vascular monitoring
352	12/4/67	320.0	1.2	Upper Rt. Arm	81.0	S.Z.	Cooling - no exercise - fixed Q
353	12/4/67	175.0	6.0	Upper Rt. Arm	72.2	S.Z.	Insulated Patch Test
354	12/4/67	125.6	14.4	Upper Rt. Arm	59.9	S.Z.	Insulated Patch Test
355	12/5/67	484.0	1.4	Lwr. Lt. Leg	80.9	S.Z.	*Vascular monitoring
355A	12/5/67	425.0	1.4	Lwr. Lt. Leg	78.8	S.Z.	*Vascular monitoring
356	12/5/67	346.0	5.0	Lwr. Lt. Leg	67.0	S.Z.	Cooling - no exercise - fixed Q
357	12/5/67	--	--	Lwr. Lt. Leg	--	J.B.	Bad data - press. line off
358	12/5/67	287.0	5.5	Lwr. Lt. Leg	68.0	J.B.	Cooling - no exercise - fixed Q
358A	12/5/67	341.0	3.5	Lwr. Lt. Leg	72.0	J.B.	Cooling - no exercise - fixed Q
358B	12/5/67	234.0	6.5	Lwr. Lt. Leg	66.8	J.B.	Cooling - no exercise - fixed Q
358C	12/5/67	439.0	2.1	Lwr. Lt. Leg	71.8	J.B.	Cooling - no exercise - fixed Q
358D	12/5/67	186.0	17.1	Lwr. Lt. Leg	67.5	J.B.	Cooling - no exercise - fixed Q
359	12/6/67	217.0	12.0	Lwr. Lt. Leg	63.2	J.B.	Cooling - no exercise - fixed Q
359A	12/6/67	240.0	10.5	Lwr. Lt. Leg	64.0	J.B.	Cooling - no exercise - fixed Q
359B	12/6/67	235.0	12.3	Lwr. Lt. Leg	61.7	J.B.	Cooling - no exercise - fixed Q
359C	12/6/67	243.0	12.0	Lwr. Lt. Leg	60.9	J.B.	Cooling - no exercise - fixed Q
359D	12/6/67	347.0	5.9	Lwr. Lt. Leg	66.8	J.B.	Cooling - no exercise - fixed Q
359E	12/6/67	382.0	5.0	Lwr. Lt. Leg	69.8	J.B.	Cooling - no exercise - fixed Q
359F	12/6/67	165.0	23.5	Lwr. Lt. Leg	66.3	J.B.	Cooling - no exercise - fixed Q
360	12/6/67	425.0	4.3	Lwr. Lt. Leg	70.9	J.B.	Ballonet eval. P_{BAL} = 20" H_2O
360A	12/6/67	266.0	13.0	Lwr. Lt. Leg	63.8	J.B.	Bad data - leak
360B	12/6/67	282.0	9.9	Lwr. Lt. Leg	62.6	J.B.	Ballonet eval. P_{BAL} = 20" H_2O
360C	12/6/67	272.0	4.7	Lwr. Lt. Leg	69.6	J.B.	Ballonet eval. P_{BAL} = 0" H_2O

Table II (page 4 of 6)

Run Number	Date	Maximum Q Patch (Btu/hr)	Run Time (minutes)	Patch Location	Minimum Skin Temperature (°F)	Subject	Remarks
360D	12/6/67	345.0	3.1	Lwr. Lt. Leg	73.7	J.B.	Ballonet eval. P_{BAL} = 0" H_2O
360E	12/6/67	381.0	2.2	Lwr. Lt. Leg	75.0	J.B.	Ballonet eval. P_{BAL} = 0" H_2O
360F	12/6/67	205.0	12.5	Lwr. Lt. Leg	66.4	J.B.	Ballonet eval. P_{BAL} = 0" H_2O
360G	12/6/67	501.0	1.3	Lwr. Lt. Leg	81.0	J.B.	Ballonet eval. P_{BAL} = 0" H_2O
361	12/7/67	465.0	3.5	Lwr. Lt. Leg	66.5	J.B.	No net performance P_{BAL} = 20
361A	12/7/67	512.0	2.5	Lwr. Lt. Leg	69.5	J.B.	No net performance P_{BAL} = 20
361B	12/7/67	293.0	9.3	Lwr. Lt. Leg	60.6	J.B.	No net performance P_{BAL} = 20
361C	12/7/67	312.0	8.3	Lwr. Lt. Leg	62.8	J.B.	No net performance P_{BAL} = 20
361D	12/7/67	383.0	4.9	Lwr. Lt. Leg	67.0	J.B.	No net performance P_{BAL} = 5
361E	12/7/67	394.0	4.0	Lwr. Lt. Leg	68.0	J.B.	No net performance P_{BAL} = 5
361F	12/7/67	290.0	8.9	Lwr. Lt. Leg	62.9	J.B.	No net performance P_{BAL} = 5
361G	12/7/67	189.0	17.6	Lwr. Lt. Leg	64.0	J.B.	No net performance P_{BAL} = 5
361H	12/7/67	274.0	9.5	Lwr. Lt. Leg	59.5	J.B.	No net performance P_{BAL} = 5
362	12/8/67	504.0	4.1	Upper Lt. Leg	71.1	J.B.	Initial checkout
362A	12/8/67	576.0	2.5	Upper Lt. Leg	75.2	J.B.	Initial checkout
362B	12/8/67	652.0	2.0	Upper Lt. Leg	78.0	J.B.	Initial checkout
362C	12/8/67	522.0	4.5	Upper Lt. Leg	70.6	J.B.	Initial checkout
362D	12/8/67	456.0	6.2	Upper Lt. Leg	65.0	J.B.	Initial checkout
362E	12/8/67	382.0	10.3	Upper Lt. Leg	59.8	J.B.	Initial checkout
363	12/8/67	373.0	9.0	Upper Lt. Leg	--	--	Performance eval. P_{BAL} = 5
363A	12/8/67	308.0	17.1	Upper Lt. Leg	61.0	J.B.	Performance eval. P_{BAL} = 5
363B	12/8/67	255.0	25.1	Upper Lt. Leg	58.8	J.B.	Performance eval. P_{BAL} = 5
363C	12/8/67	323.0	18.7	Upper Lt. Leg	58.2	J.B.	Performance eval. P_{BAL} = 5
363D	12.8/67	610.0	3.6	Upper Lt. Leg	73.2	J.B.	Performance eval. P_{BAL} = 20
363E	12/8/67	539.0	4.5	Upper Lt. Leg	69.3	J.B.	Performance eval. P_{BAL} = 20

Table II (page 5 of 6)

Run Number	Date	Maximum Q Patch (Btu/hr)	Run Time (minutes)	Patch Location	Minimum Skin Temperature (°F)	Subject	Remarks
363F	12/8/67	535.0	5.1	Upper Lt. Leg	67.2	J.B.	Performance eval. P_{BAL} = 20
363G	12/8/67	419.0	10.8	Upper Lt. Leg	65.0	J.B.	Performance eval. P_{BAL} = 20
363H	12/8/67	468.0	10.3	Upper Lt. Leg	57.3	J.B.	Performance eval. P_{BAL} = 20
364	12/11/67	447.0	7.7	Upper Lt. Leg	63.5	J.B.	Performance eval. P_{BAL} = 20
364A	12/11/67	336.0	16.1	Upper Lt. Leg	55.4	J.B.	Performance eval. P_{BAL} = 20
365	12/11/67	Max.	8.2	Upper Lt. Leg	62.0	J.B.	Performance evaluation
366	12/14/67	--	2.3	Lwr. Lt. Leg	--	S.Z.	*Cardiovascular monitoring
366A	12/14/67	229.0	5.7	Lwr. Lt. Leg	--	S.Z.	*Cardiovascular monitoring
366B	12/14/67	--	--	Lwr. Lt. Leg	--	S Z.	*Cardiovascular monitoring
366C	12/14/67	210.0	6.8	Lwr. Lt. Leg	--	S.Z.	*Cardiovascular monitoring
366D	12/14/67	249.0	5.1	Lwr. Lt. Leg	--	S.Z.	*Cardiovascular monitoring
367	12/14/67	--	--	Lwr. Lt. Leg	--	S.Z.	*Cardiovascular monitoring
367A	12/14/67	--	--	Lwr. Lt. Leg	--	S.Z.	*Cardiovascular monitoring
367B	12/14/67	--	--	Lwr. Lt. Leg	--	S.Z.	*Cardiovascular monitoring
367C	12/14/67	--	--	Lwr. Lt. Leg	--	R.W.	*Cardiovascular monitoring
367D	12/14/67	--	--	Lwr. Lt. Leg	--	R.W.	*Cardiovascular monitoring
367E	12/14/67	--	--	Lwr. Lt. Leg	--	R.W.	*Cardiovascular monitoring
368A	12/15/67	--	--	Lwr. Lt. Leg	--	S.Z.	*Cardiovascular monitoring
368B	12/15/67	--	--	Lwr. Lt. Leg	--	S.Z.	*Cardiovascular monitoring
368C	12/15/67	--	--	Lwr. Lt. Leg	--	S.Z.	*Cardiovascular monitoring
368D	12/15/67	--	--	Lwr. Lt. Leg	--	S.Z.	*Cardiovascular monitoring
369A	12/18/67	--	--	Lwr. Lt. Leg	--	E.H.	*Cardiovascular monitoring
369B	12/18/67	--	--	Lwr. Lt. Leg	--	E.H.	*Cardiovascular monitoring
369C	12/18/67	--	--	Lwr. Lt. Leg	--	E.H.	*Cardiovascular monitoring

*Tests associated with cardiovascular monitoring research - IRAD effort.

Table II (page 6 of 6)

Run Number	Date	Maximum Q Patch (Btu/hr)	Run Time (minutes)	Patch Location	Minimum Skin Temperature (°F)	Subject	Remarks
369D	12/18/67	--	--	Lwr. Lt. Leg	--	E.H.	*Cardiovascular monitoring
369E	12/27/67	260 (Avg)	5.0	Upper Rt. Arm	66.0	J.B.	Max. cooling rate
369F	12/27/67	261 (Avg)	5.0	Bottom of Foot	61.0	J.B.	Max. cooling - upper rt. arm patch used
370	12/21/67	--	--	Upper Rt. Arm	--	S.Z. H.L.	Skin temp. equilibrium runs

*Tests associated with cardiovascular monitoring research - IRAD effort.

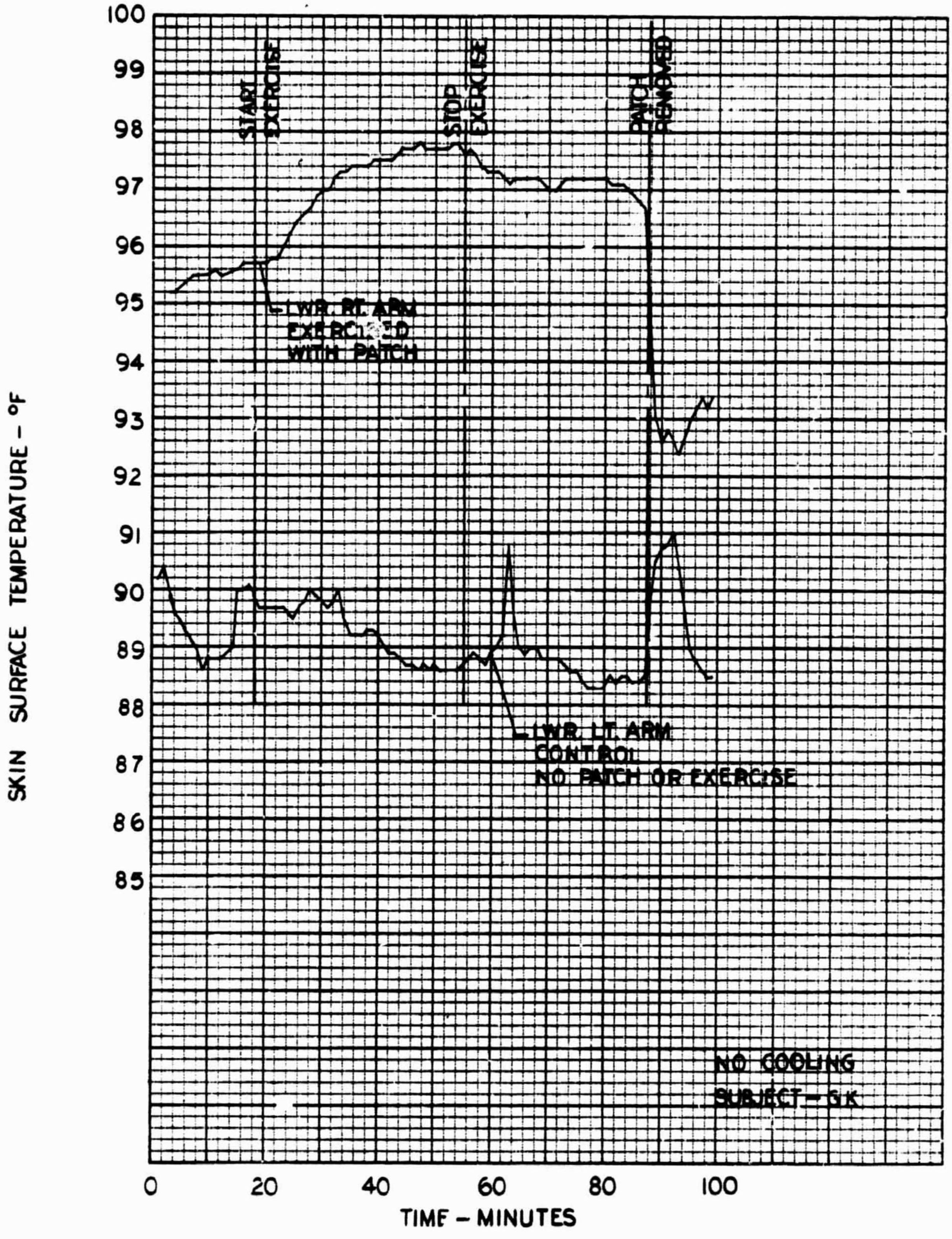

Figure 20. Skin Temperature Time History - LWR. Rt. Arm - Run 301

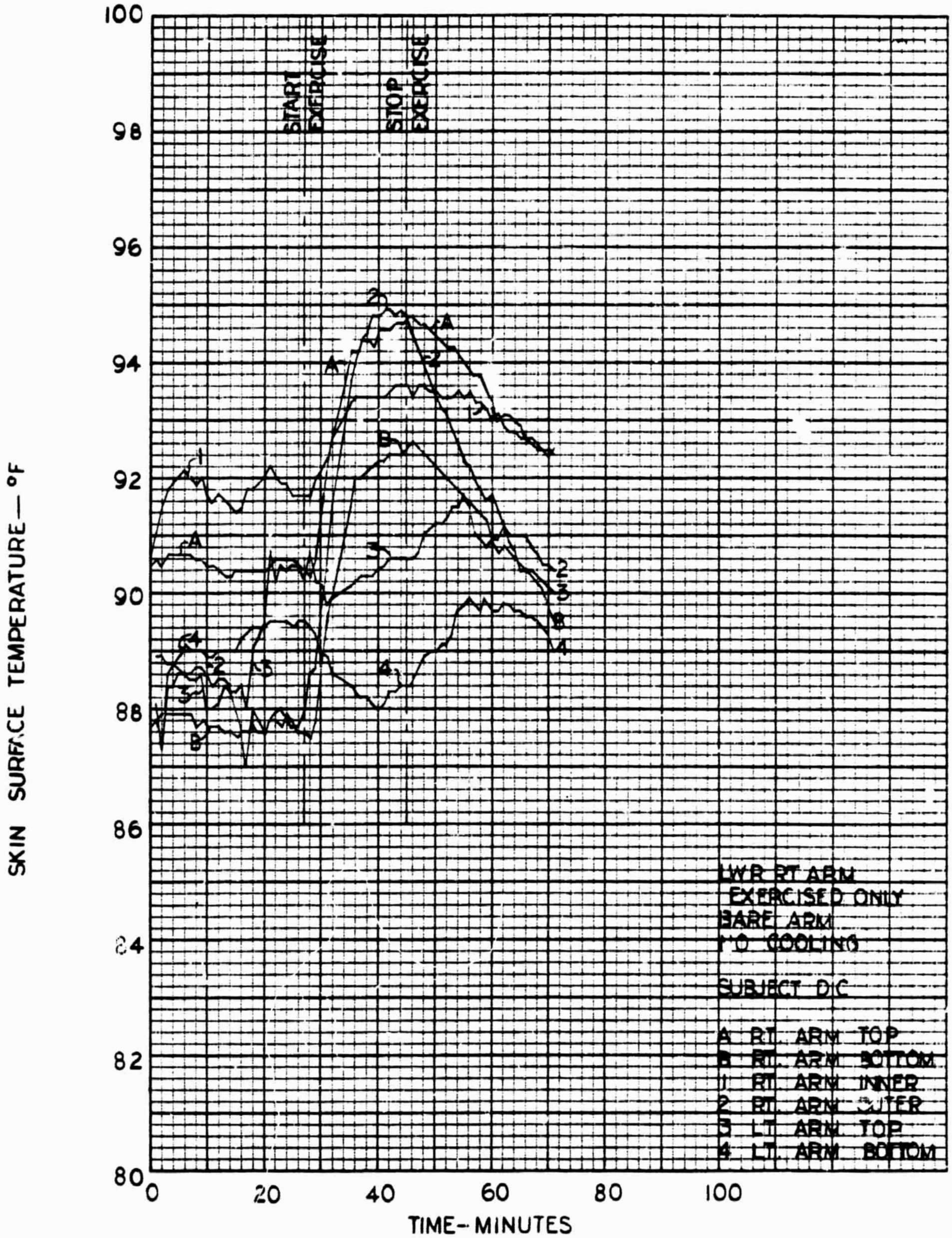

Figure 21. Skin Temperature Time History - LWR. Rt. Arm - Run 302

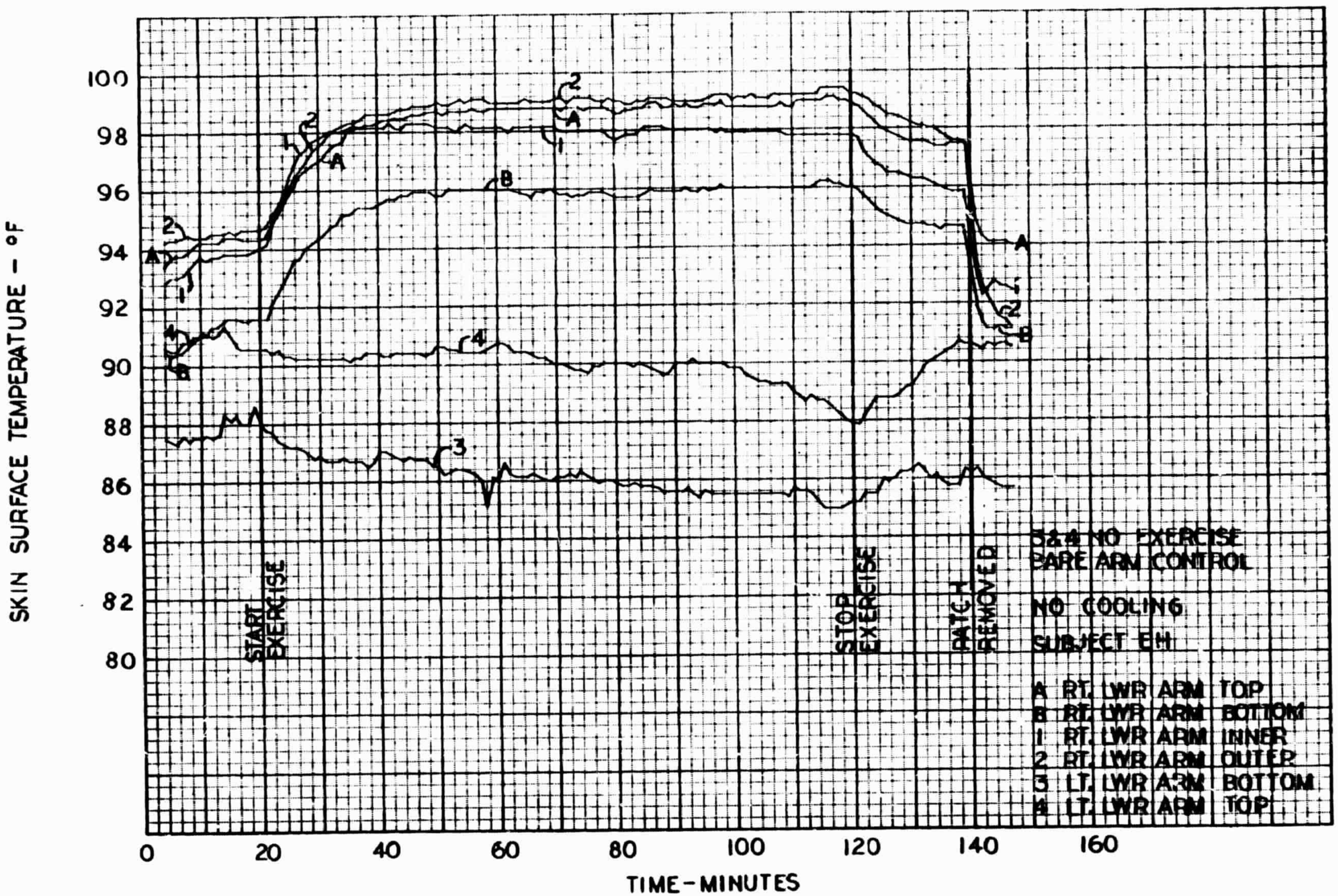

Figure 22. Skin Temperature Time History - Right Lower Arm - Run 303

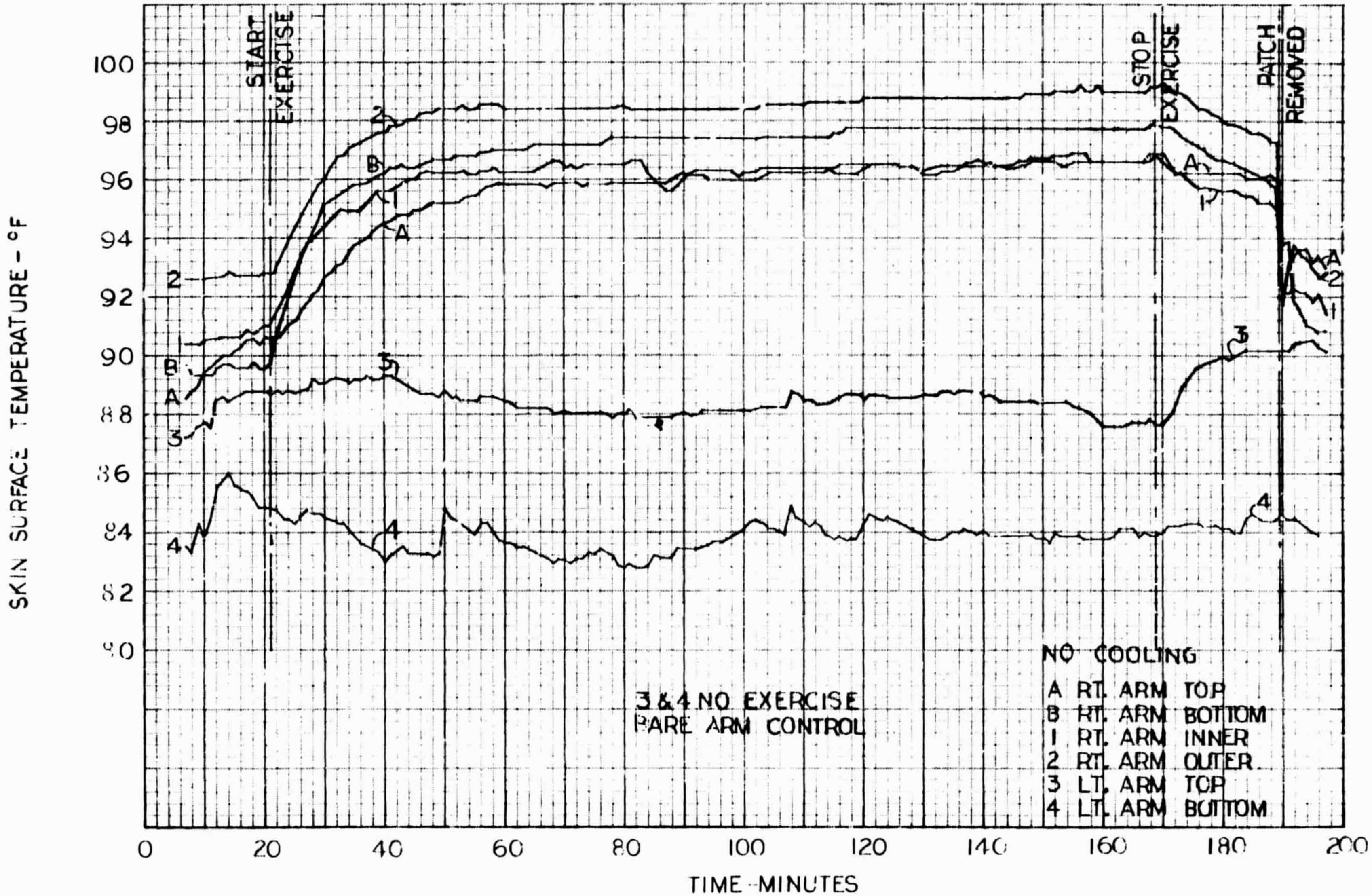

Figure 23. Skin Temperature Time History - Lower Right Arm - Run 304

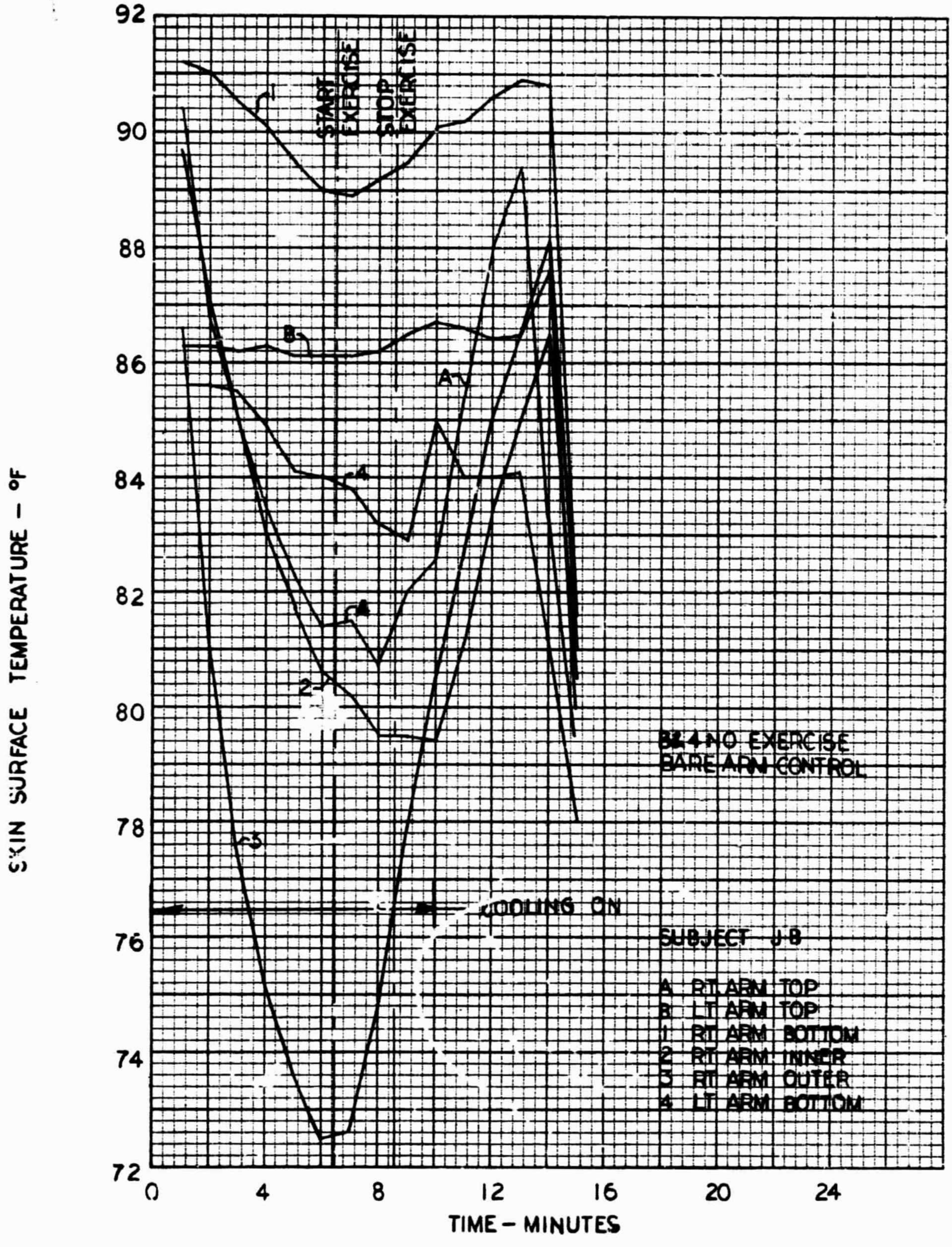

Figure 24. Skin Temperature History - LWR RT. Arm - Run 308

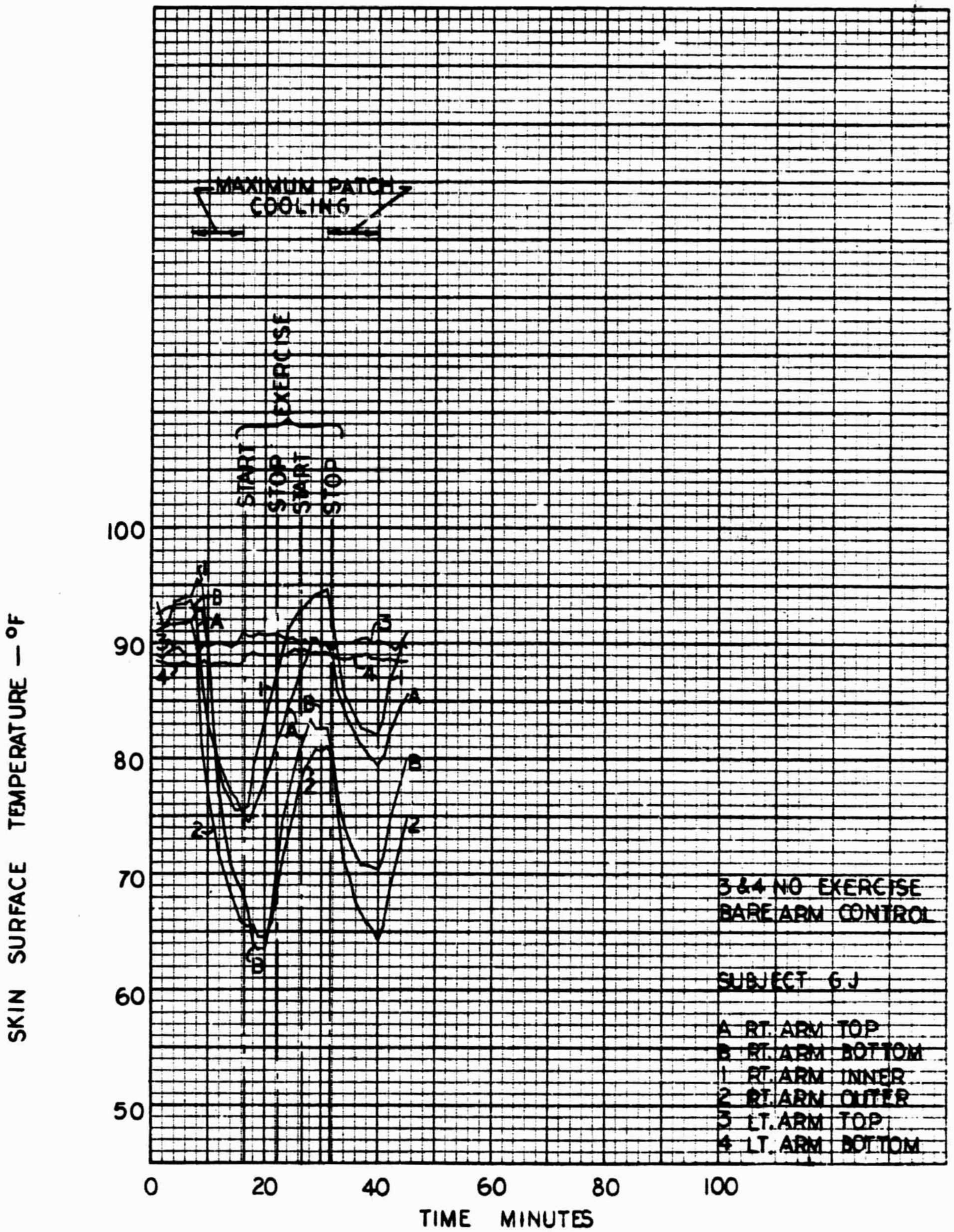

Figure 25. Skin Temperature Time History - LWR. RT. Arm - Run 309

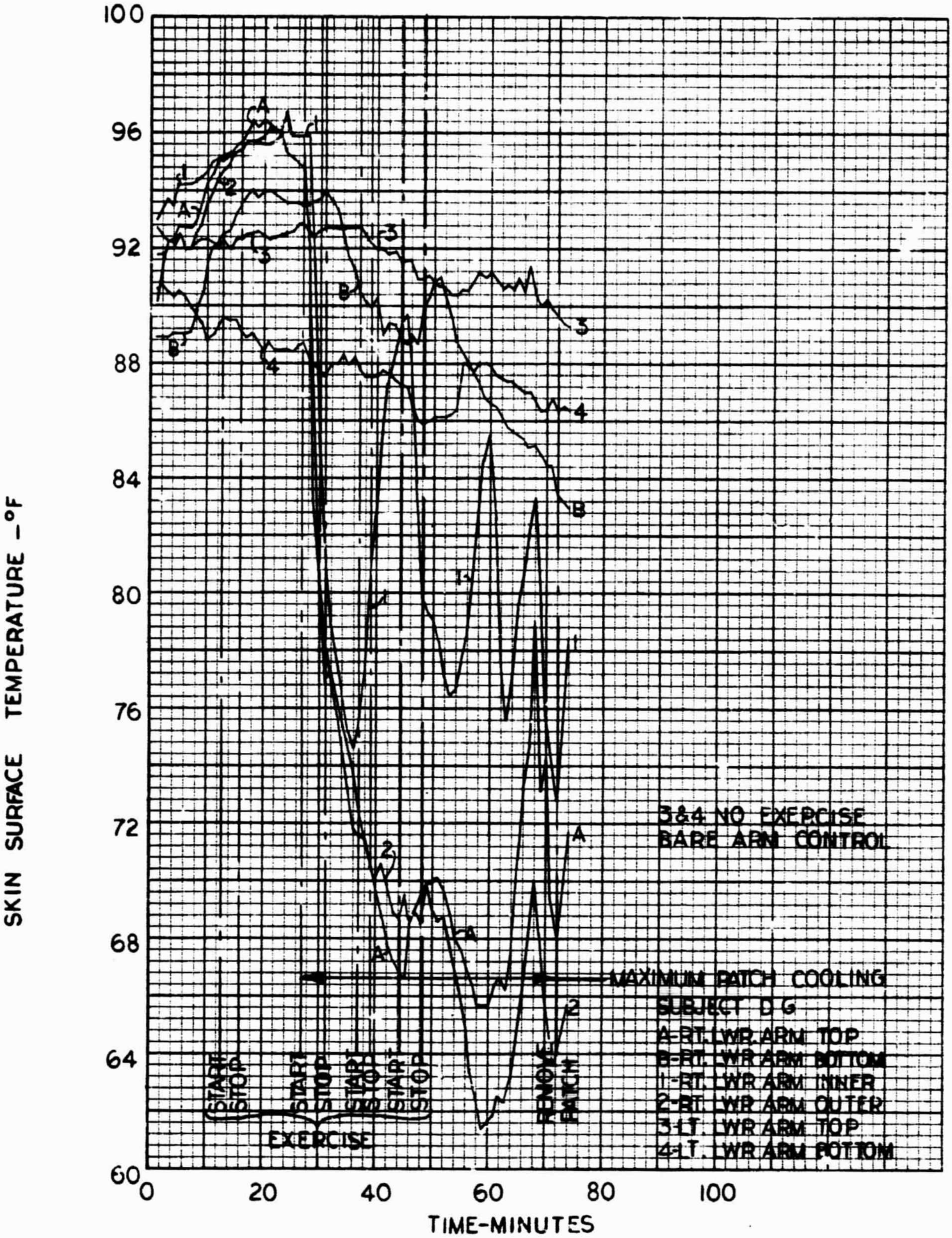

Figure 26. Skin Temperature Time History - LWR. RT. Arm - Run 310

A further series of runs (313, 314, 317, and 318) was made to evaluate two sizes of Spirap edging on the cooling patch. In these tests, the heat removal rate was maintained constant for two runs, one on the upper left arm patch (with the small Spirap) and one on the upper right arm patch (with the larger Spirap). Four pressures inside the patch were recorded along with skin temperature. Heat removal rate was calculated for each run from the weight of water removed from the patch during the cooling process. The first two runs resulted in unsatisfactory pressure data from the right arm patch. To provide as similar conditions on each patch as possible, both patches were retested (runs 317 and 318). These runs were conducted in the same manner as runs 313 and 314. The results of these tests are shown in Figures 27 and 28. It can be seen that the smaller Spirap edging increases flow resistance as evidenced by the higher pressure differentials inside the patch. Also, the patch with large Spirap shows a more rapid cooling of skin temperature than the patch with the small Spirap. Although these differences in performance exist, both patches perform sufficiently well to satisfy the cooling requirements of 5,000-Btu/hr full suit capacity. Another factor in selecting the size of edging Spirap is patch comfort and flexibility. In light of the bulky nature of the large Spirap edging and its associated increased stiffness, the small (1/8-in. diam) Spirap was selected to be used on all future patches. In areas where additional flow capacity is required, this small Spirap can be doubled up to provide the required flow capacity without adding thickness or stiffening to the patch.

One test was run in an attempt to adjust patch cooling rate to obtain stable skin temperature. This test (run 315) used the lower right arm cooling patch and exercise was accomplished with the squeeze bulb forearm exercise equipment. Unsatisfactory control of heat removal rate resulted in a final cooling sequence at maximum cooling rate. After the run, leaks were found in the patch outer membrane. The poor heat removal rate control was due to these leaks. Further testing with this patch was discontinued until it could be repaired.

The effect of overall exercise on patch cooling capacity was investigated by using an upper right arm cooling patch while the subject was walking on the

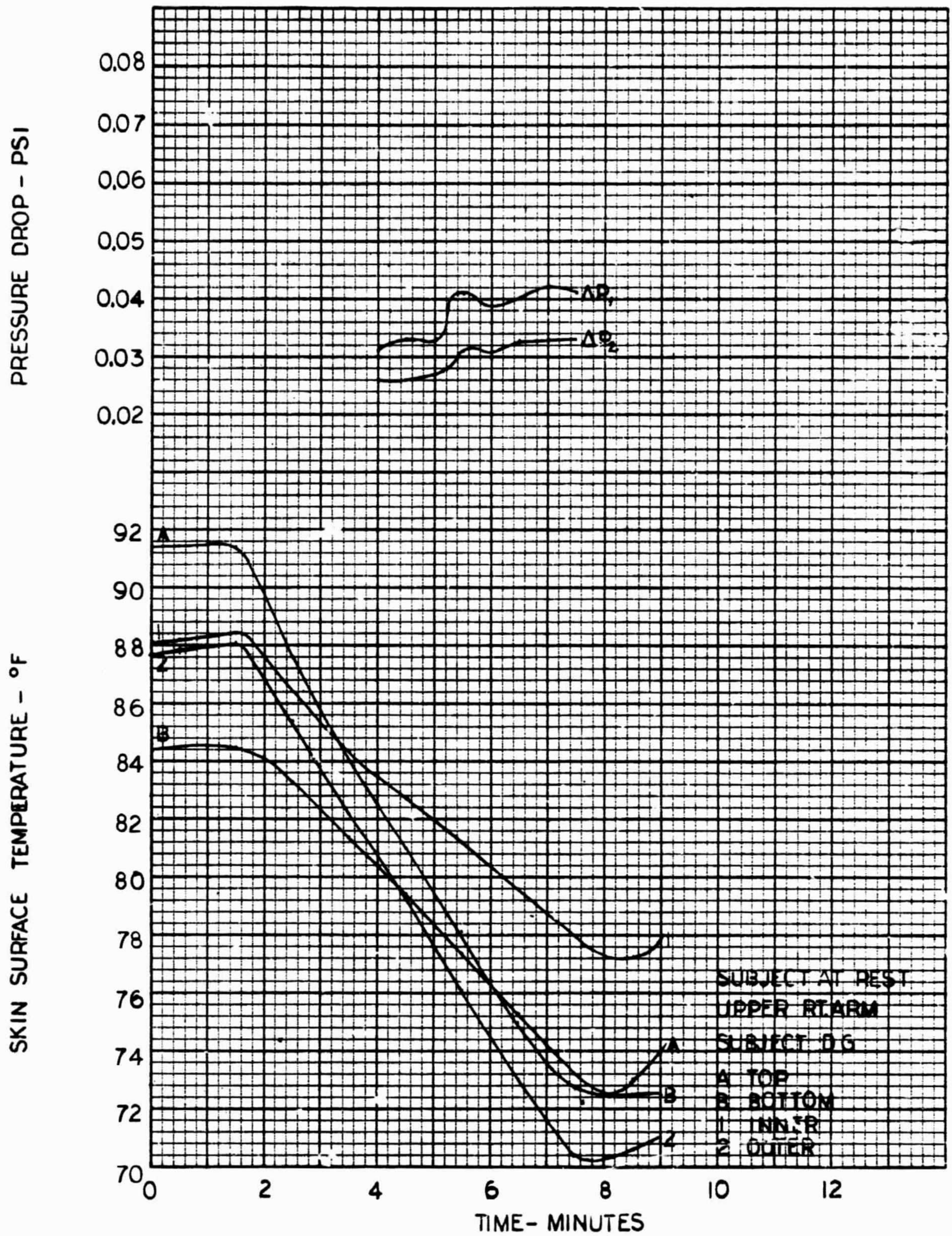

Figure 27. Spirap Size Evaluation - 1/4 Inch Spirap

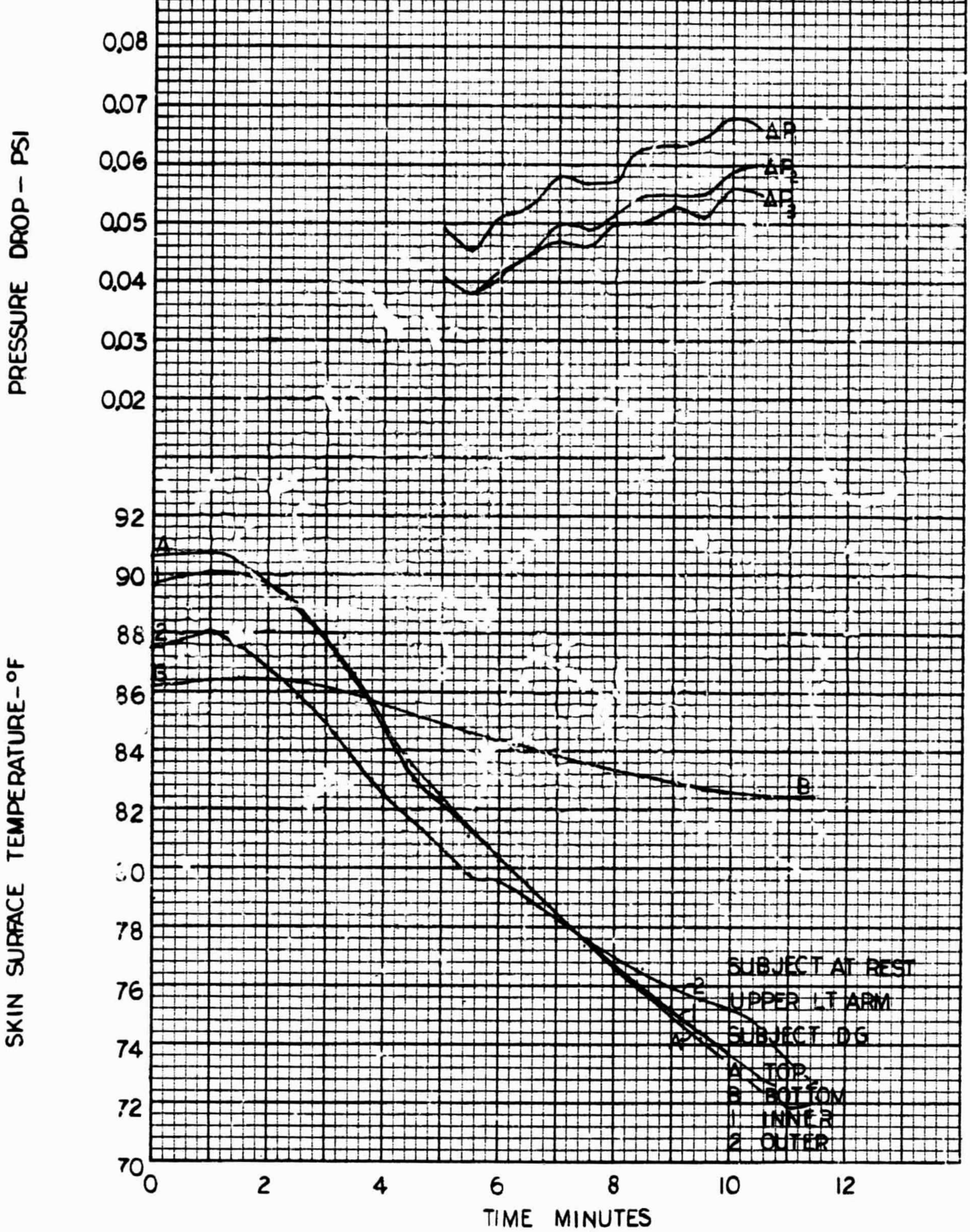

Figure 28. Spirap Size Evaluation - 1/8 Inch Spirap

treadmill. Patch cooling characteristics were observed at three different metabolic rates (based on treadmill speed and grade). Run 319 investigated upper right arm cooling at a metabolic rate of approximately 3,200 Btu/hr. Runs 339 and 340 were made at 1,200/Btu hr and runs 342, 343, and 345 were made at 1,600 Btu/hr. Figure 29 shows the skin temperature history for each of these runs. It can be seen that even at the 3,200-Btu/hr metabolic rate the patch cooling capacity was much greater than that required to maintain constant skin temperature in the nonperspiring temperature range. Run 341 was made immediately following a 1,200-Btu/hr metabolic rate run to observe the cooling characteristics under postexercise conditions. Figure 30 shows the skin temperature history for this run. Run 349 was a similar test except no exercise was done preceeding the cooling run. Figure 31 compares these two runs. The effect of exercise prior to cooling is as would be expected. The postexercise run failed to cool the skin as rapidly as the nonexercised related run. This is accounted for by the increased metabolic lev in the postexercise run; that is, more heat was being generated, and therefore t the same heat removal rate, slower skin temperature cooling occurred.

Two series of runs were made to document the performance of the upper right arm patch. Two different subjects were used, one for each series. The runs were made at fixed heat removal rates varying from equivalent full-suit cooling of 2,000 to over 6,000 Btu/hr. Run time (to patch internal pressure drop limit), heat removal rate (by the water weight change method), and skin temperature versus time was recorded for each test. All these runs were made with the subject passive, in a seated position. The data from these runs were plotted in two forms, skin temperature versus time, and run time versus heat removal rate. This data is shown in Figures 32 and 33. The skin temperature versus time curves give an indication of the heat removing capacity of the patch. Variation in these curves, even at the same heat removal rate, occurs from subject to subject. This is indicative of the difference in physiology between subjects. Even the same subject will occasionally generate different skin temperature versus time curves as a function of his physiological condition at the time of the test. The same variation applies to the run time curves. Data scatter, therefore, is apparent in all cooling tests. By careful interpretation of the test results, a reasonable band of performance characteristics

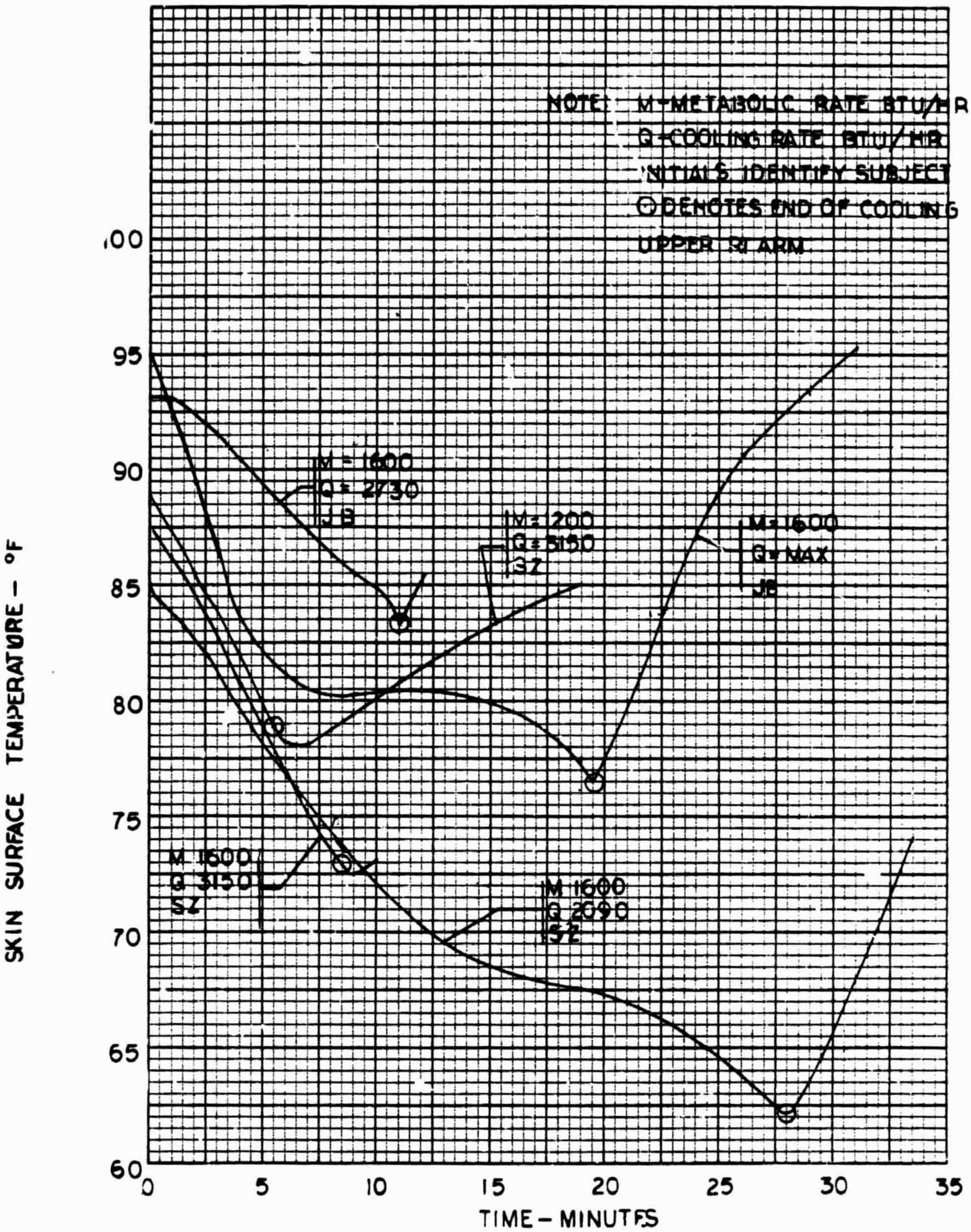

Figure 29. Skin Temperature Time History Comparison With Cooling and Exercise

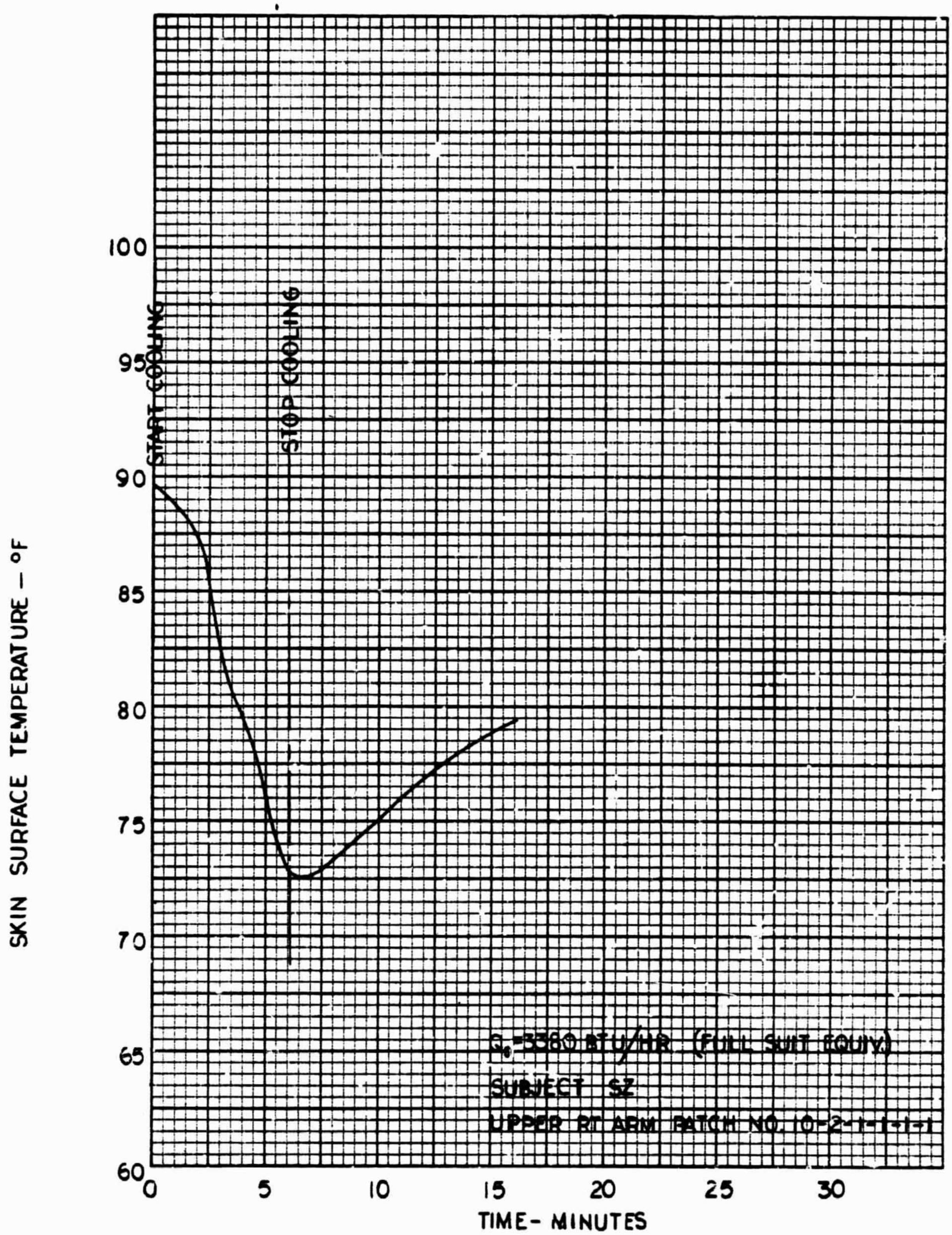

Figure 30. Skin Temperature Time History - At Rest After 1200 BTU/HR Exercise

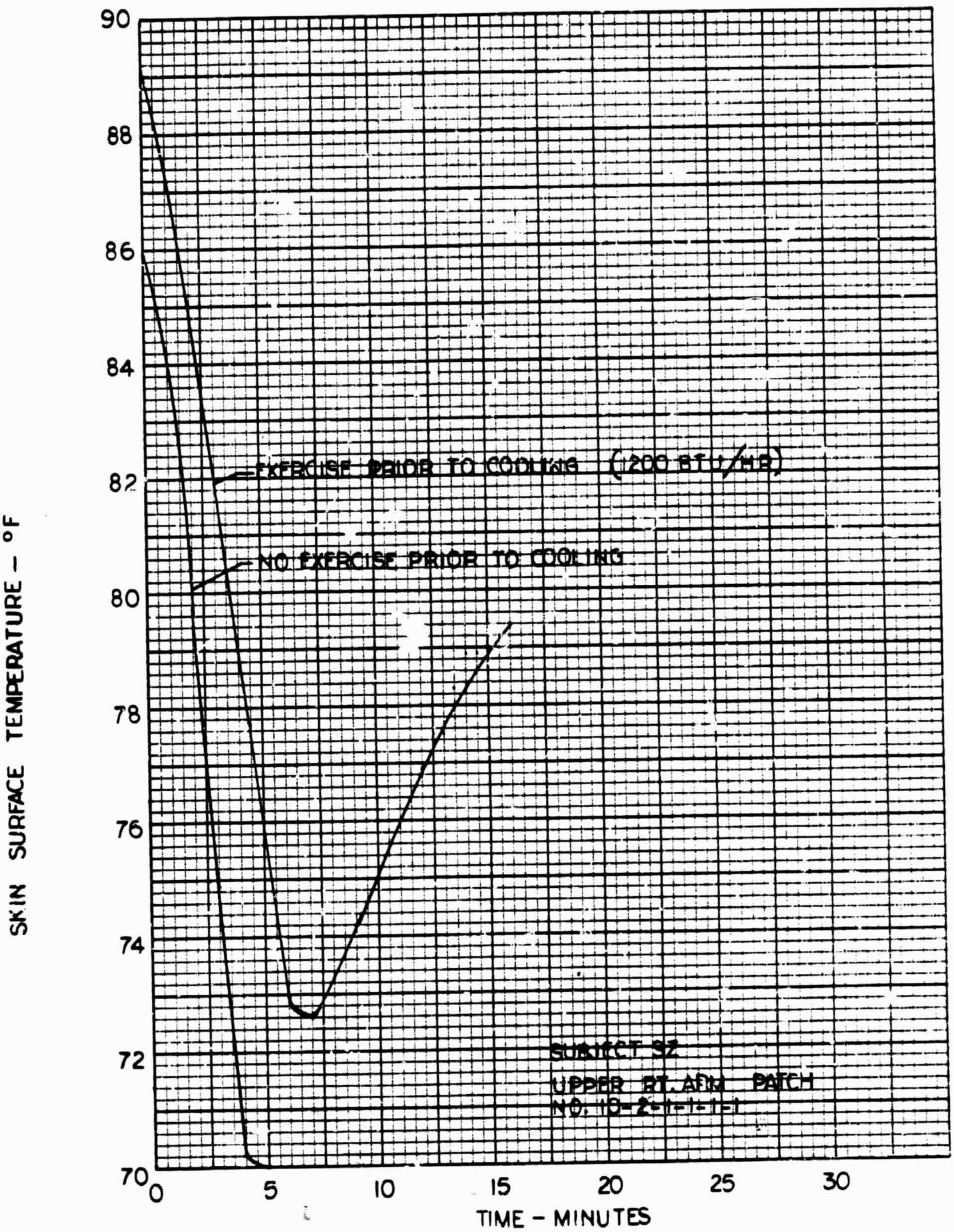

Figure 31. Comparison of Skin Cooling With and Without Prior Exercise

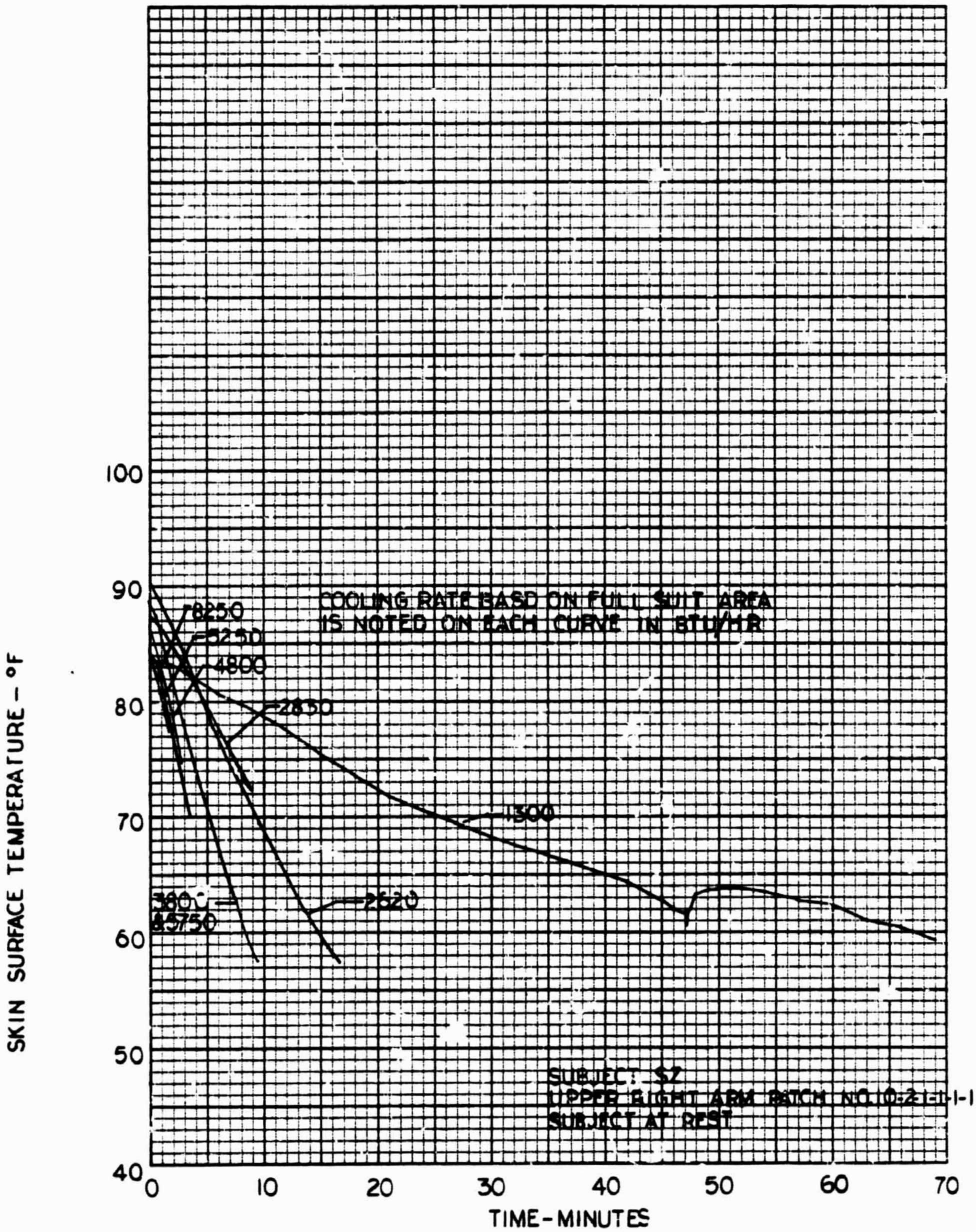

Figure 32. Skin Temperature Time History - Comparison of Different Fixed Cooling Rates

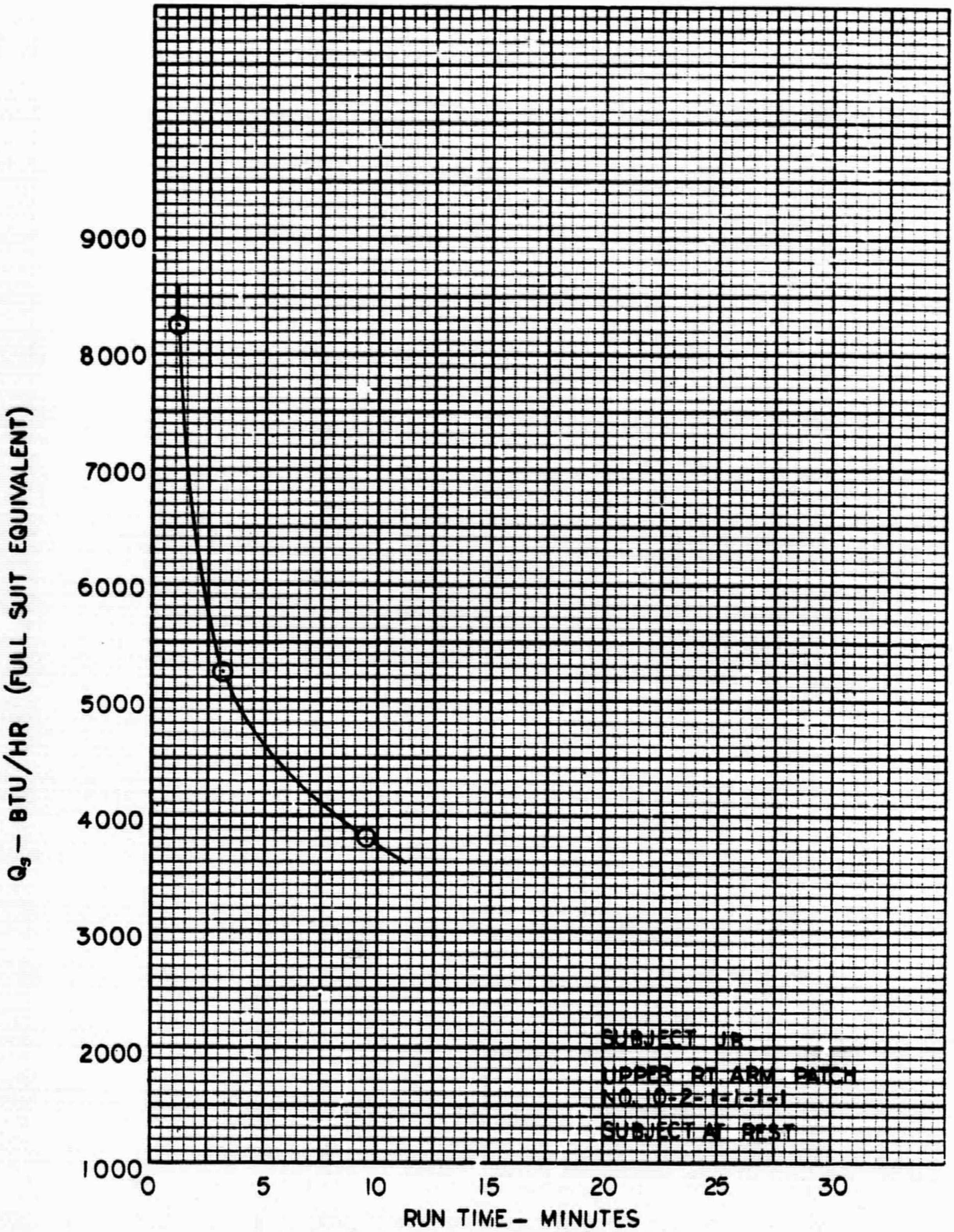

Figure 33. Run Time as Limited by Internal Patch ΔP

can be established which gives satisfactory evidence of the overall patch performance.

It can be seen that the curves of run time versus heat removal rate separate into two distinct lines, one for each subject. The basic characteristics of the curves are similar. High heat removal rates limit the run time while lower heat removal rates permit longer operation before the skin-to-patch temperature difference becomes too small to maintain a fixed heat removal rate. At higher metabolic rates, these run time curves become less sloped, with a final slope of zero when subject skin heat rejection rate equals ECGS system heat removal rate.

On two of the above mentioned runs, water was added to the patch during the cooling operation. The effect of this water addition was to momentarily raise patch pressure with a corresponding increase in patch and skin temperature. A small perturbation such as this is expected during water refill operation and should not detract from overall system performance.

Two tests were run using the upper right arm patch to evaluate the effect of external thermal insulation on patch performance. Figure 34 shows the skin temperature vs. time curve for this test compared with the skin temperature observed in a similar test without the thermal insulation. The most significant thing about the comparison is the rate of skin temperature recovery. The uninsulated patch has a much greater skin temperature recovery rate at any given skin temperature than the insulated patch. This indicates, quantitatively, that external insulation on the patch does materially prevent enough heat flow into the patch to cause observable differences. In the final patches, a layer of aluminum foil is located on the outside of the boiler void to prevent radiant heat transmission into the patch from external sources: This should eliminate a large part of the heat leak apparent in the insulated patch tests.

A series of runs was made to document the performance of the lower left leg patch. The data for these tests were recorded and plotted in the same way as those for the upper right arm patch. The same basic performance characteristics are apparent in this data as for the upper right arm. The data are shown in Figures 35 and 36. Maximum heat removal rates of over 5,000 Btu/hr,

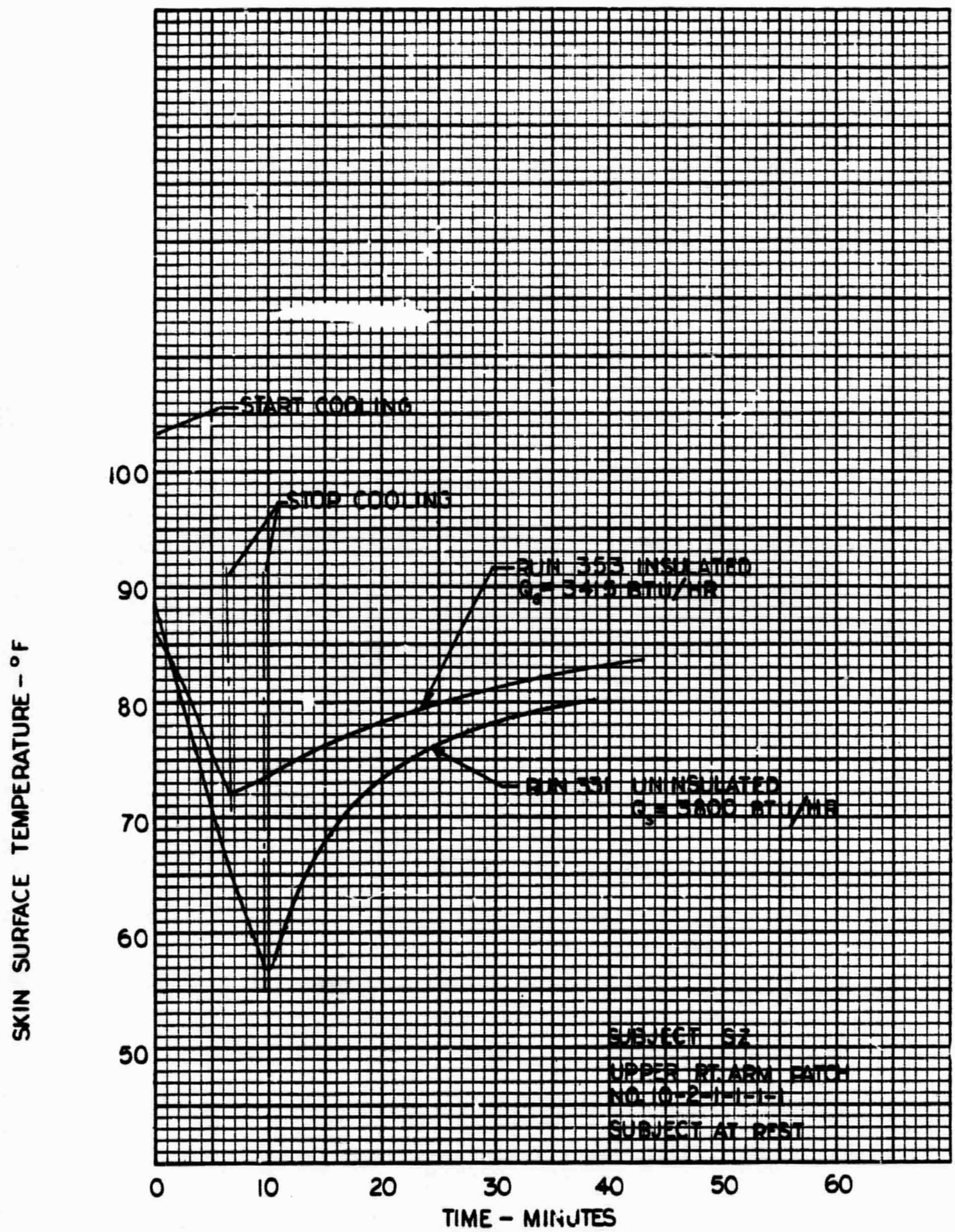

Figure 34. Effect of Thermal Insulation on ECGS Patch Performance

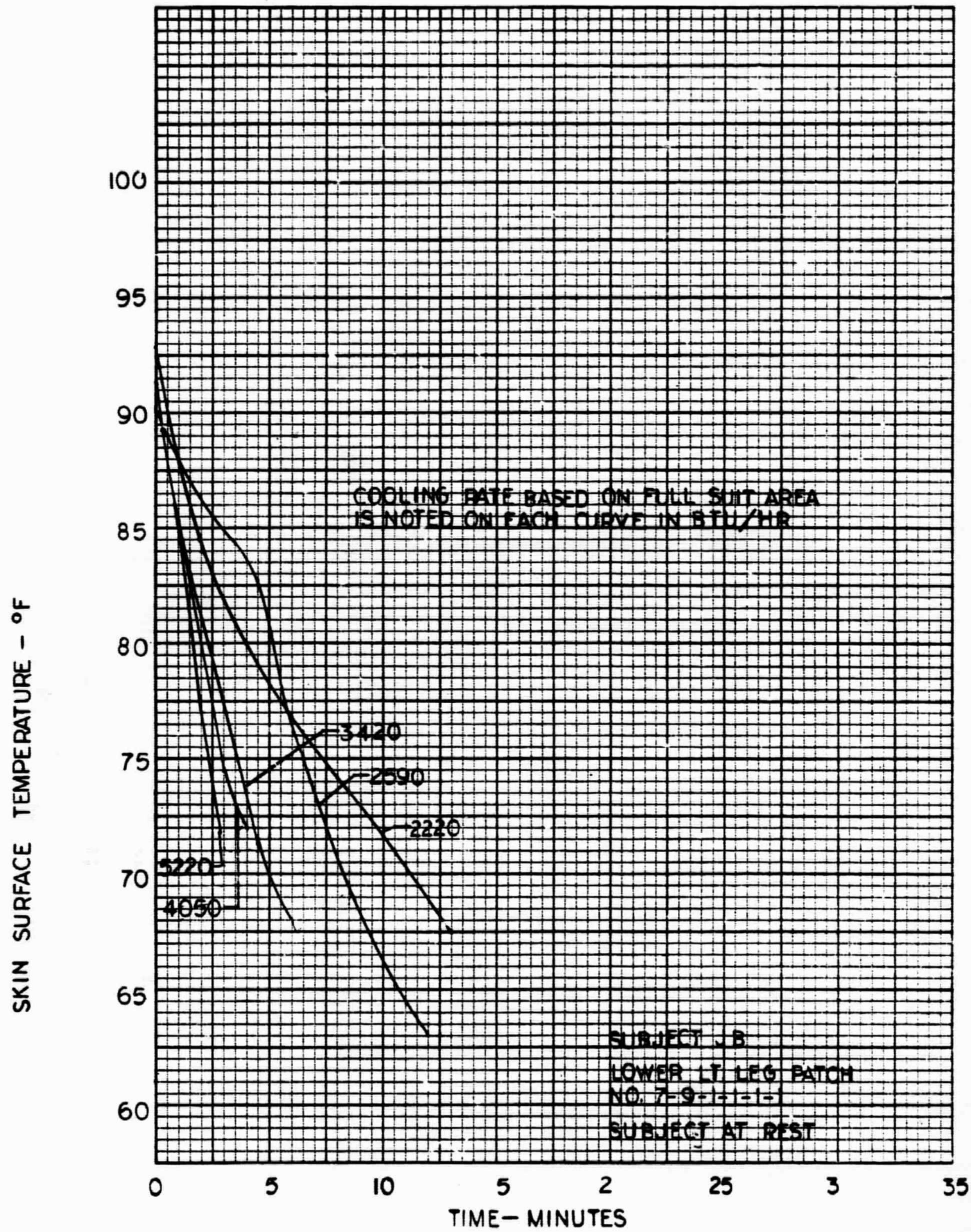

Figure 35. Skin Temperature Time History - Comparison of Different Fixed Cooling Rates

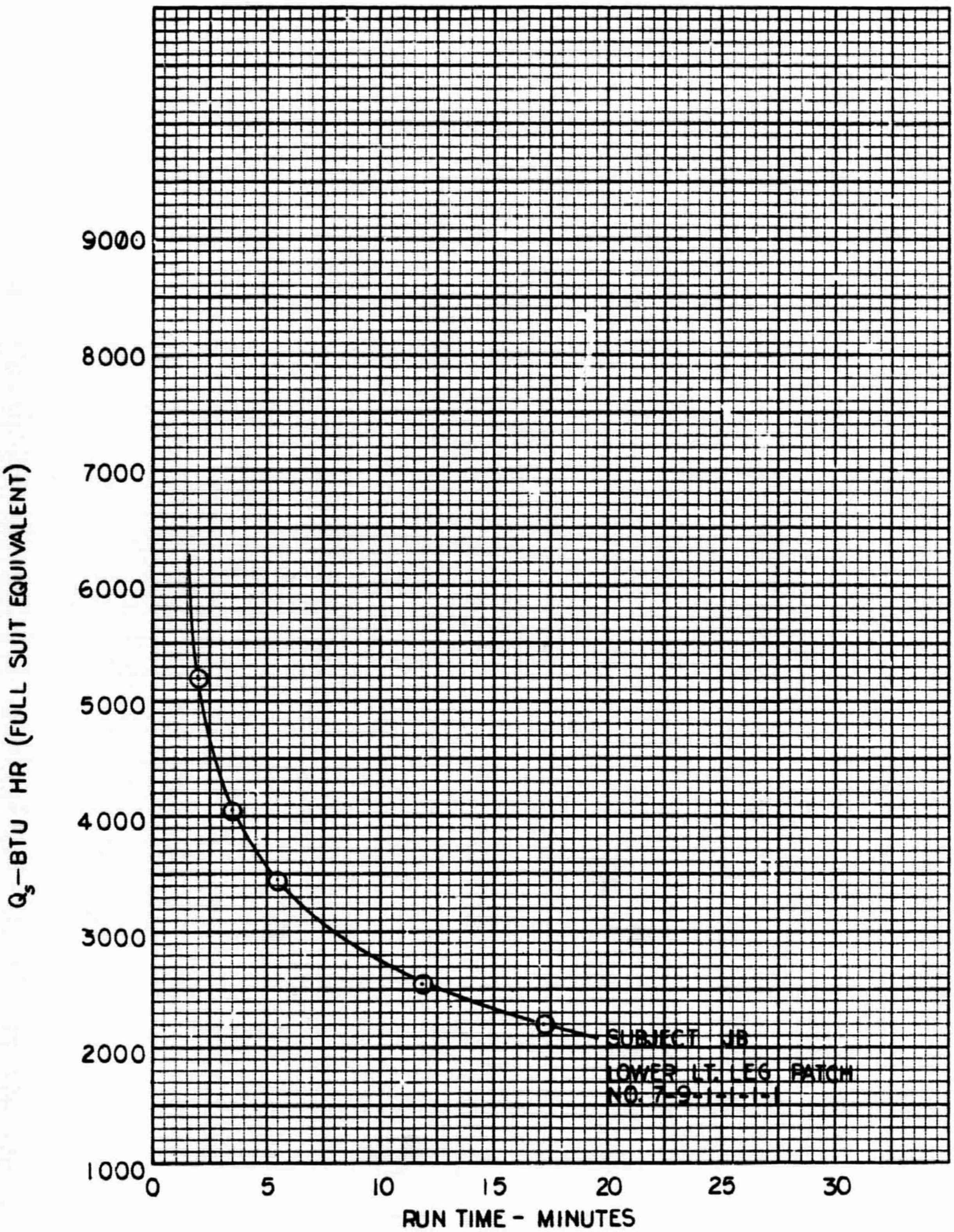

Figure 36. Run Time as Limited by Internal Patch ΔP

based on full ECGS suit area, were obtained on several runs, indicating that the patch is more than capable of removing its share of heat at a full-suit rate of 5,000 Btu/hr.

The effect on ECGS patch performance of varying ballonet pressure was determined. Several runs were made with the lower left leg patch at varying ballonet pressure from 0 to 20 in. H_2O. The results of these runs is shown in Figure 37. It can be seen that increasing ballonet pressure increases the run time at a given heat removal rate. The improvement in run time with increased ballonet pressure is due to two factors: (1) the patch is pressed into more intimate contact with the skin, lowering the thermal resistance of the patch-to-skin heat path, and (2) areas of the patch which were not contacting the skin due to the local "hills and valleys" were formed to conform more closely to the skin contours, thus increasing the skin contact area through which heat could be transferred. The improvement in performance appears to diminish with increasing ballonet pressure. Because of this trend, and the fact that lower ballonet pressures are more comfortable, a compromise pressure of 5 in. H_2O was chosen for use on fugure ECGS systems. Further testing with the full cooling garment may allow elimination of the ballonet entirely from some portions of the suit if sufficient heat can still be removed from the system as a whole.

Tests were run to determine the effect of the skin-to-patch comfort layer of nylon mesh on patch cooling performance. The results of these tests, as shown in Figure 38, shows no appreciable difference in patch performance, with or without the comfort layer. Based on this test data, the use of the comfort layer mesh will be continued in all ECGS patches.

A series of runs (362 to 365) was made to document the performance of the upper left leg patch. These runs were made at two different ballonet pressures. The data (Figure 39) show the same trend to improved performance with increasing ballonet pressure as did the lower left leg patch data. Overall performance was comparable to the other patches evaluated. A comparison of patch run time (limited by patch internal pressure drop) at constant heat removal is shown in Figure 40 for upper arm, lower leg, and upper leg patches. The

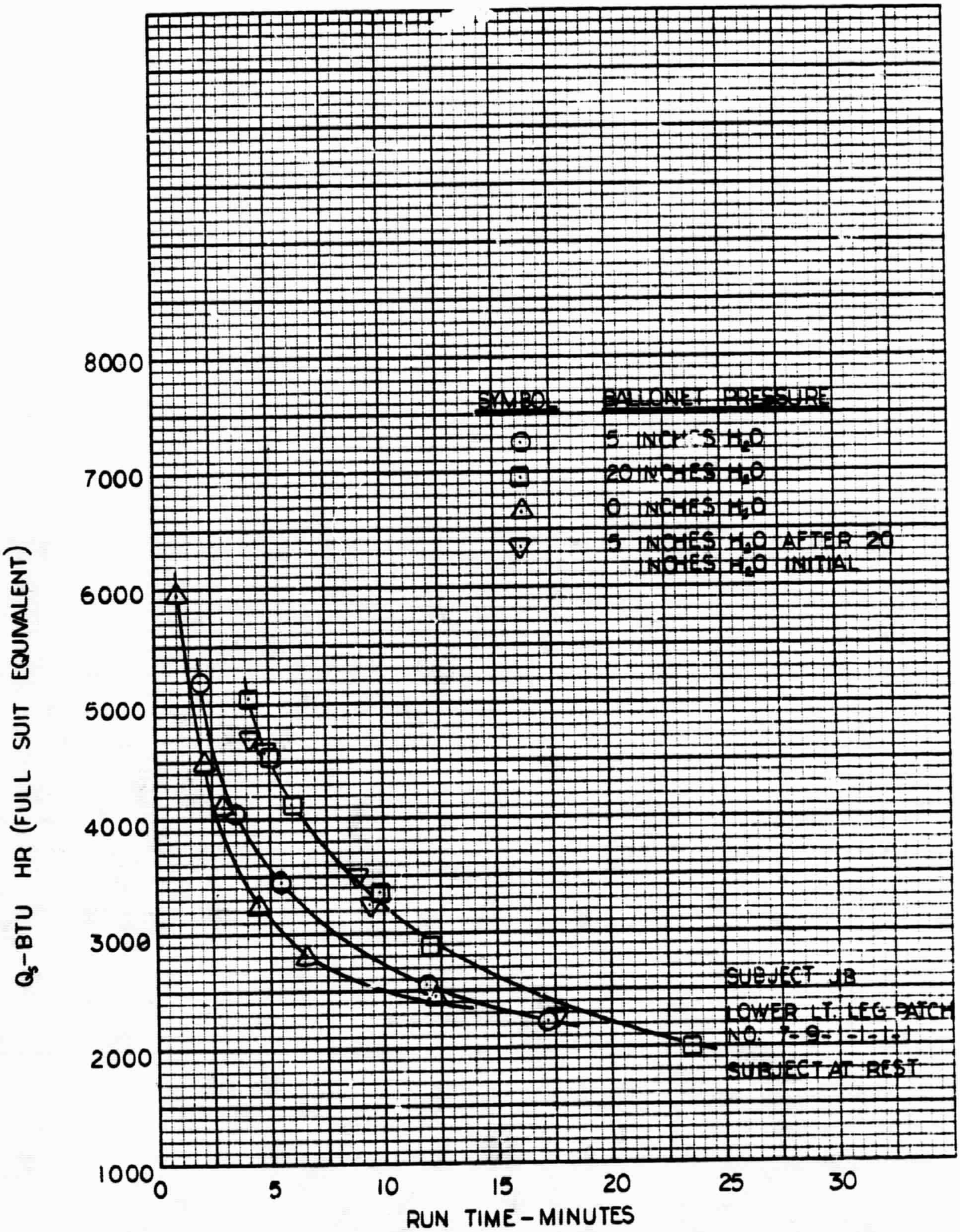

Figure 37. Ballonet Pressure Effect on Lower Left Leg Patch Performance

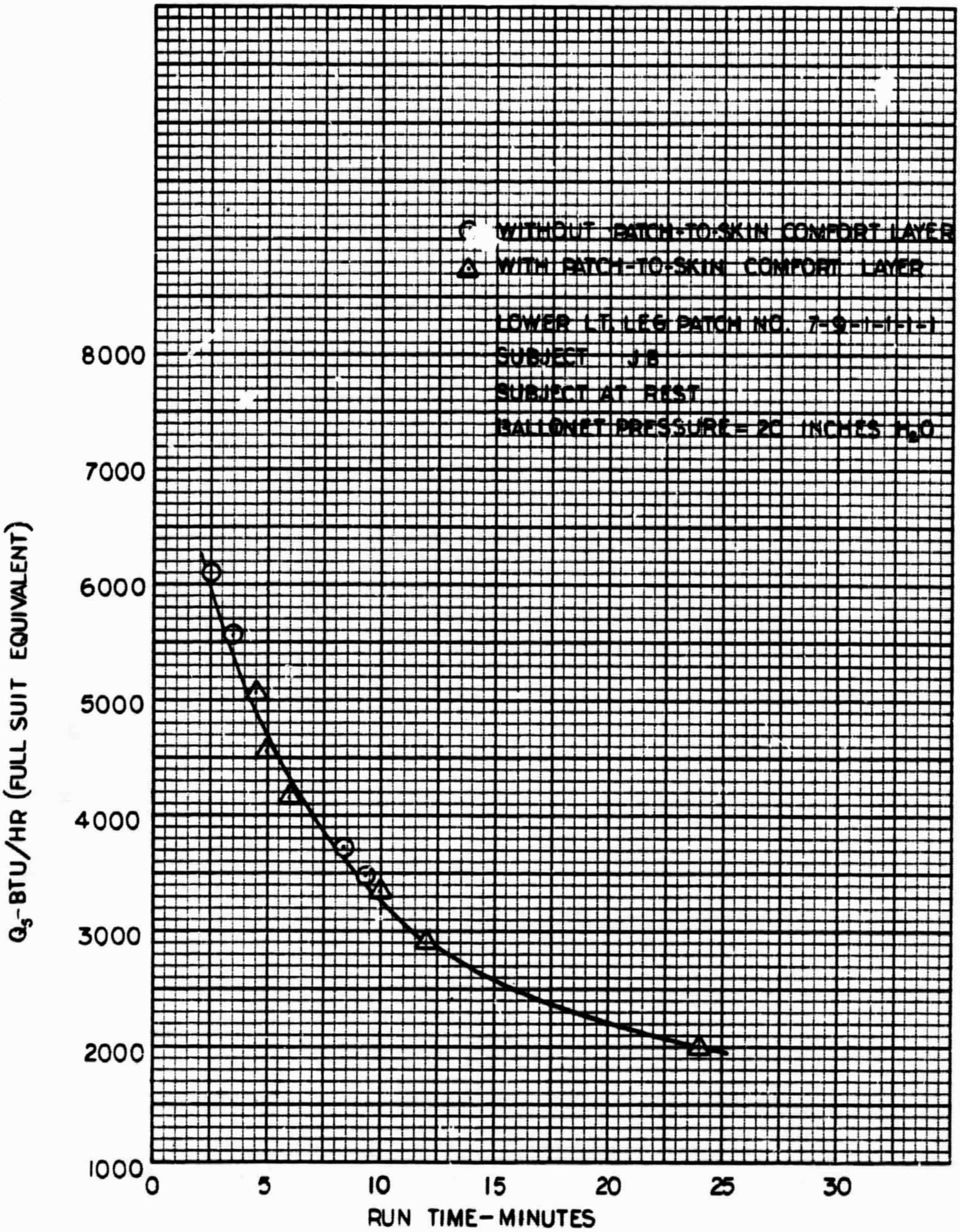

Figure 38. Effect of Skin-to-Patch Comfort Layer on ECGS Patch Performance

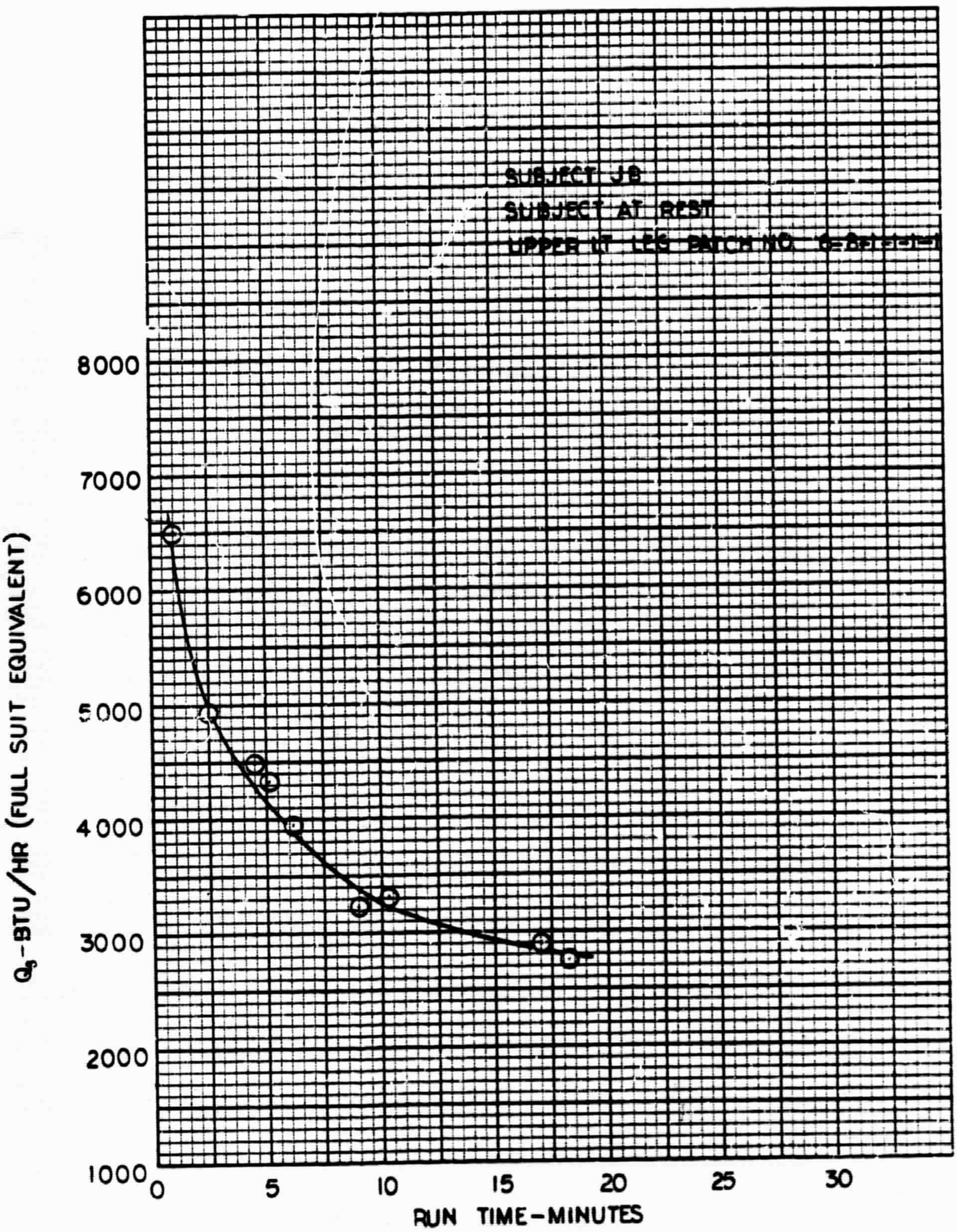

Figure 39. Upper Left Leg Patch Performance

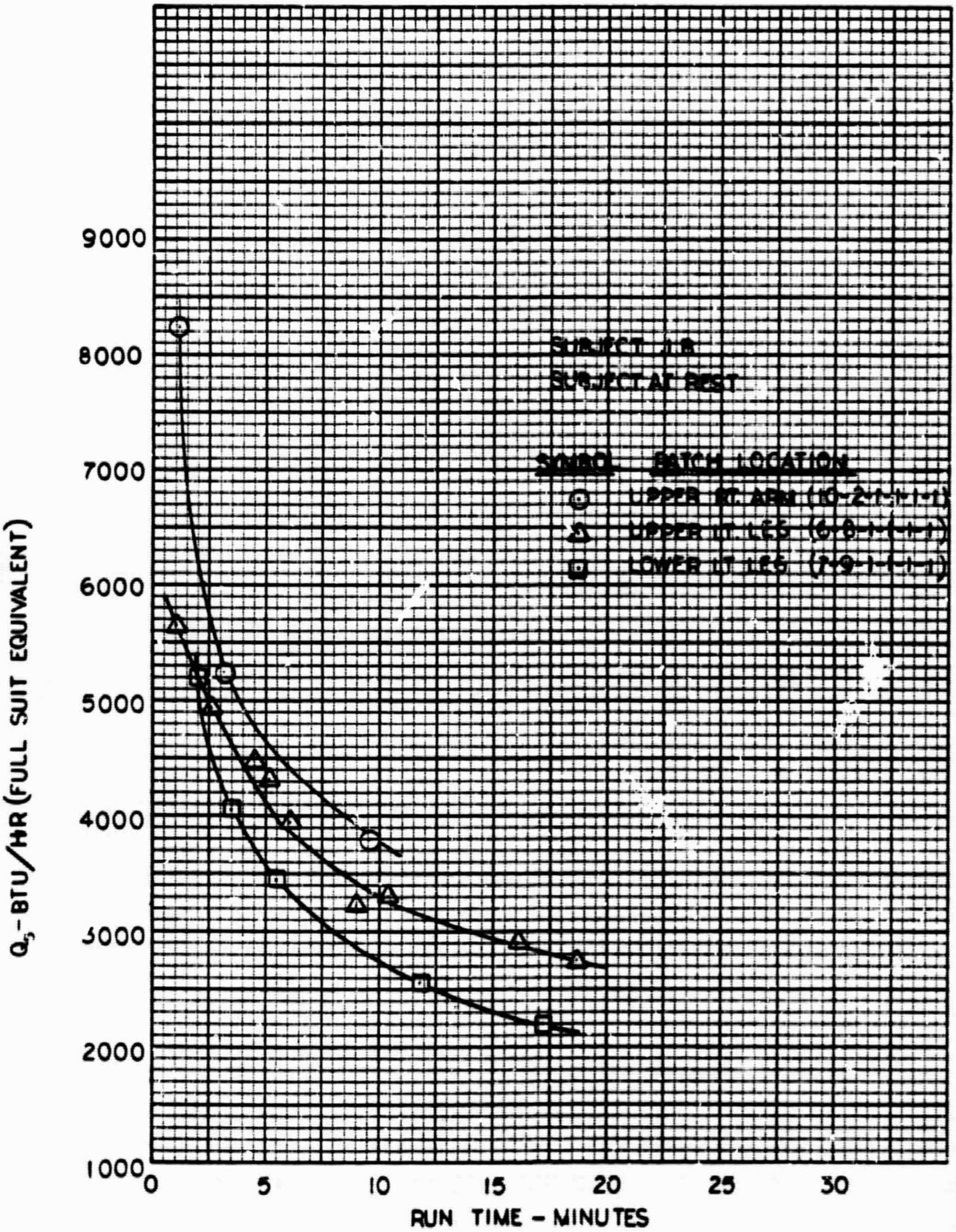

Figure 40. ECGS Patch Performance Comparison

closely similar performance for each patch indicates approximately equal cooling capacity in each patch. This is necessary if the predicted full-suit cooling performance is to be accomplished. The slight variation between the performance of the patches can be in part attributed to the varying physiology between the parts of the body which were being cooled. Further research into the quantity of heat rejected from various areas of the body under different exercise conditions is required before the precise local body cooling requirements can be specified.

Two runs (369E and 369F) were performed to evaluate the difference in heat rejection at maximum patch cooling capacity using the same patch in two different body-locations. The upper right arm patch was used on both the location for which it was designed (the upper right arm) and on the bottom of the feet. Almost identical performance was recorded for both patch locations. This indicates that, for the locations tested, the ability of the body to supply heat to the skin surface does not vary appreciably between the upper arm and the bottom of the feet.

A test was run to obtain the steady state skin temperature heat removal rates for two different test subjects. A range of skin temperatures was investigated and Figure 41 shows the results of this testing. An increase in the steady state heat removal is apparent as skin temperature is reduced. Each subject has a different skin temperature vs. heat removal rate curve. It should be noted that these tests were run with the subject at rest. Further tests with the subject at higher metabolic rates would generate data which could make a family of curves of constant subject metabolic rate. These curves would show higher heat removal rates for a given skin temperature than those in Figure 41. The range of temperatures over which steady state skin temperature can be obtained indicate the wide operating limits of the ECGS system.

By this time in the program all of the ECGS cooling patches had been fabricated and upgraded in readiness for assembly into the complete suit. Final performance tests were run with the same vacuum line plumbing (line length and ID) as would be used on the full suit. Data were taken at a range of heat removal rates with the subject at rest. Figures 42, 43, and 44 show the results of these tests. The performance of all patches

FOLDOUT FRAME

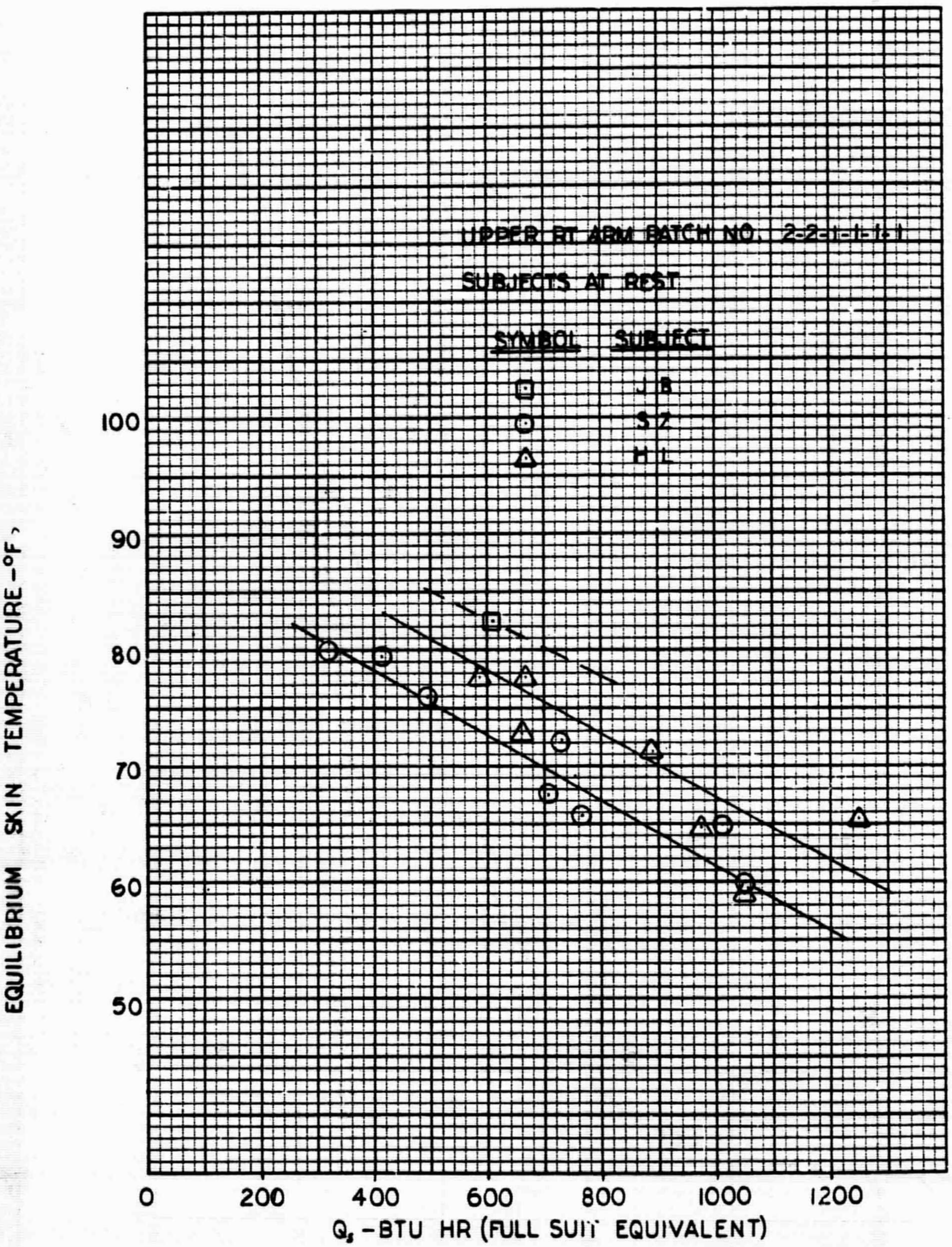

Figure 41. Steady State Skin Temperature Heat Removal Rates

FOLDOUT FRAME

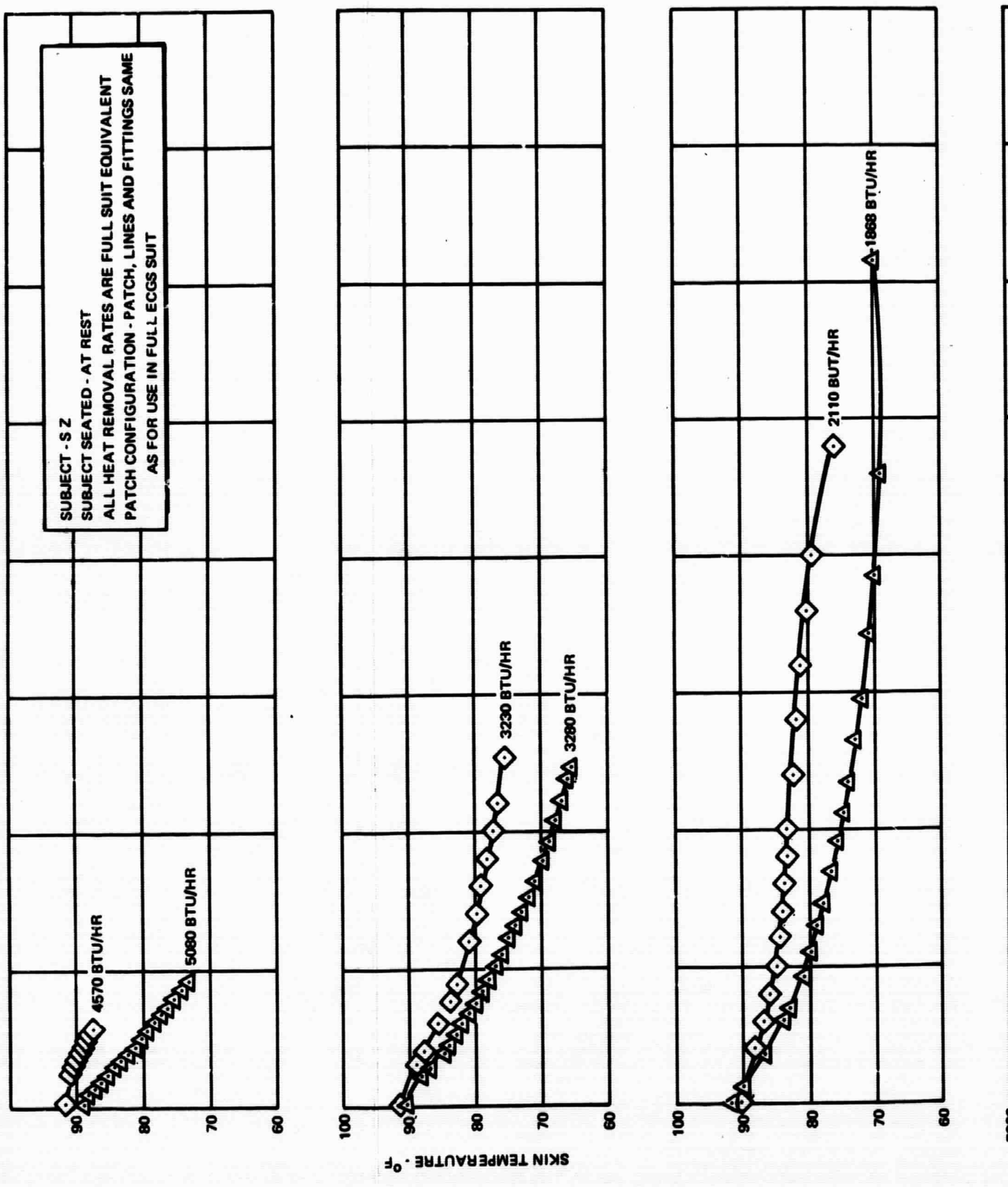

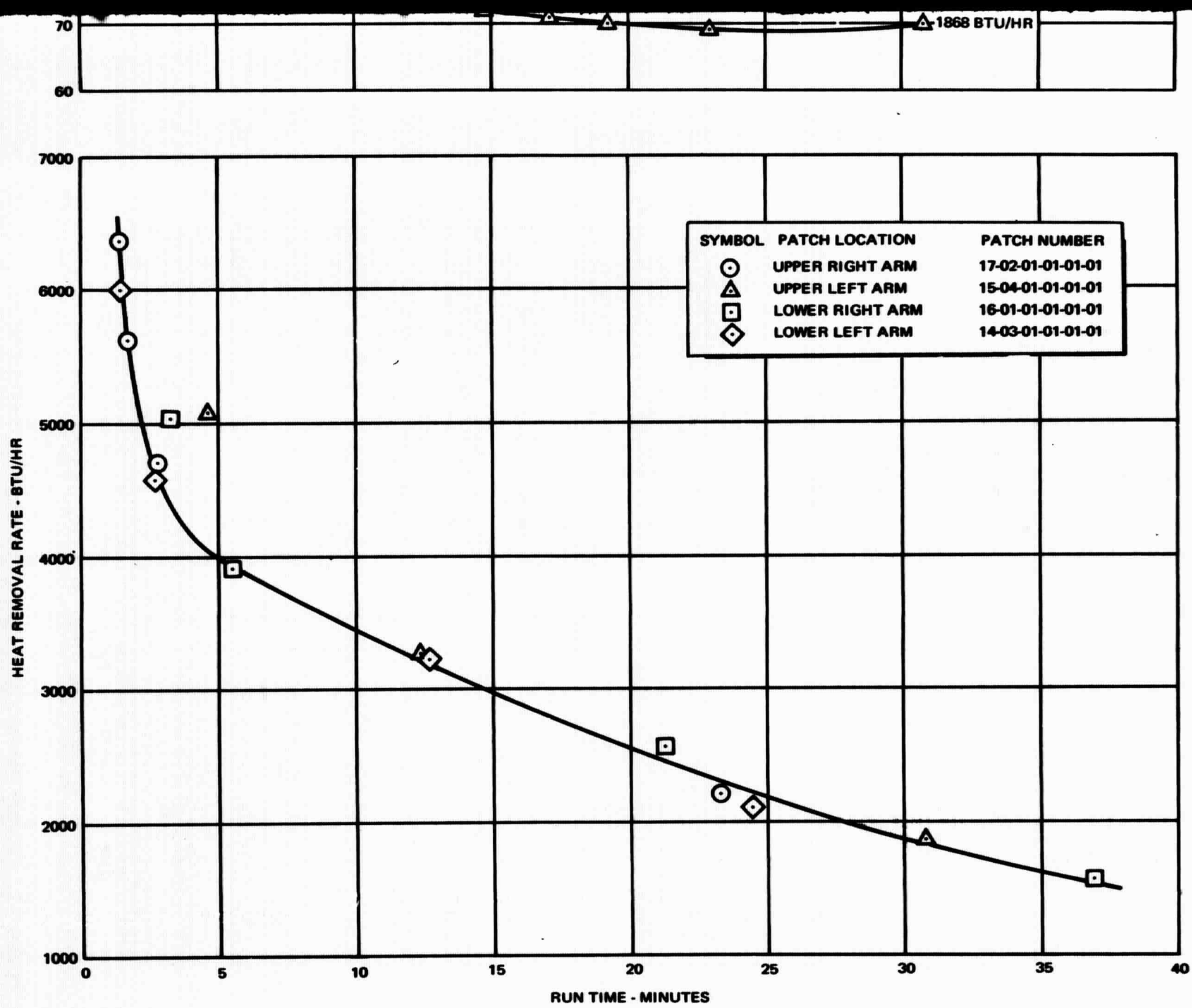

Figure 42. Full ECGS Individual Patch Performance - Upper and Lower Arms.

FOLDOUT FRAME

FOLDOUT FRAME

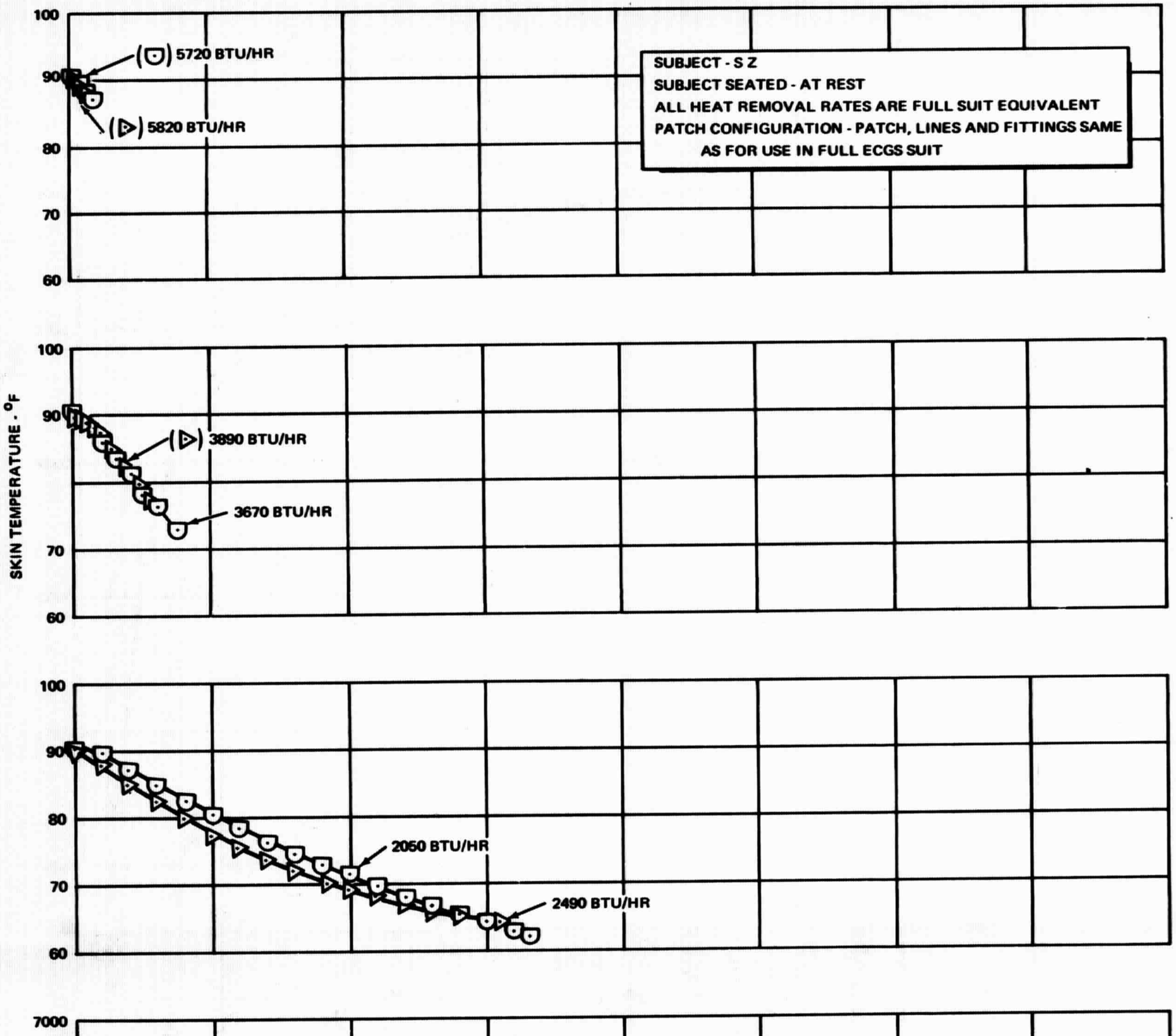

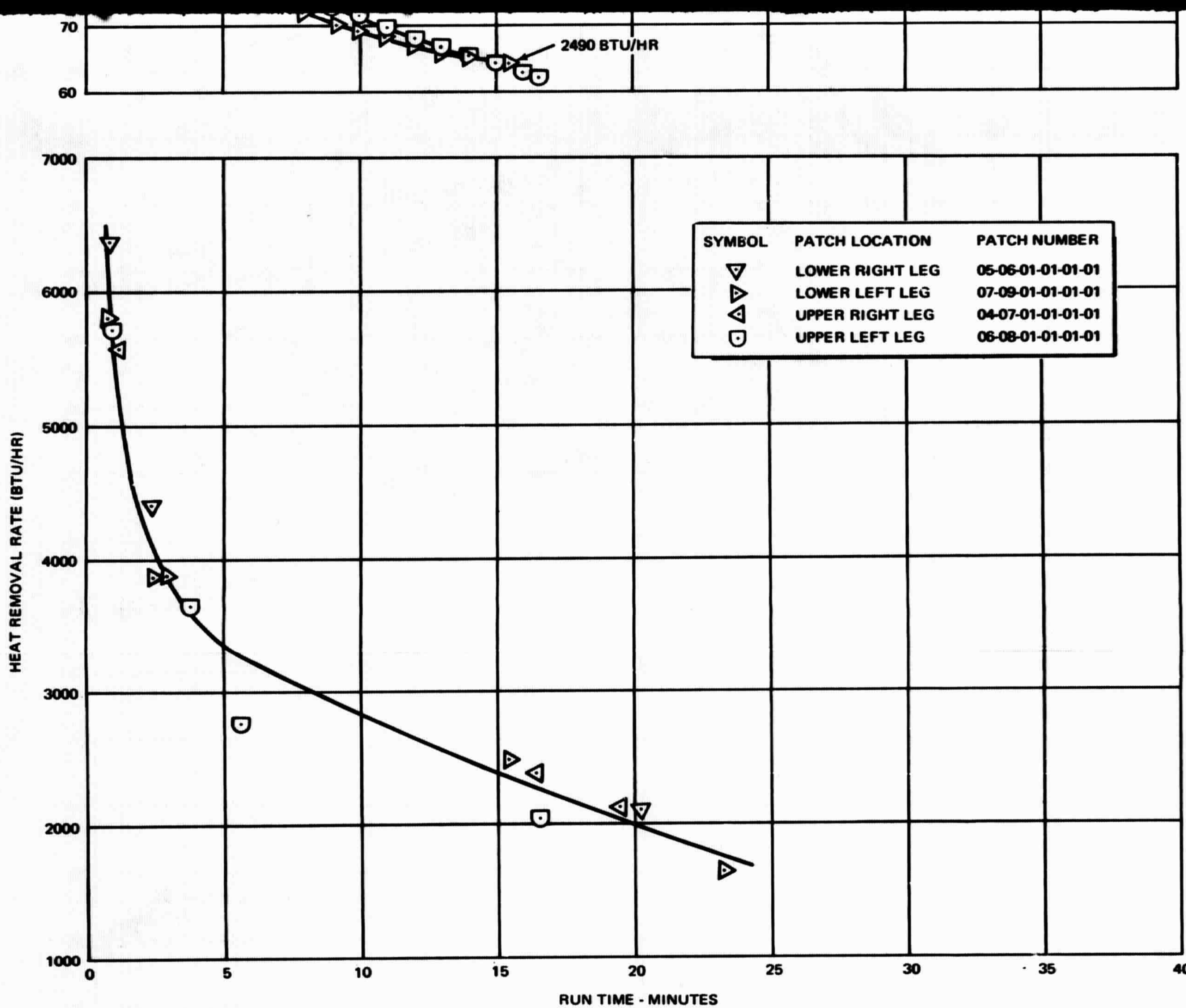

Figure 43. Full ECGS Individual Patch Performance - Upper and Lower Legs.

FOLDOUT FRAME

FOLDOUT FRAME

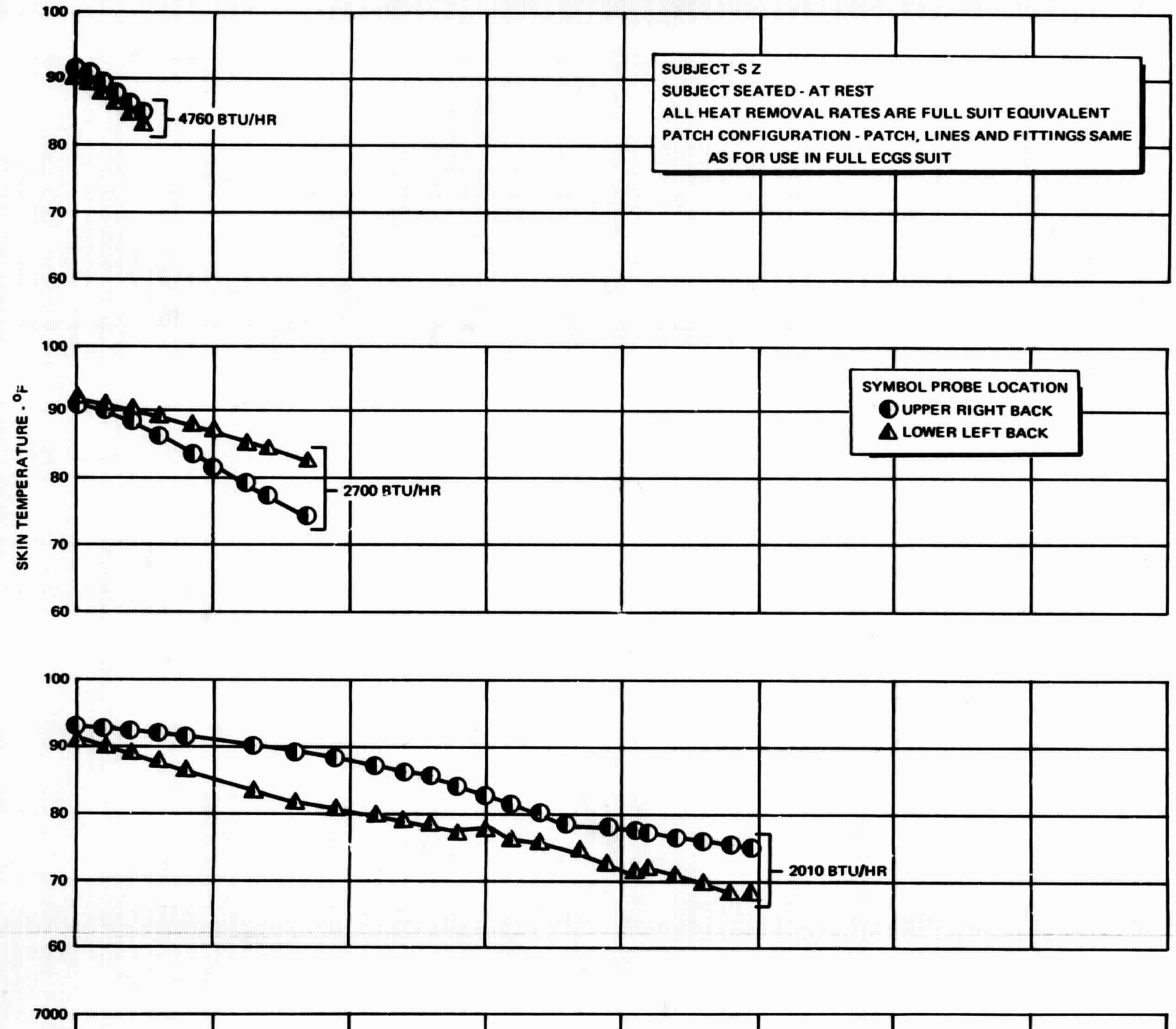

Figure 44. Full ECGS Individual Patch Performance – Torso Back (Patch Number 13-05B-01-01-01-01)

fell within a narrow range, indicating that each unit is capable of about the same performance. This is a desirable objective to assure the most uniform cooling of the subject as possible.

3.6 MEASUREMENT OF ECGS PATCH HEAT REMOVAL RATE

The measurement of the heat removal by the ECGS system is necessary in order to evaluate the system performance. Several methods of measuring this heat removal rate have been evaluated. The heat removed is directly proportional to the amount of water vapor removed from the patch. This fact makes the measurement of heat removal analogous to water vapor removal. Thus, a measurement of water vapor flow from the patch is a direct measurement of patch heat removal rate. The methods used to measure this flow include metering orifices, calibration of vacuum pump inlet pressure versus flow, and patch weight change during a run. The use of a metering orifice in the vapor removal line presents problems in obtaining accurate readings. The vacuum pressures are quite small; therefore, a very small pressure drop must be maintained across the orifice if flow is to be kept in the subsonic range. Calibration of an orifice is uncertain and measurement of the very small ΔP is difficult with any degree of accuracy. The above mentioned problems caused this method of vapor flow measurement to be abandoned early in the program. Calibration of the vacuum pumping system to determine flow of water vapor as a function of pump inlet pressure appeared to be a very simple, on-line, method of measuring the required flow. Attempts to calibrate the system included patch operation at fixed pump inlet pressure for a timed period and determination of water loss from the patch by weight difference. The results of these calibrations provided a rough indication of flow but the accuracy was not entirely satisfactory. The method finally used for most ECGS patch tests was a combination of pump calibration and weight change in the patch. During constant heat removal rate runs, the flow from the patch was throttled to maintain constant pump inlet pressure.

The test patch was accurately weighed before and after the run, giving the amount of water used. The time duration of the cooling process was recorded and, using the weight of water from patch weighings, the steady state or (in the case of variable heat removal) the average heat removal rate for the run was calculated.

PRECEDING PAGE BLANK NOT FILMED.

Section 4

DEVELOPMENT OF USAF ECGS CONFIGURATION (UPPER ARMS WITH FULL TORSO)

4.1 CONFIGURATION DISCUSSION

A contract requirement specified that two complete configurations of the ECGS be provided. The simpler of these configurations is the USAF version, which would include the front and back torso cooling patches, the upper arm patches, a water belt to supply the expendable coolant media, all vacuum lines, and all related plumbing and instrumentation. The complete ECGS was designed with this in mind; the upper and lower legs of the ECGS can be unzipped in one unit from the torso, together with the removable lower arms and headpiece. Both configurations share the water belt, the main torso vacuum-collector mainfold, and the multiple-pin thermistor plug for skin temperature instrumentation.

The ECGS torso suit splits from the hips to the armpits on both sides and the upper arm patches also split along a line that continues from the armpit to the elbow; this allows the complete garment to slip over the wearer's head like a poncho. The simple velcro zippering of the torso and arm splits and the velcro fastening of the torso bottom circumference to constant-wear slip on skin tight shorts complete the donning procedure. The water belt splits at the navel and is snapped in place with integral suspender straps. A single line connection to a vacuum source provides immediate cooling capability.

Sharp bends at the torso were not a requirement in the first phase of the program; therefore, no effort was made to provide flexibility. However, the torso suit can easily be used on the treadmill at very fast speeds without inconvenience to the wearer. If complete torso mobility is desired, it is entirely feasible to make the torso into four or more smaller articulated patches instead of the two large ones now being used.

The ECGS torso suit has been designed to integrate with the Apollo spacesuit by the simple replacement of the LCG fitting with an appropriate ECGS vacuum fitting. The spacesuit penetration holes would not have to be altered for this conversion. All water lines, together with pressure and thermistor instrumentation lines, may be routed through the LCG/ECGS penetration hole if desired. These lines are required only for test and evaluation and not for flight hardware.

4.2 PRELIMINARY PERFORMANCE TESTS

The heat rejection rates of the torso suit were converted to the full garment area, as was the case for the individual patch tests, to compare torso suit performance more easily with the 5,000-Btu/hr maximum-metabolic-rate design cooling objective.

Two typical performance tests on the ECGS torso suit configuration were made on the treadmill as shown in Figure 45.

Analysis of the data has established time-temperature curves for skin surface temperatures at selected areas under the cooling patches. These data are shown in Figures 46 and 47. On the first run (Figure 46), the system was operated with no throttling of the vacuum exhaust until one of the skin temperatures ceased to decrease. This was interpreted as an indication that the ECGS patch cooling in that area was running out of water. The cooling was shut off at this point, and the skin temperatures were allowed to recover at a normal rate during exercise. Throughout the entire run, the subject was walking on the treadmill at 4.5 mph and on a 2% grade. This corresponds to about 2,700-Btu/hr metabolic rate. The average ECGS torso suit heat removal rate, based on water used, was 1,895 Btu/hr or 4,630 Btu/hr for the full suit equivalent. The heat removal rate was an average value, because under the full open outlet vacuum valve type operation the heat removal rate begins initially high and then decreases as patch pressure and temperature decrease. In later runs, fixed heat-removal-rate tests were made to simplify the reduction of test data and to give better control of skin temperature.

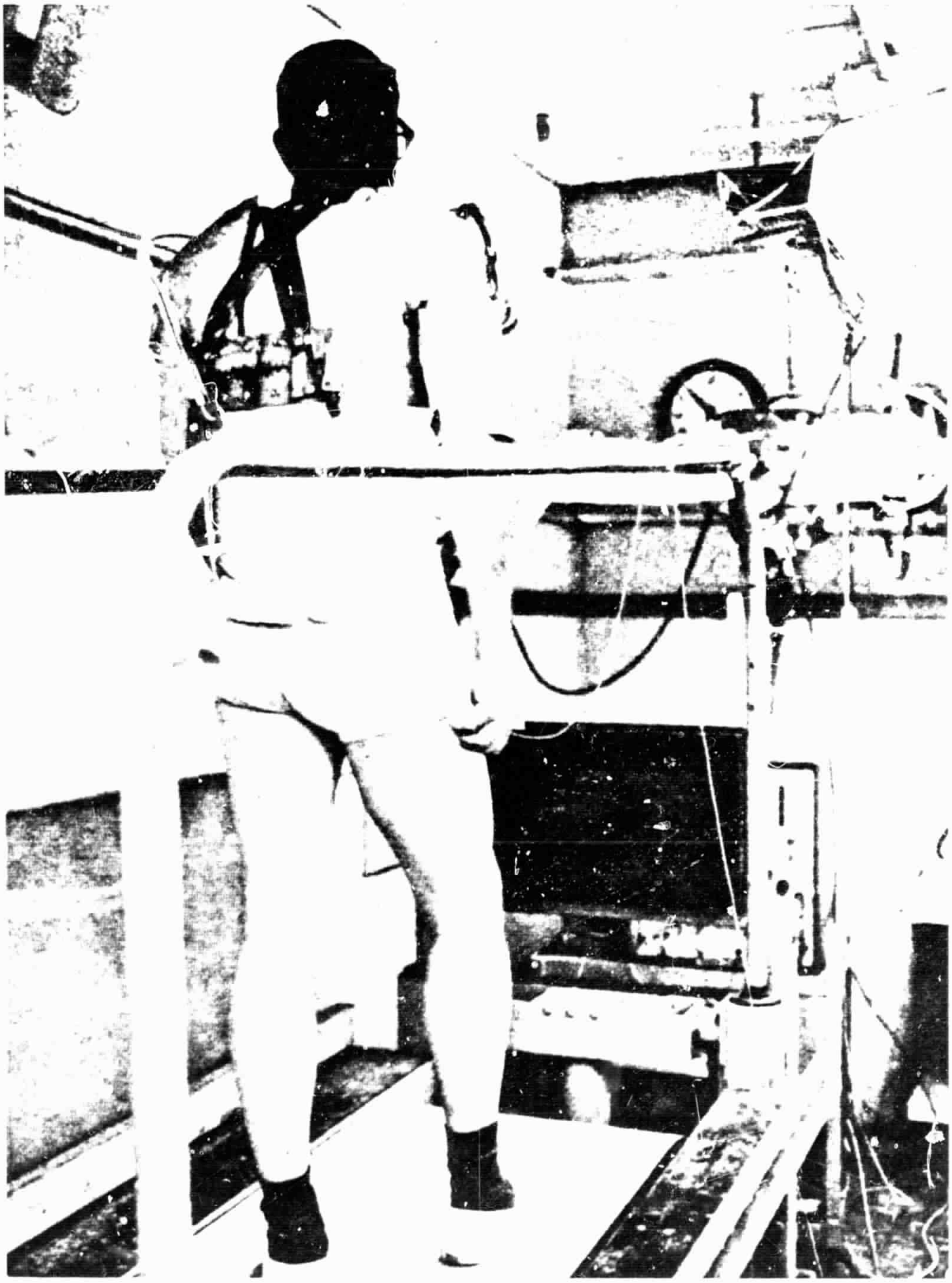

Figure 45. USAF Configuration

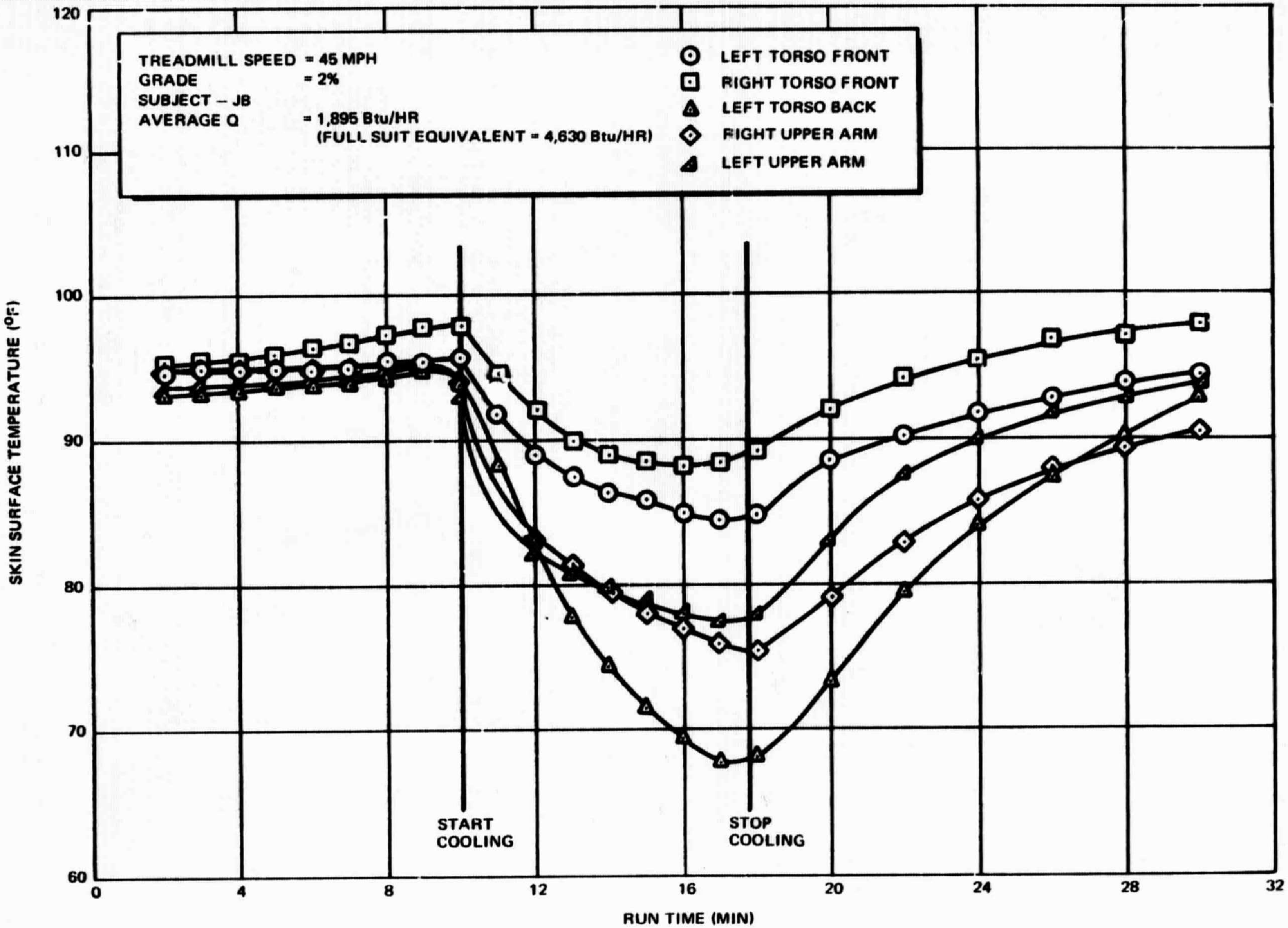

Figure 46. Skin Temperature Time History, Upper Arm and Torso Garment

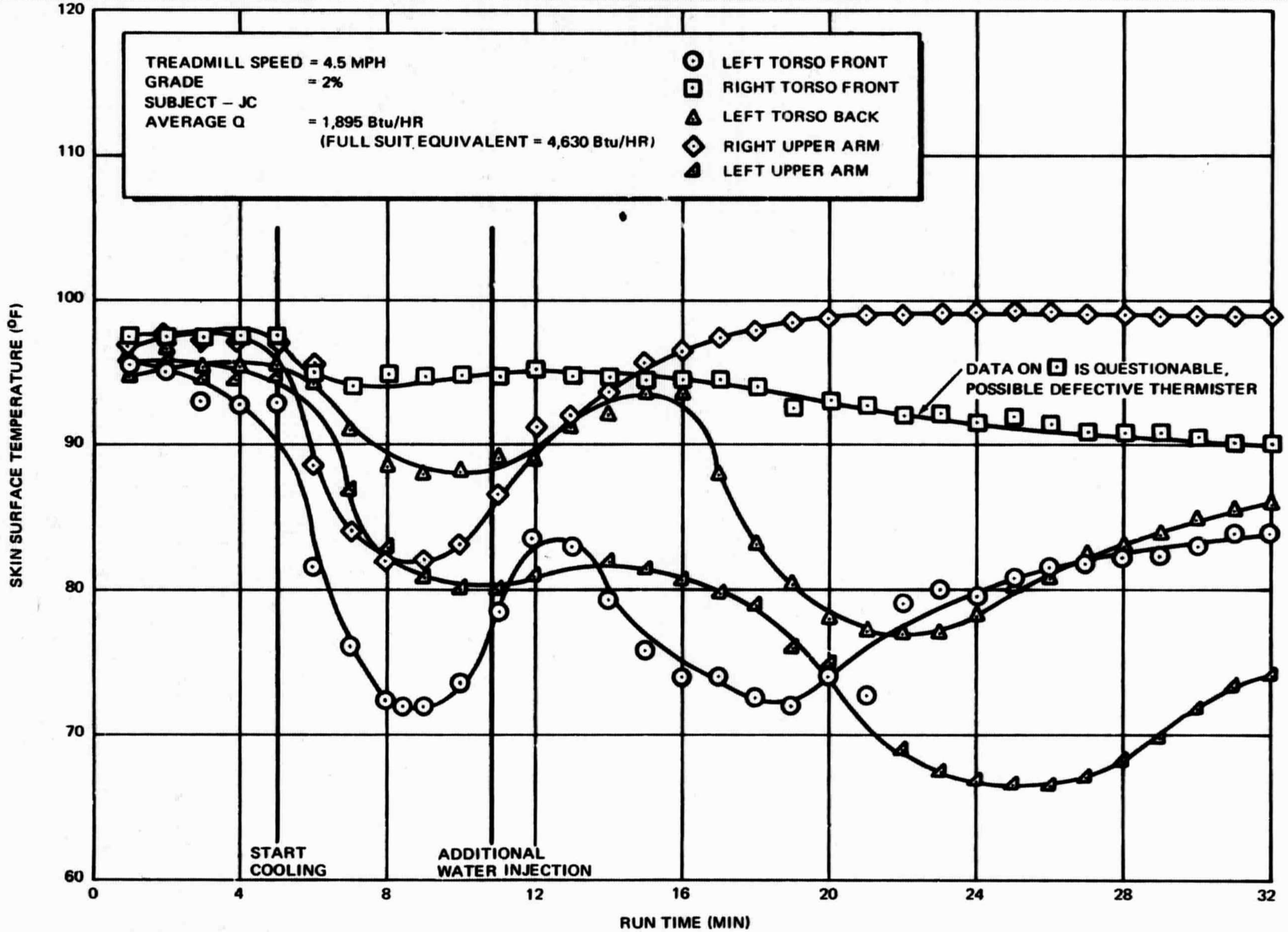

Figure 47. Skin Temperature Time History, Upper Arm and Torso Garment

The data from the second run (Figure 47) show approximately the same initial cool down. When the point at which the patches stopped reducing skin temperature was reached, water was injected into all of the patches at the theoretical use rate. It was found, however, that too much water was injected into some of the patches and this caused some liquid carry-over into the vacuum lines. This loss of water made it impossible to calculate an accurate heat removal rate for this run. The test subjects exercised at the same rate as in the first run (4.5 mph, 2% grade) for the entire run. Further experimentation will determine the time and quantity of water that must be injected into each patch to prevent liquid carry-over. Because of a transducer calibration error, recorded patch pressures are not reliable for either of these two runs.

Two additional runs were made with the steam exit throttle valve wide open. The subject was wearing shorts and the USAF ECGS upper arm and torso garment configuration. Exercise level for both tests was 3,420 Btu/hr, which was obtained by having the subject walk on the treadmill at 4.5 mph and on a 4% grade. Figures 48 and 49 show the skin temperature versus time for these runs. Steady state conditions were not obtained in these tests. Figure 50 shows the maximum and minimum pressure recorded in each patch during the second run. Figures 51 and 52 show the pressure drop inside each patch and from each patch to the collector respectively. The back torso pressure level is higher than the other patch pressures; this may indicate a higher heat output of this part of the body.

Two more runs were made to determine the suit performance at fixed heat removal rates. Skin temperature versus time for these runs is shown in Figures 53 and 54. In both cases, the exercise level was maintained at 4.5 mph and on a 4% grade on the treadmill; this produced an energy expended level of 3,420 Btu/hr. In run 502 (Figure 54), a severe leak developed in the collector fitting at about 30 min into the run. The exact time when the leak began is not known, so the last half of these data is questionable and is shown for reference only.

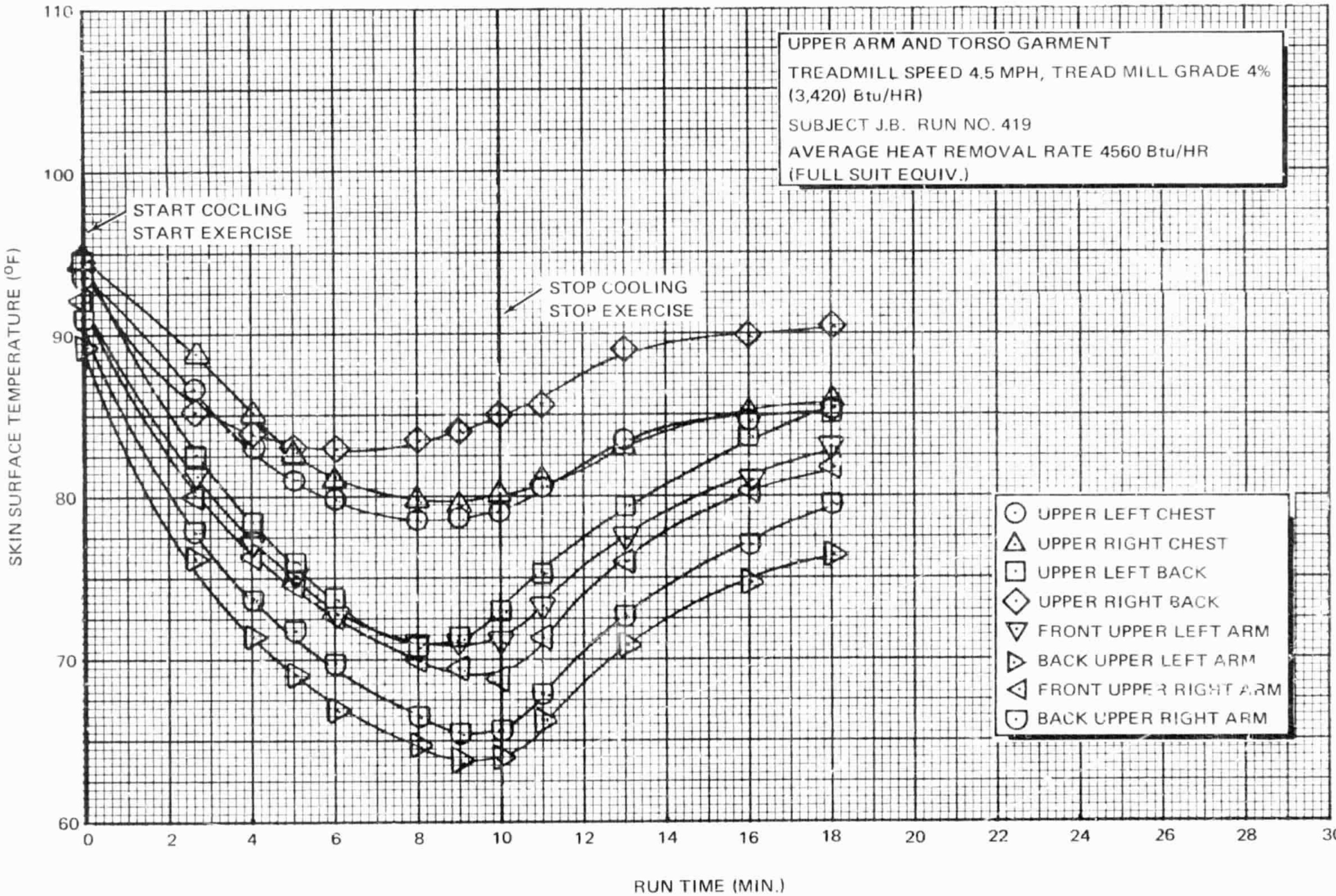

Figure 48. Skin Temperature Time History – Run 419

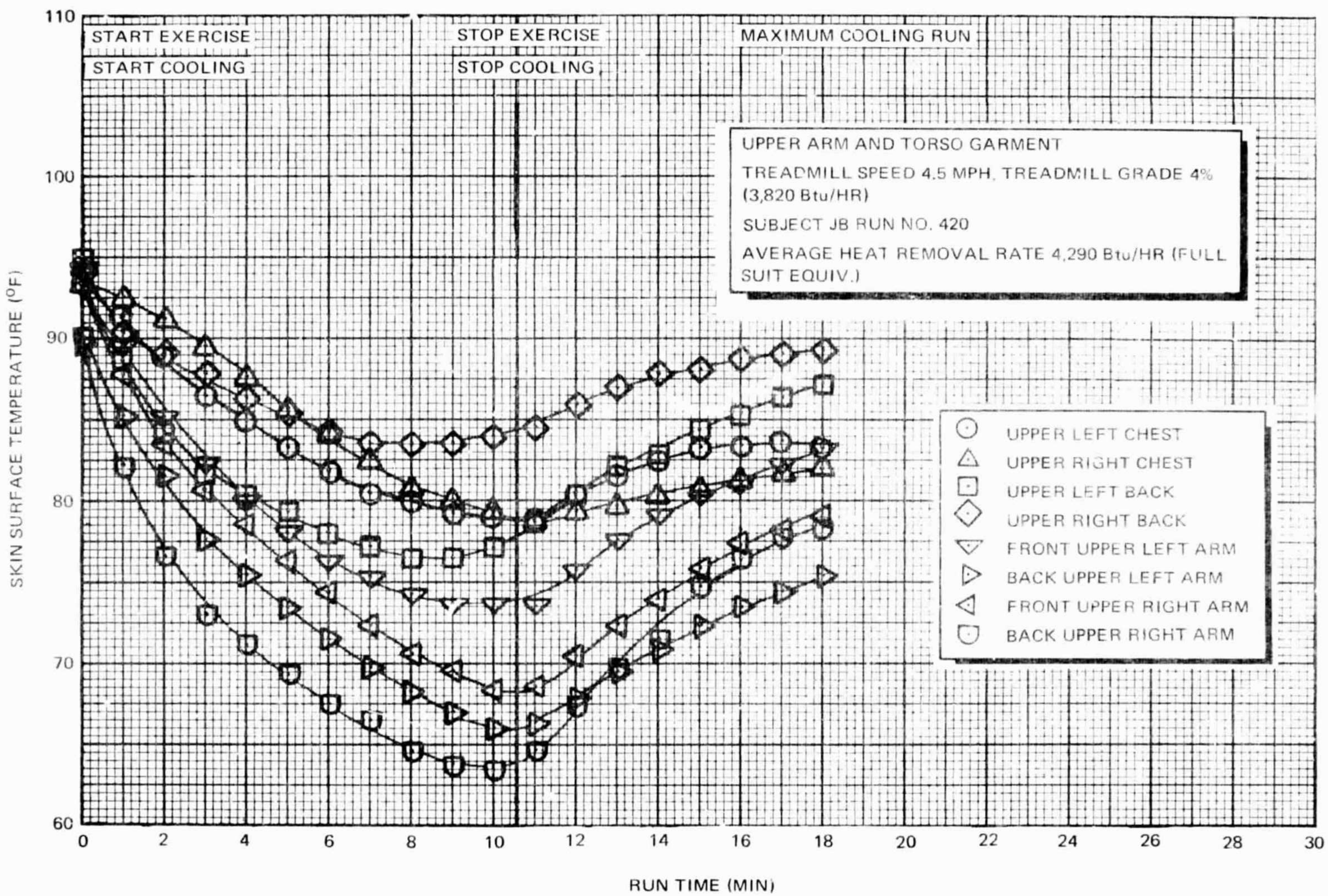

Figure 49. Skin Temperature Time History – Run 429

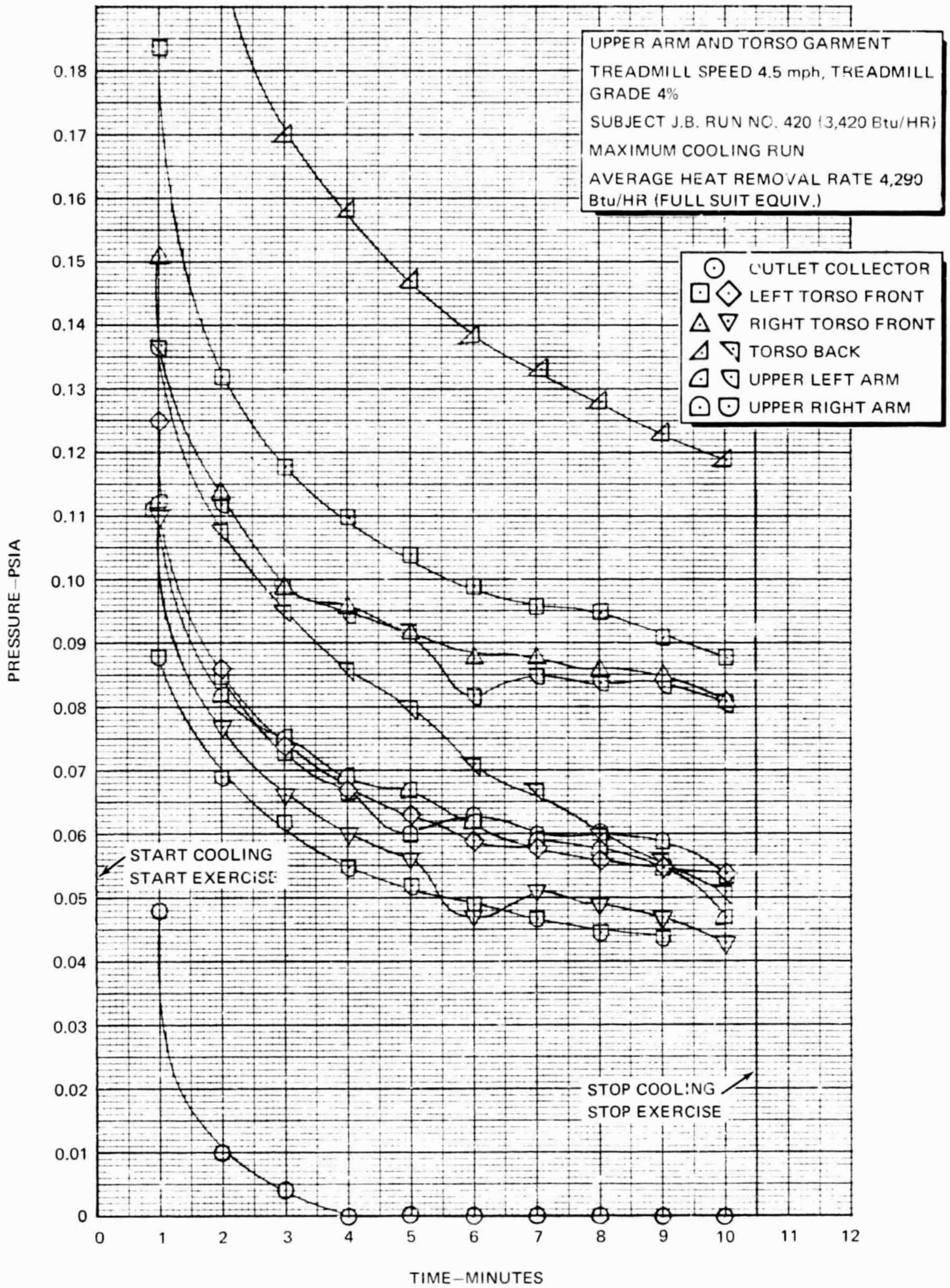

Figure 50. Patch Pressure Time History – Run 420

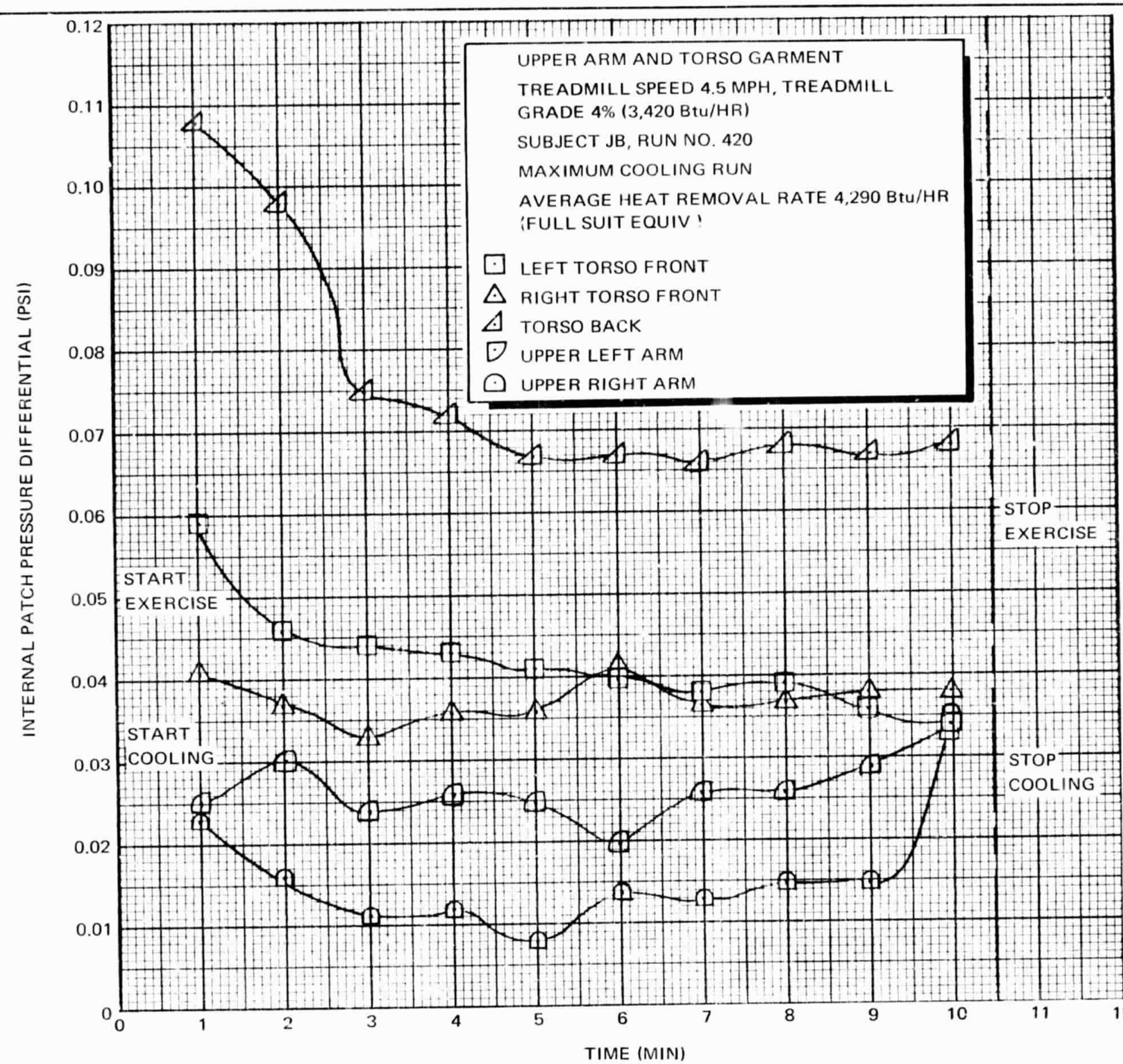

Figure 51. Patch Pressure Differential Time History – Run 420

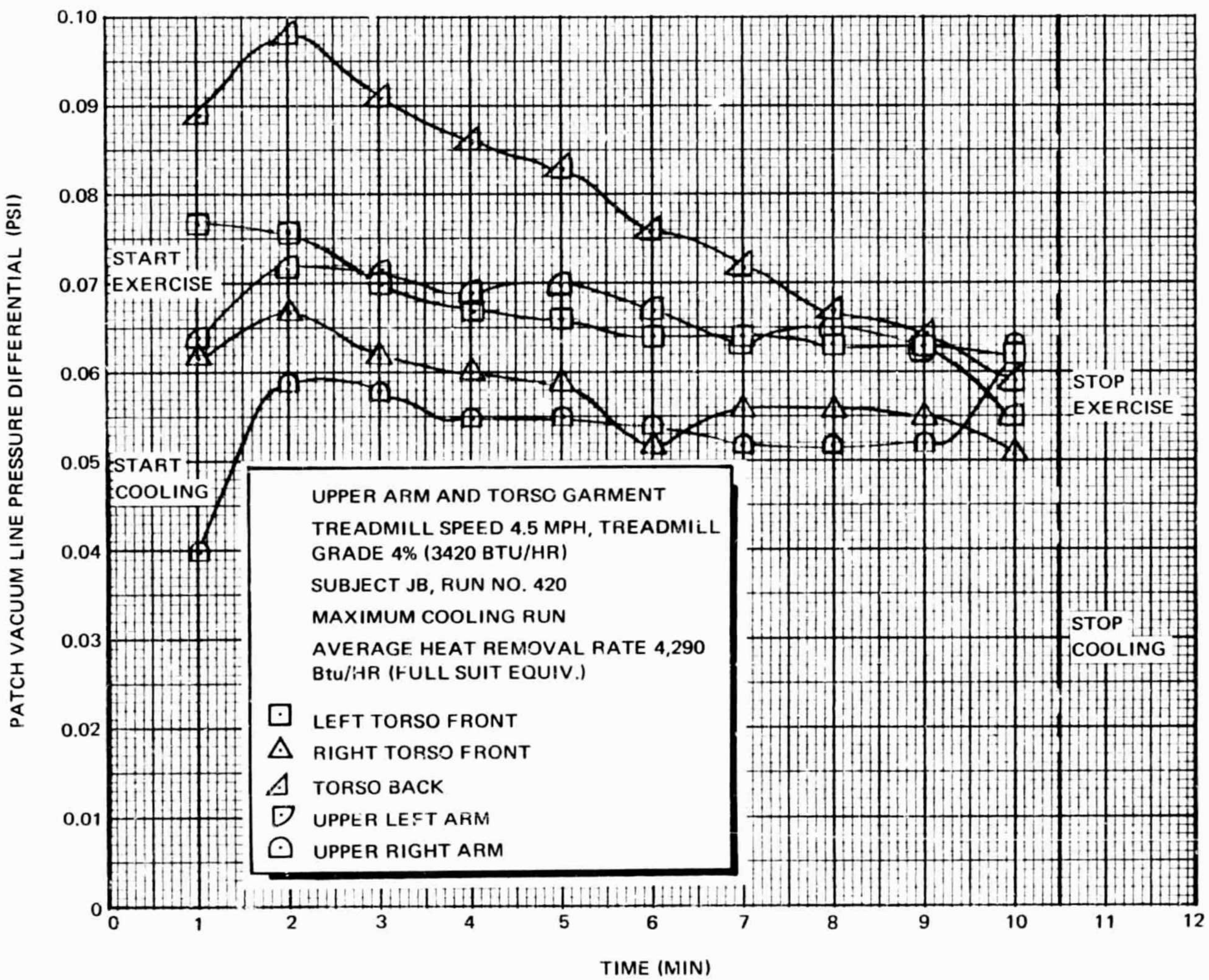

Figure 52. Patch to Outlet Pressure Differential Time History – Run 420

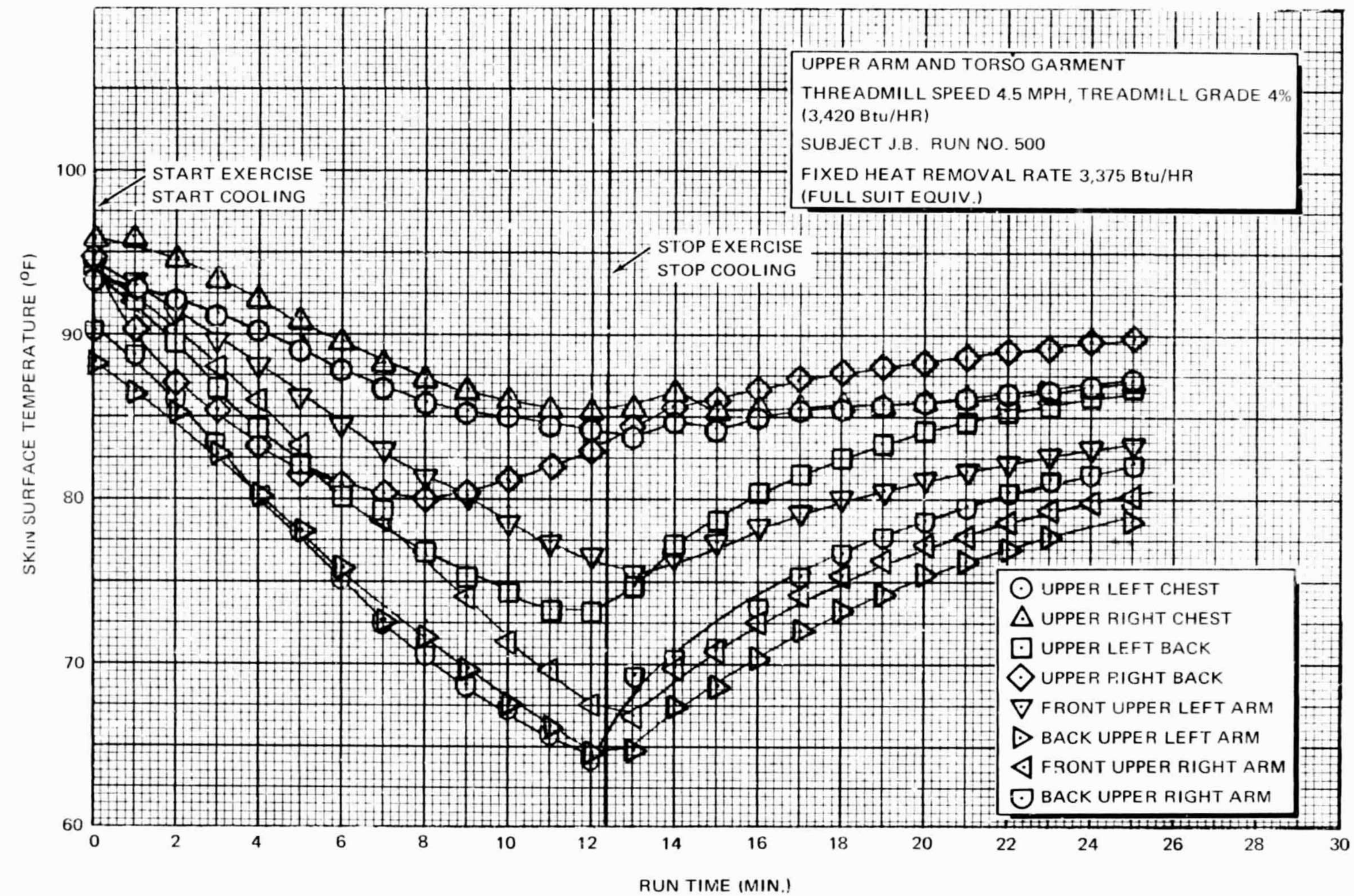

Figure 53. Skin Temperature Time History – Run 500

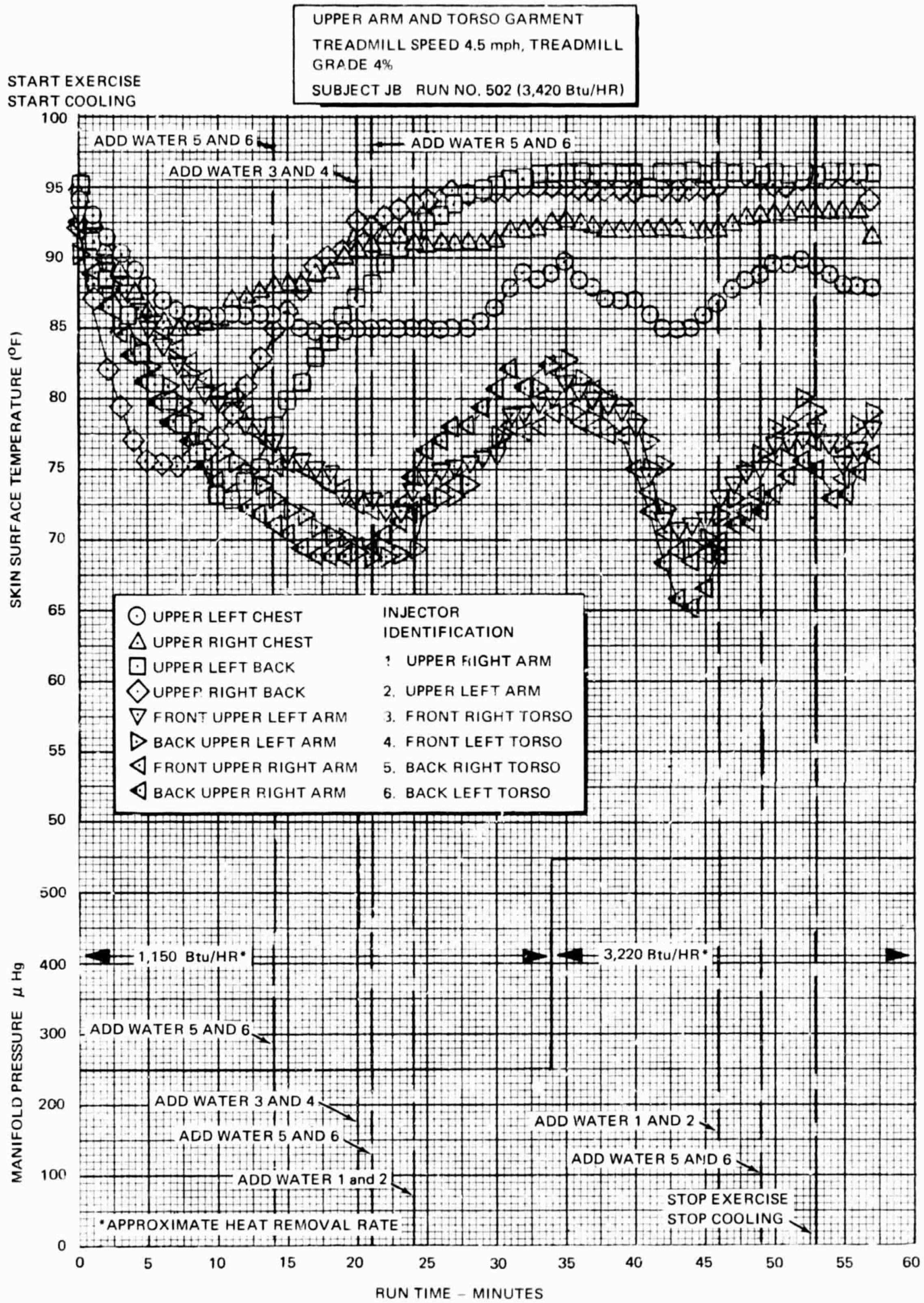

Figure 54. Skin Temperature Time History – Run 502

A test was made to determine the conditions that were required to maintain stable skin temperatures in the torso area. The data from this run are shown in Figure 55. At each exercise level, vacuum manifold pressure (an indicator of steam flow) was adjusted to obtain a stable skin temperature in the 85° to 90°F range. Insufficient time was allowed for conclusive stability determinations in this first attempt; however, the temperature time data indicate that some degree of stability was obtained at each exercise level, except that the peripheral blood circulation in the upper arms appears to have been reduced during the last half of the run.

Water was injected into the patches when it seemed, by skin temperature, that the patch was not being cooled. The times when water was injected and the patches to which water was added are shown in Figure 55.

In addition to the above data, heart rate was recorded during all the test runs. These data are shown in Figure 56. Further analysis of cooled versus uncooled heart rate will be made to evaluate the effect of various cooling rates combined with exercise on a subject's heart rate.

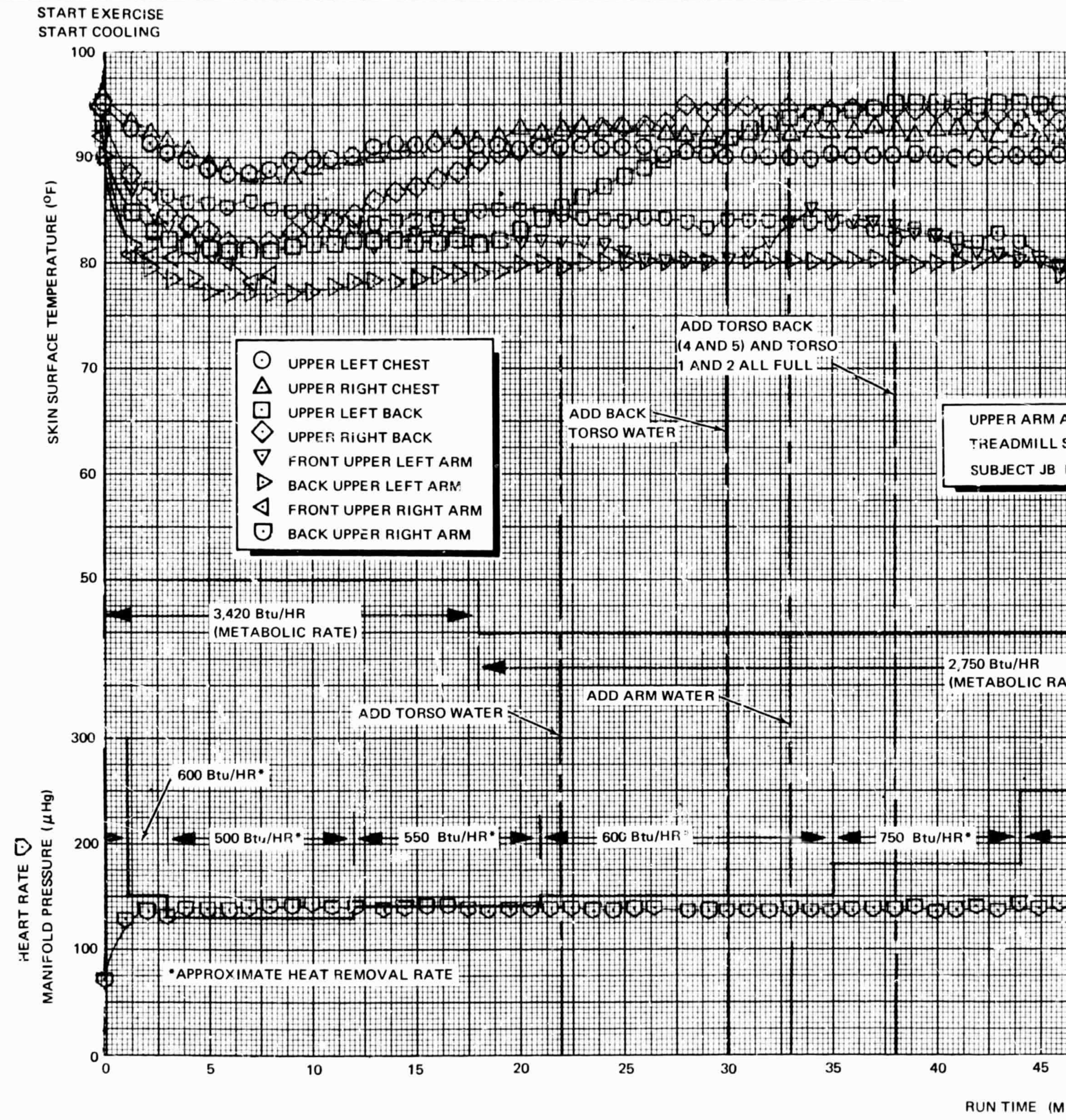

START EXERCISE
START COOLING
SKIN SURFACE TEMPERATURE (°F)
HEART RATE
MANIFOLD PRESSURE (μHg)
UPPER LEFT CHEST
UPPER RIGHT CHEST
UPPER LEFT BACK
UPPER RIGHT BACK
FRONT UPPER LEFT ARM
BACK UPPER LEFT ARM
FRONT UPPER RIGHT ARM
BACK UPPER RIGHT ARM
ADD TORSO BACK (4 AND 5) AND TORSO 1 AND 2 ALL FULL
ADD BACK TORSO WATER
3,420 Btu/HR (METABOLIC RATE)
2,750 Btu/HR (METABOLIC RA
ADD ARM WATER
ADD TORSO WATER
600 Btu/HR*
500 Btu/HR*
550 Btu/HR*
600 Btu/HR*
750 Btu/HR*
*APPROXIMATE HEAT REMOVAL RATE
UPPER ARM A
TREADMILL S
SUBJECT JB
RUN TIME (M

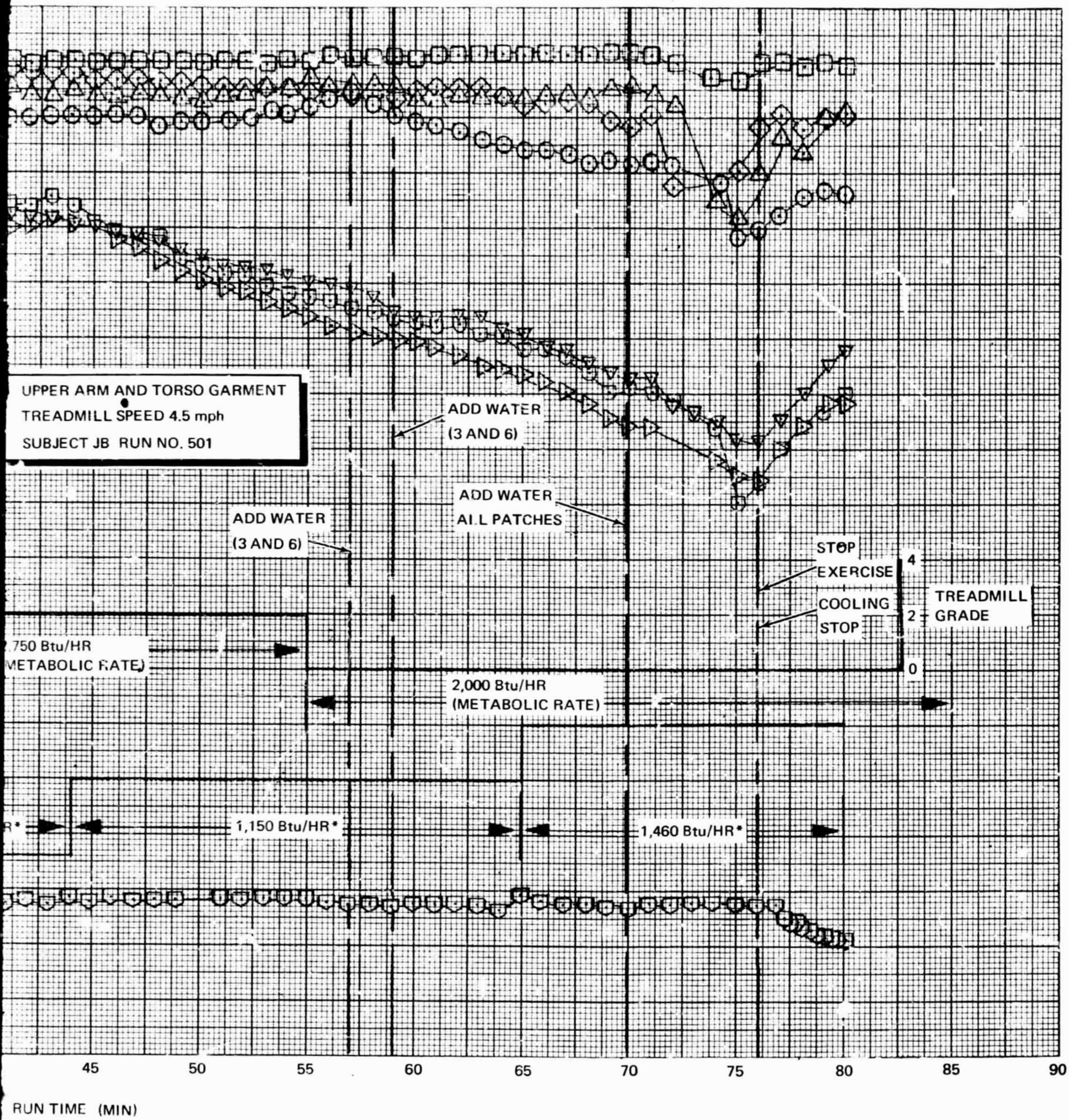

Figure 55. Skin Temperature Time History – Run 501

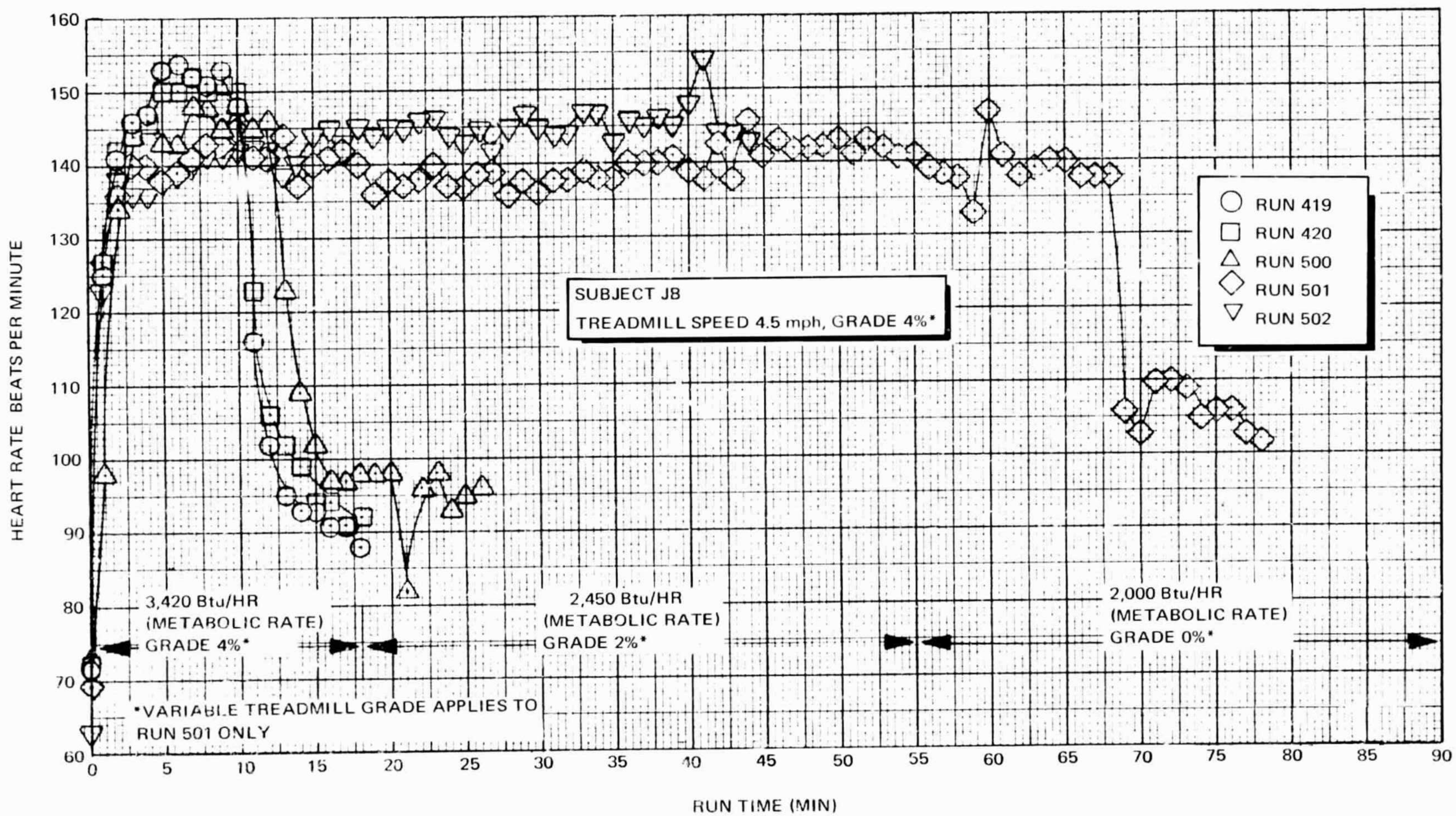

Figure 56. Heart Rate Comparison – Upper Arm and Torso Cooled with ECGS

Section 5
DEVELOPMENT OF NASA ECGS CONFIGURATION
(UPPER AND LOWER ARMS AND LEGS WITH FULL TORSO AND HEAD COOLING)

5.1 CONFIGURATION DISCUSSION

Aside from performance, the primary purpose of the complete ECGS suit design was to develop a garment that could be comfortably worn for extended periods and for at least 4 hours of sustained heavy treadmill work. The required criteria were that full running mobility would be attained and that no part of the suit would sag or get out of position during the exercise period. A time-consuming process of trial and testing was required before these criteria were met satisfactorily. Some of the typical problems were as follows:

- Lower arm slippage to wrist.
- Lower leg slippage to ankle.
- Torso, arm, and leg patch abrasions at the corresponding split lines.
- Shoulder bone discomfort.
- Hip abrasions of torso.
- Suit adjustments to compensate for subjects varying from 140 lb (5 ft, 10 in.) to 190 lb (6 ft, 2 in.).
- Test subject recovery from skin abrasions.
- Upper arm abrading armpit.
- Torso expansion to allow sustained deep breathing.
- Wearing out of flexing parts during many hours of testing.
- Abrasions caused by multiple thermistor harness (now integrated with the ECGS).

On several occasions, the cooling effectiveness was so great that the subjects were insensitive to pain at the low skin temperatures and therefore had bleeding skin abrasions that were caused by friction with suit imperfections. As much as 2 weeks was sometimes required before the subjects healed enough to be able to don the suit again for a high activity run (by this time, the suit difficulty had been corrected).

During the time that the suit was not being tested or calibrated, it was being modified to increase wearing comfort. These "bugs" have been worked out so that the same suit can now be worn by either of two subjects (one 30 lb lighter than the other) during a 4-hour treadmill run with no discomfort.

Wearing comfort and ease of donning were both considered in the design of the ECGS garment. Although the capability is not a requirement in the current program, it is forseeable that the wearer of the ECGS could don the garment without assistance.

The ECGS cooling headpiece was designed and tested under the MDAC IRAD program, and was developed for use as a part of the complete ECGS system. The headpiece includes a forehead and back-of-the-head skull cap with a wide-band cooling chin strap. The chin strap can be alternately positioned on the front and sides of the neck directly below the jaw. Heat rejection tests to determine which position produces the most cooling have been inconclusive. The headpiece also includes the standard NASA Apollo earphone/microphone gear, which is fully integrated with the ECGS.

5.2 INTEGRATION WITH SPACESUIT

The primary problem in integrating the ECGS with the Apollo space pressure suit was to provide adequate clearance between the two suits. The problem was accentuated by the size of the Apollo pressure suit that was provided for the contract as GFE; this suit was somewhat tight for the 6-ft, 180-lb test subject. Each patch was provided with an elbow exhaust vacuum fitting that protruded from the patch surface about 1 in. This caused interference problems, particularly in the lower arms and legs. Subsequent to the first design, all fittings were replaced by thin-wall, elliptical cross-section elbows that protruded less than around a curve, would fatigue in time, and the patch would have to be repackaged. Further development in this area could not be afforded, so the use of PVC was elected as a compromise.

Membrane-to-Fitting Attachment

The patches had to be designed so that body weight (such as the weight from leaning against the back torso vacuum fitting) would not tear away the 4-mil thickness membrane to which it was attached. This problem was avoided by sewing the fitting to the interior of the patch and leaving the membrane unloaded, except for its vacuum sealing duty. There were occasional membrane-to-fitting leaks, but not once was a vacuum fitting torn loose from a patch.

Highly Flexible Vacuum Lines With Low Pressure Drop

All patches are vacuum connected to the ECGS "octopus collector" manifold located near the heart. This requires that the arm, leg, and headpiece patches have flexible vacuum lines at least in every body articulation area, such as the knee joint. During a typical treadmill run of 2 hours at 4.5 mph, the knee joint will flex through an angle of about 30° about 7,580 times; this is sufficient to cause metal fatigue. Early in the program, Teflon corrugated vacuum tubing made by Penntube Plastics Company was ordered to be used on flexible joints. This tubing had excellent flex characteristics but the inside-diameter sizes, internal pressure drops, and vacuum fitting sealing problems led to the use of brass flex bellows tubing. The brass flex had all the advantages of the Penntube product, but the weight was high, and fatigue soon caused leaks at the highly used articulation joints on the body. The brass flex tubing was then encased in PVC thin-wall tubing with end joints sealed by heat shrinkable plastic tubing; this solved most of the leak problems but not metal fatigue. The final solution was to use both materials (brass and Teflon flex) in different parts of the ECGS. An acceptable performance compromise has been reached on the delivery hardware, but reliability, weight, and bulk factors can be improved.

half the original distance. The vacuum lines and all of the plumbing and instrumentation that would normally be outside of the patches were covered by a zippered liner to keep the entire outer surface of the ECGS smooth and free of obstructions. The only exception to this was the single outlet vacuum fitting near the heart that served as the penetration through the LCG fitting in the pressure suit. The changes allowed integration of the ECGS with the Apollo pressure suit. Even the largest subject could don both suits and move with relative ease. Figure 57 shows a subject in the completed ECGS.

There turned up an unexpected bonus on the donned ECGS with an open vacuum valve, which will help the astronaut both with and without the spacesuit (during IVA). All cooling patches are normally loaded with a wick water supply, and roughly one-half the body area is in contact with this wet wicking as separated by the thin patch to skin membrane. It was found that a 5-psia pressure exposed to the open vacuum valve produces enough phase change as a result of normal evaporation of wick water, to provide low level cooling. This could reduce or possibly eliminate the space suit ventilation air requirement during certain low-level resting conditions.

A modified vacuum collector has been devised that can enclose all ECGS water supply lines, pressure instrumentation lines, and each patch vacuum line; all of these lines pass through the single LCG penetration on the spacesuit. A sketch of this fitting is shown in Figure 58. The new fitting restricts the steam flow passage more than the previous design, but eliminates the need for a second suit penetration for water and instrumentation lines. Any part or all of this restriction can be removed, but this depends on the percentage of the pressure instrumentation used.

5.3 DESIGN AND FABRICATION PROBLEMS

There were numerous areas in the design of the ECGS garment that required special attention. In every area, off-the-shelf materials and parts were used; the sole objective was to get something quickly that would work well enough to show the feasibility of the total concept in the laboratory. In many

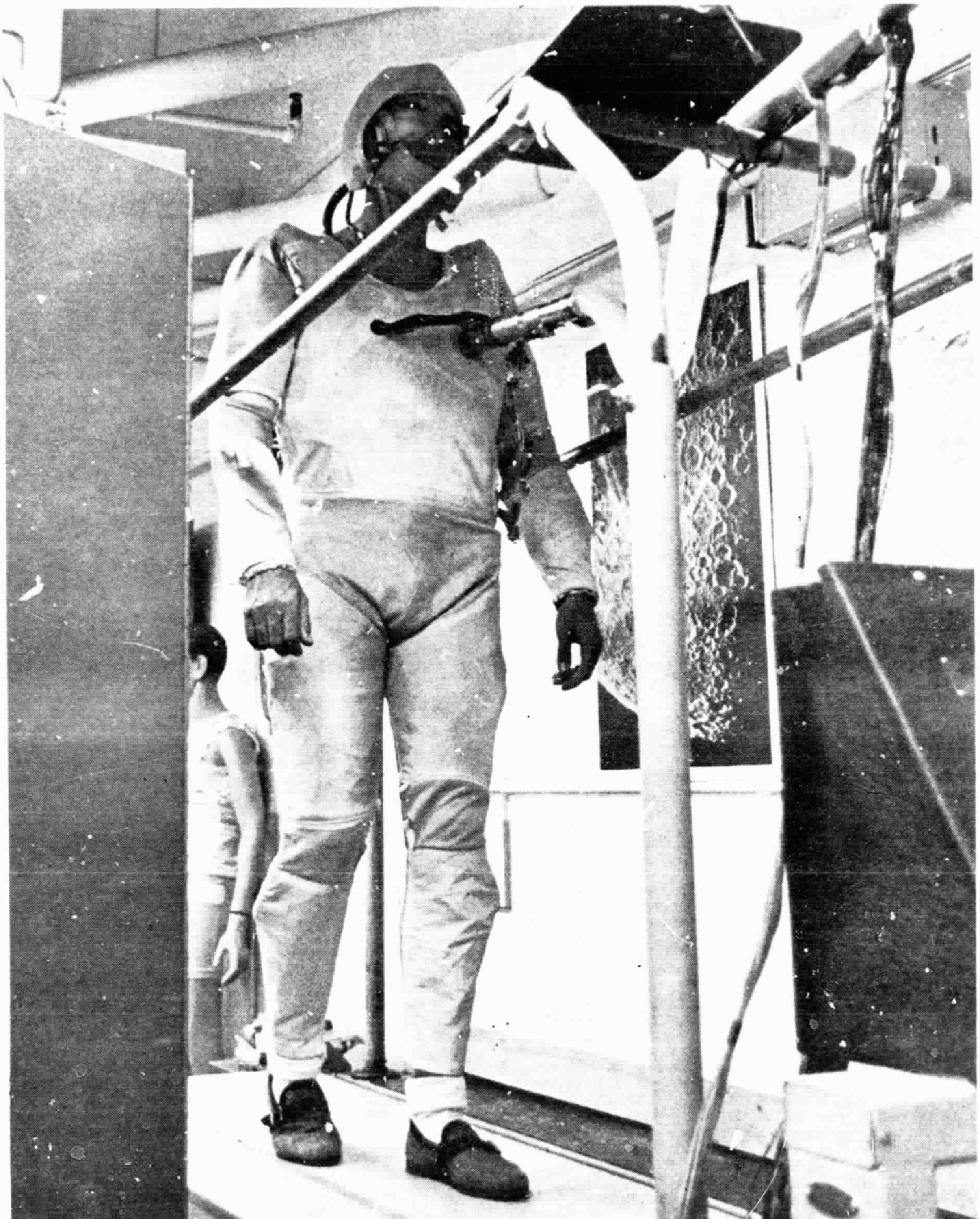

Figure 57. Completed ECGS

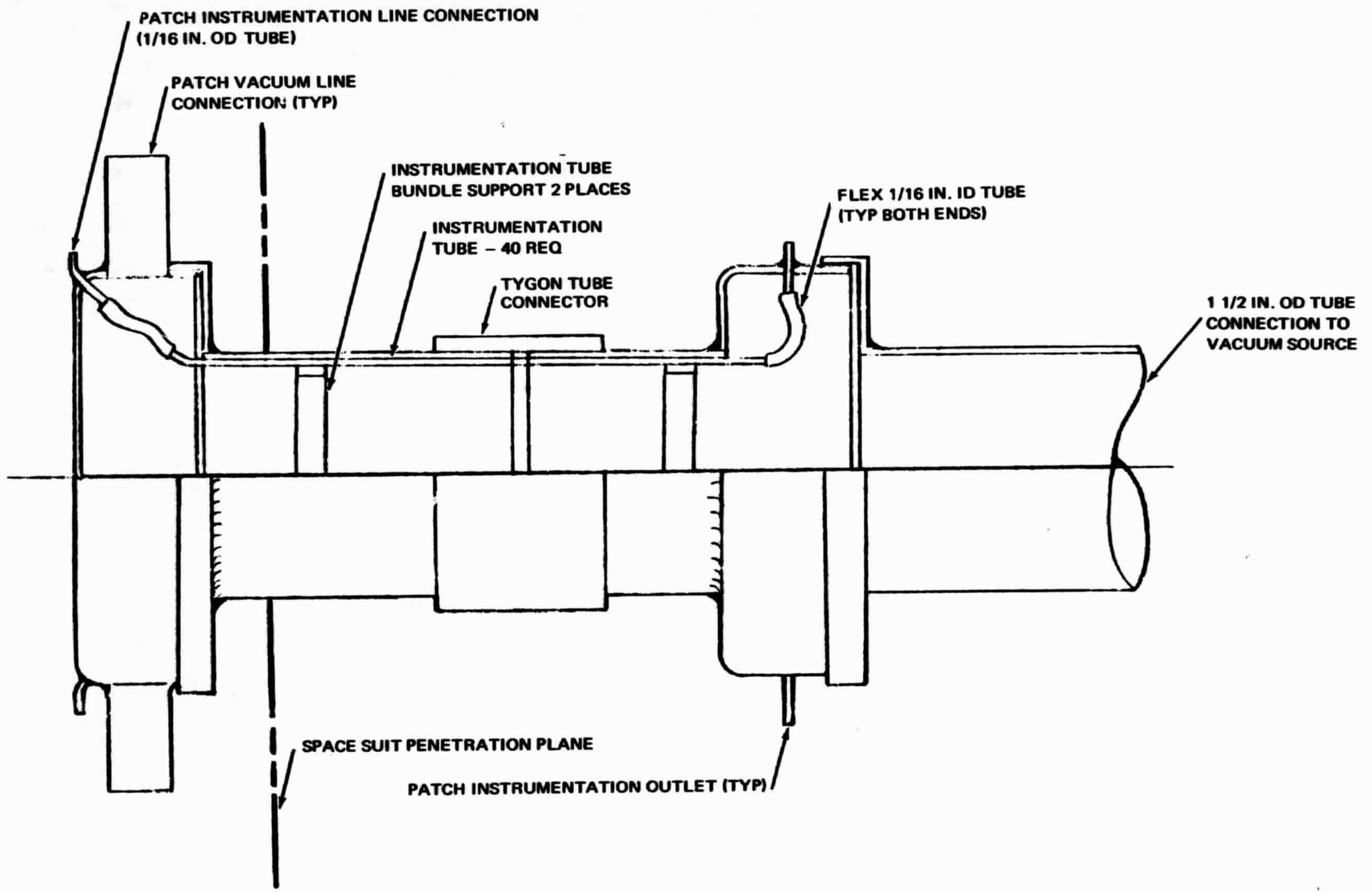

Figure 58. ECGS–Spacesuit Penetration Fitting

instances, poor or improper materials and/or parts were used that caused problems; however, these problems were tolerated in the interests of time and economy. The design approach, by necessity, was strictly one of serendipity, with no formal drawings and very few sketches. A typical component was conceived, built under oral instructions, tested, and modified on the spot as required; modifications were strictly guided by function and performance. Reliability and quality assurance, again by budgetary necessity, were not considered during the program.

The following list presents typical design problem areas; each will be discussed in later paragraphs.

- Membrane-to-membrane sealing.
- Membrane-to-fitting attachment.
- Highly flexible vacuum lines with low pressure drop.
- Attachment of patches to vacuum lines.
- Water-line penetration.
- Pressure-tube penetration.
- ECGS vacuum collector.
- Thermistor harness.
- Leaks in the vacuum system.
- Wearing comfort (see Section 5.1).

Membrane-to-Membrane Sealing

Two membrane materials were chosen for the patches, but neither of these should be considered to be near the optimum. The materials were PVC and Vacpac, each of which had advantages for the initial program. PVC heat-seals very easily, but it has very poor abrasion resistance and cannot stand rough treatment. PVC is also quite porous for vacuum work. Vacpac, on the other hand, has excellent physical properties, but heat-sealing techniques were unknown. Experiments on a heat-sealing machine showed, however, that the material could be sealed; and it appeared that an easy, early solution had been found to the material problem, but such was not the case. It turned out that a heat-sealed joint, and particularly an overlapping seal that had progressive tangential line seals

Attachment of Patches to Vacuum Lines

The normal maintenance and upgrading of the patches required that all connections to these patches be quickly removable, such as vacuum, water, and pressure lines. Soft gum rubber sleeves have excellent vacuum characteristics when connecting two pieces of tubing, except for the need to resist tension at the joints. On several occasions, some of these joints have parted during heavy treadmill activity, and shutdown has been required to permit reconnection. Again, a laboratory compromise route was taken.

Water Line Penetration

Early in the program, the water lines had their own separate penetration points into the patches. This caused undue complications and leak sources. Subsequently, the patch water lines were terminated within the patch outlet vacuum fitting; a slip-on connection is made through the fitting wall prior to attachment of the vacuum flex line. This procedure works very well and only one external water line per patch is required. Internally, the single water line feeds a manifold that has multiple outlets to all regions of a given patch. An internal patch water leak cannot be detected, and if one should occur, the patch performance should not be grossly affected.

Pressure Tube Penetration

Pressure tube instrumentation would not be required for flight hardware except as necessary for a sensor input in an automatic control heat rejection mode of operation. Each patch has a six-tube pressure penetration through a single hole. This hole is sealed by a type of bulkhead fitting similar to the vacuum outlet fitting; internal pressures at six different locations can be measured if desired. A second static pressure measurement penetration is located in the patch outlet vacuum fitting, which can allow internal patch pressure drops to be measured. A second static pressure top is installed at the ECGS "octopus collector" manifold, which can allow each vacuum line pressure drop to be measured.

Thermistor Harness

Skin temperature measurements were very important in the ECGS development; the thermistors were initially taped on various parts of the body, which required considerable setup time for each run. A thermistor harness was designed into and became a part of, the final delivery hardware. Several times the thermistor leads were rerouted to minimize wearing discomfort because the patches are gently pressured into intimate contact with the body by means of the ballonet. The best solution was to route the leads on the edge of the patch split lines; in this position, they could not be felt by the test subjects.

Leaks in the Vacuum System

The cost of eliminating leaks in any vacuum system approaches an asymptote with limiting zero absolute pressure. Therefore, in the interests of economy in laboratory research, a hard vacuum should be avoided wherever possible. The ECGS program was not an exception, and it was determined early that the highest suit leakage rate should be allowed for all tests, provided that this leakage would not appreciably affect cooling performance. The design criterion for the maximum leak rate was fixed by the pumping capacity of the two-stage laboratory vacuum pumps while pumping off air leakage and water vapor at the rate of 8 lb/hr, which corresponds to an ECGS heat rejection rate of about 8,300 Btu/hr. The air leakage rate for this condition was approximately 0.62 scfm; this value, therefore, was the maximum allowable ECGS suit leakage for any test. Most tests, however, were run at a much lower value, and some patches consistently operated as low as 0.0024 scfm. It was an easy matter to determine the leakage rate of the ECGS garment or of any of its parts, by connecting it to the laboratory vacuum manifold and noting the pressure rise while the pumps were in normal operation. As long as the leakage pressure rise did not exceed 260μ of mercury for the total system, the part was judged acceptable for test.

A study was made of the number of opportunities for leakage in the delivery hardware. For purposes of discussion, a "leak opportunity" is defined as one leak per homogenous piece of material. For example, a single unbroken sheet of membrane material is one "leak opportunity." A component consisting of a plate soldered to a tube and connected to another tube by means of plastic sleeve would have seven "leak opportunities"; namely the plate, the solder joint, the two tubes, and the two ends of the sleeve mating the tubes and the sleeve itself. Any leak, whether it may be in series or in parallel in the system, contributes to the manifold pressure rise as the ECGS is designed.

The "leak opportunities" on the design verification test series reached the surprising number of 888. Of this total, 485 could be attributed to instrumentation requirements and 403 to the basic ECGS. The current design comprises 10 body patches. Of this total, it averaged out that each patch as connected to the complete ECGS system has an average of 24 "leak opportunities."

We have looked at foreseeable design refinements and can predict that eventual flight hardware could have as few as six "leak opportunities" per patch. This low number, with individual patch valve redundancy, could assure that the ECGS will provide adequate cooling with any predictable failure situation.

5.4 PRELIMINARY PERFORMANCE TESTS

At this time in the program, a complete ECGS suit, including the cooling headpiece, was available for testing. All prior runs gave indications that cooling could be expected at metabolic rates of 5,000 Btu/hr based on full suit equivalent values; however, at first, it was not known if the human physiology would allow heat levels of this amount to be conducted through the skin for extended duration activity.

The following data directly lead to the maximum heat rejection run. The skin temperatures on the second series, in general, dropped at a faster rate than the torso suit, thus showing greater heat removal rate. The subject at the end of the 10-min. 5,200-Btu/hr run was uncomfortably cold, indicating the ECGS cooling effectiveness.

The first series of tests was run at a fixed heat removal rate. The skin temperatures are plotted versus time in Figures 59 through 66. The full suit

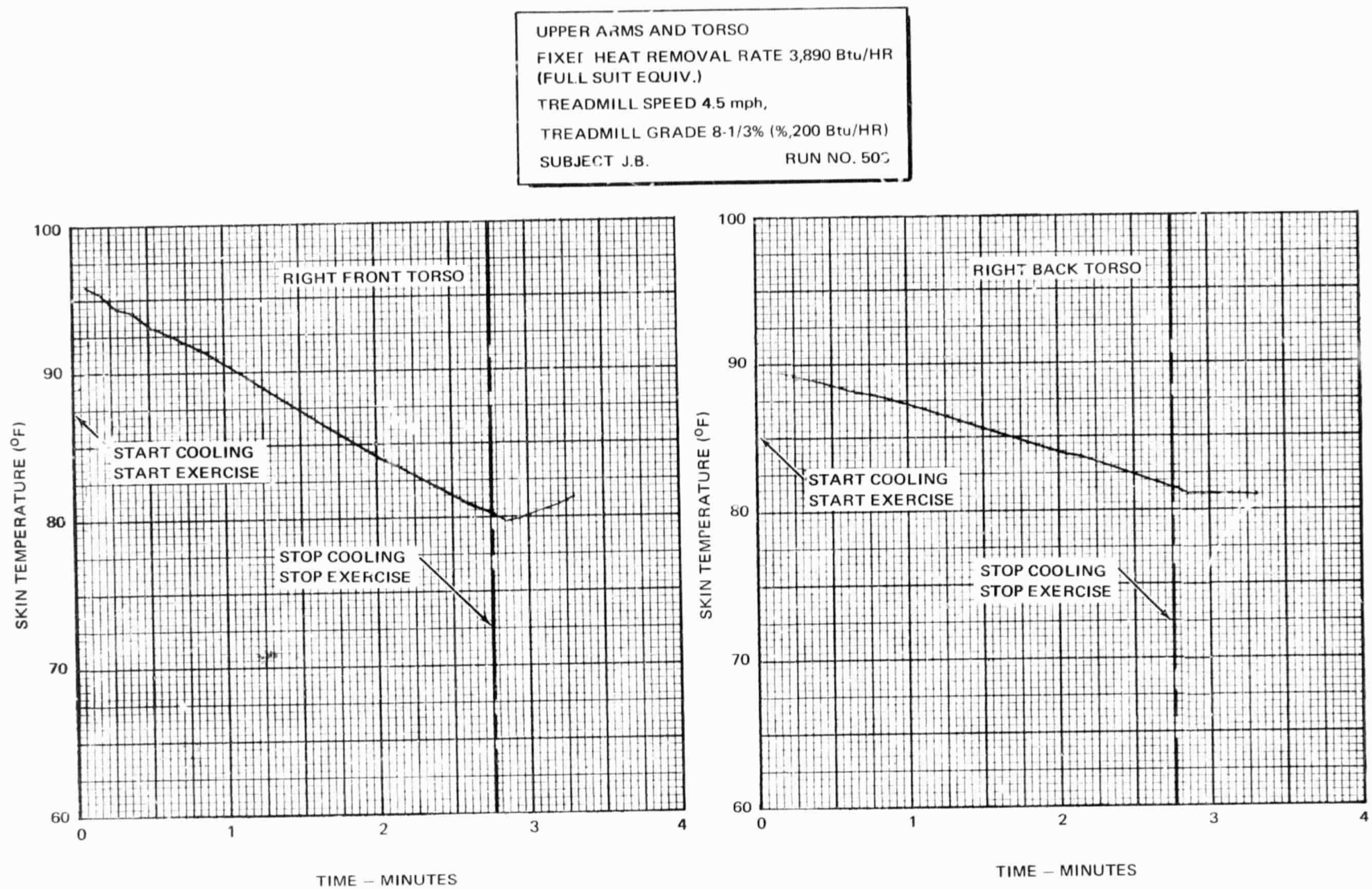

Figure 59. Skin Temperature Time History Right Front and Back Torso – Run 503

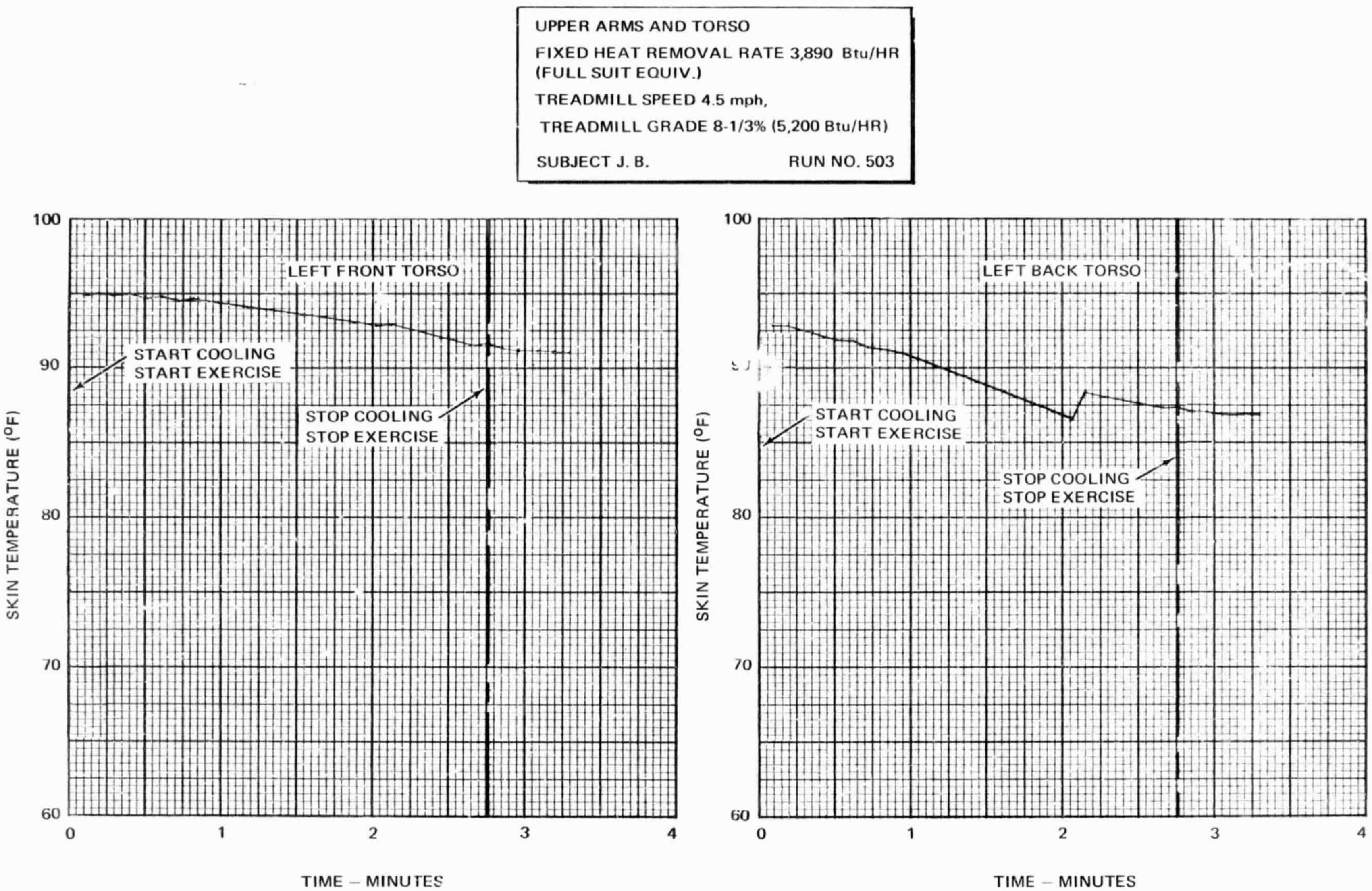

Figure 60. Skin Temperature Time History Left Front and Back Torso – Run 503

UPPER ARMS AND TORSO
FIXED HEAT REMOVAL RATE 3,890 Btu/HR
(FULL SUIT EQUIV.)
TREADMILL SPEED 4.5 mph,
TREADMILL GRADE 8 1/3% (5,200 Btu/HR)
SUBJECT J.B. RUN NO. 503

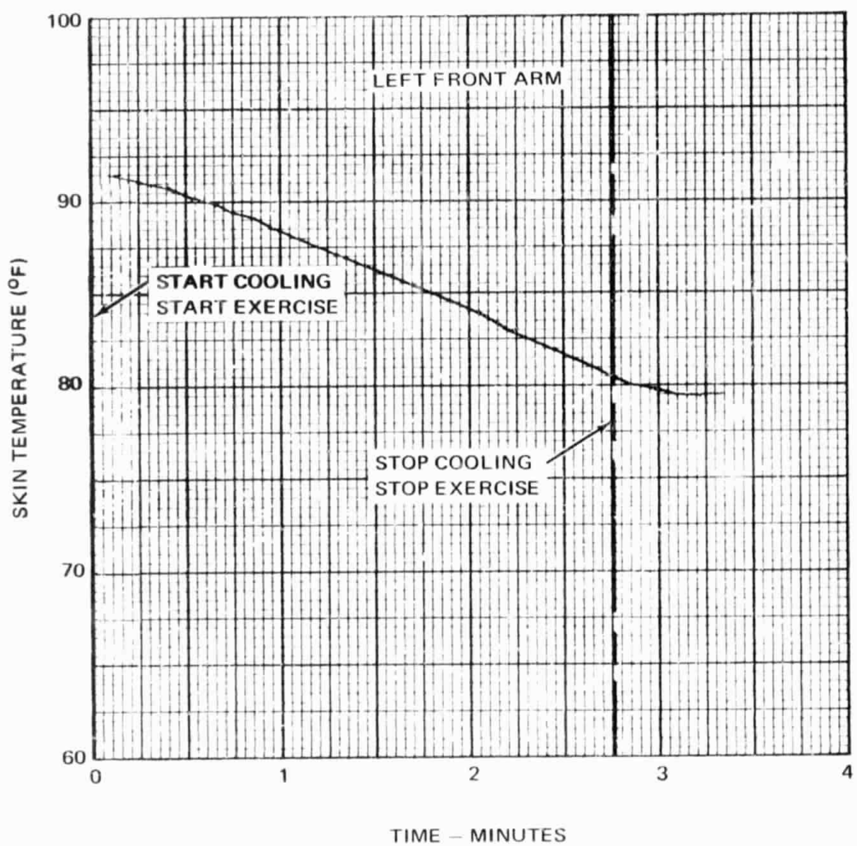

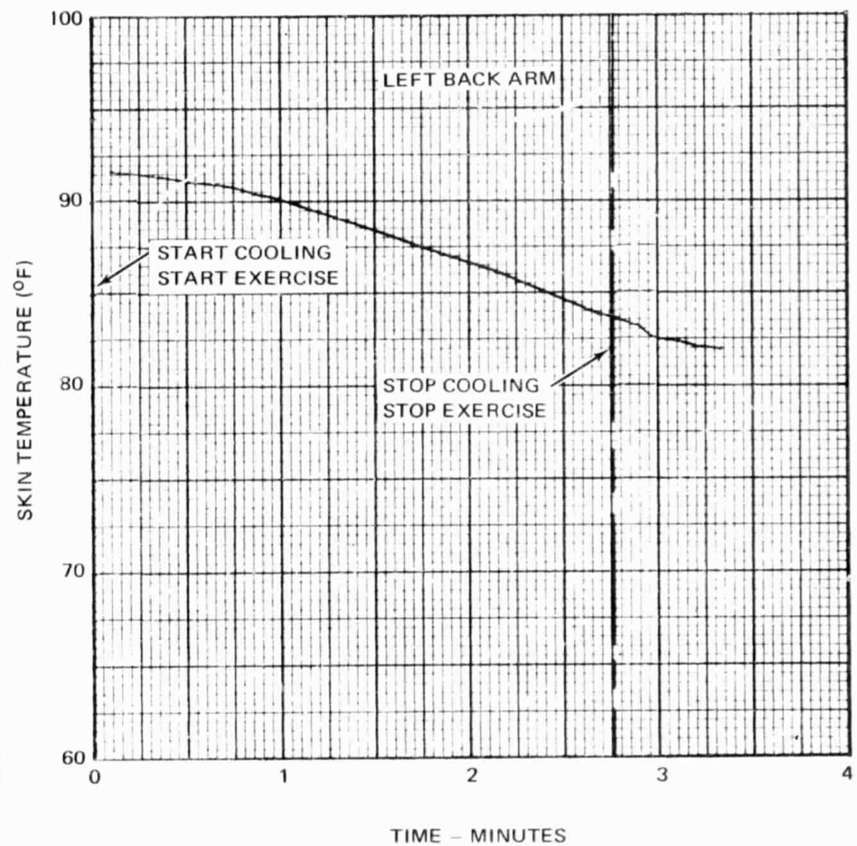

Figure 61. Skin Temperature Time History Front and Back of Left Arm – Run 503

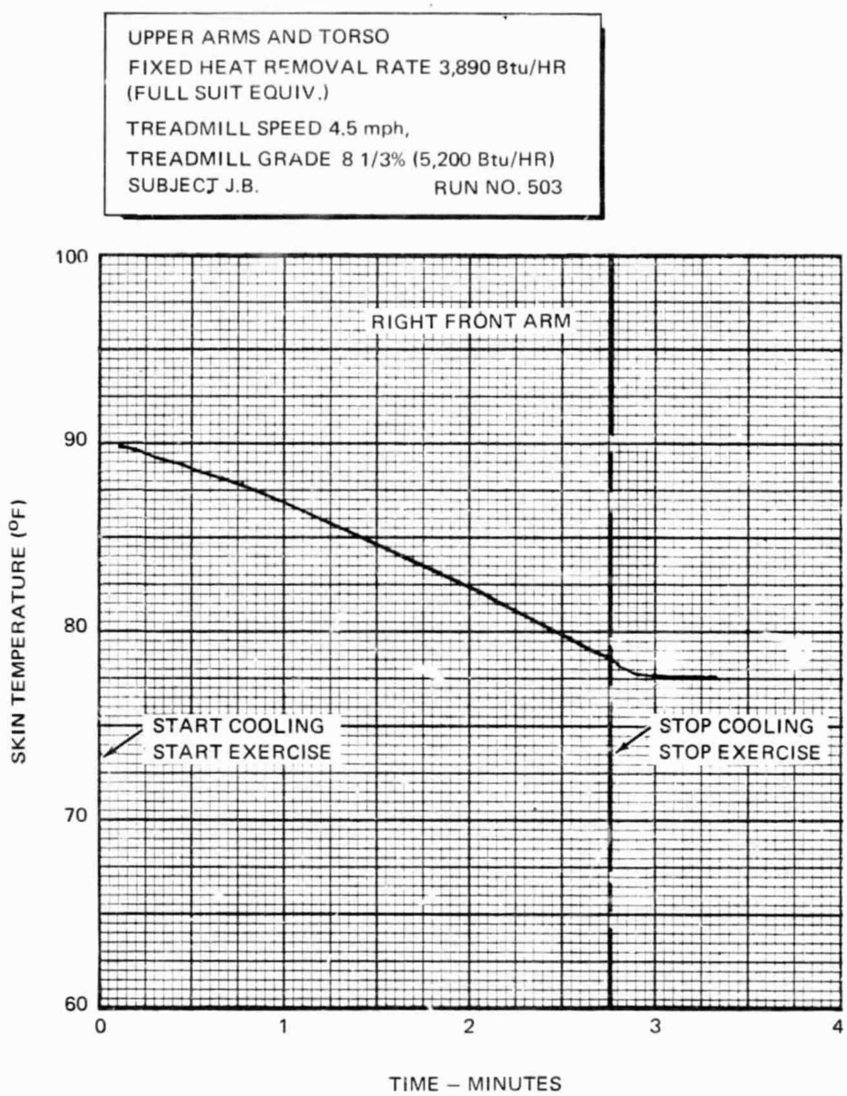

Figure 62. Skin Temperature Time History Right Front Arm – Run 503

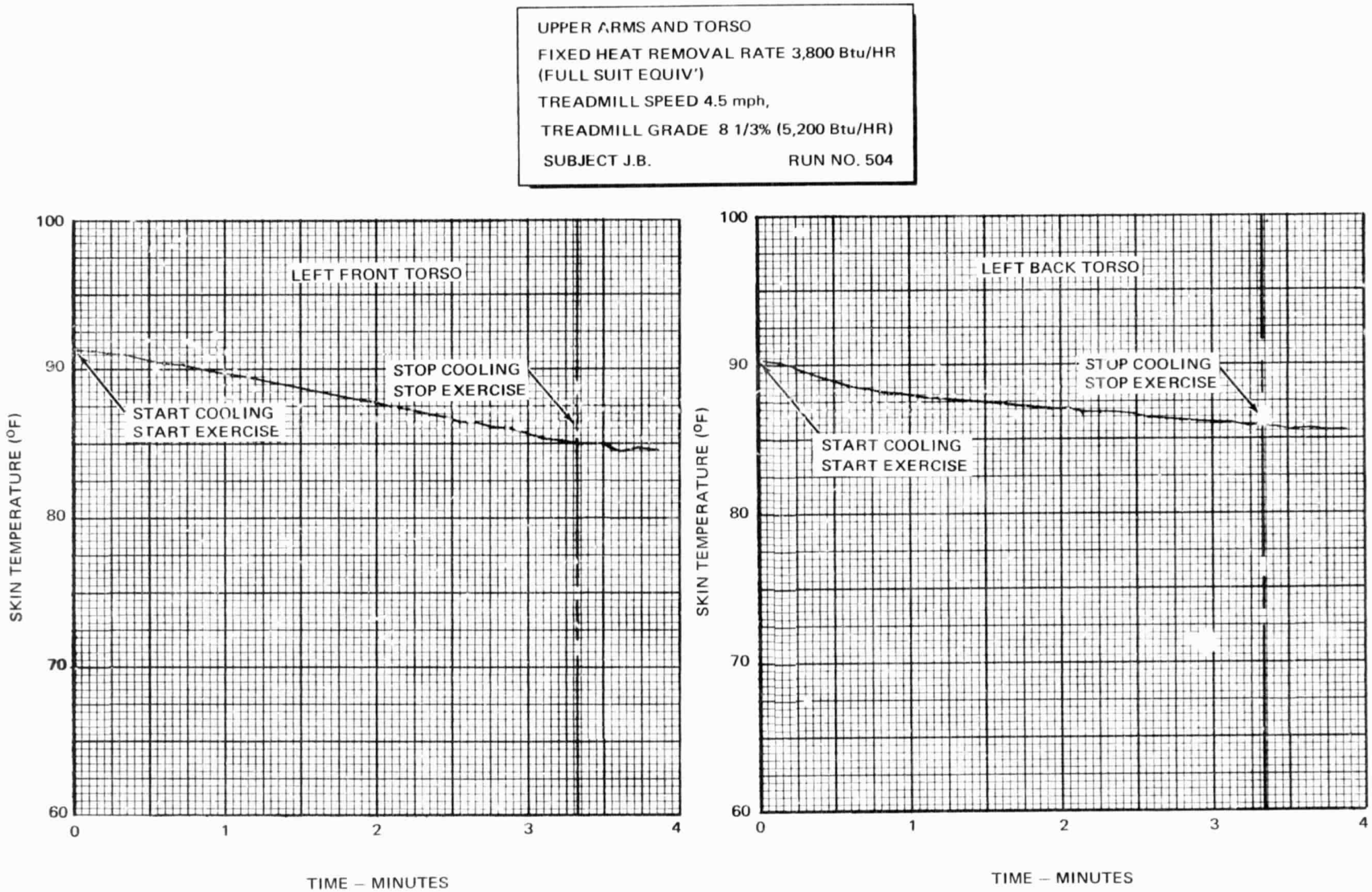

Figure 63. Skin Temperature Time History Left Front and Back Torso – Run 504

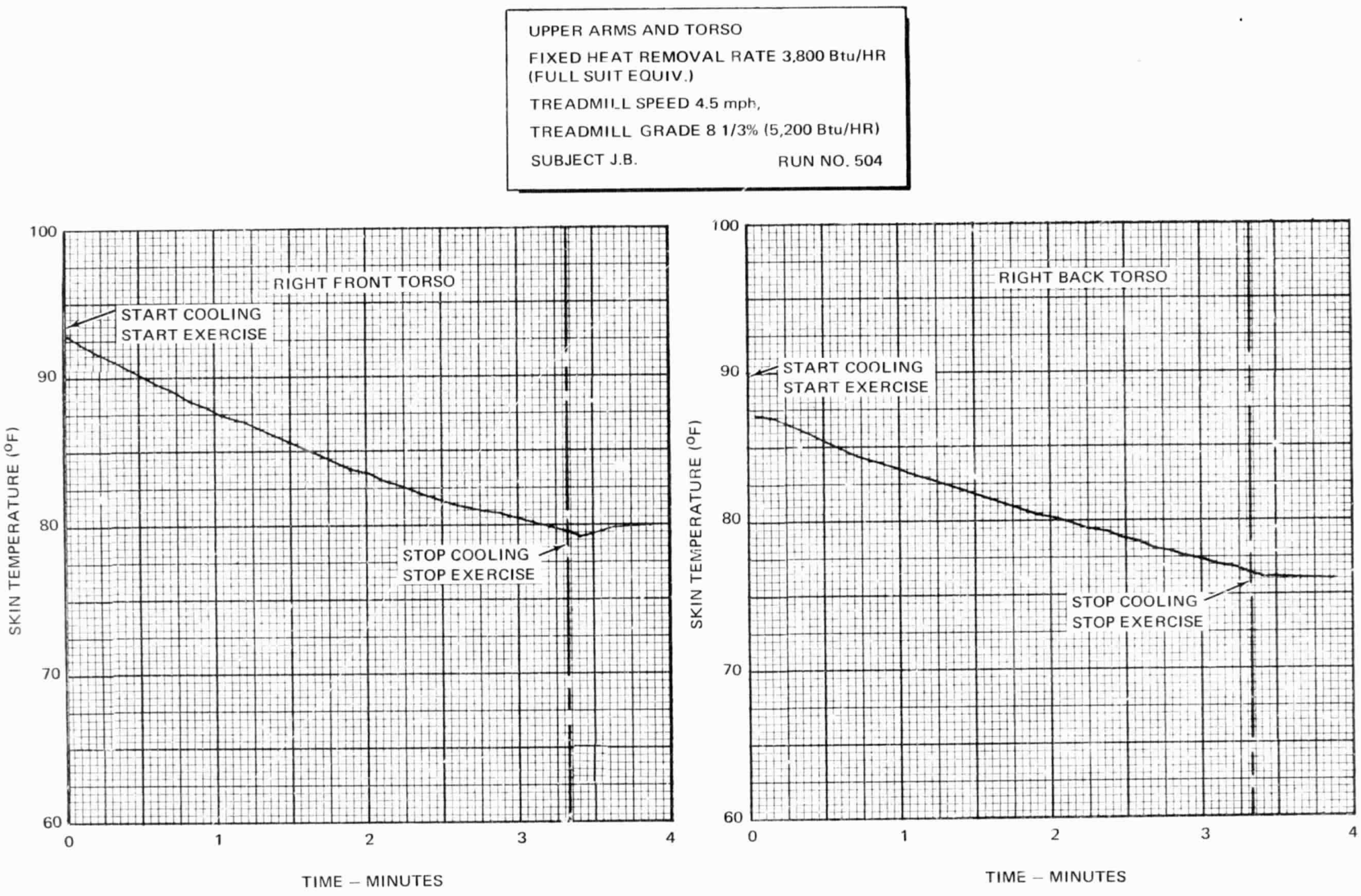

Figure 64. Skin Temperature Time History Right Front and Back Torso – Run 504

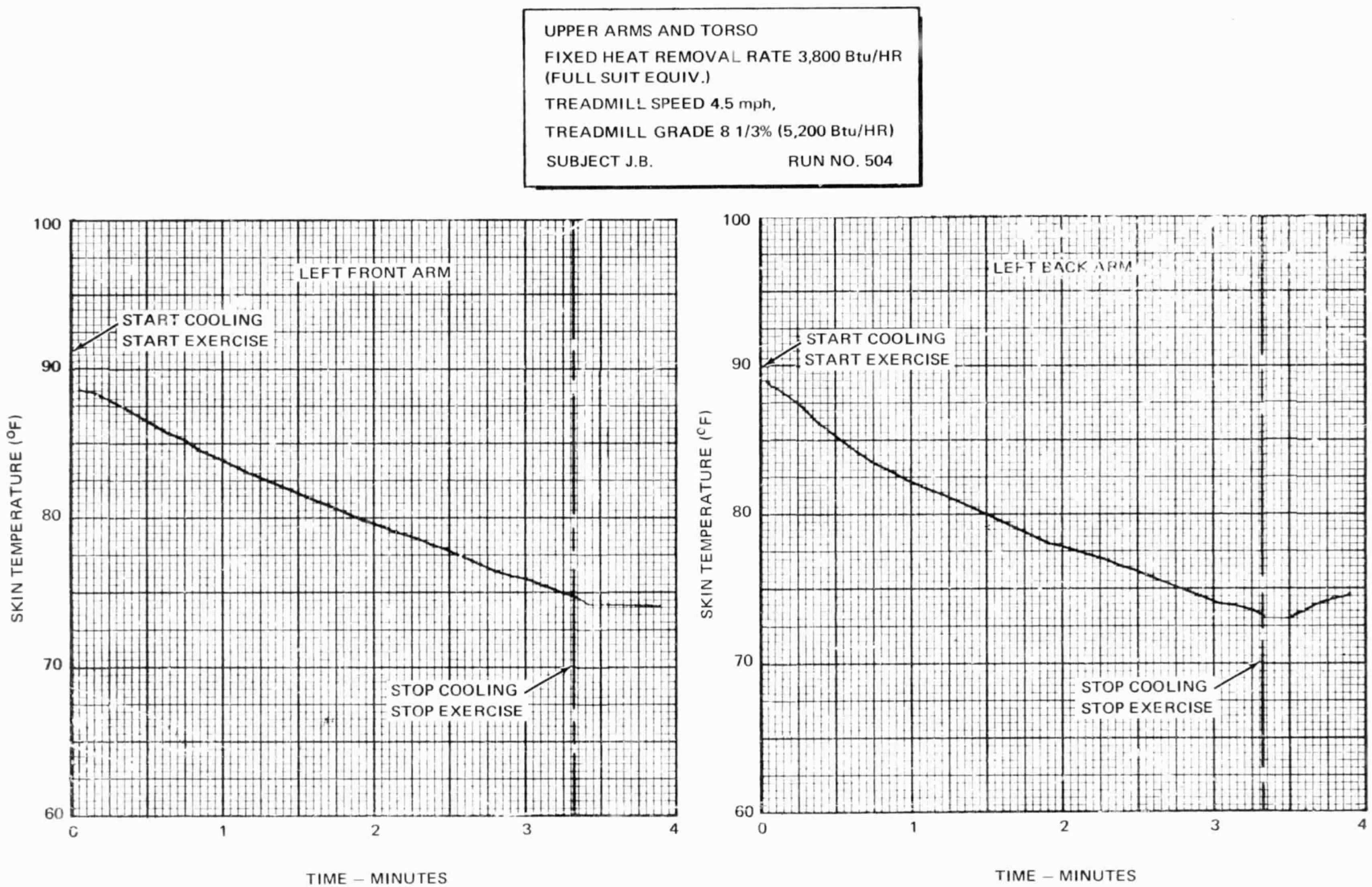

Figure 65. Skin Temperature Time History Front and Back of Left Arm – Run 504

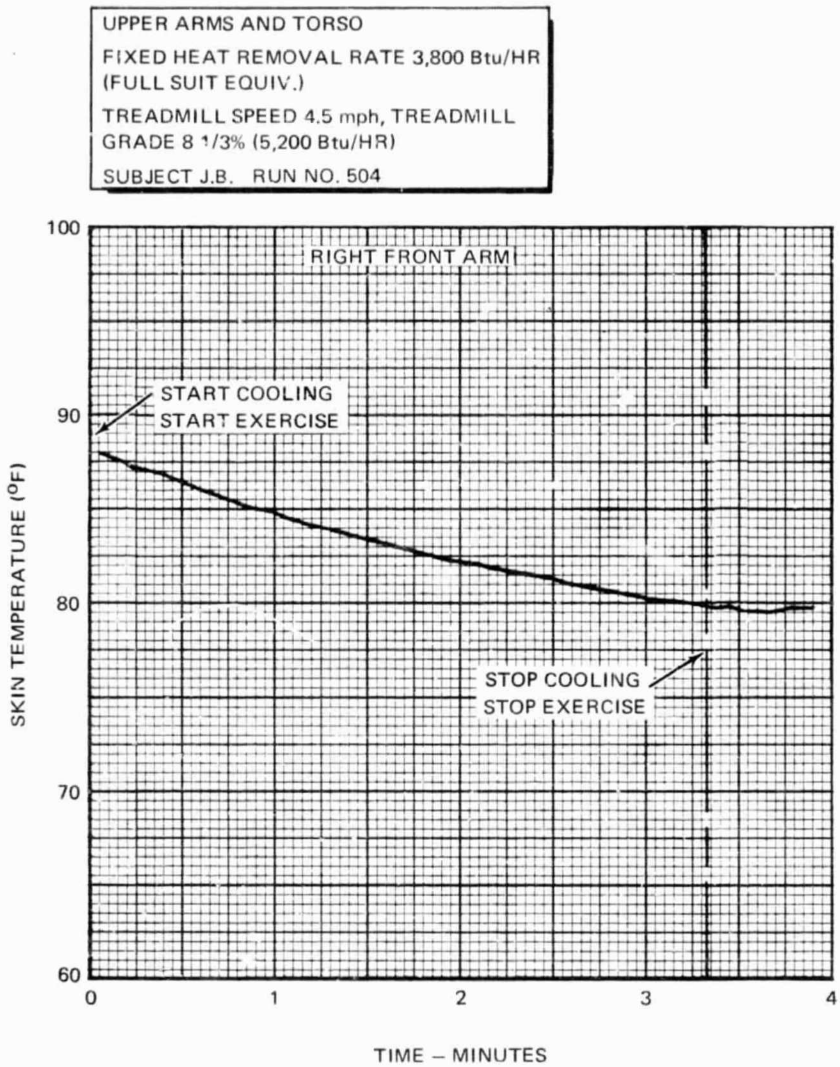

Figure 66. Skin Temperature Time History Right Front Arm – Run 504

equivalent heat removal rate was 3,890 and 3,800 Btu/hr. The skin temperature constantly decreased, indicating that steady state heat balance had not been obtained. This is to be expected in runs of such short duration. Lower metabolic rate runs allow longer operation and provide sufficient time to establish thermal equilibrium (if physiologically possible).

The second series was made to check the performance of the full ECGS without the headpiece. The run was made with maximum cooling and a subject metabolic rate of 5,200 Btu/hr. Figures 67 through 70 show the test data. Figure 67 shows heart rate versus time, and the other figures show the various skin temperatures versus time. Pronounced cooling occurred in all patches. The upper right front leg and upper right back torso show a marked decrease in cooling rate at about 6 to 8 in. into the run. This is probably an indication of water depletion in these patches. The average heat removal rate based on water usage was 3,410 Btu/hr. No sweating was experienced by the subject during the cooling run. Higher average heat removal rates can be expected when water is added at the proper intervals.

A series of tests was made to obtain run time limits on the torso, upper arm suit, and on the leg patches. These data are compared with individual patch performance in Figure 71. The data follow a general curve as shown in the figure with some variation between the several configurations tested.

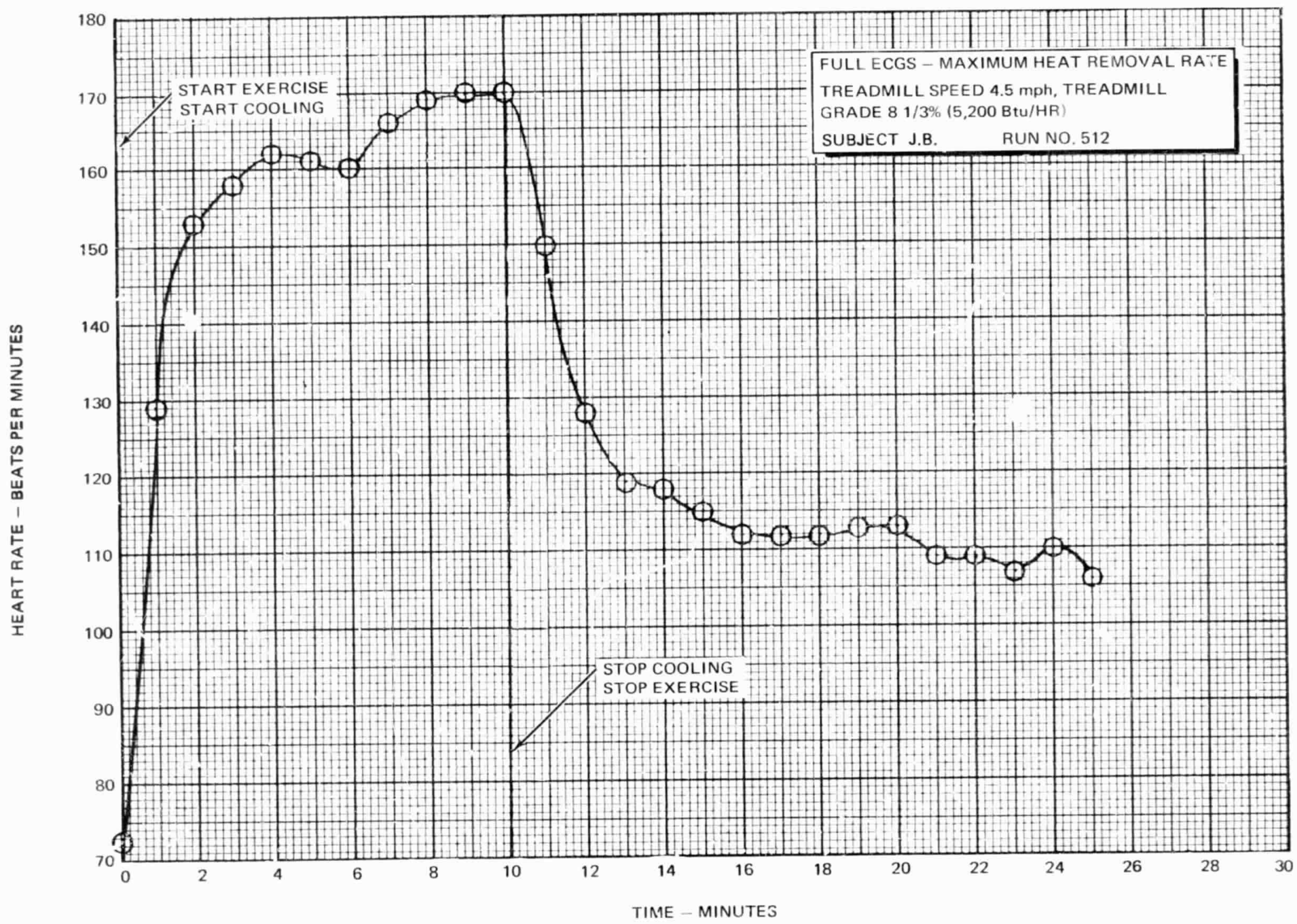

Figure 67. Heart Rate Time History – Run 512

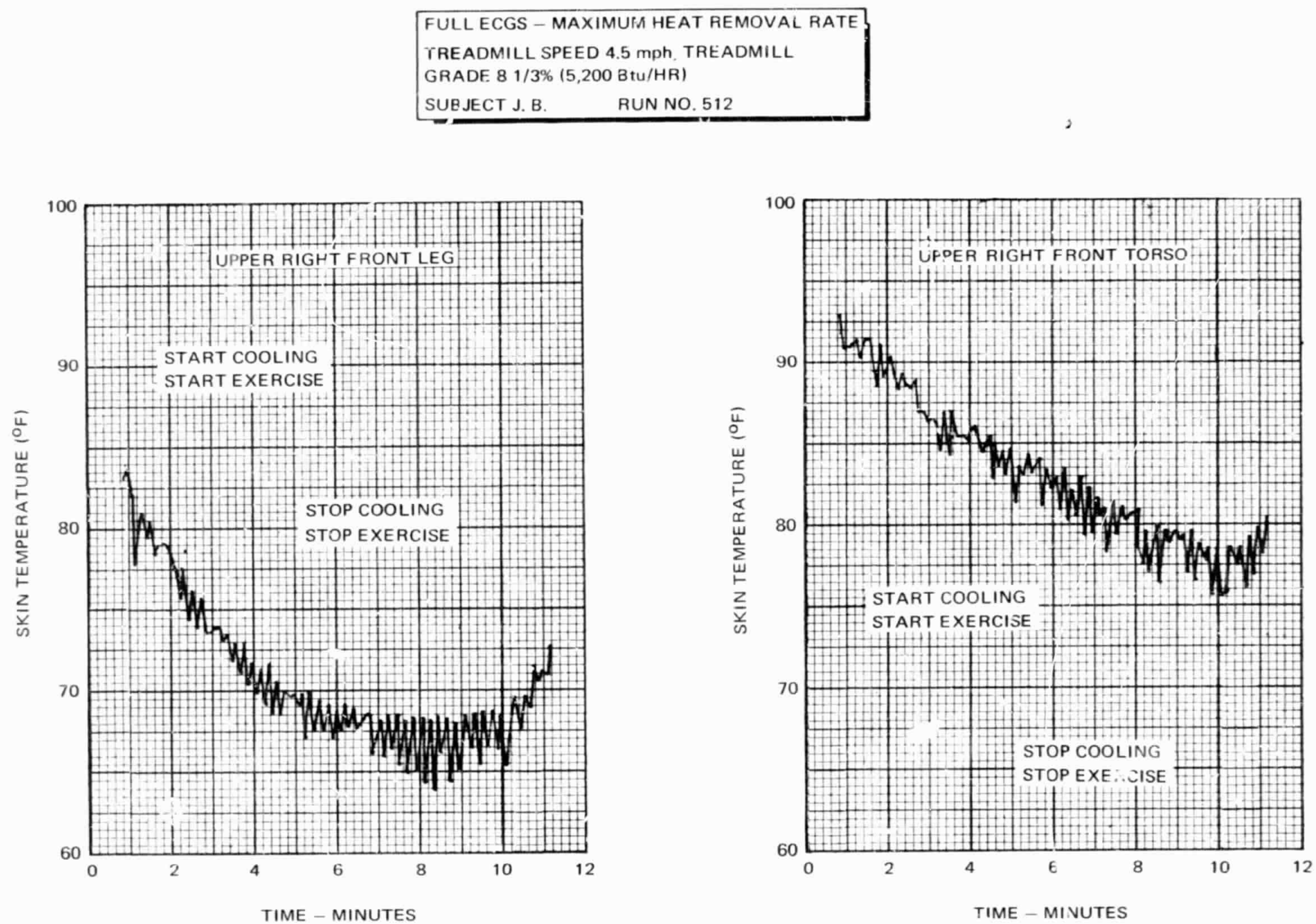

Figure 68. Skin Temperature Time History Upper Right Front Torso and Leg – Run 512

FULL ECGS – MAXIMUM HEAT REMOVAL RATE
TREADMILL SPEED 4.5 mph, TREADMILL GRADE 8 1/3% (5200 Btu/HR)
SUBJECT J.B. RUN NO. 512

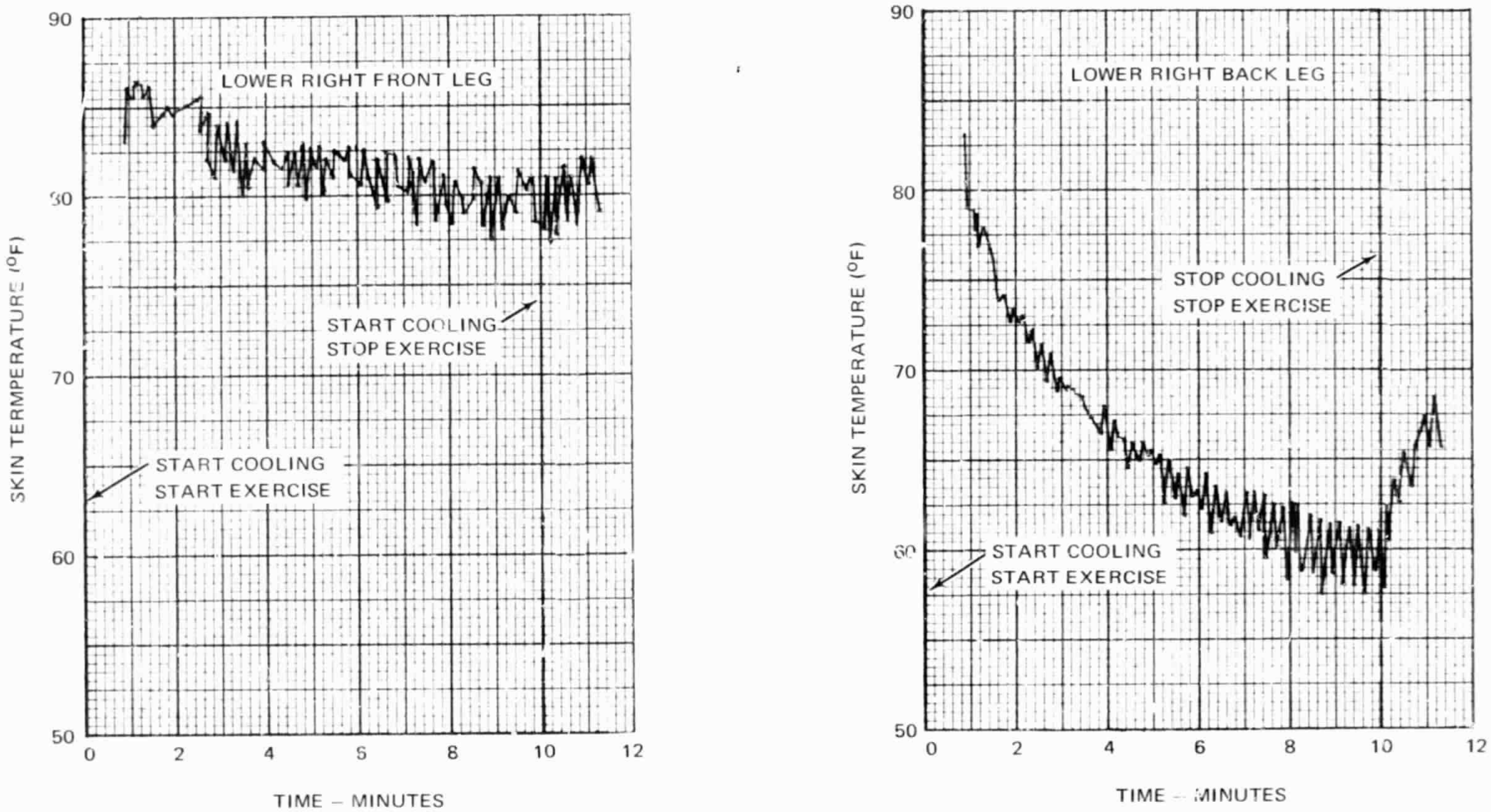

Figure 69. Skin Temperature Time History Lower Front and Back of Right Leg – Run 512

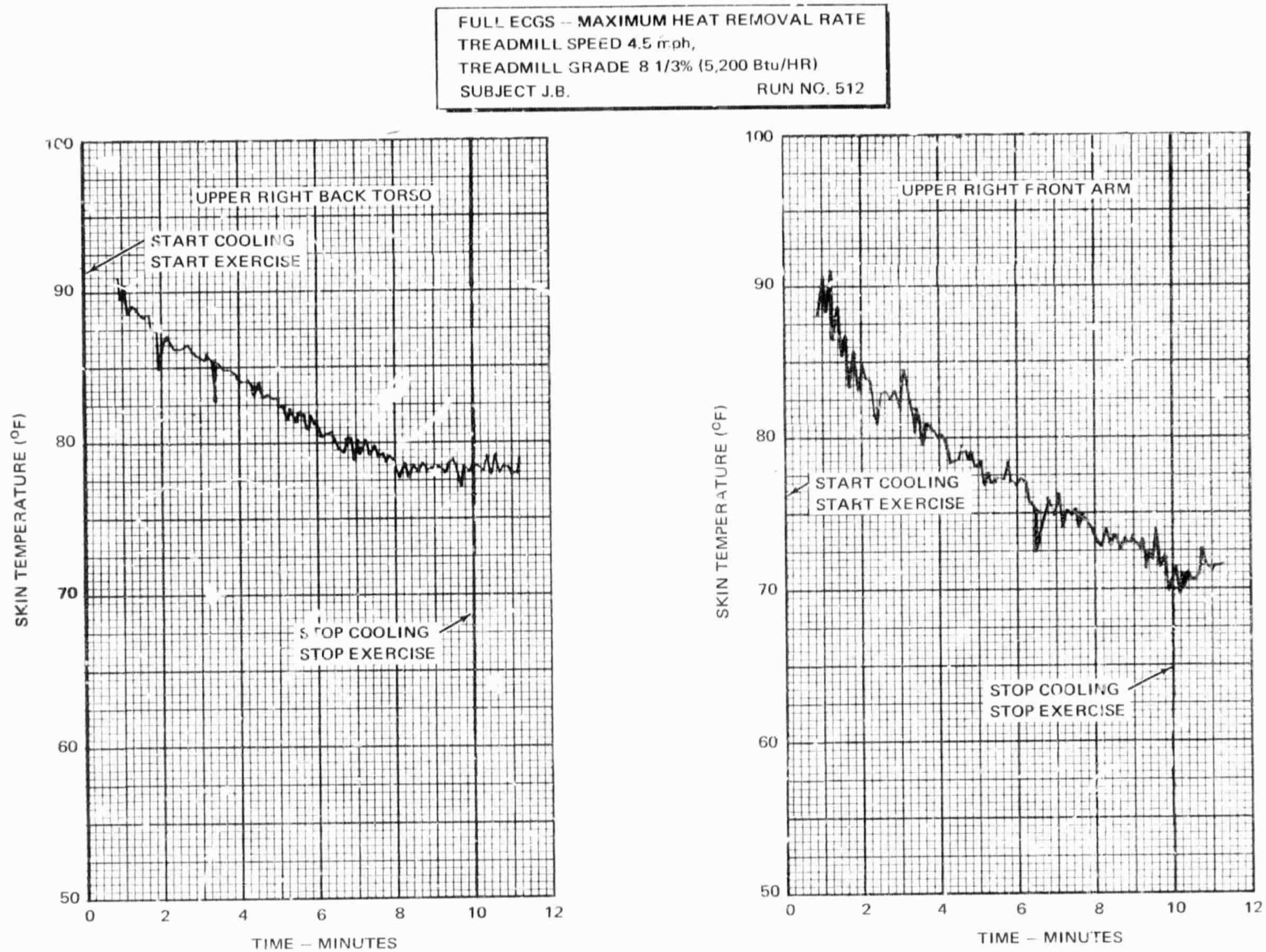

Figure 70. Skin Temperature Time History Upper Right Back Torso and Upper Right Front Arm – Run 512

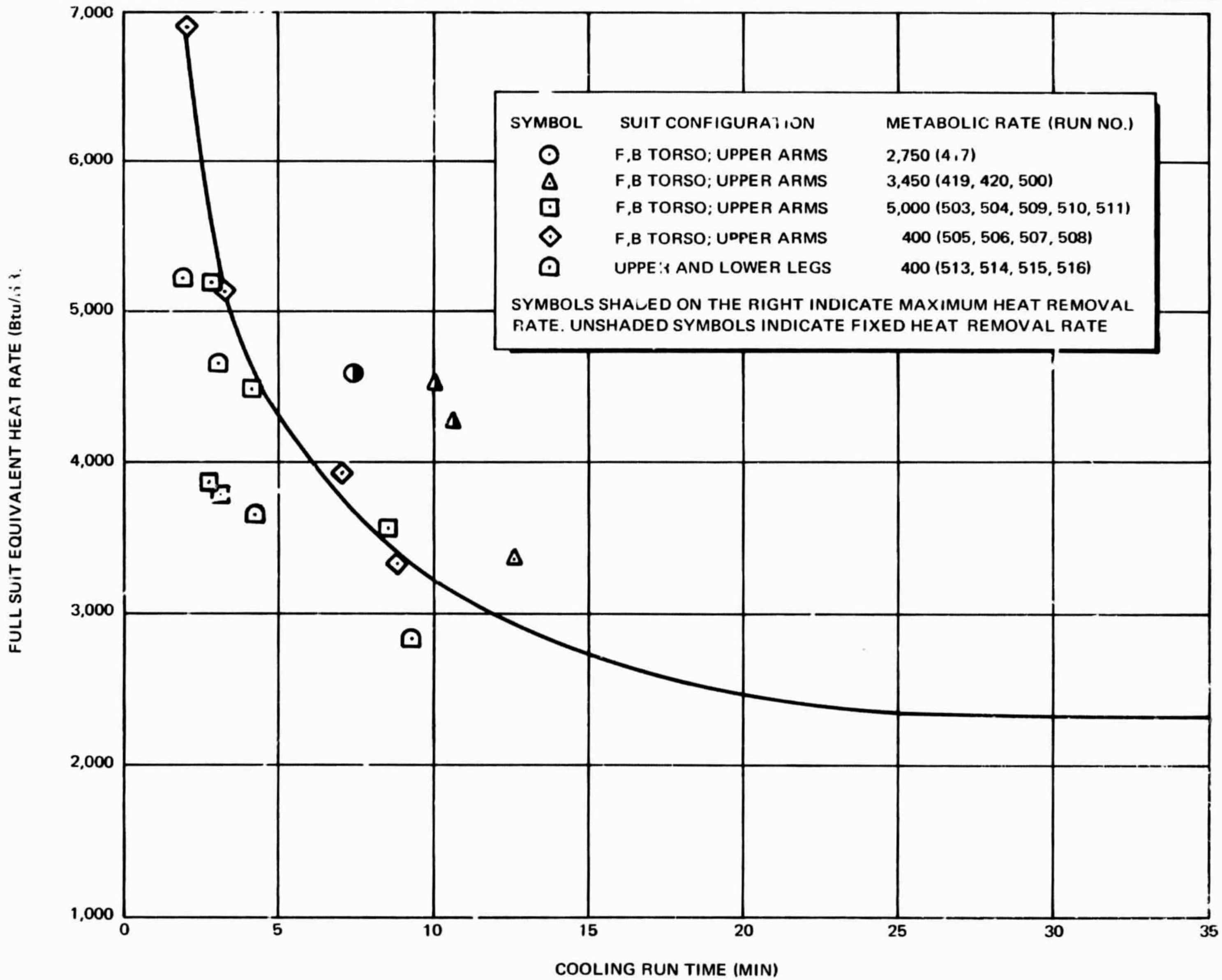

Figure 71. ECGS Delivery Hardware Preliminary Performance

Section 6

FORMAL DESIGN VERIFICATION TESTS

6.1 TYPICAL EVA MISSION PROFILE

The program performance objective was to provide cooling for a typical EVA mission work rest cycle of 4 hours, which would lead up to 5,000 Btu/hr metabolic rate for the last 20 mins. Figure 72 shows the mission profile together with equivalent treadmill walking speeds. The energy expenditure during this period is equal to a nonstop walk of 17.5 miles at an average speed of 4.39 mph. This schedule obviously will tax human effort and endurance and it was hoped that the heat produced would be removed without a physiological barrier. The ECGS had shown that extremely high heat removal rates were possible, but to sustain these rates in a practical case could only be proved by demonstrating cooling in a thermal insulated garment at work levels such as those postulated in the EVA mission profile. The profile then became the target design specification for not only the ECGS, but also for the subjects who were to demonstrate the delivery hardware.

6.2 TRAINING OF SUBJECTS ON TREADMILL

At about the program midpoint, it was discovered that healthy young athletic male subjects could not perform the 20-min stint at 5,000 Btu/hr. This was the crucial heat production case and was compounded by the difficulty of trying to accomplish this work level at the end of an already strenuous 4-hour treadmill run. It soon became apparent that a treadmill training program was required. Seven subjects were selected on the basis of athletic prowess, demonstrated by their ability to pass an Air Force Class A flight physical. Subsequent to this, the subjects were given an

EVA MISSION PROFILE

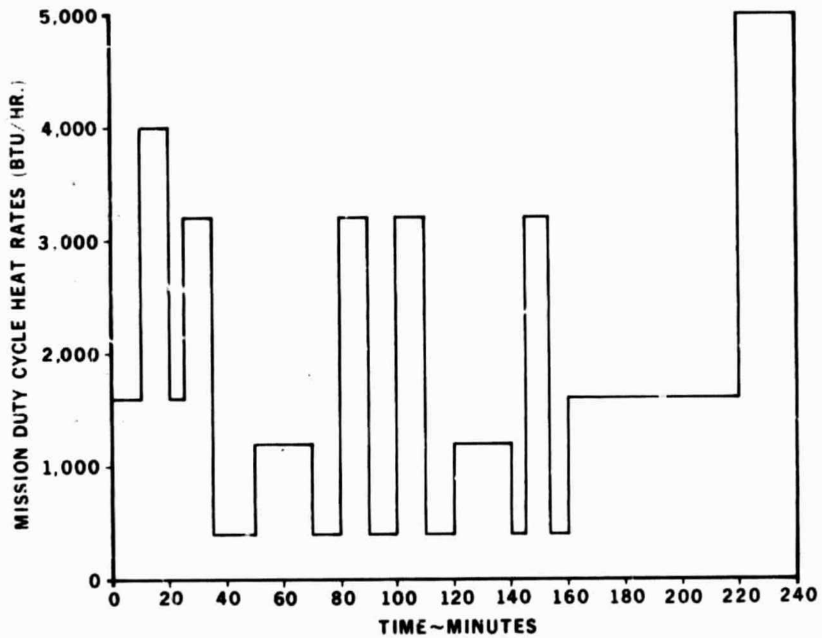

EQUIVALENT TREADMILL PROFILE

(AVG. SPEED 4.39 MPH)

ACTIVITY	ACTIVITY DURATION (MINUTES)	ACCUM. DURATION (MINUTES)	SPEED (MI./HR.)	HEAT OUTPUT BTU/HR.	DISTANCE PER ACTIVITY (MILES)	ACCUM. DIST. (MILES)
WALK	10	10	4.4	1600	.733	.733
RUN	10	20	8.7	4000	1.456	2.183
WALK	5	25	4.4	1600	.367	2.550
RUN	10	35	7.0	3200	1.167	3.717
SIT AT REST	15	50	—	400	—	3.717
WALK	20	70	3.65	1200	1.216	4.933
SIT AT REST	10	80	—	400	—	4.933
RUN	10	90	7.0	3200	1.167	6.100
SIT AT REST	10	100	—	400	—	6.100
RUN	10	110	7.0	3200	1.167	7.267
SIT AT REST	10	120	—	400	—	7.267
WALK	20	140	3.65	1200	1.216	8.483
SIT AT REST	5	145	—	400	—	8.483
RUN	$7\frac{1}{2}$	$152\frac{1}{2}$	7.0	3200	.875	9.358
SIT AT REST	$7\frac{1}{2}$	160	—	400	—	9.358
WALK	60	220	4.4	1600	4.400	13.758
RUN	20	240	11.7	5000	3.800	17.558

Figure 72. Metabolic Test Profile

altitude pressure chamber indoctrination course, which they all passed; one subject was also given the Air Force pressure suit training course to make him knowledgeable in spacesuit operations.

During the treadmill training, five of the seven subjects dropped out for one or more of the following reasons, when the metabolic rates were reaching high levels:

1. Leg and muscle cramps.
2. Inability to reduce pulse rate fast enough during training.
3. Limitations due to loss of breath.
4. Lack of motivation.

The two remaining subjects completed the training and each was brought to an almost identical level of performance. Heart rates, endurance, and high energy runs were also remarkably similar at the end of the program. The younger of the two subjects (E.H., age 25, 6 ft, 150 lb) had been an old "pro" on the treadmill for various tests during the previous 2 years, and required less training to reach the required competence level. The second subject (J.B., age 49, 6 ft, 180 lb) had difficulties, but was highly motivated and finally made the grade.

Periodic physicals were given to the subjects during the training period; these physicals included exercise electrocardiograms as heart rates were pushed up to the 180 level during sustained treadmill runs.

A constant treadmill training speed of 4.5 mph was selected for two reasons; first the average speed on the EVA mission was 4.39 mph, and any higher speed would have required a running gait, which was believed to be dangerous if the subject were to fall when exercising to fatigue.

Specialized pulse rate instrumentation was developed for and utilized on all training runs. This system automatically records in a digital conversion the average pulse rate for each 10 beats of the heart; this provides for the observation of dynamic heart rate changes in intervals as short as 10 secs and yet assures an averaging function during the 10-beat count. The three electrodes were placed on the sternum and symmetrically at the side of the third rib location; no signal artifacts were observed even during the heaviest exercise. An oscilloscope was provided for visual inspection of the ECG; strip-chart recordings could be taken, and, simultaneously, pulse rates were printed out on paper tapes.

A training run could be terminated for any one of the following reasons:

1. The medical monitor.
2. Test subject fatigue.
3. Limiting pulse rate of 180 (mandatory termination).
4. Any of the program personnel observing the test subject for any reason.

Since endurance at high work levels was the goal, the training protocol was to have the test subjects work out at least 3 days each week on the treadmill at 4.5 mph to the previously mentioned run termination point. Exceptions were made to this when a subject was too sore, ill, or had foot blisters, which were common. Any given run was continuous, with no rest allowed. Endurance was built up at each grade to a point of apparent diminishing returns, and then the next grade angle jump of 2% was instigated. The lower grades resulted in endurance up to 2-1/2 hours (11-1/4 miles), which culminated at training peak of 5,000 Btu/hr for 1/2-hour duration.

Pulse rate versus time plots were prepared for all training runs. The advantages of training in producing a progressive lowering of pulse rate at a given work level were observed for all subjects. A complete pulse rate training history from beginning to end for the older of the two remaining subjects is presented in Figures 73 through 79. The younger subject did not have this complete a record, because he started from a much higher conditioned level. The figures do show, however, that a healthy individual, although older, can be conditioned to exceedingly high levels of endurance and work.

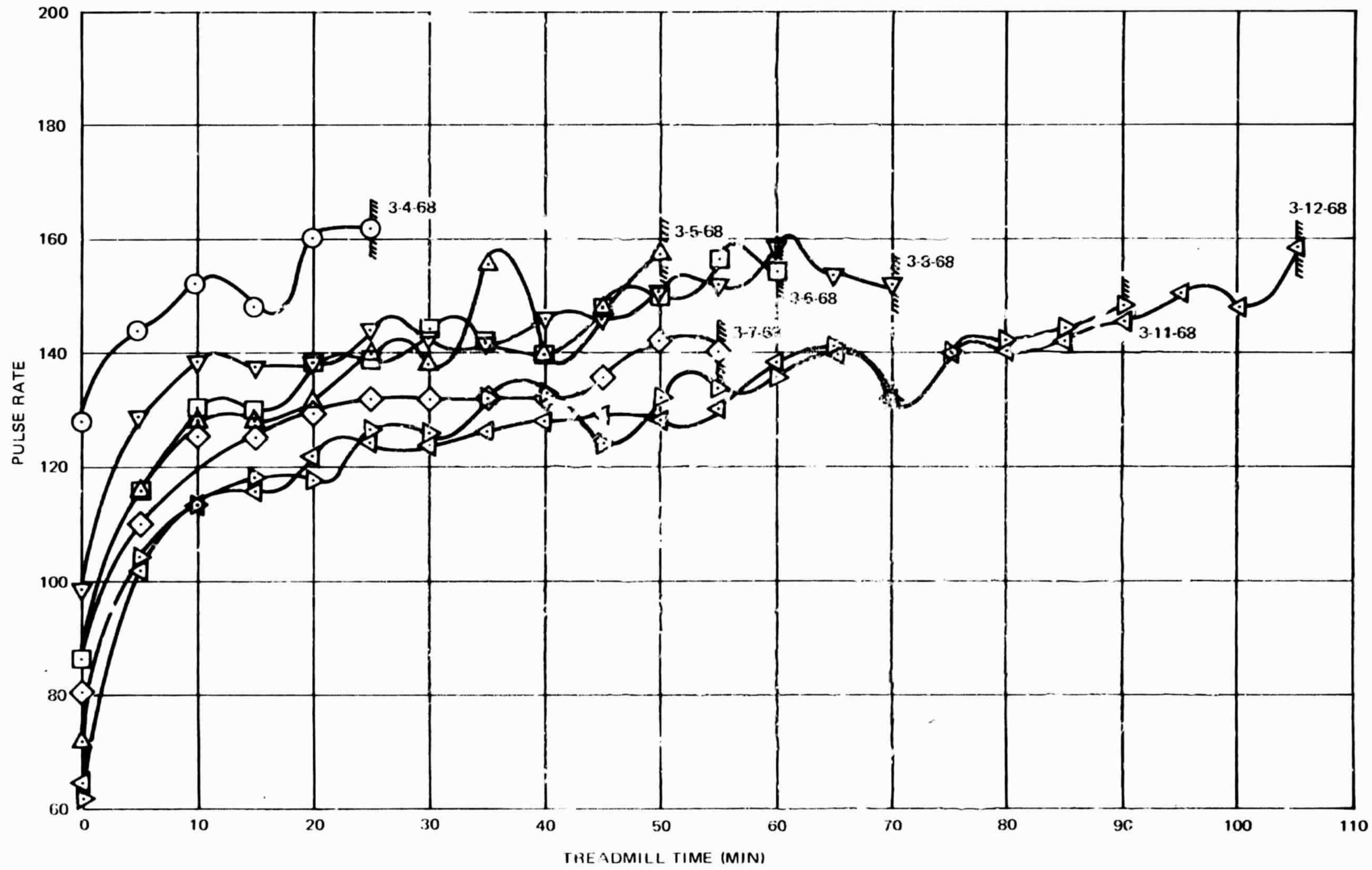

Figure 73. Treadmill Training – 0% Grade

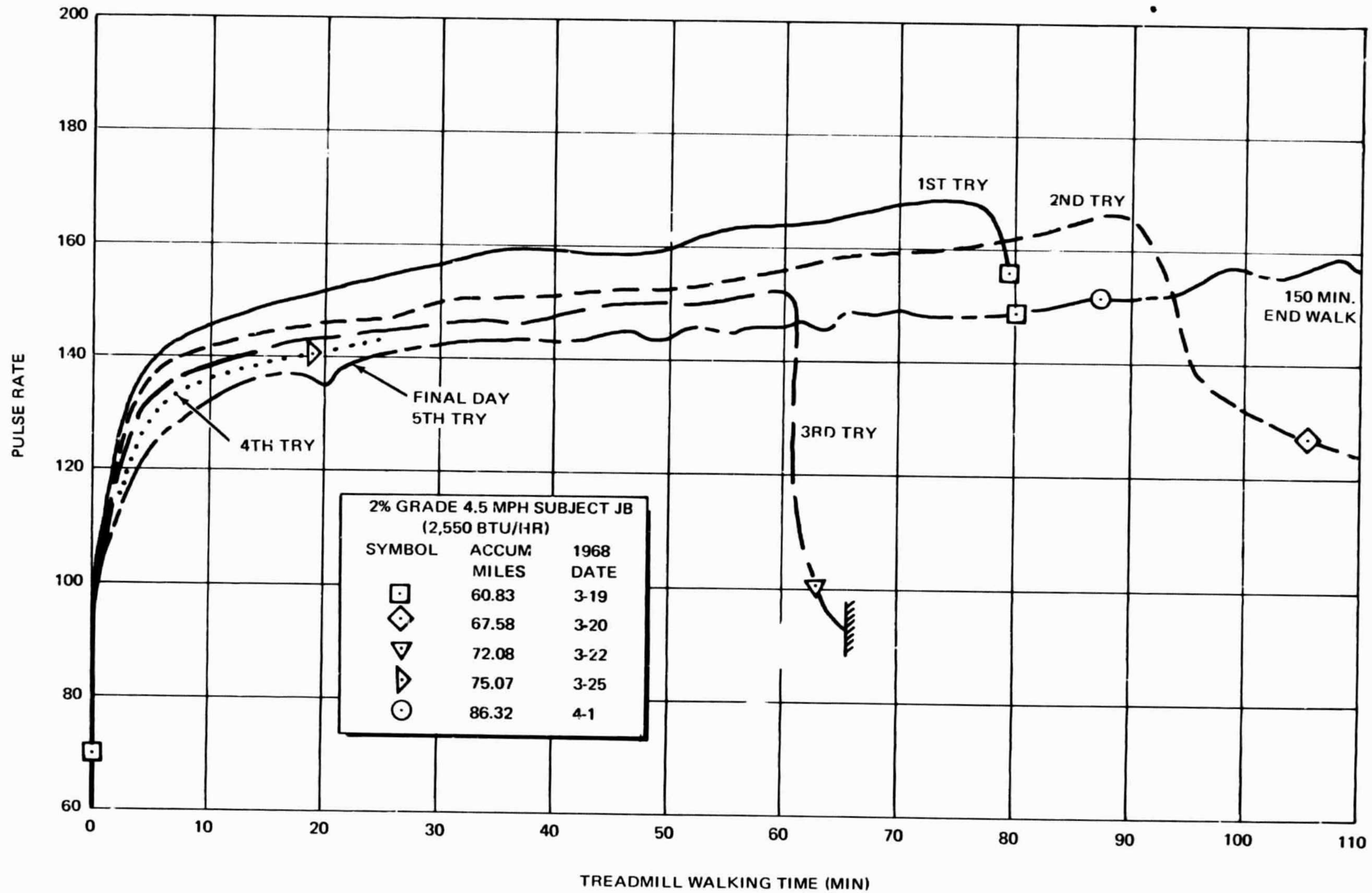

Figure 74. Treadmill Training – 2% Grade

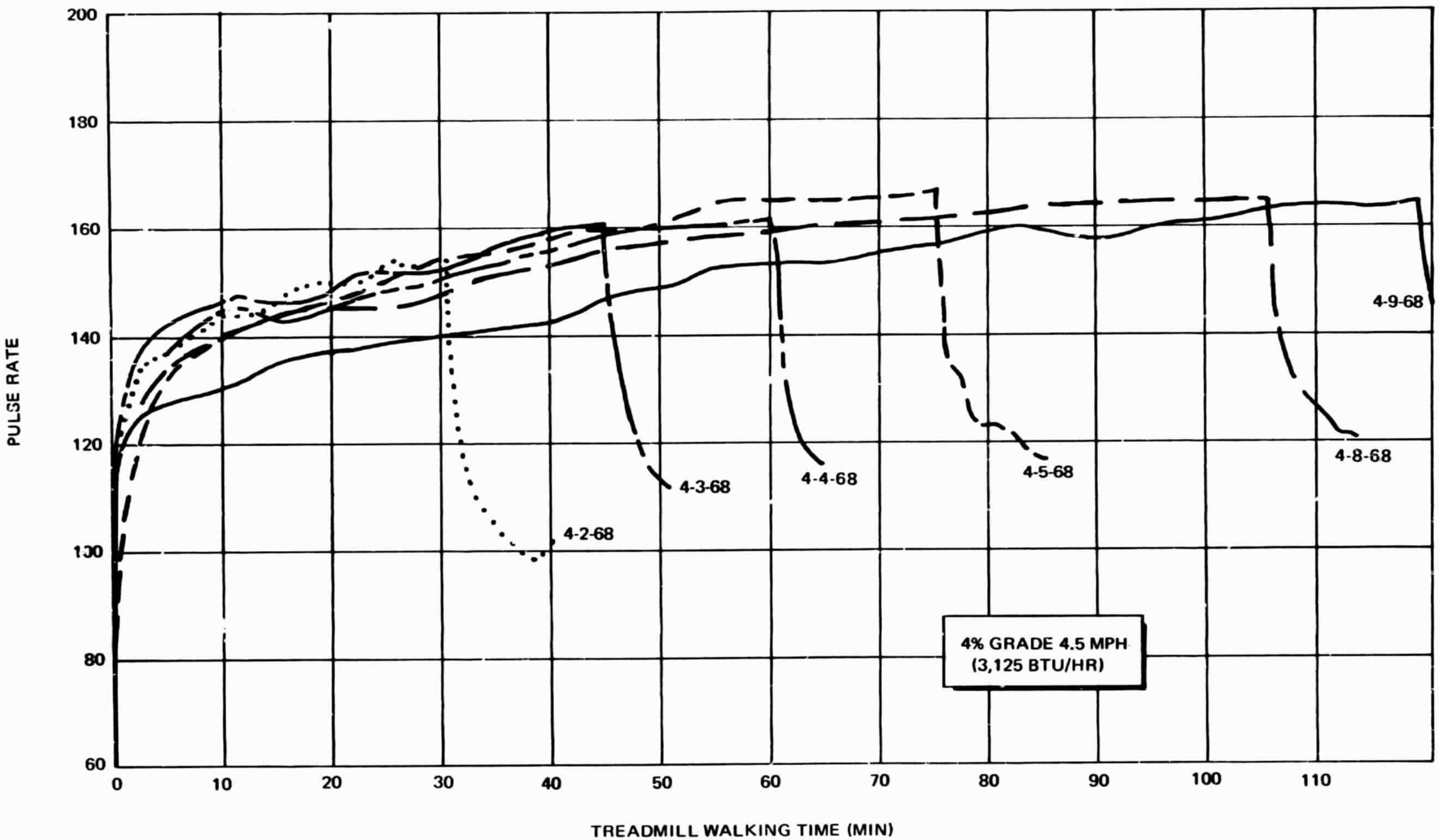

Figure 75. Treadmill Training – 4% Grade

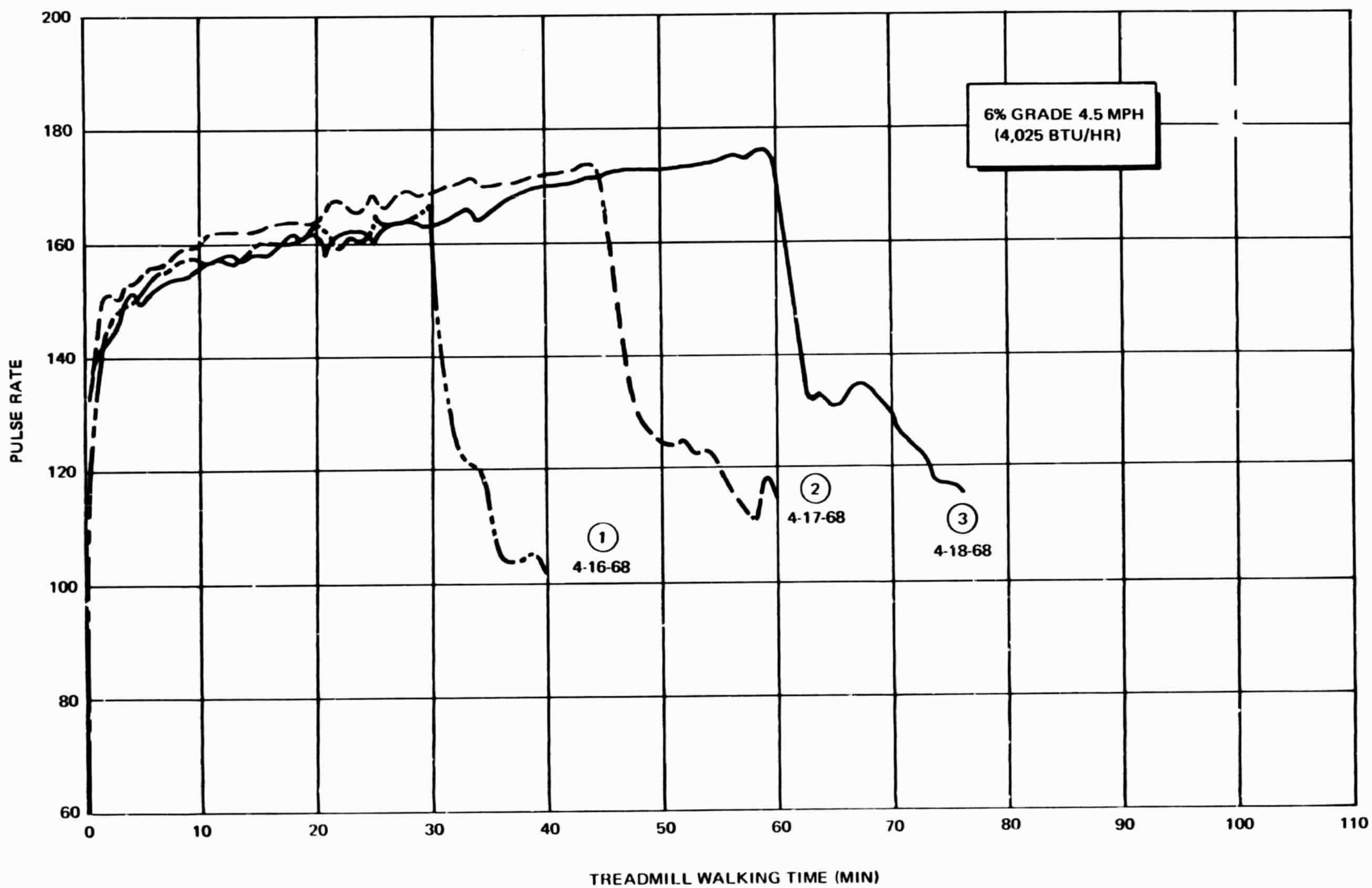

Figure 76. Treadmill Training – 6% Grade

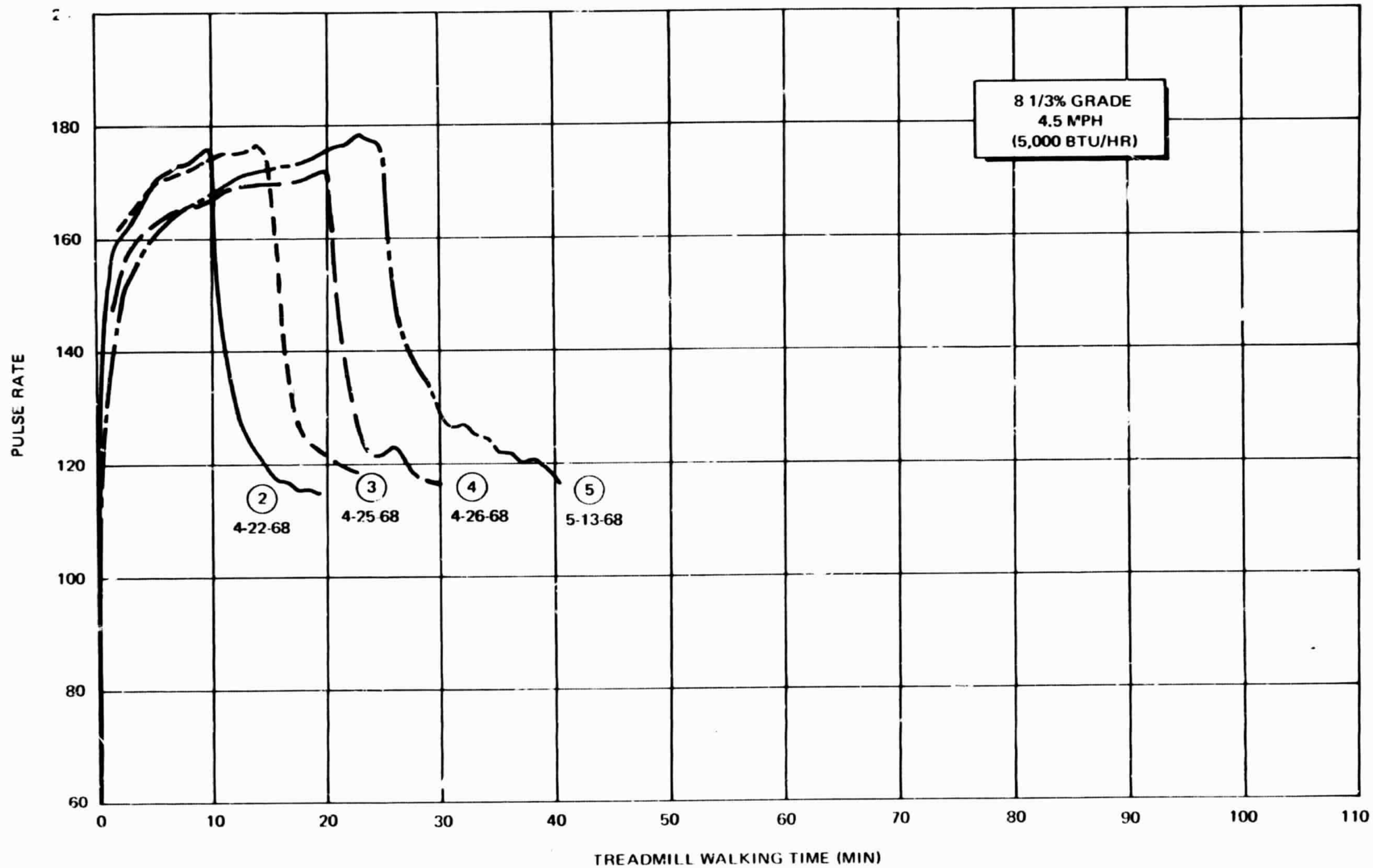

Figure 77. Treadmill Training – 8% Grade

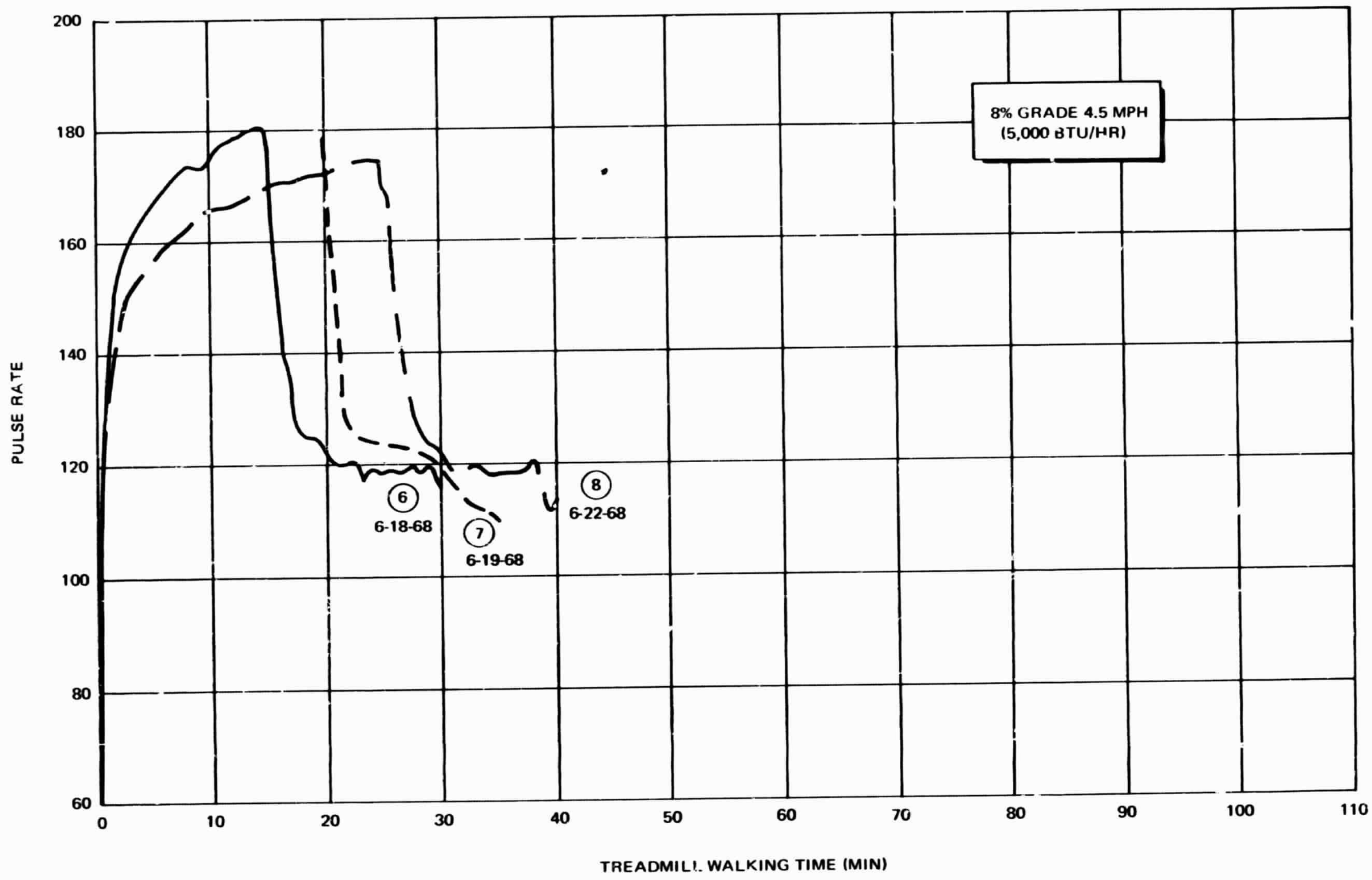

Figure 78. Treadmill Training – 8 1/3% Grade

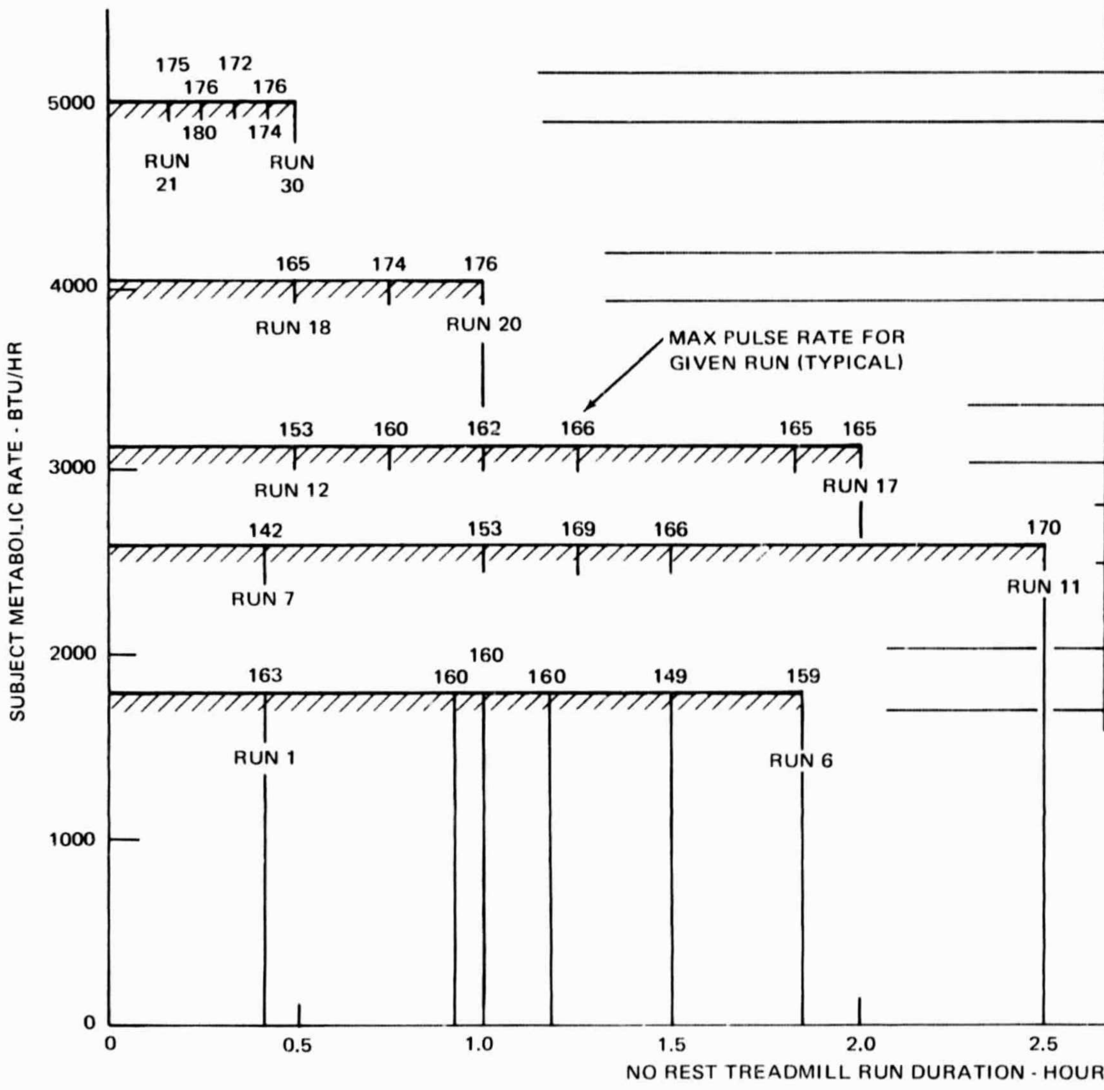

EXERCISE GRADE LEVEL %	MAX EQUIVALENT ENERGY MILES AT 0% GRADE	STEADY STATE % ENERGY OVER 0% GRADE	MAX DURATION RUN PULSE RATE BEFORE JUMP IN GRADE
8.33	5.92	163	174
6.00	9.53	112	176
4.00	14.80	64	165
2.00	15.10	34	170
0	8.33	0	159

- PERIOD OF TRAINING 3-4-68 THROUGH 6-22-68
- SUBJECT JB TEST DATA SHOWS TYPICAL TREND OF SEVEN SUBJECTS

Figure 79. 4.5 MPH Treadmill Physical Conditioning Test Results of 30 Runs Exercised to Fatigue

6.3 EFFECT OF ECGS AND ARCTIC GARMENT ON METABOLIC RATES

An Air Force arctic garment that had full body insulation, except for the face, was used on all design verification test runs. This suit is a double thickness; the inner layer consists of quilted torso and pants, which are snapped together, and an outer single piece that is a zippered rubberized fabric liner. Thick insulated gloves and a headpiece are parts of the suit assembly. The outer suit has a tight rubber seal at the wrists and the neck to preclude any body thermal loss from internal to external heat transfer. The arctic garment cannot, therefore, be worn without cooling provisions for more than a few minutes at resting metabolic rates; without such provisions, the wearer would become extremely uncomfortable and would sweat profusely.

A minor modification was made to the arctic garment to permit it to be worn over the complete ECGS cooling suit (Figure 80). This modification required two penetration ports, one for the LCC/ECGS vacuum line fitting and the second for instrumentation leads. The arctic suit-ECGS combination was quite restrictive to mobility, particularly that of the 6 ft, 180 lb subject; however, either suit worn alone did not cause such a problem. The test configuration mobility problems increased the work loads at any given speed, probably near to what may be expected with the space pressure suit, which actually helped in simulating the typical EVA mission. Since the treadmill physical conditioning training runs were made with shorts only (track clothing), the metabolic rates increased greatly for any given treadmill grade and speed.

Figures 81 through 85 present theoretical treadmill performance curves that can be typically compared with the actual test data shown in Figure 86. The effect of an increased metabolic rate at a given treadmill condition with the ECGS-arctic garment combination is shown in Figure 83.

6.4 FINAL WORK LOAD CALIBRATION TESTS

The EVA mission profile of Section 6.1 was broken down into specific ranges of work levels that had to be set during the final design verification test. Each condition had to be set on the treadmill for the final two test subjects who, in turn, varied in weight by about 30 lb. The setting of

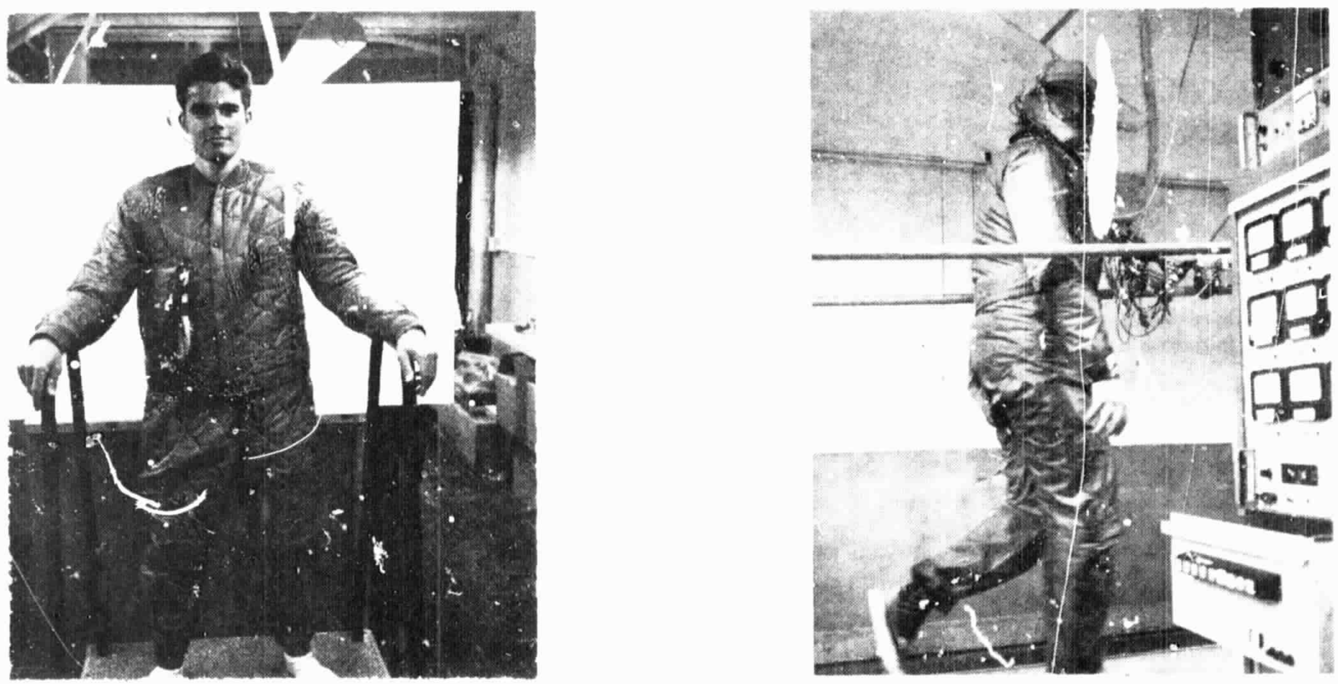

Figure 80. ECGS and Arctic Suit

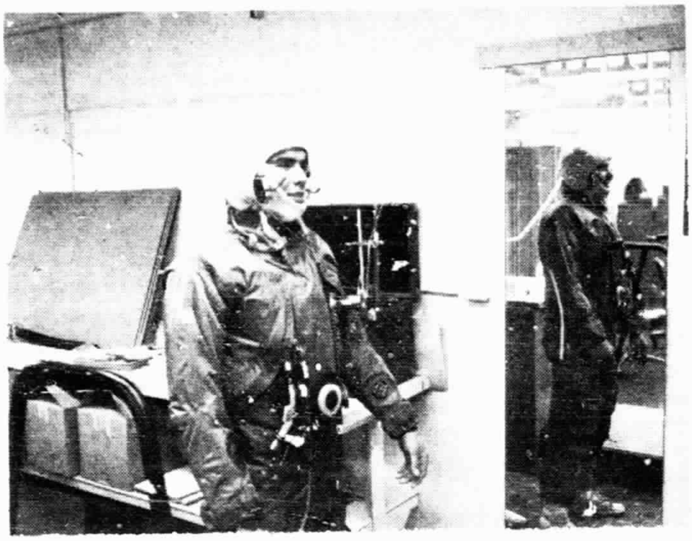

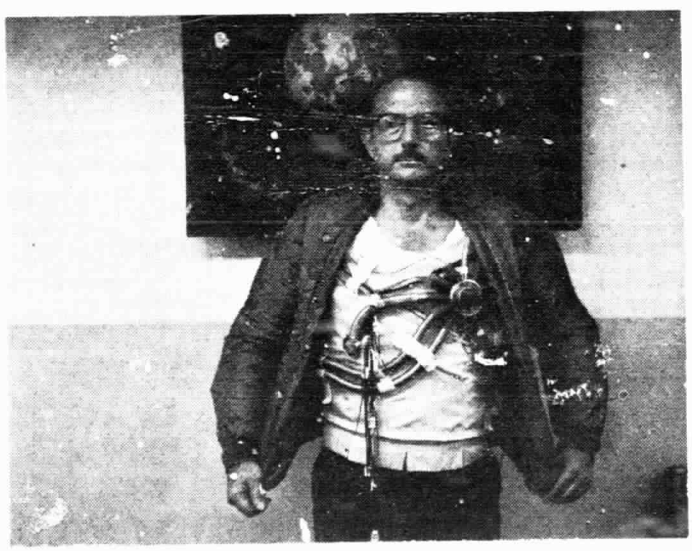

Figure 80. ECGS and Arctic Suit (Continued)

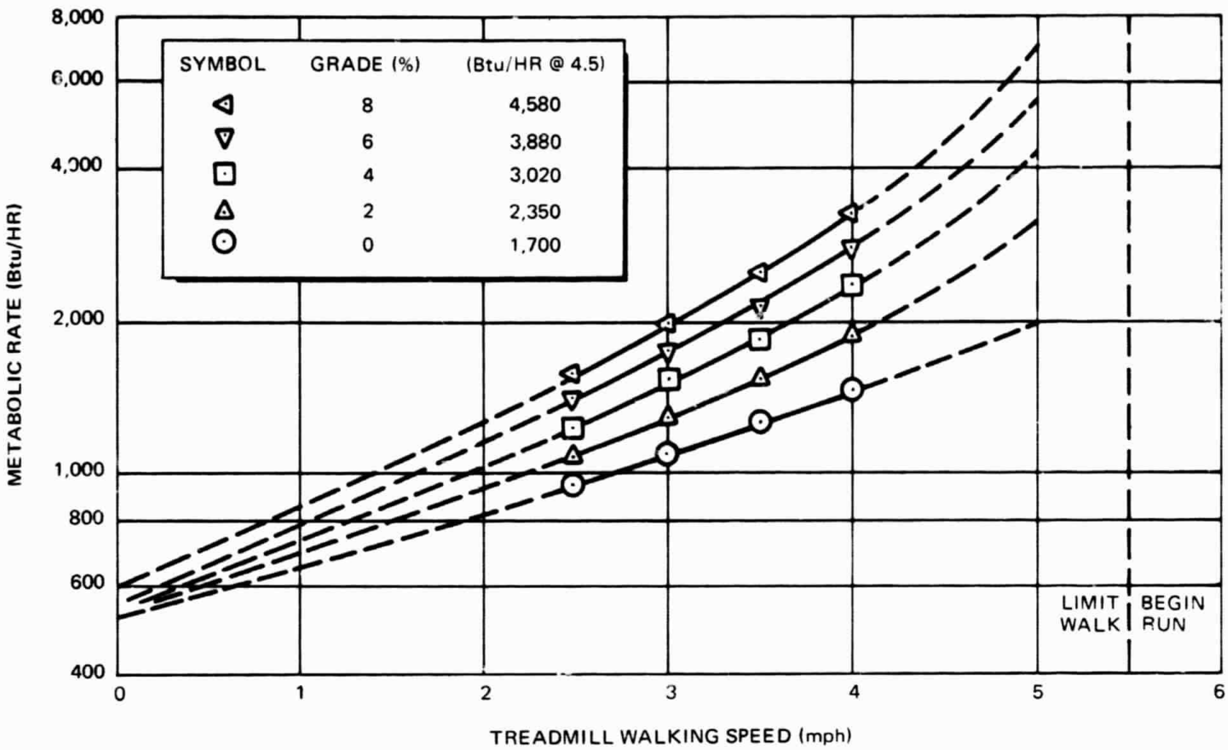

Figure 81. Walking Energy (160 lb Man)

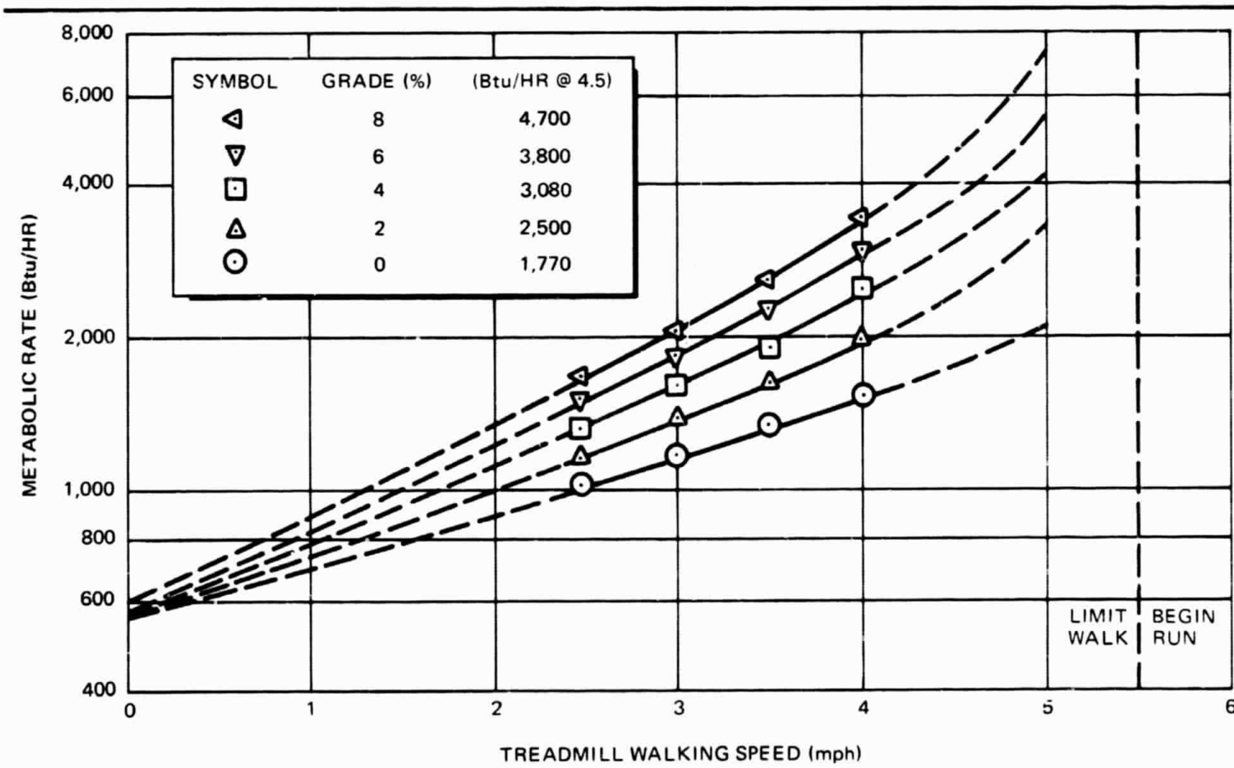

Figure 82. Walking Energy (170 lb Load/Weight Man)

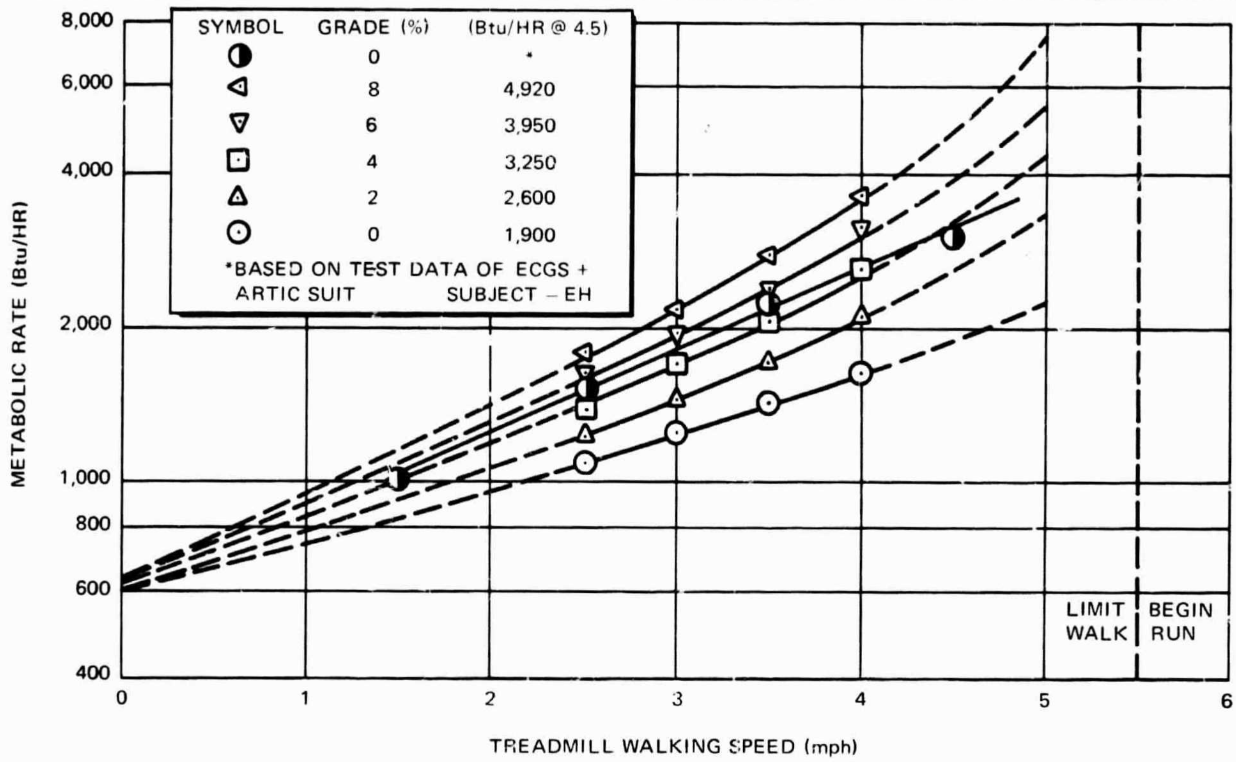

Figure 83. Walking Energy (180 lb Load/Weight Man)

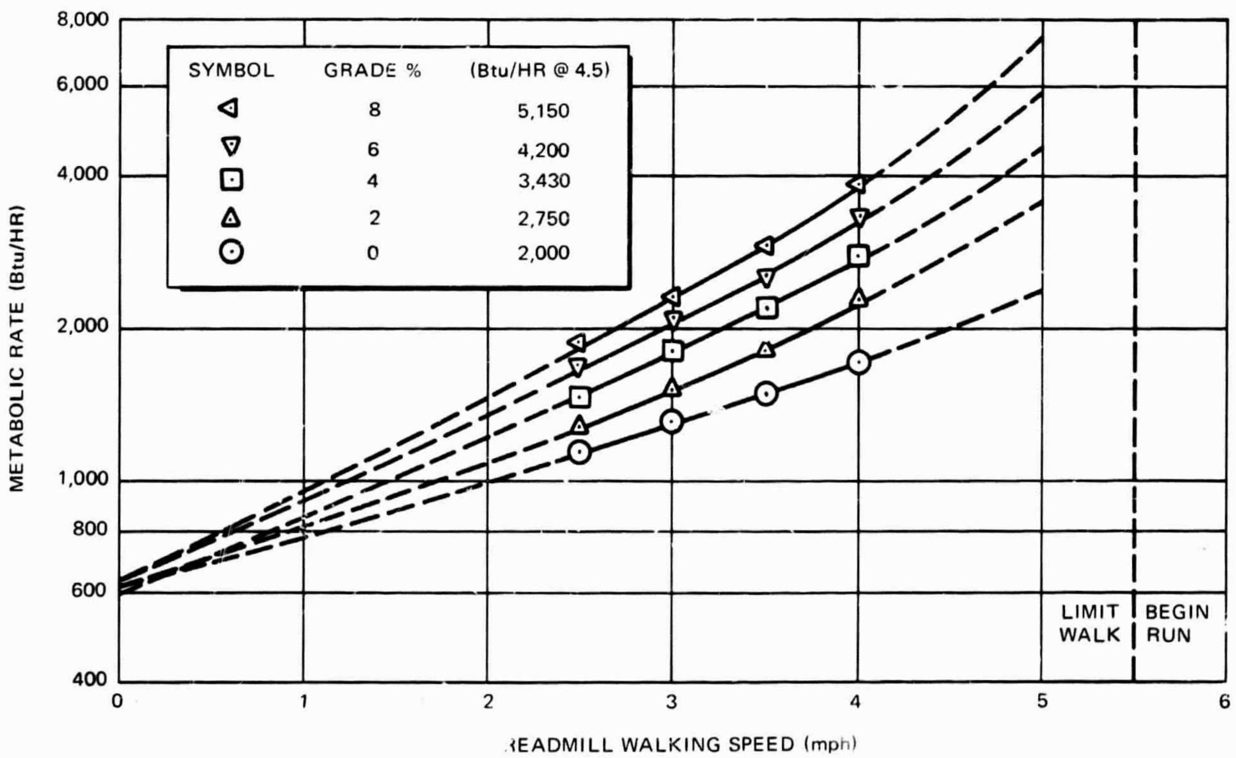

Figure 84. Walking Energy (190 lb Load/Weight Man)

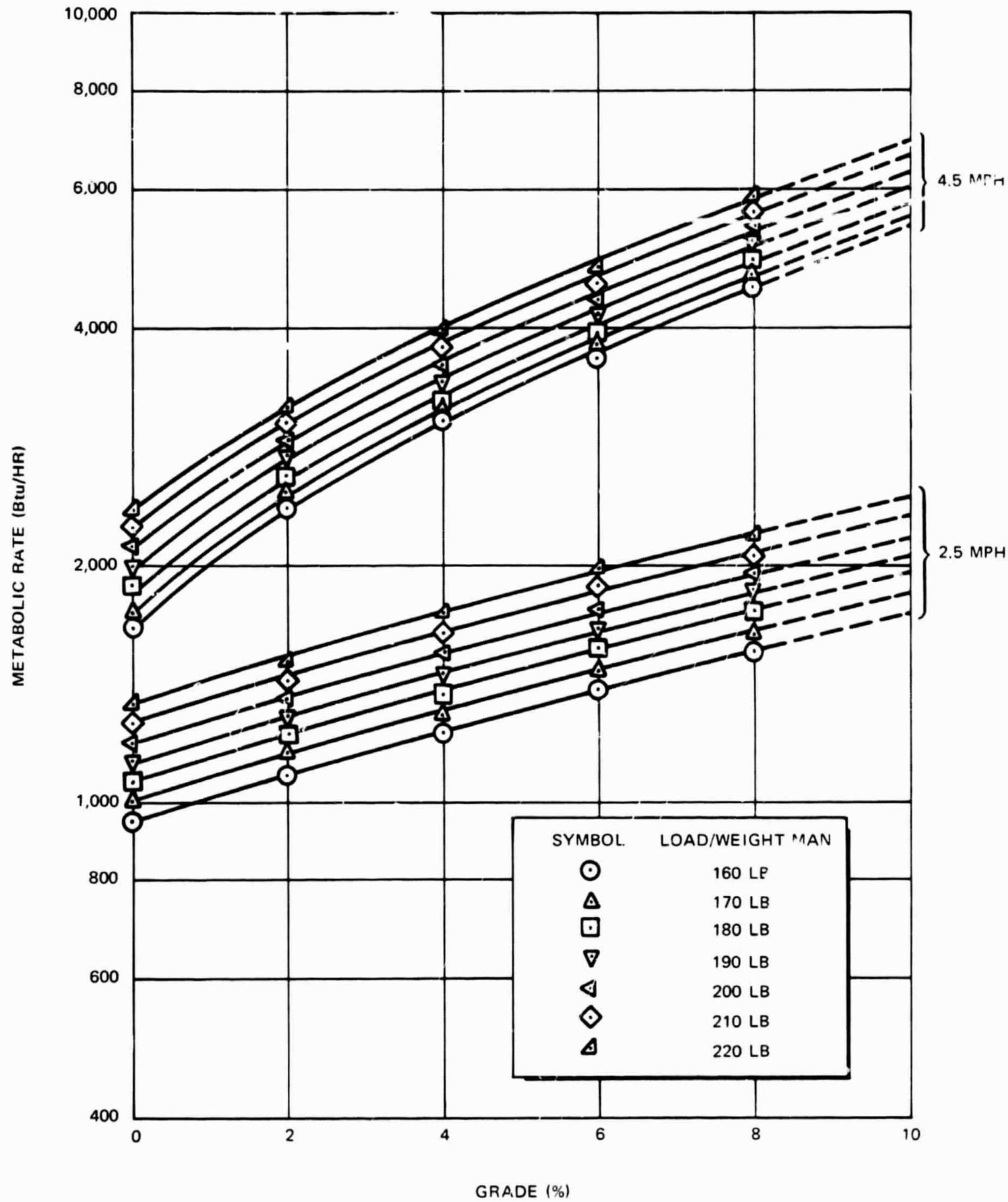

Figure 85. Walking Energy at 2.5 and 4.5 MPH

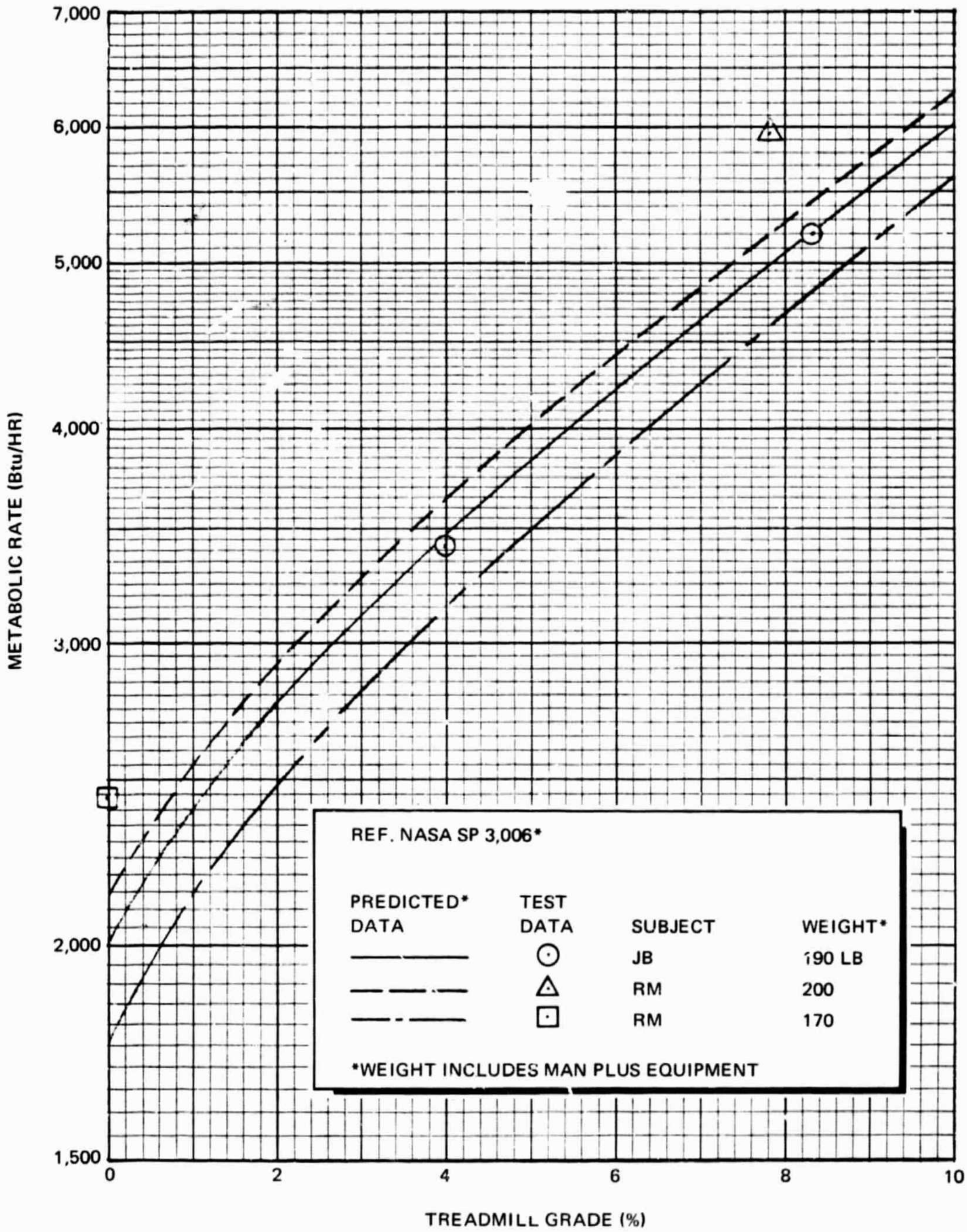

Figure 86. Comparison of Measured and Predicted Metabolic Rate Versus Treadmill Grade at 4.5 mph

proper treadmill conditions was not a simple matter because of the following variables:

1. The normal increase in metabolic rate with time from the beginning of any given run.
2. Treadmill speed.
3. Treadmill grade.
4. Restrictions in mobility over the normal training run condition (Section 6.3).
5. Changes in metabolic rate with removal of heat stress during a cooling run.
6. The effect of training enhancement with repetitive runs (Section 6.2).
7. Normal metabolic rate instrumentation errors (believed to be better than 3%).
8. Whether the maximum aerobic capacity had been exceeded (undetermined factor).
9. Dietary variation on the energy equivalent per unit volume of oxygen consumed (all data based on average diet, yielding 545 Btu/ft^3 oxygen).

The most significant of the above factors will be discussed as relating to the final runs as follows:

Metabolic Rate Increase With Time

Most of the EVA work load changes were to take place after a prior 10-min run. It was therefore desirable to obtain the point in time during any given 10-min run at which the metabolic rate should be measured. Figure 87 indicates that the peak values do fall near the 10-min point; prior to this, anaerobic energy probably has some contributary effect to the lower values until the body is physiology stabilized. Therefore, in long duration runs like the 30-min design verification fixed level tests, the metabolic rate was sampled at the 15-min point; shorter high rate runs such as the 15-min 5,000 Btu/hr tests were sampled at the 10-min point.

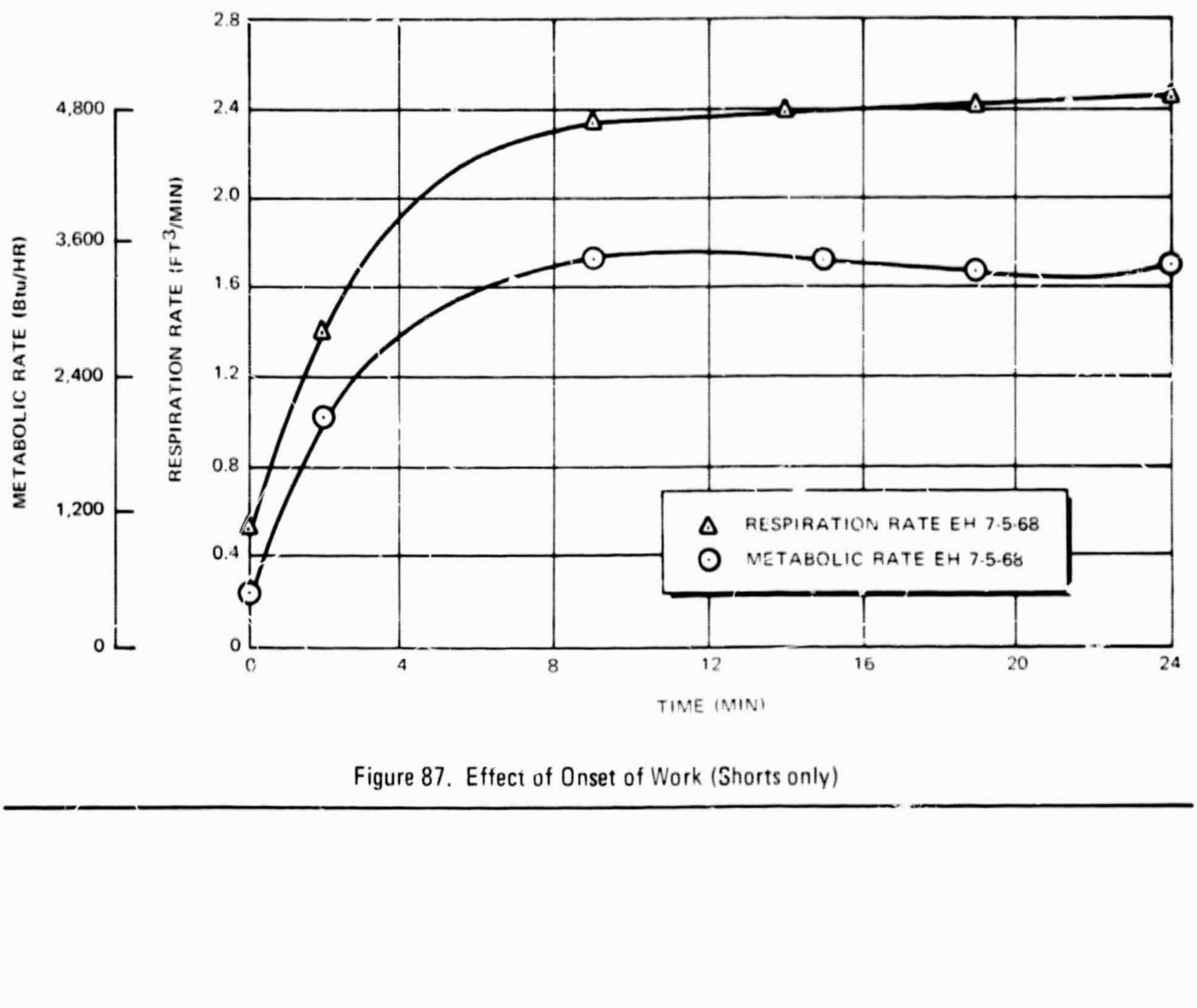

Figure 87. Effect of Onset of Work (Shorts only)

Treadmill Speed and Grade

Since all training runs were made at 4.5 mph with varying grade, an attempt was made to maintain to this value in the design verification runs. Any values above 4.5 mph were deemed dangerous in the event of a fatigue fall on the treadmill; none occurred.

Heat Stress on Metabolic Rate

Heat stress at high work loads is probably the most significant and (at present) the least understood of all the factors that relate to metabolic rate. The metabolic calibration curves shown in Figure 88 for the condition of full operational cooling ECGS plus arctic suit are based on cooling rates that were, in each case, set by the desires of the exercising test subject. The design verification runs of constant work load at several fixed heat removal rates produced heat stress at low heat-removal rates, and overcooling at the high heat-rejection rates; these factors complicated the setting of any particular run, but the final results were quite close to predictions.

When the data of Figure 88 were compared on the two subjects for a metabolic rate per pound of body weight (plus load), it was shown that the apparent discrepancy between subjects was less than 10%, which is quite good. It was then concluded that the final calibration for each subject was adequate.

6.5 CALIBRATION OF VACUUM FACILITY FOR VARIOUS ECGS HEAT REJECTION RATES

A technique was devised for a direct readout of the ECGS heat removal rate as a function of vacuum pumping machinery characteristics. When a synchronous speed vacuum pump evacuates a storage tank, eventually the tank pressure equilibrium will be reached; the time depends on the pump capacity and the tank volume. A fixed leakage is introduced into the tank, measured by a sensitive flowmeter; from this, a pressure-leakage flow rate relationship can be established which then simulates any object that may be coupled to the pressure tank such as the ECGS.

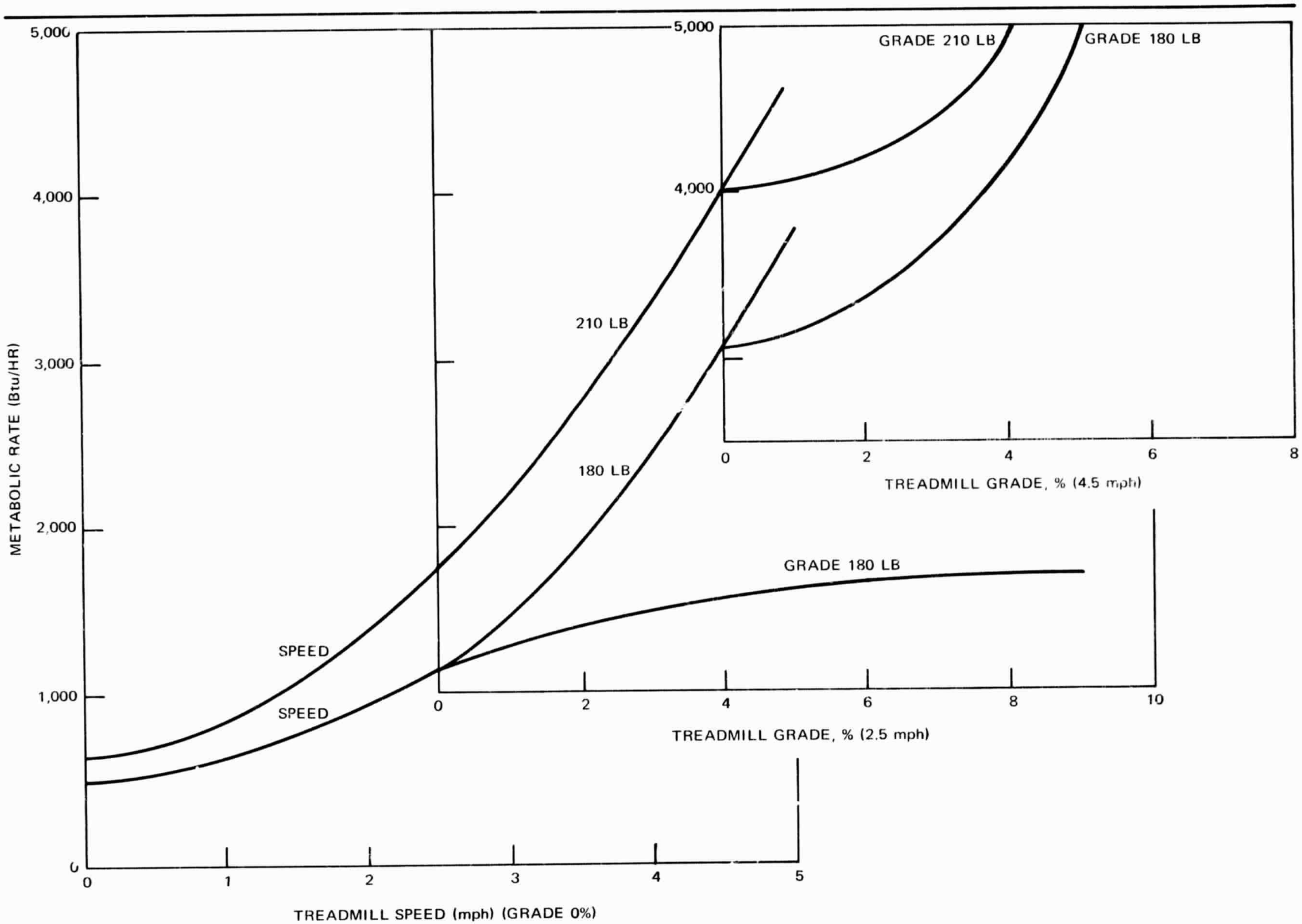

Figure 88. Treadmill Work Rates with ECGS and Arctic Suit

A large warm water filled flask was then connected by a throttle valve to the laboratory vacuum-supply manifold. Precise weighing of the flask and contents to ± 0.01 gram was made before and after setting the throttle valve at a particular manifold pressure setting. Water temperatures during boiloff in the flask were recorded to obtain the steam table heat of vaporization data, which in turn was integrated, thus resulting in a heat removal vs manifold pressure. Curves such as this were very accurately obtained for various leakage rates as explained in the prior paragraph. The family of pressure vs heat removal rates at various preset leakage rates were than cross-plotted to the several design verification plan heat removal rates. These data are shown in Figure 89. Checks were made by water weight loss in ECGS body patches in cooling operation with nearly perfect correlation. ECGS heat rejection rates can be instantly set or measured by this technique, which is believed accurate to within 2%.

A micron pressure gage is a rather fast response instrument; monitoring this gage (and the calibration curves) instantly shows the ECGS heat removal or cooling characteristics on a real-time basis.

6.6 TYPICAL TEST OPERATION

A typical complete suit ECGS test operation can be described as follows (Figure 90 shows a typical test):

1. The test subject tapes on the ECG electrodes and is then assisted into the ECGS garment. (Skin thermistors are a part of the ECGS.)
2. The arctic suit is donned and the inner ear thermistor is installed.
3. The subject gets on the inoperative treadmill, the LCG/ECGS vacuum umbilical line is connected.
4. The basic ECGS/instrumentation leakage rate is established prior to periodic injection of feed water. This determines which heat rejection calibration curve is to be used; a rest heat removal rate of 275 Btu/hr is set.

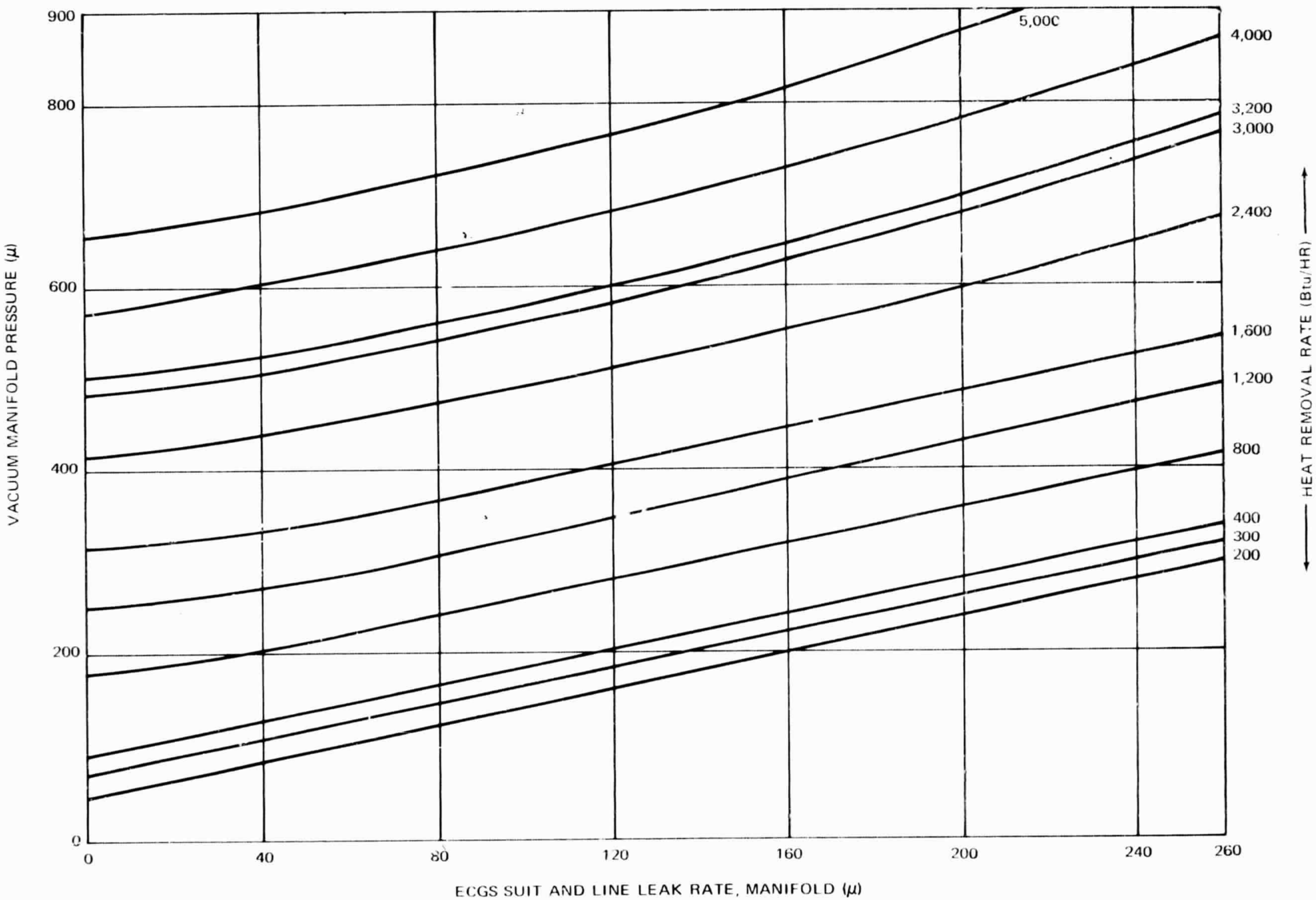

Figure 89. Vacuum Manifold Calibration

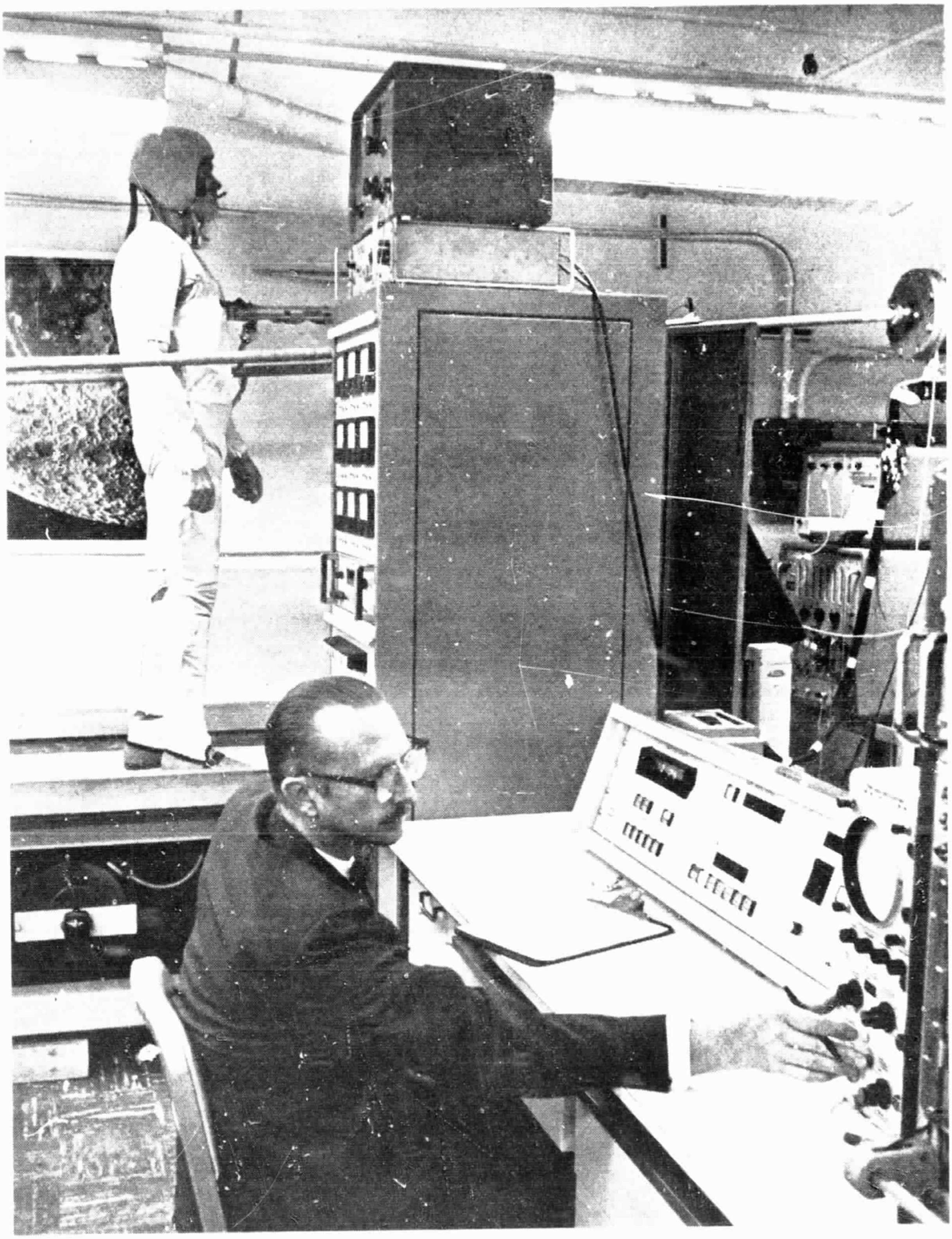

Figure 90. Laboratory and ECGS Run

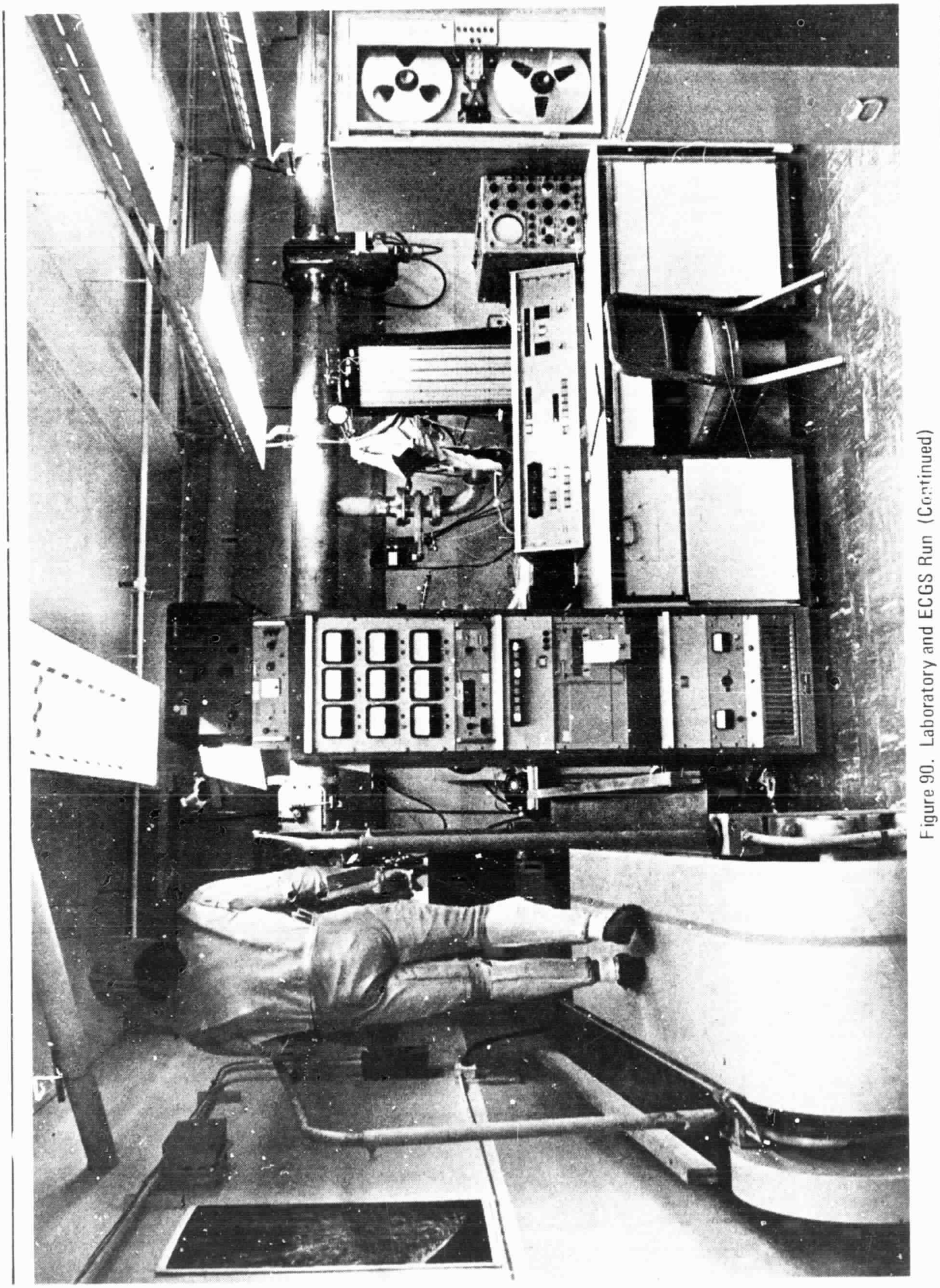

Figure 90. Laboratory and ECGS Run (Continued)

5. The thermistor harness plug is connected to the data acquisition system, and all instruments are trim-calibrated in readiness for the run.
6. The ECG recorder is turned on, and a basal pulse recording is obtained.
7. The treadmill is started after it has been checked for speed and grade.
8. A countdown is started, and at time zero the subject steps from a stationary straddle position to the walking belt position.
9. The data system immediately starts recording all instrumentation.
10. A test engineer monitors and controls (as required) the vacuum throttle value, thus setting heat rejection rate, which is brought to the predetermined rate in less than 2 sec.
11. The test conductor monitors all crew members and the data being generated.
12. Metabolic rate determinations are started by collecting expired air into a Douglas bag at predetermined times.
13. Oxygen consumption analysis is started on a Beckman E2 oxygen analyzer after four samples of 250 ml each are drawn out. The Douglas bag is then evacuated through a sensitive flowmeter to obtain minute volume, and metabolic rate is then calculated. Short interval runs rely on bag storage for later analysis.
14. Subject comments are recorded during run; heart rates are observed by the medical monitor as are other visual functions for subject safety.
15. The treadmill run is carried to completion or is aborted by any member of the operating crew for subject safety reasons.
16. At run conclusion, a 5- to 15-min recovery recording is made; during which time the heat rejection rate is set at 275 Btu/hr.
17. The subject is assisted out of the test setup in reverse to the order described above, or, in case of another run, a skin temperature stabilization period back to about 92° to 95°F is watched for and the next run begun.

6.7 PERFORMANCE RESULTS, CONSTANT WORKLOADS WITH FIXED LEVELS OF HEAT REJECTION

A series runs with full ECGS plus arctic garment were conducted in preparation for the formal 4-hour EVA mission profile tests. The purpose of these runs was to establish the best estimate for cooling rates at steady state conditions and to determine the maximum sustained cooling performance of the ECGS without the necessary consideration of body comfort. In every test, the cooling and metabolic rates were held constant for 30 min; each metabolic work level run was comprised of three 30-min levels of cooling. The only exception to this routine was the reduced duration runs at 5,000-Btu/hr work rate which was run to a maximum of 15 min because of human endurance considerations.

Much ECGS operational experience was gained from this test series. The only difficulty experienced was failure to inject the boiler water at the proper time at high cooling rates. For example, if the water injection was delayed too long, one or more patches would go dry and necessitate refilling immediately to maintain full cooling efficiency. Occasionally too much water was injected; this resulted in either the excess flowing out of the umbilical vacuum line in the liquid phase or freezing in the ECGS "octopus collector". It was found that the proper monitoring of temperatures and patch pressures would provide injector information that could be used to eliminate the flooding or freezing problems. For example, enough experience had been gained during these runs to allow completion of both 4-hour simulated EVA profiles without problems.

Tables III and IV and Figure 91 present the design verification test plan; all runs were completed except for the 4-hour mission profiles at cooling rates of 25% and 50% of the various step function metabolic rate levels. This deletion was mandatory for subject safety because heat prostration resulted almost immediately at these low cooling ratios at any reasonable exercise level. The 100% cooling rate case (cooling equal to metabolic rate) was also eliminated because extreme cold discomfort was reflected by the subjects and an alarming reduction in skin and core temperature that was deemed medically unsafe. The cooling headpiece was used on all runs, and by subject comment appears to be mandatory to sustain cooling comfort at high metabolic rates.

FOLDOUT F...

Table I

ECGS DESIGN VERIFICATION TES

Type of Run	Configuration	Metabolic Rate (Btu/Hr)	Subject	Treadmill Speed (Mph)	Treadmill Grade (%)	Heat Removal Rate (Btu/Hr)	Run Durati (Min)
Fixed heat removal	Full ECGS with Thermal Insulating garment (No Headpieces)	400	1	0	0	200	To Sta or 30
		400	2	0	0	200	
		400	1	0	0	300	
		400	2	0	0	300	
		400	1	0	0	400	
		400	2	0	0	400	
		1,600	1	Figure 88		800	
		1,600	2	Figure 88		800	
		1,600	1	Figure 88		1,200	
		1,600	2	Figure 88		1,200	
		1,600	1	Figure 88		1,600	
		1,600	2	Figure 88		1,600	
		3,200	1	Figure 88		1,600	
		3,200	2	Figure 88		1,600	
		3,200	1	Figure 88		2,400	
		3,200	2	Figure 88		2,400	
	Full ECGS with Thermal Insulating garment (No Headpiece)	3,200	1	Figure 88		3,200	
		3,200	2	Figure 88		3,200	To Ste or 30
		5,000	1	Figure 88		3,000	
		5,000	2	Figure 88		3,000	To Ste or 15
Fixed heat removal		5,000	1	Figure 88		4,000	

FOLDOUT FRAME

Table III

[C]GS DESIGN VERIFICATION TEST OUTLINE (Page 1 of 2)

[Trea]dmill [Spe]ed [(mp]h)	Grade (%)	Heat Removal Rate (Btu/Hr)	Run Duration (Min)	Instr Req	Test Objective	General Notes
	0	200	To Stability or 30 min	Table IV		
	0	200				
	0	300				
	0	300				
	0	400				
	0	400				
[Fi]gure 88		800				
[Fi]gure 88		800				
[Fi]gure 88		1,200			To determine optimum heat removal rate vs metabolic rate	
[Fi]gure 88		1,200				
[Fi]gure 88		1,600				
[Fi]gure 88		1,600				
[Fi]gure 88		1,600				
[Fi]gure 88		1,600				
[Fi]gure 88		2,400				
[Fi]gure 88		2,400				
[Fi]gure 88		3,200				
[Fi]gure 88		3,200	To Stability or 30 min			
[Fi]gure 88		3,000				
[Fi]gure 88		3,000	To Stability or 15 min			
[Fi]gure 88		4,000		Table IV		

FOLDOUT FRAME

Table III (Page 2 of 2)

Type of Run	Configuration	Metabolic Rate (Btu/Hr)	Subject	Treadmill Speed (Mph)	Treadmill Grade (%)	Heat Removal Rate (Btu/Hr)	Run Duration (Min)
Fixed heat removal		5,000	2	Figure 88		4,000	To Stability or 15 min
		5,000	1	Figure 88		5,000	
		5,000	2	Figure 88		5,000	
		5,000	1	Figure 88		5,000	
Fixed heat removal	See Gen Notes	5,000	2	Figure 88		5,000	To Stability or 15 min
Mission profile without space suit	Full ECGS with Thermal insulating garment	Fig. 88	1	Figure 88		25% M.R.	Figure 88
			2	Figure 88		25% M.R.	
			1	Figure 88		50% M.R.	
			2	Figure 88		50% M.R.	
			1	Figure 88		75% M.R.	
			2	Figure 88		75% M.R.	
			1	Figure 88		100% M.R.	
		Fig. 88	2	Figure 88		100% M.R.	Figure 88
Mission profile with space suit	Full ECGS with space suit	Fig. 88	1	Figure 88		See General Notes	Figure 88
		Fig. 88	2	Figure 88			Figure 88

FOLDOUT FRAME

on	Inst Req	Test Objective	General Notes
bility min	Table IV	To determine optimum heat removal rate vs metabolic rate	
bility min	Table IV	To determine optimum heat removal rate vs metabolic rate	Configuration for these runs to include head piece, full ECGS, and thermal insulating garment.
88	Table IV	To demonstrate ECGS performance at a range of cooling levels	5,000 Btu/Hr metabolic rate will be run at the option of the test subject and the medical monitor on all mission profile runs.
88	Table IV	To demonstrate ECGS performance with best heat removal rate in space suit.	Heat removal to be adjusted to best level as determined from preceding runs.
88	Table IV		
88	Table IV		

Table IV

ECSG FULL SYSTEM TEST INSTRUMENTATION

Parameter	Sensor	Range	Readout	Number Req
**Skin Temperature	Thermistor	40-150°F	Visual and Continuous Recording	9 visual-72 total
**System Pressure	Static Tap to Press Transducer	0-2.0 psia	Continuous Recording (multiplexed)	48
Reference Pressure	T/C Vacuum	0-500 mmHg	Visual and Continuous Recording	1
Ballonet Pressure	Manometer	0-20 in. H_2O Gage	Visual	1
Treadmill Speed	Speedometer	0-10 mph	Visual	1
Treadmill Grade	Scale	0-16%	Visual	1
EKG	Std EKG Electrodes		Strip Chart Recording	1
*Metabolic Rate ($_pCO_2$, $_pO_2$, min. Vol.)	Douglas Bag		Visual	1
Rectal or Inner Ear Temperature	Thermistor	90-110°F	Visual and Continuous Recording	1
Respiration Rate (Typical Values During Rest)			Visual	1
Blood Pressure (Pre and Post Test Values)			Visual	1

*Several samples will be taken during tests to verify existing treadmill calibration.
**Skin temperature and patch pressure locations to be monitored are shown in Figure 91.

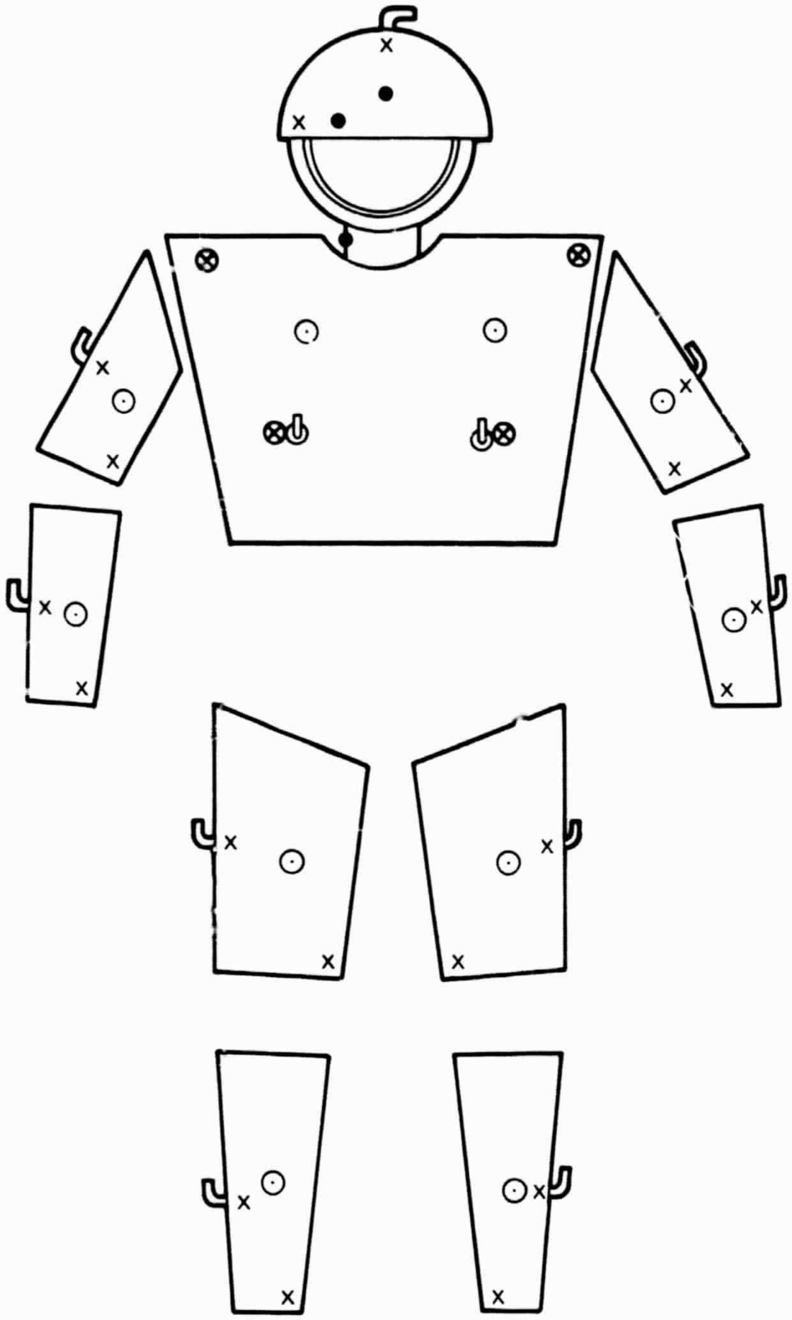

*PRESSURES

X FRONT SIDE OF SUBJECT ONLY

⊗ FRONT AND BACK SIDE OF SUBJECT

SKIN TEMPERATURES

● FRONT SIDE OF SUBJECT ONLY

⊙ FRONT AND BACK SIDE OF SUBJECT

*PATCH PRESSURES WILL BE MEASURED AT THE VACUUM OUTLET AND AT THE POINT FARTHEST AWAY FROM THE VACUUM EXIT INSIDE THE PATCH

Figure 91. Pressure and Temperature Locations ECGS Design Verification Tests (Basic Minimum Requirements)

Typical detailed temperature, pressure, cooling rate, and metabolic data are presented in Appendix E. From these results, summarized analyses that cover all the fixed level cooling runs were made and this information is presented in Figures 92 through 103.

The fixed level cooling runs can be further summarized by the following subjects, each of which will be discussed in detail:

- Reduction of pulse rate by elimination of heat stress.
- ECGS capable of overcooling at 5,000-Btu/hr metabolic ratio.
- Apparent increase in work output with proper cooling rate.
- Preliminary values for skin comfort temperatures at high work rates suggested.
- Preliminary values for heat rejection to maintain thermal balance at high metabolic rates.

Reduction of Pulse by Elimination of Heat Stress

The lowering of any stress situation will result in a lowered pulse rate. The quantitative values for complete removal of heat stress at limit work loads are virtually unknown; however, the high rate ECGS cooling provides some of these data and the results are presented in Figures 104 and 105. From Figure 104, the maximum cooling torso suit has lowered the pulse rate from 172 to 150 or a 13% reduction at 5,000-Btu/hr metabolic rate. The tests were run for the same duration on the same highly conditioned subject on consecutive days, thereby minimizing any training advantage. The effect of heat stress at 2,000-Btu/hr as compared to the full ECGS suit cooling is similarly spectacular.

Figure 106 shows three pulse rate time histories at a metabolic rate of 5,160-Btu/hr and also shows the effects of removing heat stress. This particular test series was conducted on the same highly conditioned subject on consecutive runs a few minutes apart (the high cooling rate run last and the lowest run first). The normal trend at constant cooling would have been to show a higher pulse rate on the last run caused by the extreme energy output and fatigue buildup. The trend was decisively reversed by increased cooling.

TREADMILL SPEED 2.75 MPH, TREADMILL GRADE 0% (METABOLIC RATE 1600 BTU/HR)						
RUN NO.	HEAT REMOVAL RATE BTU/HR	SUBJECT E H COMMENTS	MIN CORE TEMP	MAX CORE TEMP	MEASURED METABOLIC RATE BTU/HR	AVERAGE PULSE RATE
610 ⊙	800	TOO WARM	93.9	96.8	1585	92.0
611 △	1200	COMFORTABLE	94.2	95.2	1674	98.0
612 ⊡	1600	TOO COLD	93.1	95.2	1784	99.0

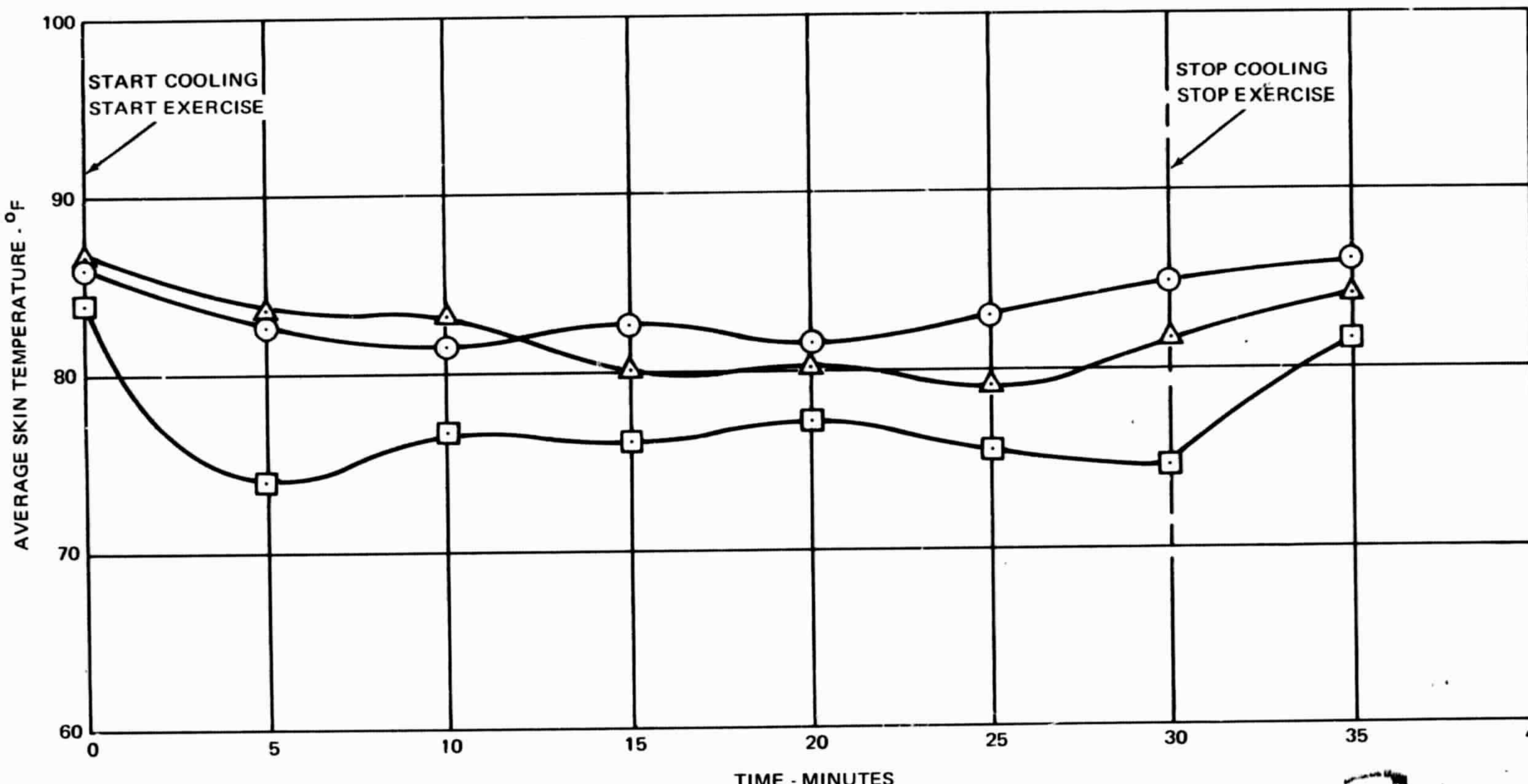

Figure 92. Skin Temperature Time History – Full ECGS with Arctic Suit

TREADMILL SPEED 4.5 MPH, TREADMILL GRADE .25% (METABOLIC RATE 3200 BTU/HR)						
RUN NO.	HEAT PEMOVAL RATE BTU/HR	SUBJECT E H COMMENTS	MIN CORE TEMP	MAX CORE TEMP	MEASURED METABOLIC RATE BTU/HR	AVERAGE PULSE RATE
613 ⊙	1600	TOO WARM	98.3	99.0	2735	133.3
614 △	2400	COMFORTABLE	97.7	98.1	2889	137.9
615 ⊡	3200	TOO COLD	98.0	98.8	2744	139.4

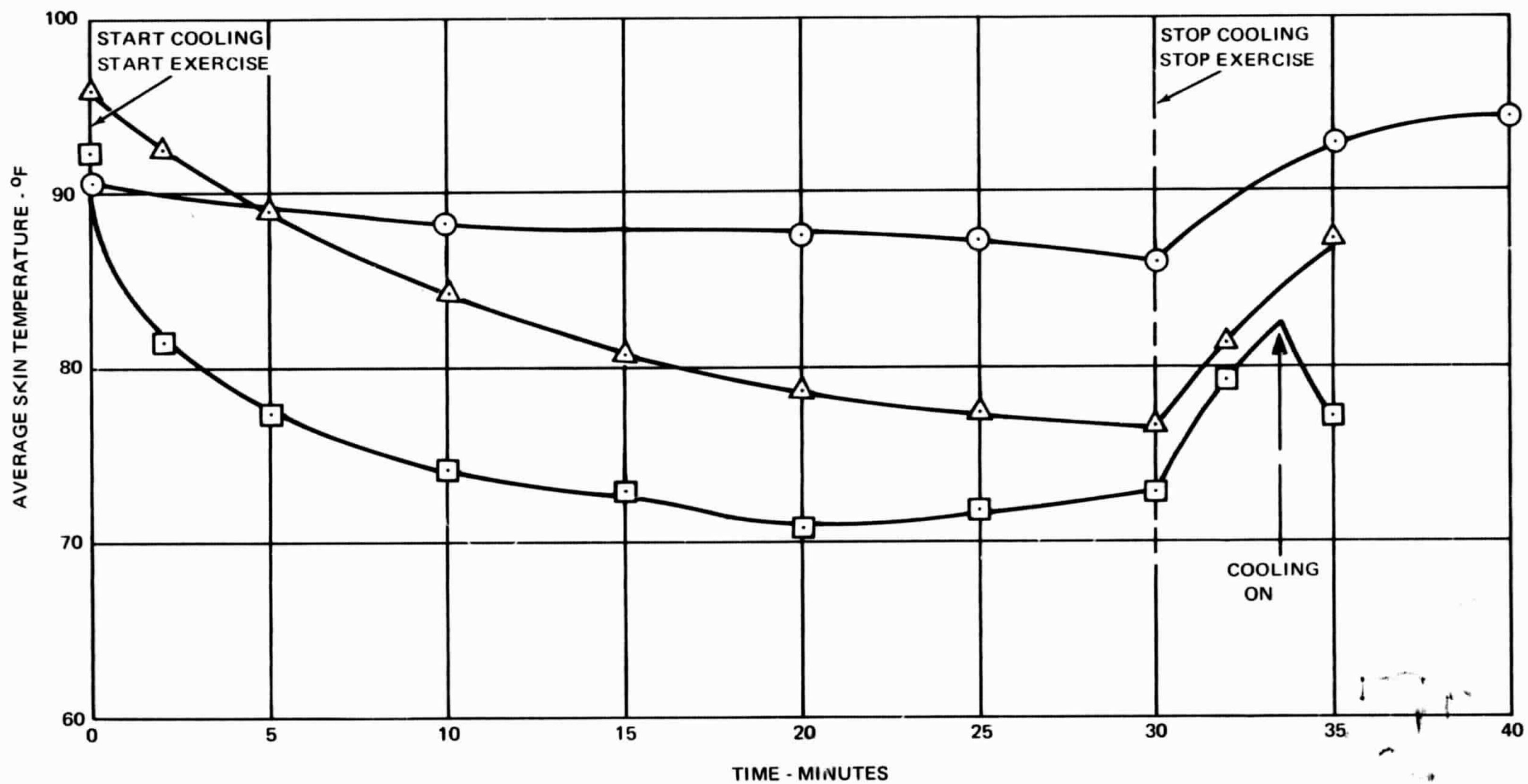

Figure 93. Skin Temperature Time History – Full ECGS with Arctic Suit

TREADMILL SPEED 4.5 MPH, TREADMILL GRADE 6% (METABOLIC RATE 5000 BTU/HR)						
RUN NO.	HEAT REMOVAL RATE BTU/HR	SUBJECT E H COMMENTS	MIN CORE TEMP	MAX CORE TEMP	MEASURED METABOLIC RATE BTU/HR	AVERAGE PULSE RATE
622 ⊙	3000	COMFORTABLE	97.3	99.1	4480	160.4
623 △	4000	TOO COLD	97.0	98.0	4410	170.9
624 ⊡	5000	TOO COLD	96.0	98.5	4322	167.6

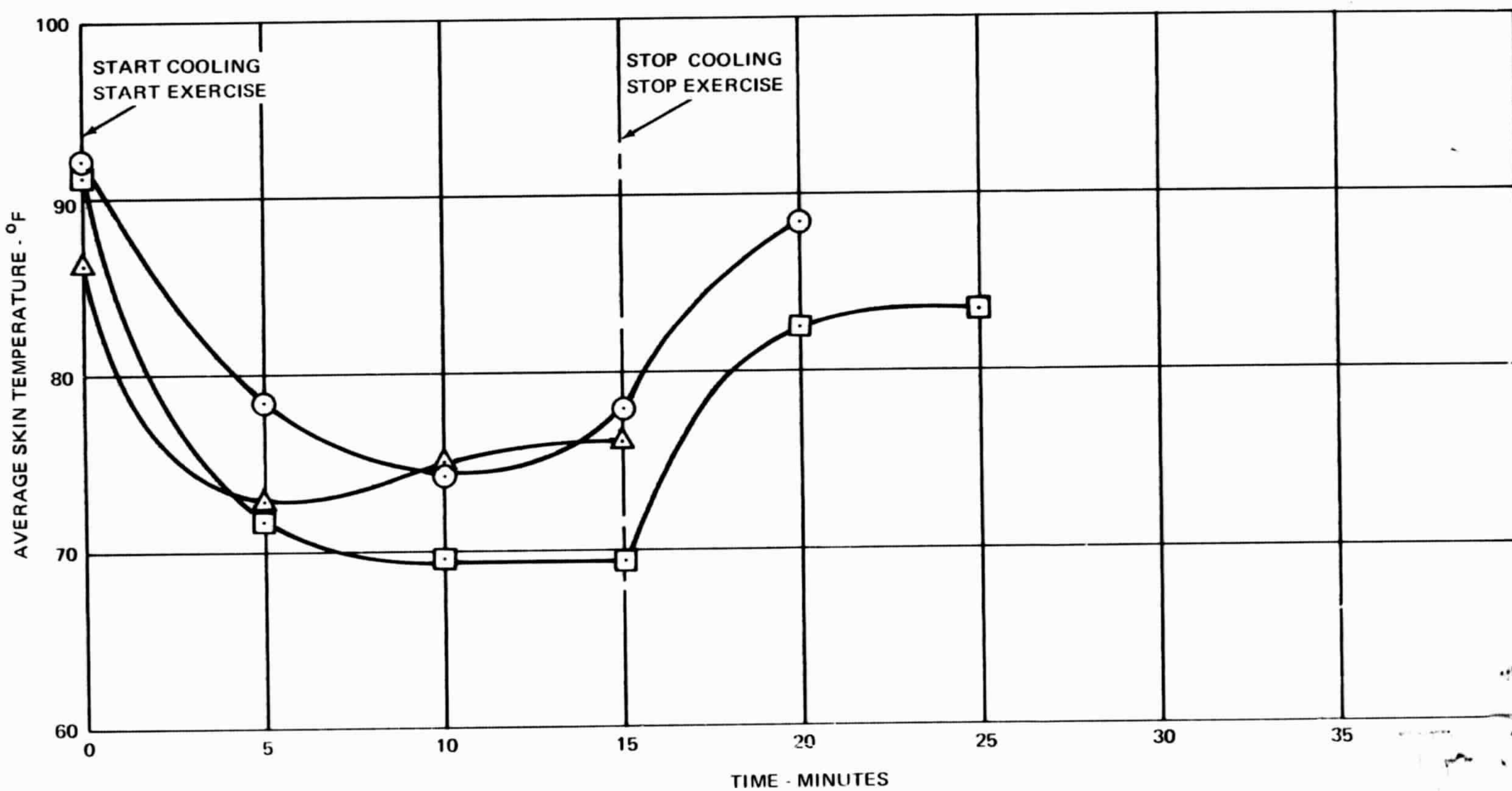

Figure 94. Skin Temperature Time History – Full ECGS with Arctic Suit

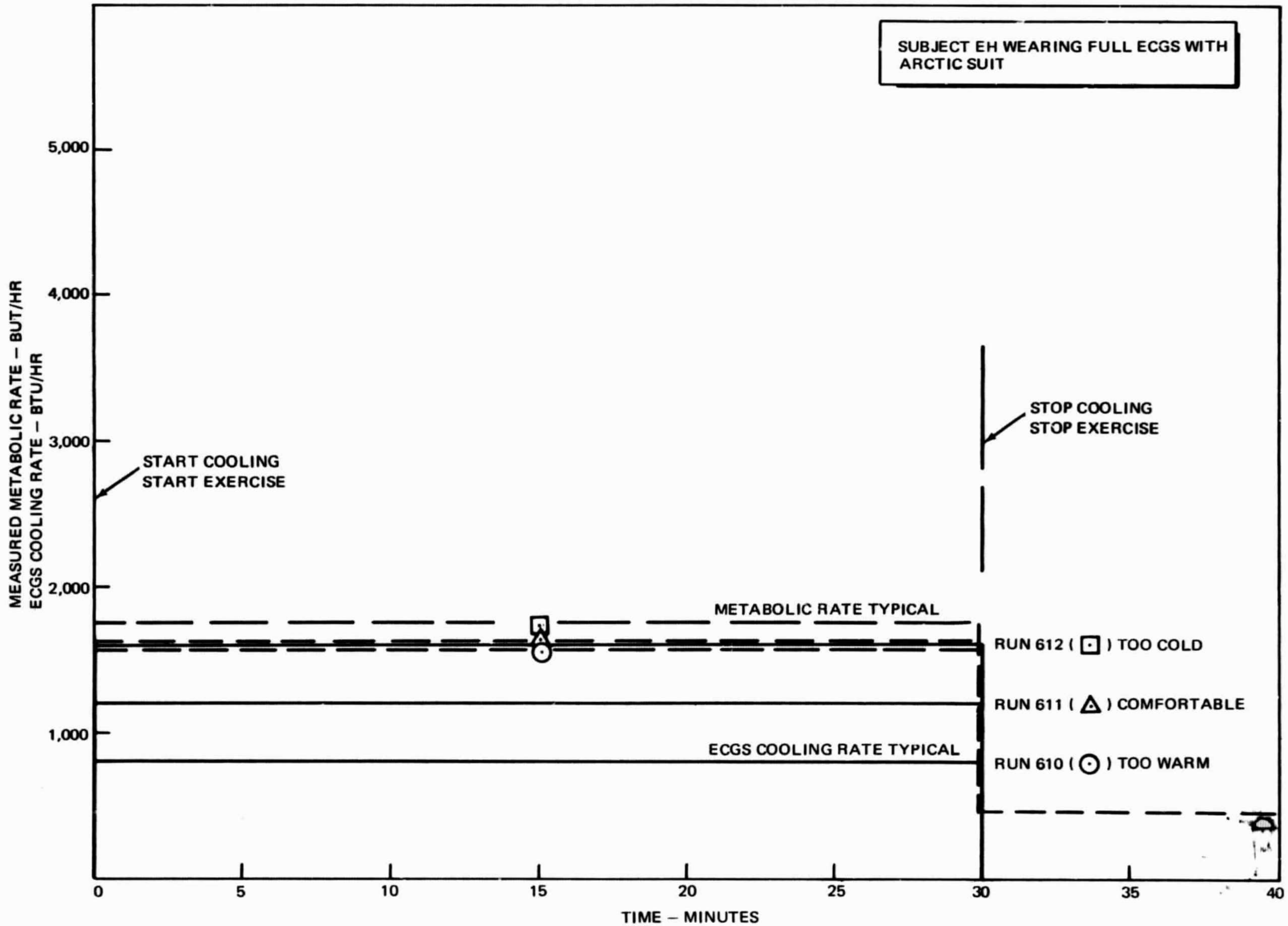

Figure 95. Work and Cooling Rate Time History

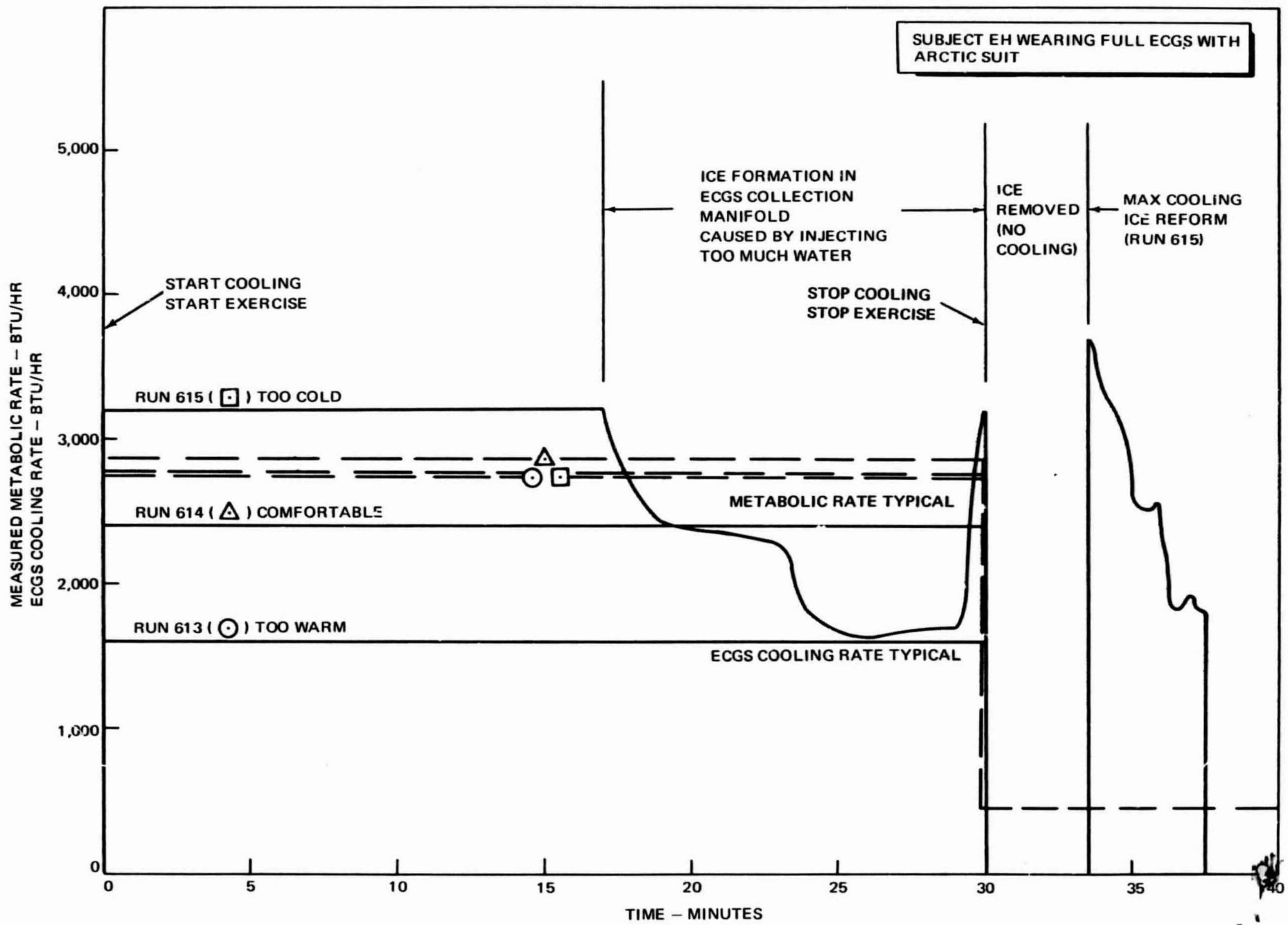

Figure 96. Work and Cooling Rate Time History

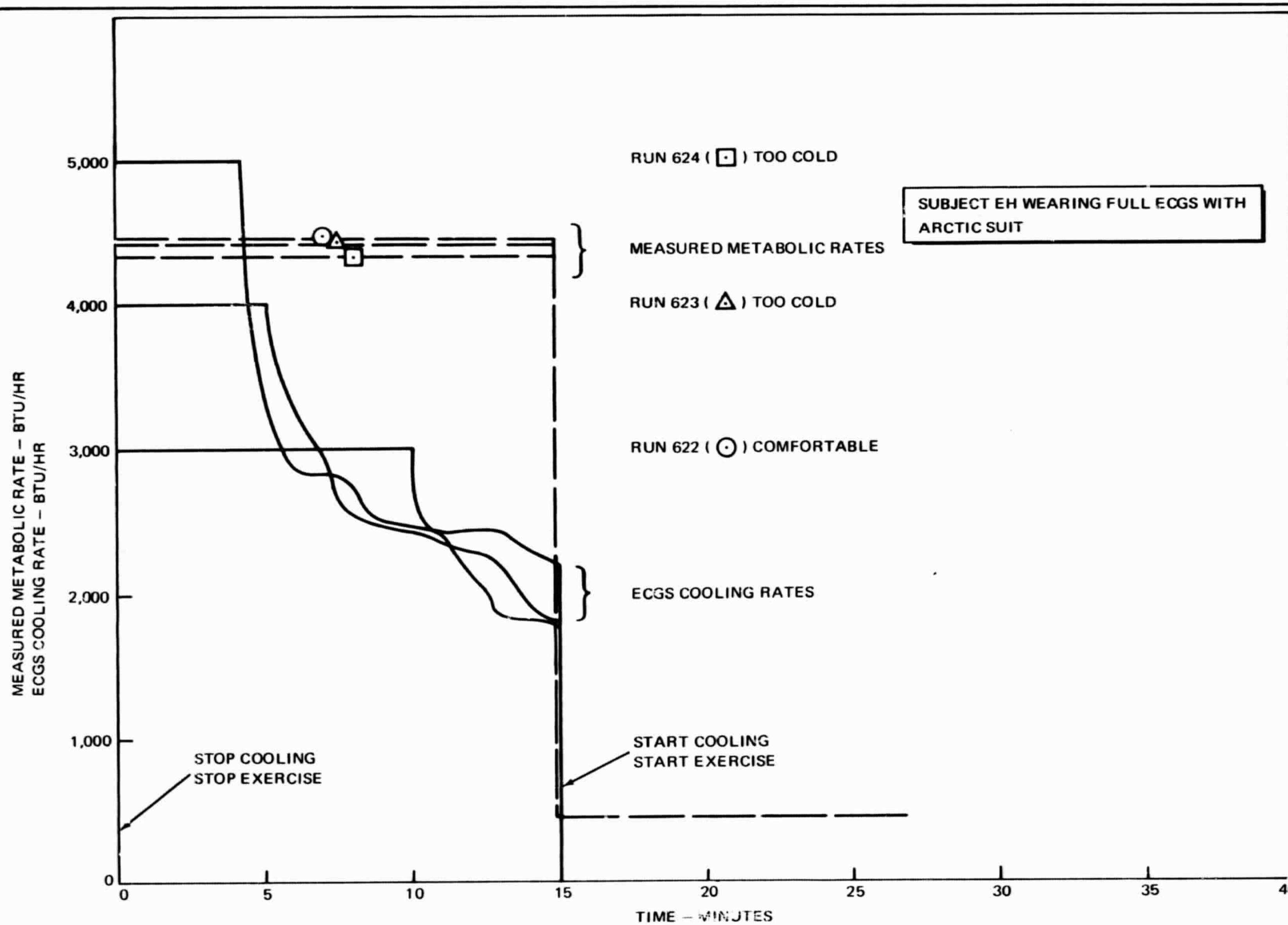

Figure 97. Work and Cooling Rate Time History

TREADMILL SPEED 2 MPH, TREADMILL GRADE 0% (METABOLIC RATE 1600 BTU/HR)						
RUN NO.	HEAT REMOVAL RATE BTU/HR	SUBJECT J B COMMENTS	MIN CORE TEMP	MAX CORE TEMP	MEASURED METABOLIC RATE BTU/HR	AVERAGE PULSE RATE
610 ⊙	800	TOO WARM	95.9	97.0	1737	98.5
617 △	1200	COMFORTABLE	96.6	97.0	1597	98.3
618 ⊡	1600	TOO COLD	96.1	96.8	1612	101.8

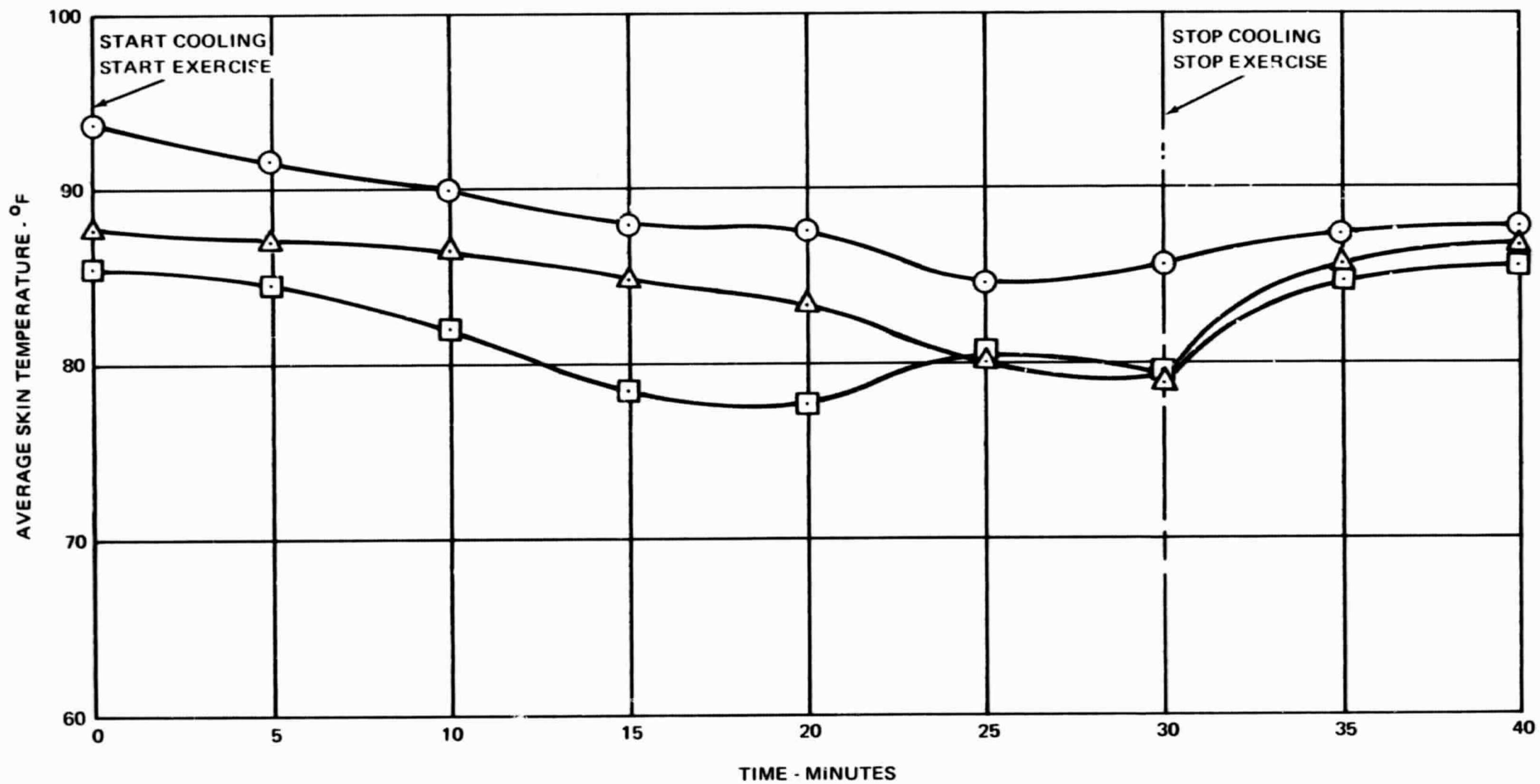

Figure 98. Skin Temperature Time History – Full ECGS with Arctic Suit

TREADMILL SPEED 3.9 MPH, TREADMILL GRADE 0% (METABOLIC RATE 3200 BTU/HR)						
RUN NO.	HEAT REMOVAL RATE BTU/HR	SUBJECT JB COMMENTS	MIN CORE TEMP	MAX CORE TEMP	MEASURED METABOLIC RATE BTU/HR	AVERAGE PULSE RATE
619 ⊙	1600	TOO WARM	95.0	98.0	3181	135.7
620 △	2400	COMFORTABLE	96.0	98.9	2982	147.2
621 ⊡	3200	TOO COLD	95.8	97.1	3063	154.1

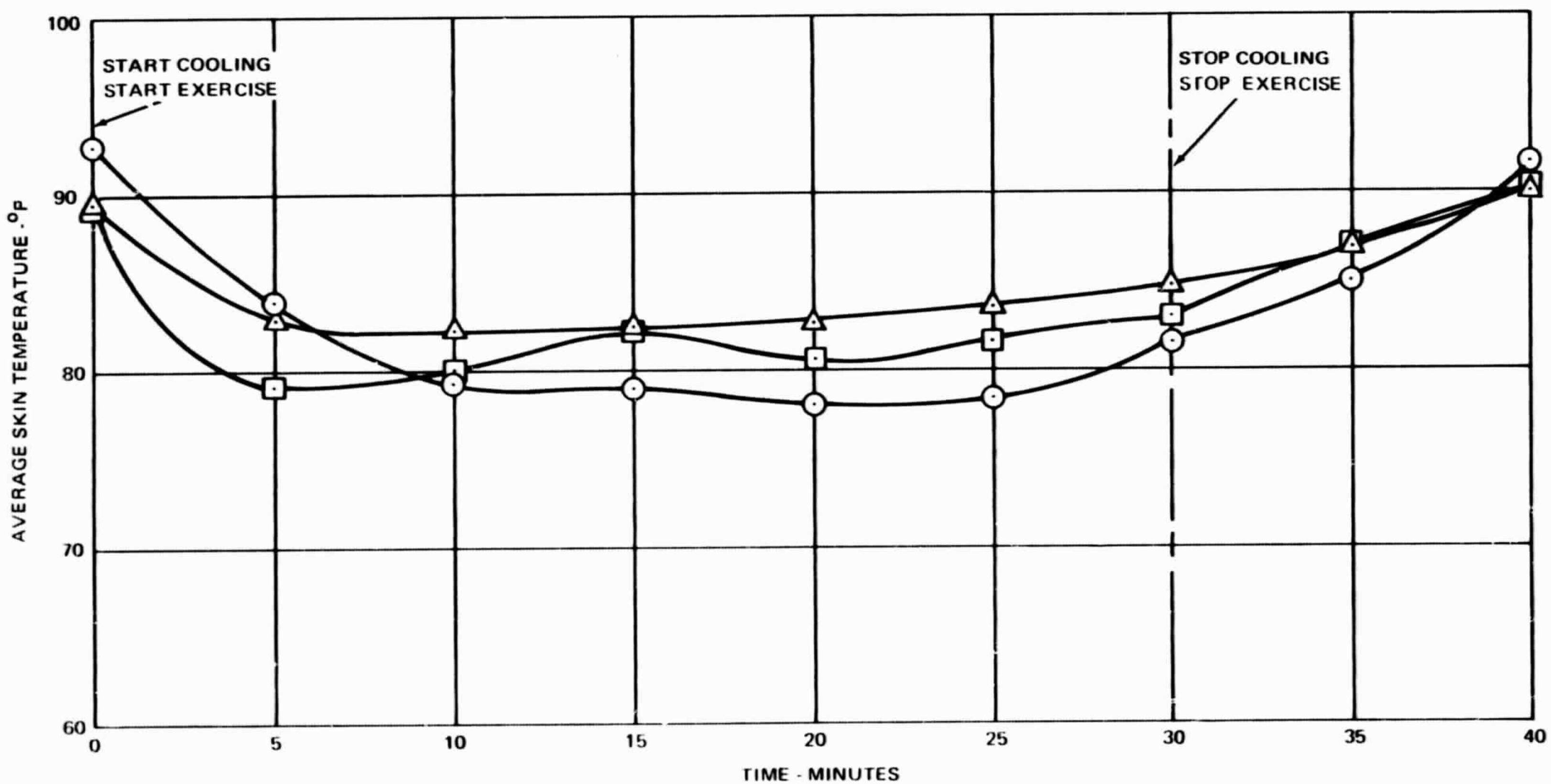

Figure 99. Skin Temperature Time History – Full ECGS with Arctic Suit

TREADMILL SPEED 4.5 MPH, TREADMILL GRADE 3.5% (METABOLIC RATE 5000 BTU/HR)						
RUN NO.	HEAT REMOVAL RATE BTU/HR	SUBJECT J B COMMENTS	MIN CORE TEMP	MAX CORE TEMP	MEASURED METABOLIC RATE BTU/HR	AVERAGE PULSE RATE
625 ⊙	3000	SLIGHTLY WARM	99.1	99.7	5157	166.2
626 △	4000	COMFORTABLE	97.8	98.8	—	160.4
627 ⊡	5000	TOO COLD	97.1	97.8	—	152.2

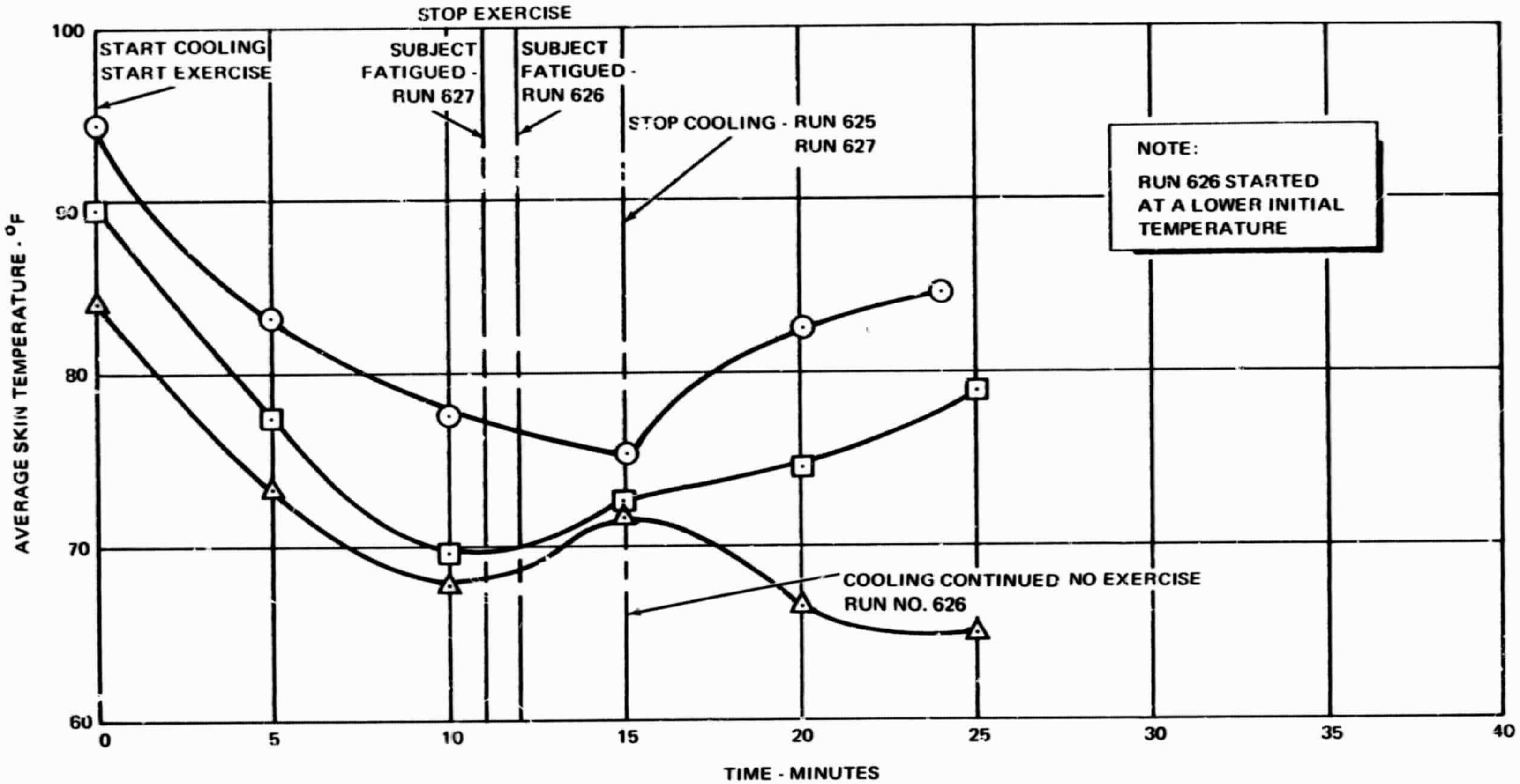

Figure 100. Skin Temperature Time History – Full ECGS with Arctic Suit

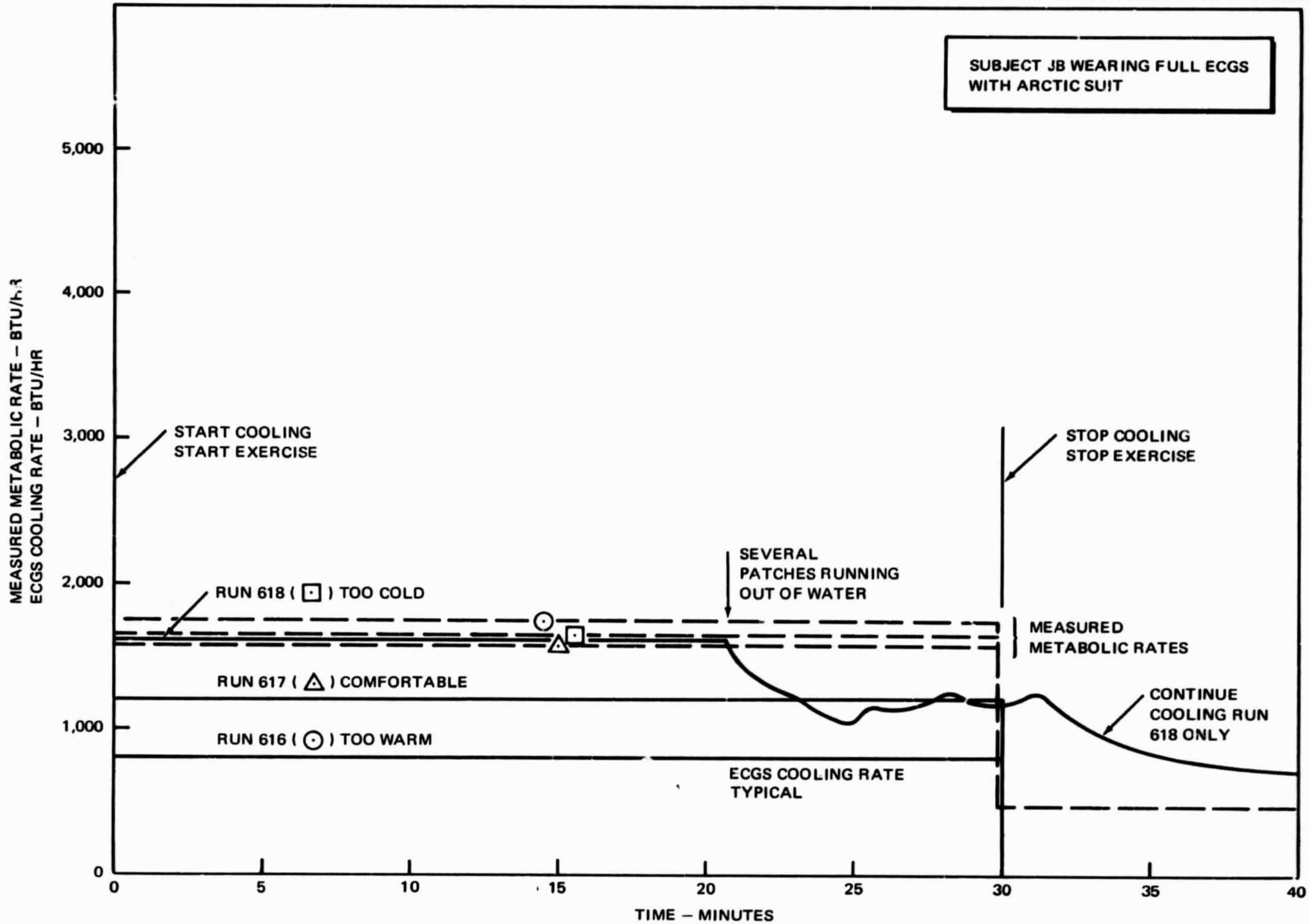

Figure 101. Work and Cooling Rate Time History

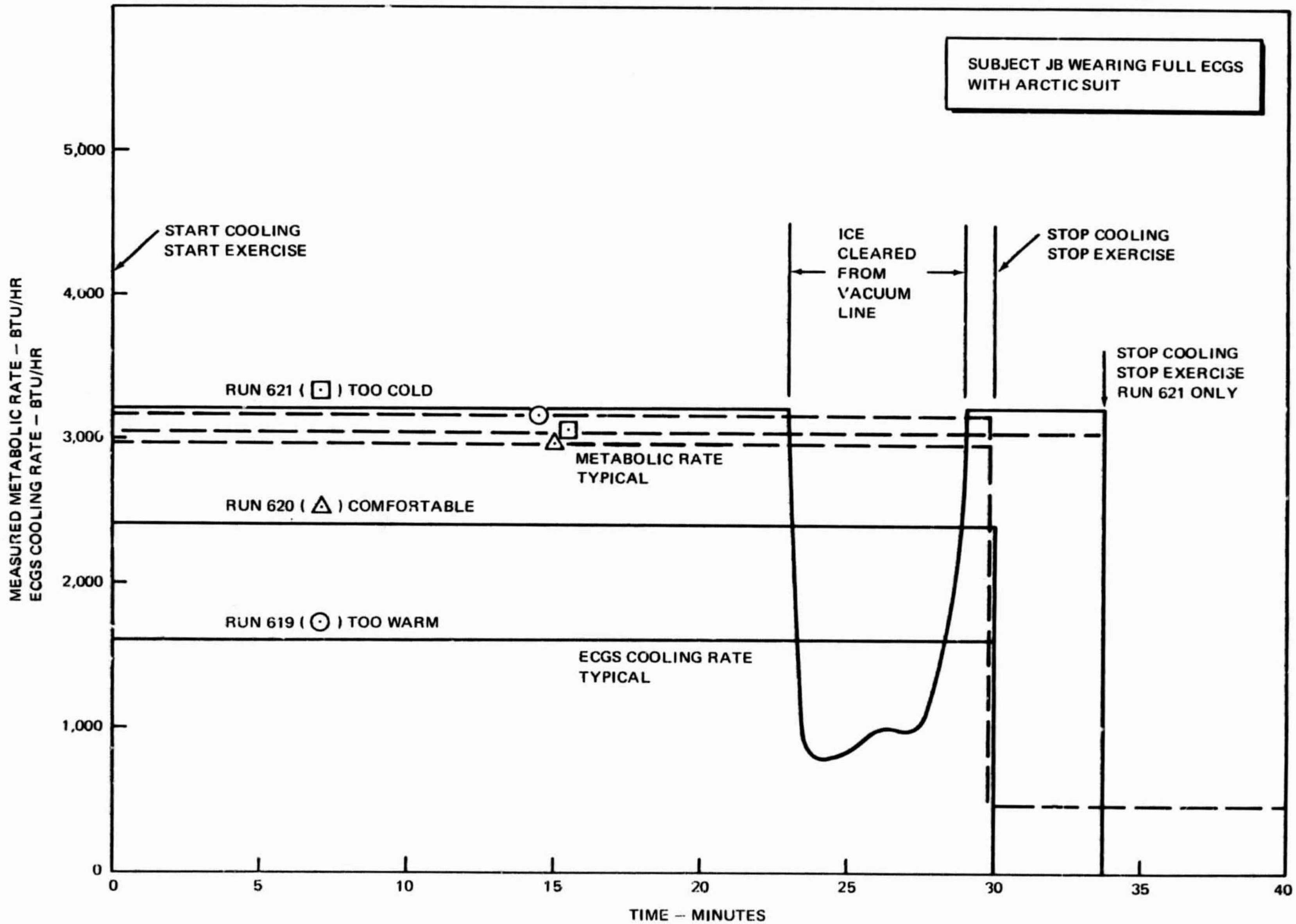

Figure 102. Work and Cooling Rate Time History

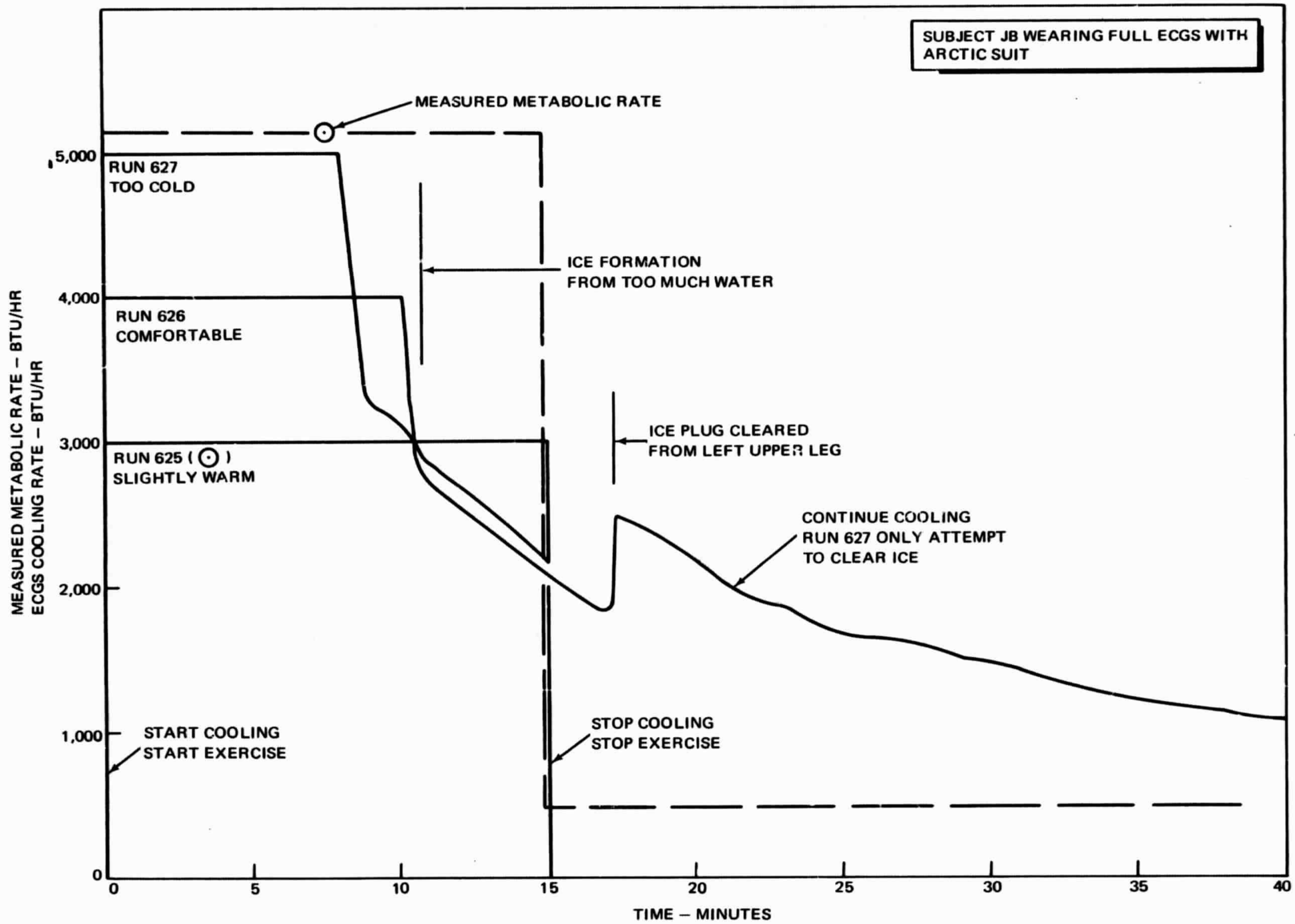

Figure 103. Work and Cooling Rate Time History

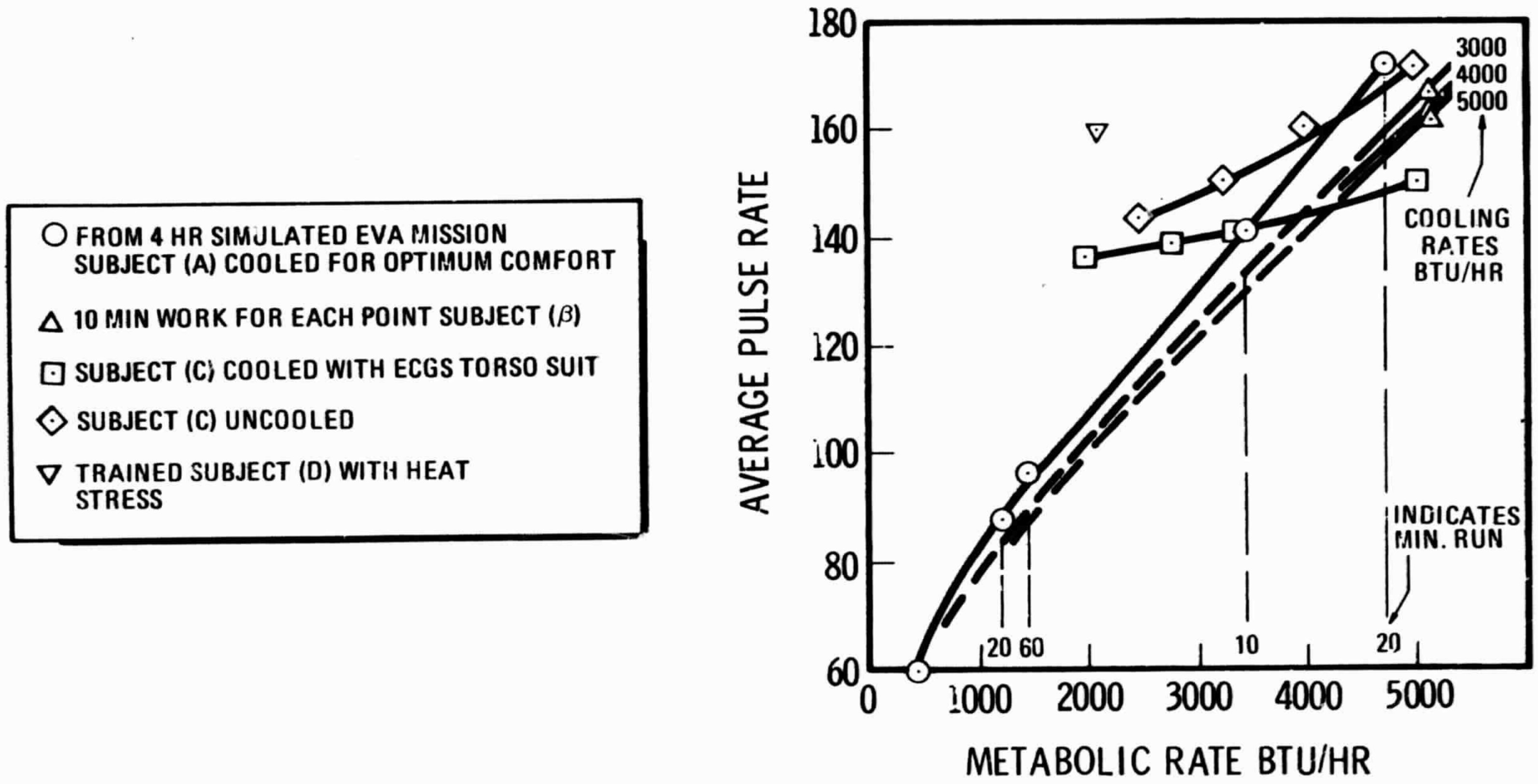

Figure 104. Effect of ECGS Cooling on Heart Rate during Heavy Work Loads

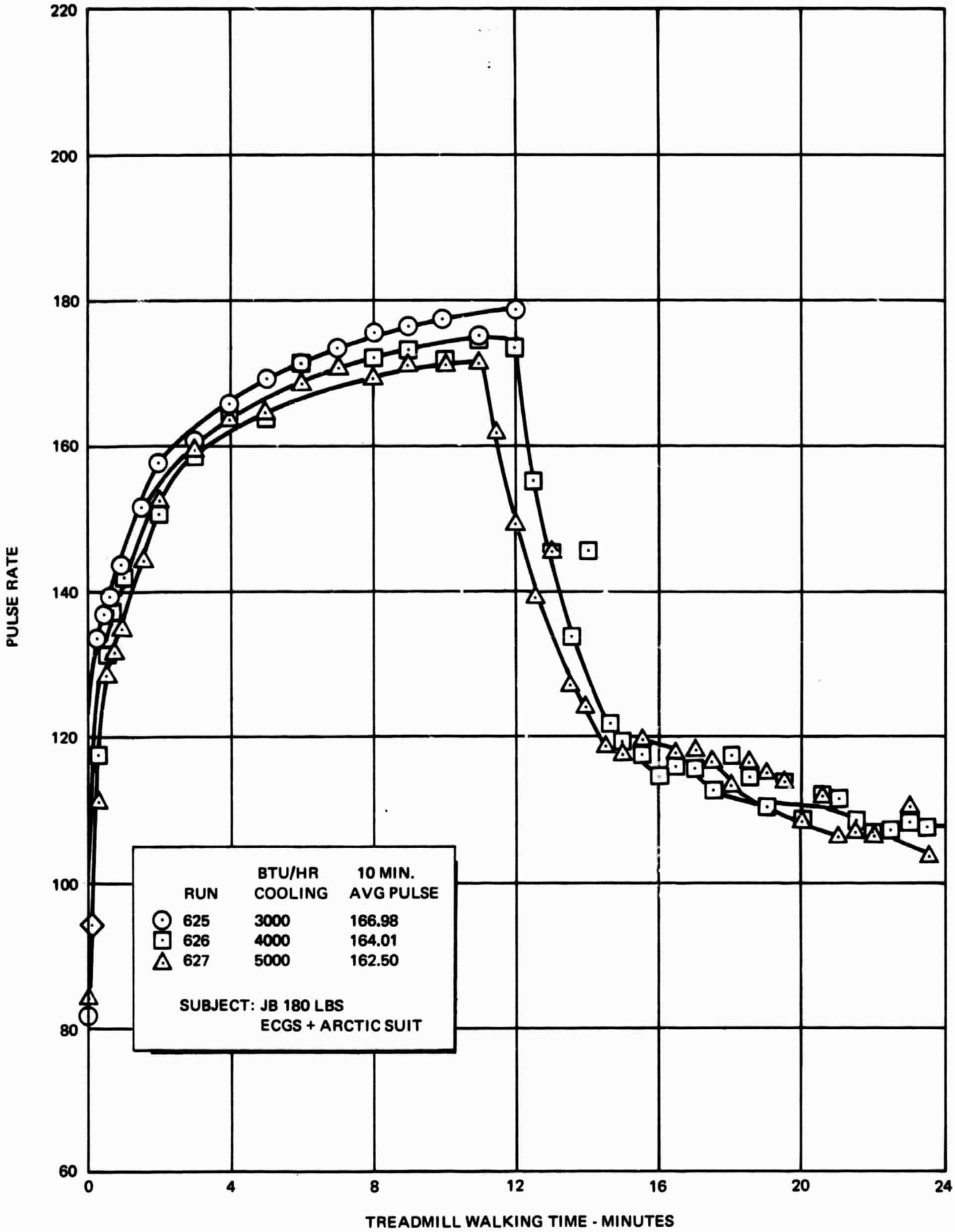

Figure 105. Effect of ECGS Cooling on Pulse Rate at Metabolic Rate of 5170 Btu/HR (4.5 MPH 3.5%)

SYMBOL	CORE AND SKIN TEMP.	SUBJECT WEIGHT	METABOLIC RATE	AVG. PULSE
••••••••••••	LOWERED	150	.400	60
————	LOWERED	150	4404	166
—— ——	LOWERED	180	5160	160
——•——	LOWERED	180	3060	154
— — —	LOWERED	180	2980	147

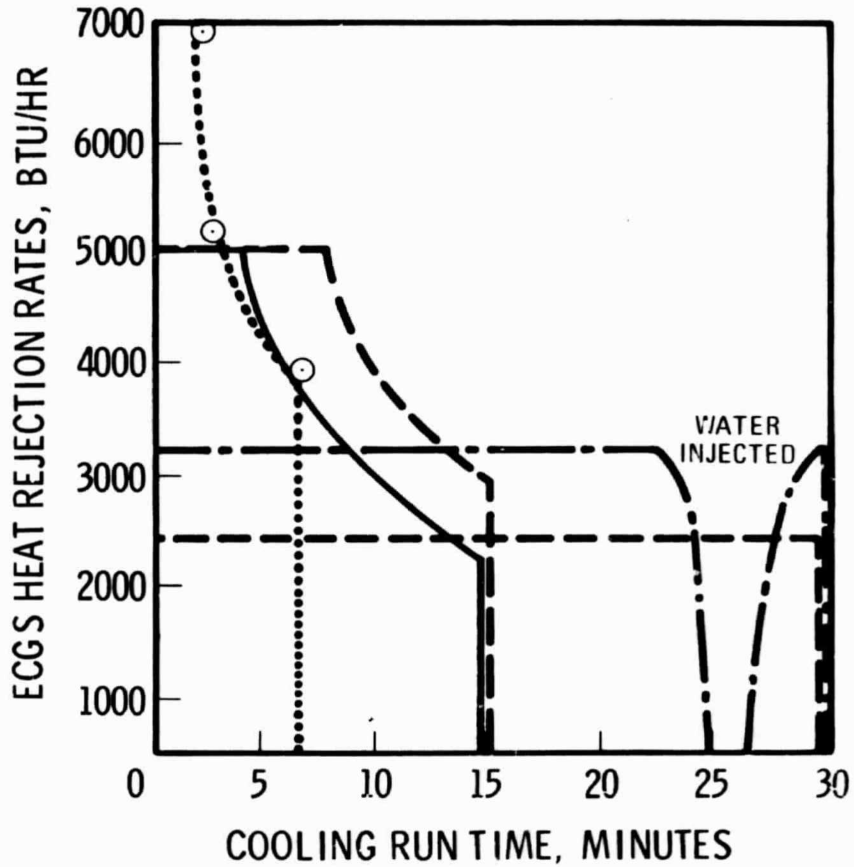

Figure 106. ECGS Maximum Heat Rejection Performance Full Suit

ECGS Capable of Overcooling at 5,000-Btu/hr Metabolic Rate

Figure 106 presents a summary of the boundary cooling conditions of several full-suit cooling runs. For example, the test run at 5,160-Btu/hr metabolic rate resulted in excessive cooling as evidenced by a reduction in both skin and core temperatures and the subject complained of being too cold during the entire run. It would appear that the ECGS in its current design therefore has a cooling capability that exceeds the approximate limits of human sustained effort. The cooling dropoff with increasing time (except for the water injection area) is caused by a continual lowering of skin temperature with the net result in an inability of the body to reject the normal quantas of heat through the skin. This then becomes a thermal-physiological limit that is controlled by the blood flow in the skin capillaries. Because the cooling patches in this condition are operating near freezing, no other cooling device could remove more heat unless the cooled area were incerased. The current ECGS area is 12.62 ft^2 which is about 62% of the surface area of an average Air Force male of mean height and weight (5 ft, 9 in., 164 lb).

Apparent Increase in Work Output with Proper Cooling

There have been numerous indications that if the cooling rate is set equal to or near the metabolic rate, then less energy is consumed to do a given task on the treadmill. For this reason it has been difficult to preset a target work level with optimum cooling. The usual result has been to undershoot the target metabolic rate in the 4,000- to 5,000-Btu/hr range by about 7%; man's apparent work capacity or efficiency is increased by about 7% in the high work level ranges if full thermal balance without heat stress or sweating occurs. This shows another advantage of using the ECGS as a body cooling system.

Preliminary Skin Comfort Temperatures

The steady state cooling runs provided subject comments on the various cooling rates at constant metabolic rates. These data are plotted for both subjects and are reflected to the corresponding average skin temperatures for the particular runs. This gives midpoint temperature boundary for the entire metabolic range; values above this line were hot and promoted sweat, and below tended to be too cold. The summary data for this condition can be seen in Figure 107, which also shows the LCG comfort zone boundary as determined under Contracts NAS 9-723, 9-3535. It should be pointed out that the new ECGS data are too limited to be conclusive, but they are indicative of general trends up to the higher metabolic rates tested.

Thermal Balance Heat Rejection Rates

A preliminary analysis of the steady state runs indicated that the high level cooling rates should range from about 67% to 78% of the metabolic rates for a fully insulated cooling suit. When the metabolic rates are sustained at 5,000-Btu/hr, the optimum cooling rate should be about 72% of this value, approximately 3,600-Btu/hr. This tentative conclusion is based on core temperatures, skin temperatures, pulse rate, work performance, and subject comments.

Figure 107 presents two heat rejection curves versus metabolic rate for two subjects. Core temperatures are also shown for these runs. The upper curve shows a dropping core temperature, indicating too high a heat rejection rate at the 5,200-Btu/hr point; the lower curve depicts the opposite effects at the 4,600-Btu/hr level. A compromise between these values might have been the best choice. Further discussion on this will be continued in Section 6.8.

6.8 4-HOUR SIMULATED EVA MISSION PROFILE COOLING RUNS

Near the conclusion of the contract, all techniques, run procedures, calibrations, operational experience, subject conditioning and the full ECGS delivery hardware were ready for the 4-hour simulated EVA mission runs. It was most gratifying to observe and record that every contract performance target specification was met during these runs and also to note that cooling capacity and work rates were not taxed during the final tests.

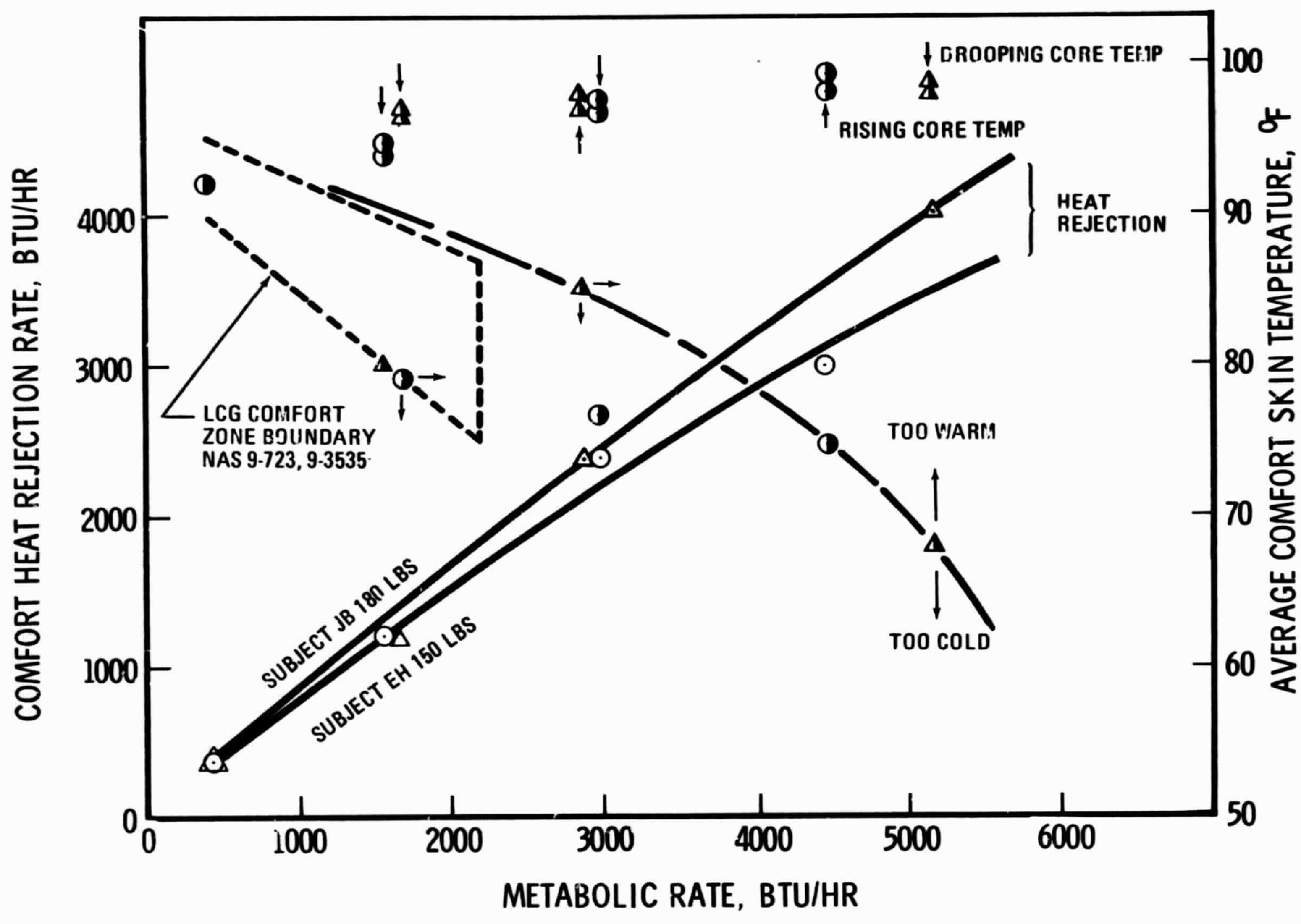

Figure 107. ECGS Cooling Comfort Performance Summary

The final runs were made with the complete ECGS and head cooling, while the subject was fully insulated with the double arctic garment worn over the ECGS. The test protocol is described in Section 6.6. Neither of the two tests was aborted during the runs nor did they require reruns caused by some subsystem malfunction. It was originally intended that the EVA mission profiles would be conducted within the A-6L spacesuit, but this was not possible because the A-6L was returned to NASA-MSC by their request prior to the final tests. The runs with the arctic garment were far more demanding on the ECGS cooling requirements as no cooling ventilation within the arctic garment was possible. This would not have been the case with the spacesuit. All answers should therefore be conservative as compared to an actual spacesuit operation. The arctic garment tests did point out one important conclusion. The spacesuit ventilation for body cooling comfort may not be necessary with an operational ECGS at any metabolic rate because body sweating was not observed. Dampness was noticed on the ECGS, which was believed to be caused by condensing water out of the air; however, the subjects were dry and cool (except for the face) even after the 4-hour run culminating in 20 min of nearly 5,000-Btu/hr metabolic rate.

The ECGS heat rejection rates were measured according to the calibration runs of Section 6.5 and set at predetermined levels as shown in Figure 107 of Section 6.7. Metabolic rates were required as indicated in Section 6.1 and were set as walking tasks on the treadmill as indicated in Section 6.4.

Figures 108 and 109 present the time history results of the 4-hour EVA simulated mission profile. All variables such as average skin temperature, core temperature, and pulse rates show remarkably similar trends.

In each case where rest periods were set up, the skin temperatures can be seen to rise in a positive slope curve. Conversely during high cooling rates, such as at the beginning of the runs, the temperature-time slopes are negative. During constant work rate periods longer than 10 min, the tendency for skin temperatures to stabilize was observed as in the first run at time 160 to 220 min. The core temperatures for both runs were essentially constant at all times, indicating good thermal balance had been maintained by the ECGS cooling.

FOLDOUT FRAME

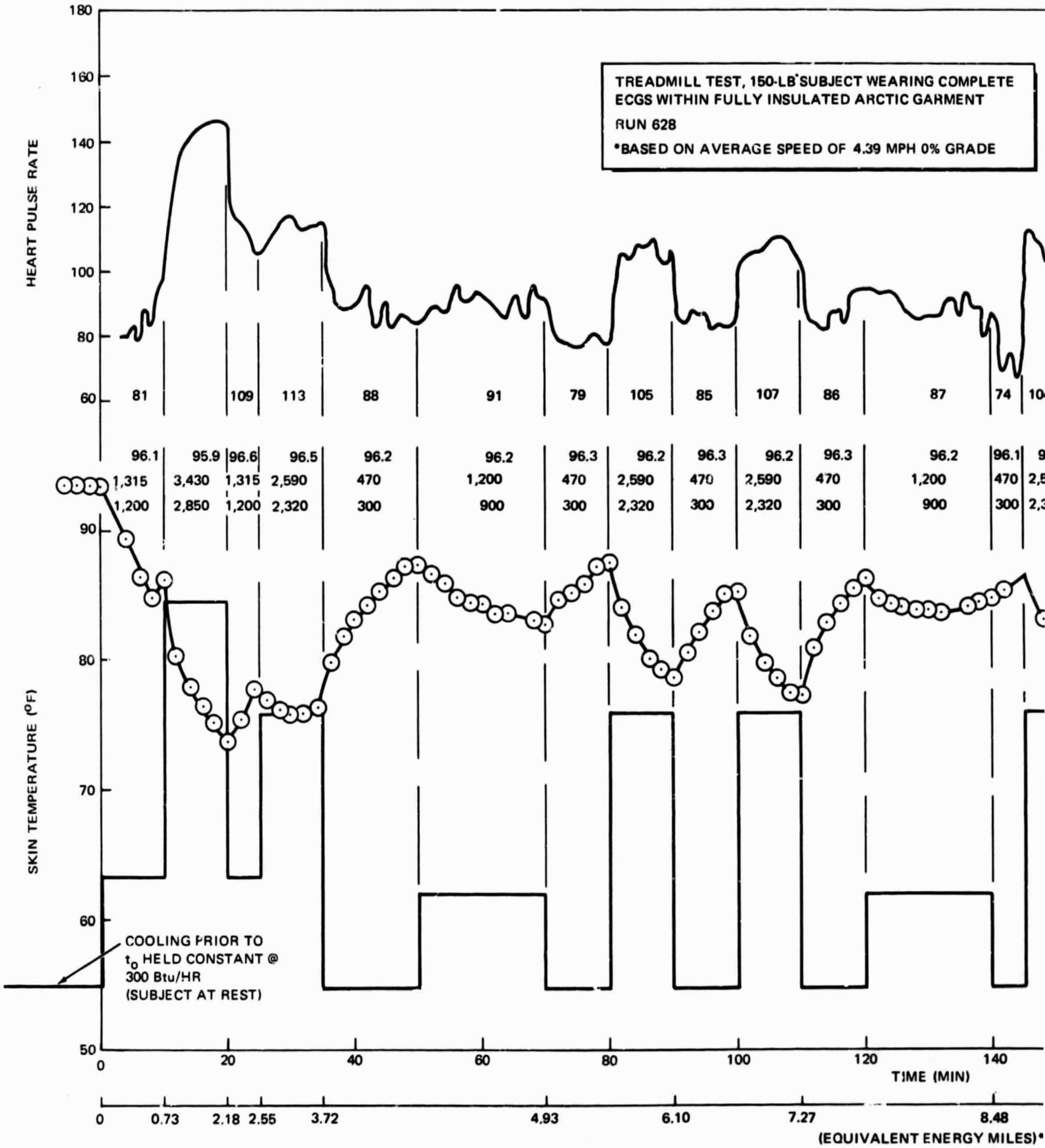

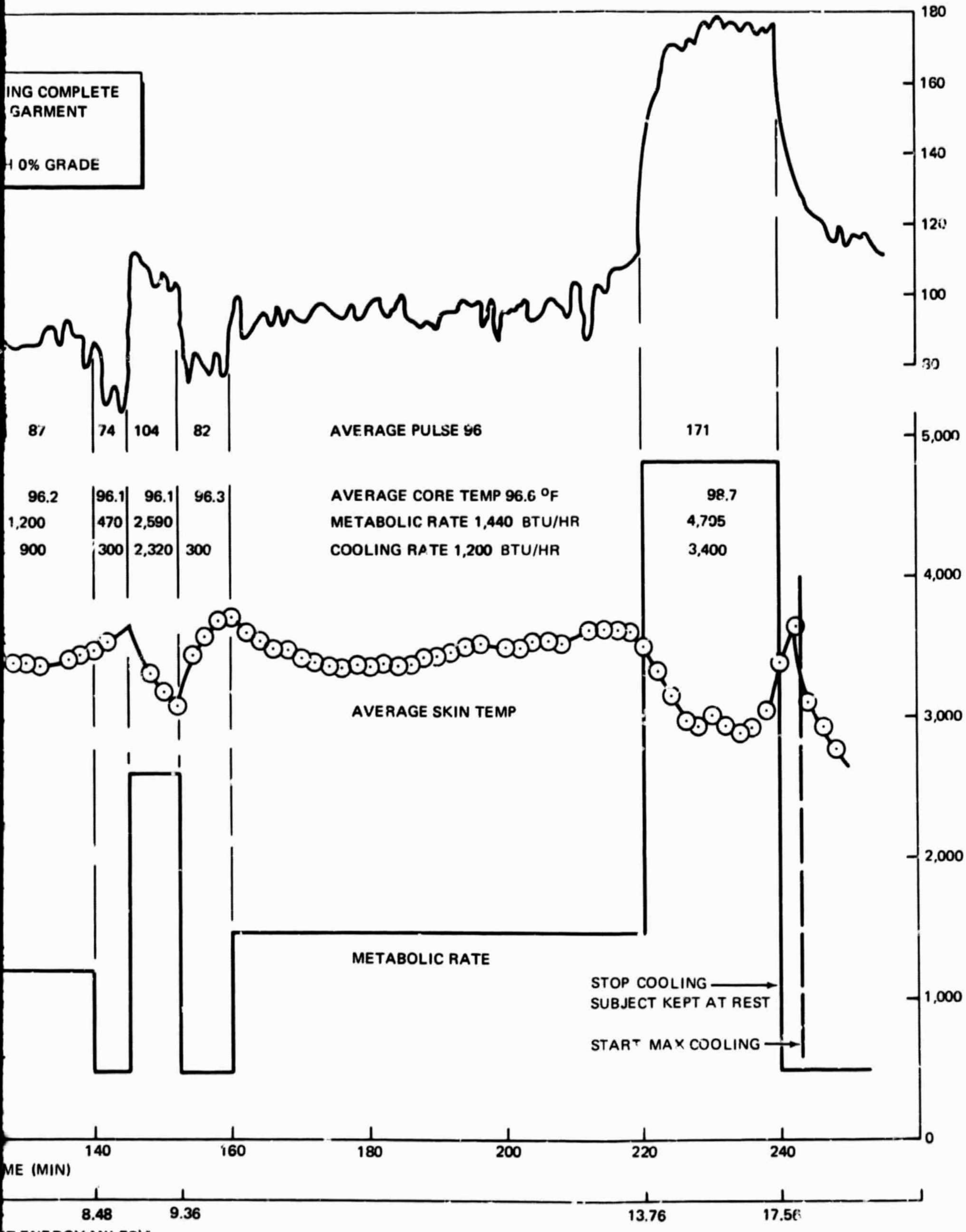

Figure 108. ECGS Cooling Performance Results – 4-hour Heavy Work Load Simulated EVA Mission (150-lb Subject)

FOLDOUT FRAME

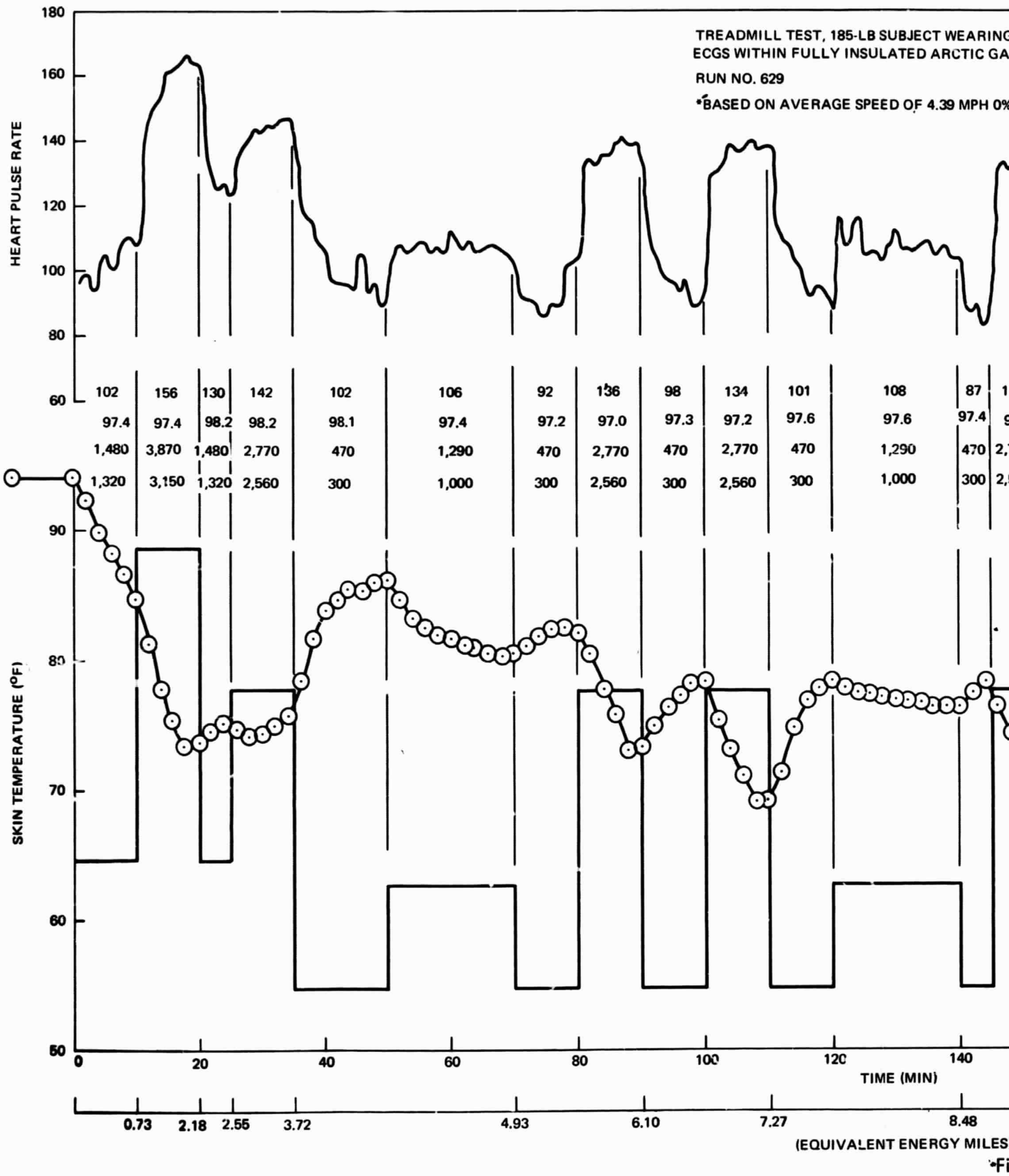

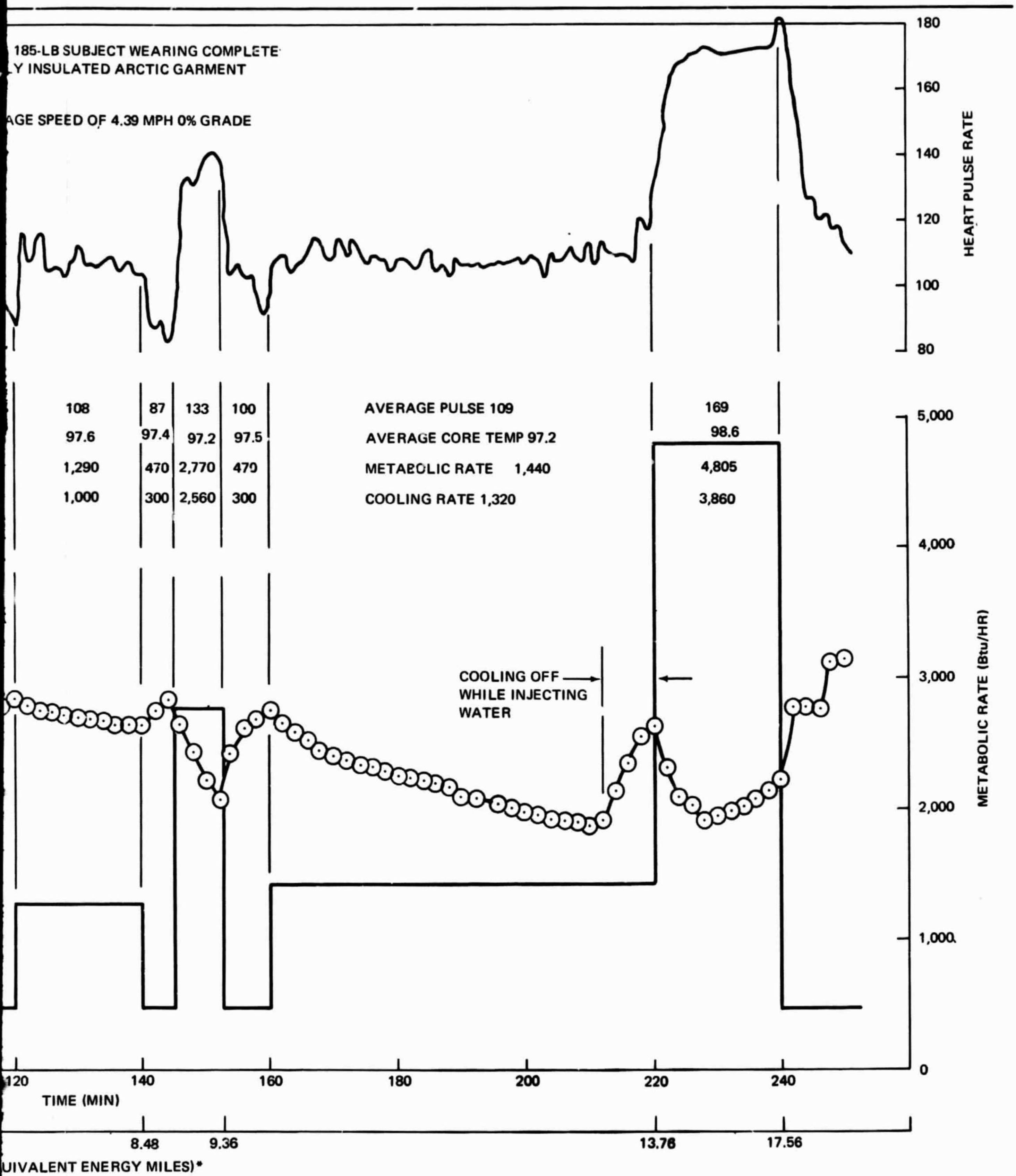

*Figure 109. ECGS Cooling Performance Results – 4-hour Heavy Work Load Simulated EVA Mission (185-lb Subject)

Figure 110 points out the average pulse rates during the design verification runs and suggests that this parameter may be used in the automatic control of cooling rate as a future development.

Both subjects apparently built up an anxiety stress just prior to entering into the last 20-min burst of energy, as shown by the pulse rates from 215 to 220 min. After cessation of exercise at the end of the first run, maximum cooling was set up for a 10-min period during recovery to demonstrate that cooling capacity was still available. The second run had the cooling stopped at the end of the run and therefore showed the immediate rise in skin temperature as would be expected.

Each of the runs was further analyzed to explain the trends in skin temperature and core temperature as a function of metabolic rate. These data are shown in Figures 111 and 112. The first run (628) shows that a nearly perfect thermal balance had been established in the resting area, and also in the 1,300- to 1,500-Btu/hr metabolic rate range; above this value a slight warming tendency was observed, even though the test subject stated that the cooling felt at optimum comfort during the entire run. The second run (629) displayed a tendency for overcooling even though the core temperatures did not vary more than ±0.6°F. The test subject felt on the slightly cool side during the entire run, which can be seen in the gradual downward slope of skin temperature from beginning to end.

Figure 113 shows the preselected cooling rates against the measured metabolic rates for the two runs. If one were to recommend the optimum cooling it could only be selected between the two curves, with slightly higher cooling for the 150-lb subject at the highest work rate and slightly less cooling for the 185-lb subject at the lower work rates.

The two subjects were in supposedly peak training just prior to the design verification runs; at that time the final work load calibration tests were completed as described in Section 6.4 utilizing the full ECGS plus the double-thickness arctic suit. The lighter subject tended to improve on

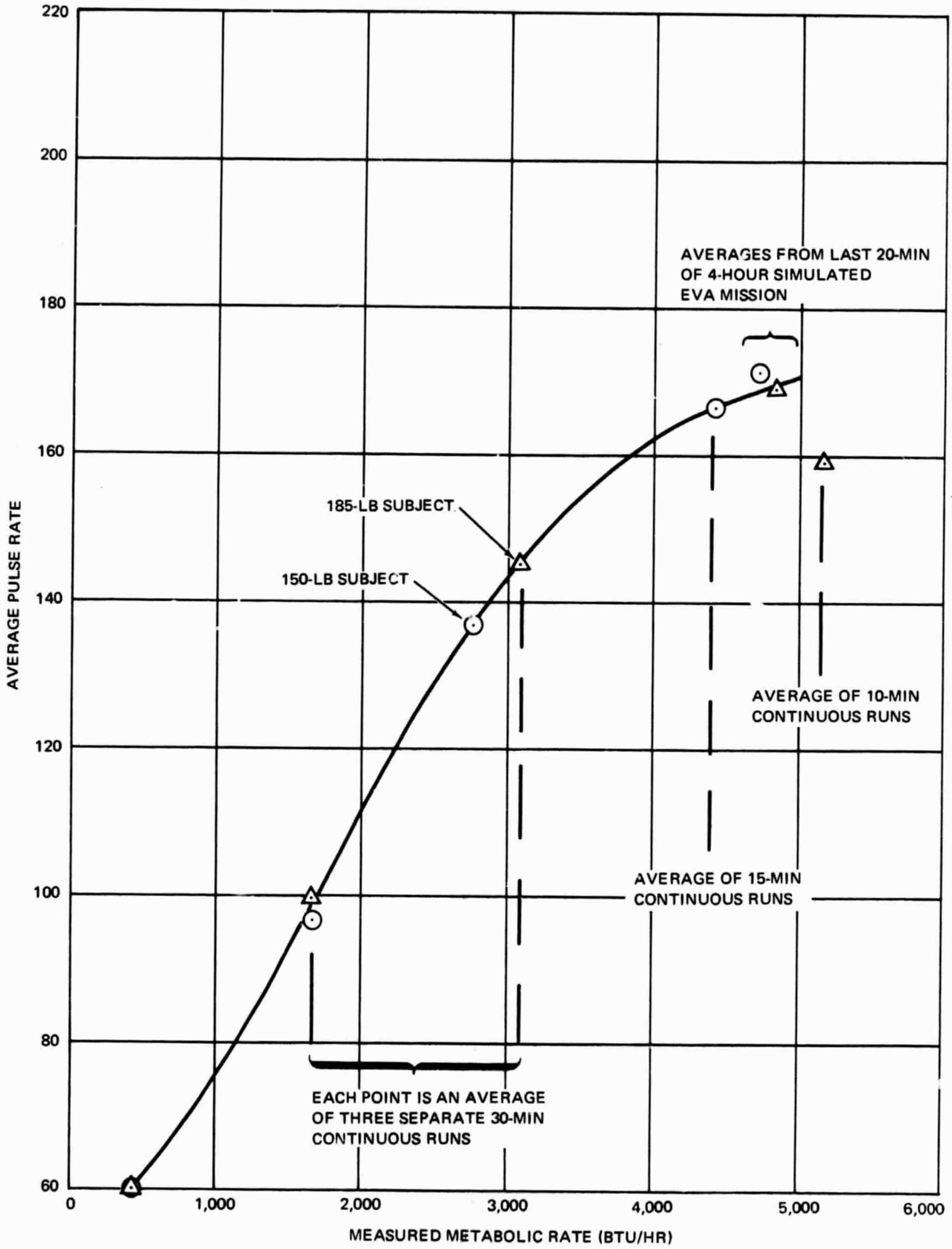

Figure 110. Pulse Rate Averages from Design Verification Runs Subjects Cooled by Full ECGS and Wearing Arctic Suit

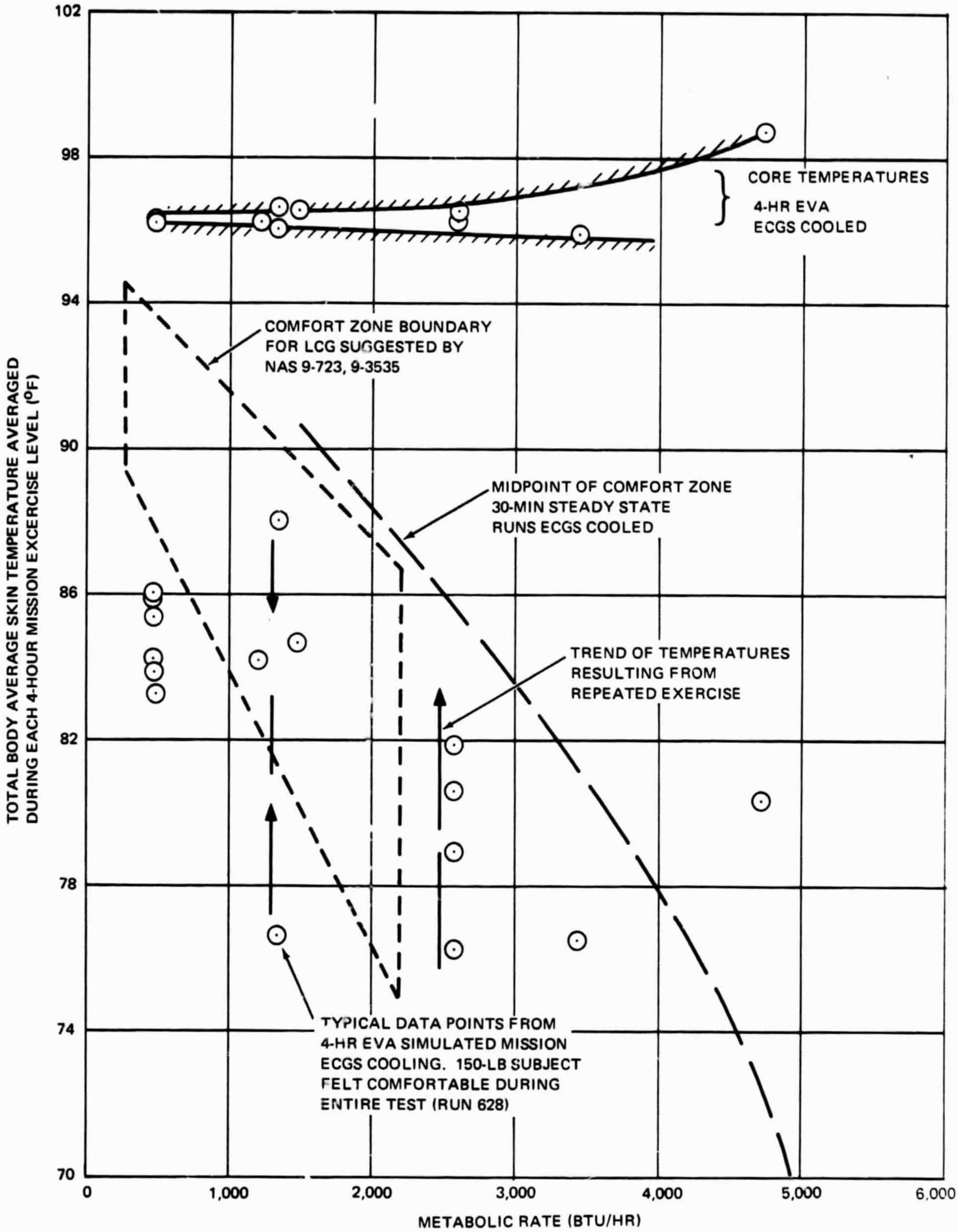

Figure 111. Summary Temperature Data – ECGS Cooled 4-hour EVA Simulated Mission (150-lb Subject)

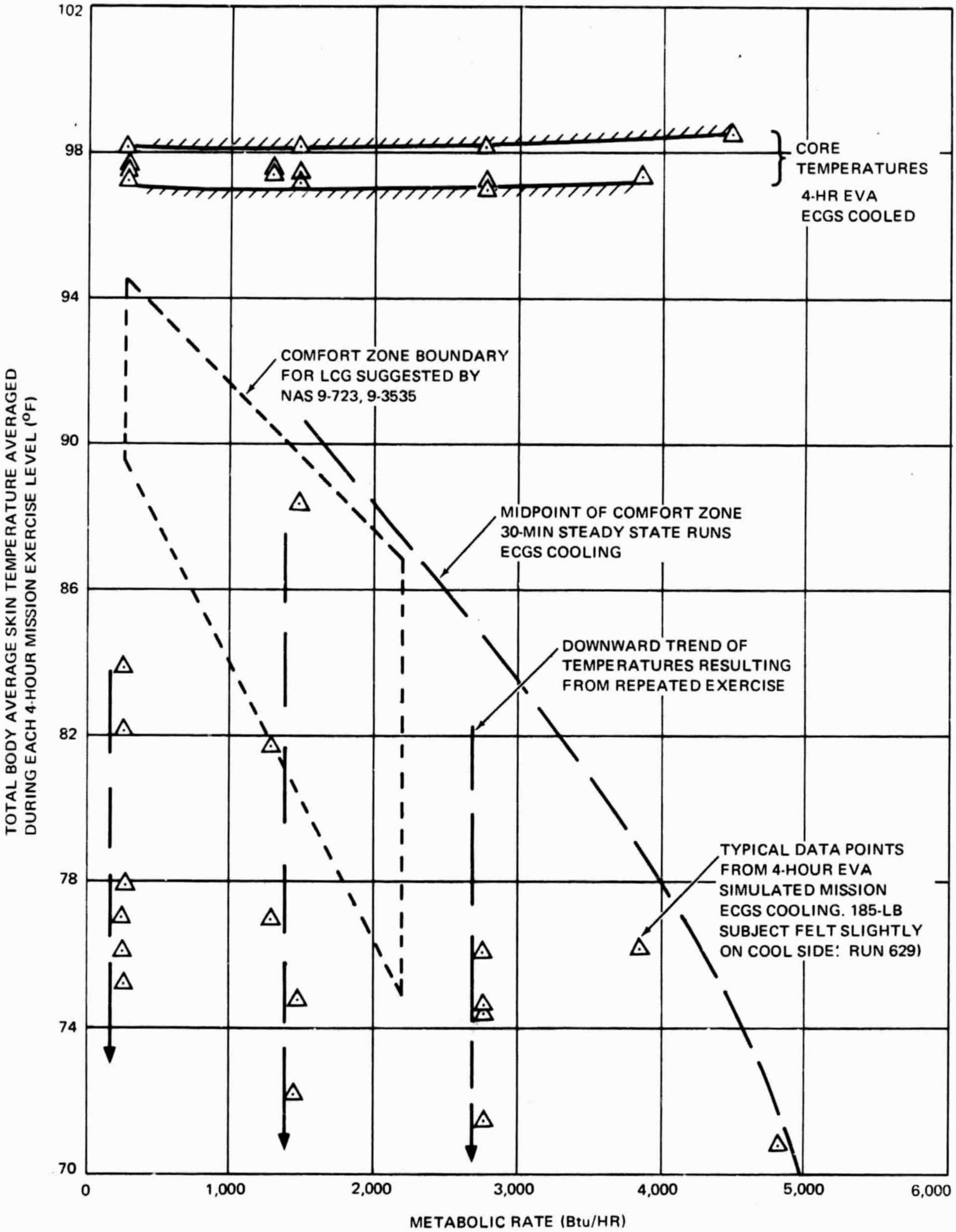

Figure 112. Summary Temperature Data – ECGS Cooled 4-hour EVA Simulated Mission (185-lb Subject)

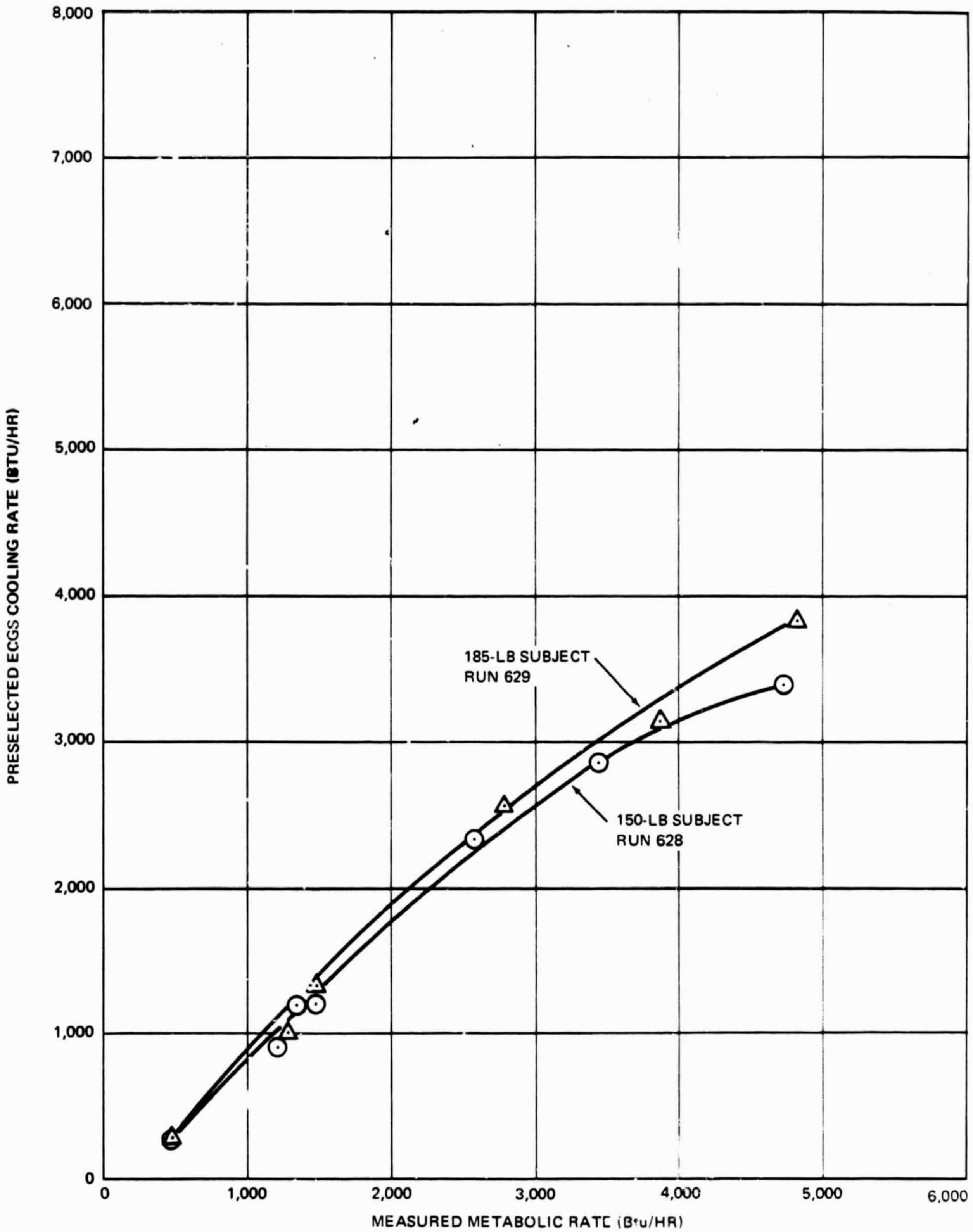

Figure 113. Summary Cooling and Metabolic Rates for 4-hour Simulated Eva Mission

subsequent runs; he was able to complete progressively a given treadmill task at a slightly lower metabolic rate than indicated by the prior calibrations. The same tendency was noted for the heavier subject, but not to such a great extent. The trend can be observed in the data of Section 6.7 where the lighter subject usually ended up with a slightly lower metabolic rate than the target value. Figure 114 shows this "training effect" for both subjects as a result of the design verification tests that directly followed the work load calibration runs; the greatest variance shows up in the 2,000- to 4,000-Btu/hr metabolic rate.

The cooling data described in this report were derived from many threadmill runs. The final two test subjects have logged over 300 miles and still the "training effects" continue to be appreciable. This fact is brought up as it may relate to an EVA operation in weightlessness. The astronaut training in EVA tasks at Earth gravity or in neutral bouyancy are also faced with the "training effect". Training will allow a given task to be accomplished at a lower metabolic rate. It would require large numbers of duplicate training tasks to minimize the metabolic rates for a given task, and if training is carried out to the point of diminishing returns, nothing short of extensive additional training in actual orbiting 0 g will allow the full training optimization to take place. The astronaut training described to reduce metabolic rates for a given EVA task is not economically practical. Therefore our spacesuit life support systems should be prepared to provide an environment capable of supporting the highest feasible metabolic rates.

It is impossible to design a system that can guarantee man will not sometime need to use his maximum sustained work capacity to cope with an emergency. This program has demonstrated that useful work can be performed at 5,000-Btu/hr metabolic rates for at least 20-min duration following 3 hours, 40 min of heavy activity and be cool and comfortable at this task without sweating. The ECGS performance breakthrough should therefore suggest a similar higher level of performance requirement for other spacesuit life support system parameters.

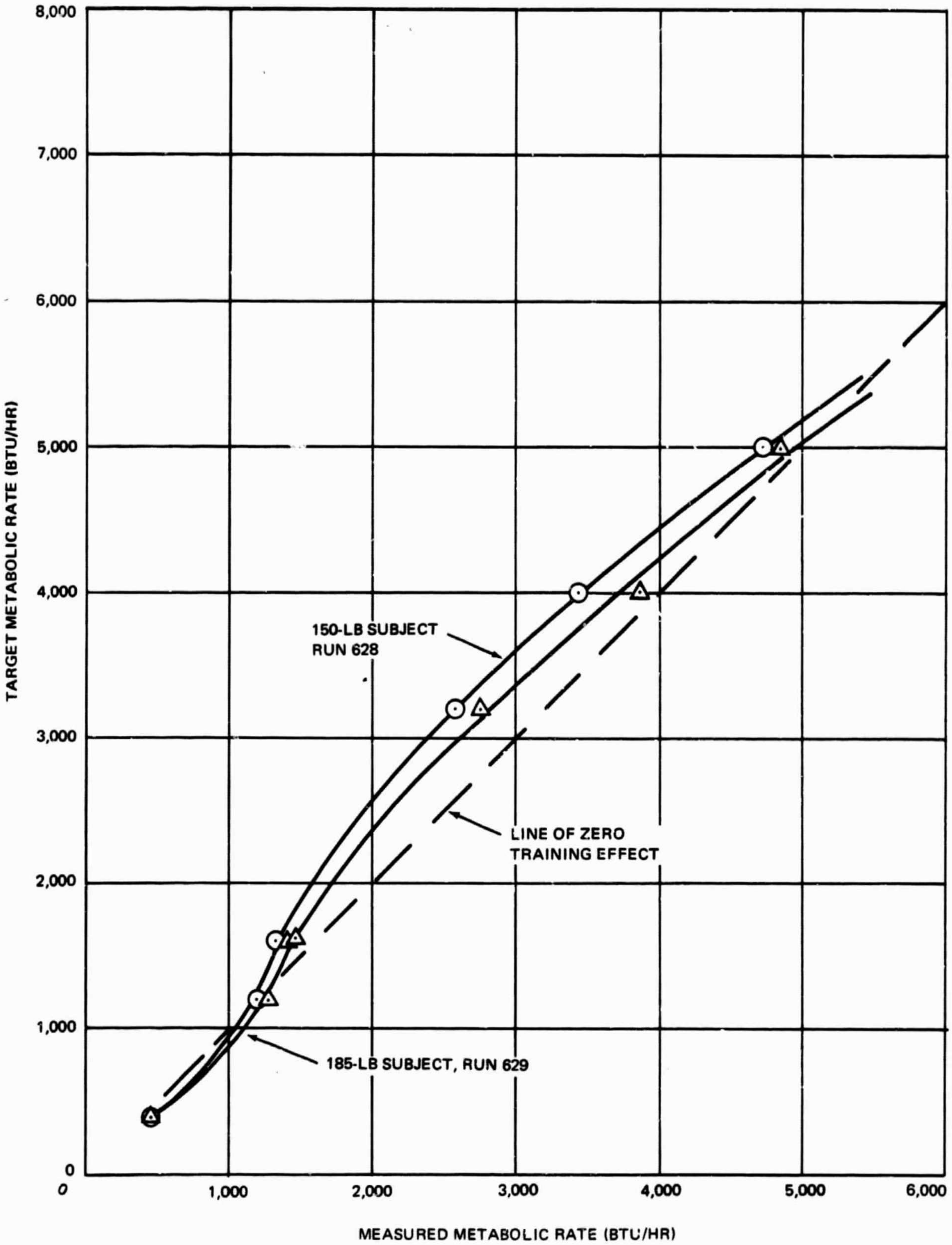

Figure 114. Summary of Predicted and Measured Metabolic Rates for 4-hour Simulated EVA Mission

6.9 GOVERNMENT REPRESENTATIVES WHO HAVE WORN THE ECGS

The following representatives from various government agencies have worn the full ECGS suit with cooling headpiece under high work capacity treadmill conditions. Tests ran up to 40-min duration and included short period metabolic rates in excess of 4,000 Btu/hr. In each case, the ECGS had a reserve cooling capacity that was greater than was deemed necessary to maintain a comfortable heat balance. Overcooling could be established within a few seconds in any work mode attempted.

1. NASA-MSC Crew Systems Division, represented by Mr. Fred Spross.
2. NASA-ARC Biotechnology Division, represented by Dr. Alan B. Chambers.
3. USAF-SAMSO Bioastronautics MOL represented by Capt. C. B. Harrah.

Section 7
CONCLUSIONS AND RECOMMENDATIONS

7.1 CONCLUSIONS

The evaporative cooling garment system (ECGS) contract was programmed through the research tasks of theory and design, basic laboratory tests, engineering model fabrication, design verification tests, and documentation with hardware delivery. The development was carried within 14 months from a working proof of principle concept to functioning hardware that was tested with very heavy work loads simulating a 4-hour EVA mission profile. Numerous problems came up with solutions covering the gamut from the search for highly specialized materials, to the development of test techniques designed to evaluate the ECGS cooling effectiveness on man working near the limits of endurance and energy consumption.

It was most gratifying to the ECGS project team and to management to observe that all aspects of the program were accomplished in accordance with contract requirements; and that the target cooling performance was easily met. It was shown that the test result cooling levels would push the prior state of the art by over 250%. Not only were the high cooling rates demonstrated, but it was shown that man could work in comfort using the ECGS at levels heretofore believed improbable of attainment.

Specific conclusions derived from the ECGS program are as follows:

1. The ECGS has demonstrated its ability to exceed every cooling requirement of the contract specified 4-hour heavy work load EVA mission profile.
2. Short run cooling rates exceed 7,000 Btu/hr; and any duration at this level over 2 min is limited only by the cardiovascular system's ability to transmit internal body heat via the bloodstream capillary bed to the skin surface.

3. Maximum cooling rates can be instigated in less than 1 sec.
4. Heat rejection rates have been controlled to less than 1% variation in laboratory test hardware.
5. 1,500 Btu-hr of heat rejection are stored within the current ECGS patches in the form of water; the cooling quanta can be released in 15 min or extended through 10 hours before adding water.
6. The ECGS requires no power with a manual controlled vacuum valve.
7. ECGS cooling of human activity up to 5,000-Btu/hr metabolic rate carried to the limit of human endurance results in no measurable body sweating while maintaining thermal equilibrium.
8. The ECGS has mobility limits comparable with the full pressure suit, wearing comfort is adequate for long-duration running speeds on the treadmill.
9. The ECGS plus the double liner arctic suit have been worn with full comfort and operated for 10 continuous hours during which 8.9 miles were walked on the treadmill.
10. The ECGS has been worn with the A-6L full pressure suit. Full integration needs only the addition of a steam vacuum fitting to the pressure suit.
11. A cooling headpiece has been developed as a part of the complete ECGS which has been integrated with full pressure suit intercom gear.

7.2 RECOMMENDATIONS

The following recommendations are made:

1. Continue development of the complete ECGS into potential space flight hardware.
2. Initiate the development of automatic cooling valves and controls.
3. Study the problems of skin temperature comfort zones at high metabolic rates and establish performance boundaries for same.
4. Optimize all components and materials.
5. Increase mobility and maintain full comfort with the increased flexibility.